Identifying Injustices in Urban Green Infrastructure Connectivity: 4 Case Studies

Zane William Havens

Albion, Michigan

Bachelor of Arts, Albion College, 2012

Master of Arts, University of Virginia, 2019

A Dissertation submitted to the Graduate Faculty

of the University of Virginia in Candidacy for the Degree of

Doctor of Philosophy

Department of Environmental Sciences

University of Virginia

May 2024

Identifying Injustices in Urban Green Infrastructure Connectivity: 4 Case Studies

Zane William Havens

(ABSTRACT)

Urban centers are complex systems, formed and influenced by both external environmental variables like climate and geography, and by the residents who participate in the systems. As the global climate warms, these already complex systems are likely to change in ways that will negatively impact their residents, and certain resources will be required to mitigate and abate these changes. However, these resources are not always fairly distributed amongst participating communities within these systems, particularly populations considered socially vulnerable. One such resource is urban green infrastructure (UGI), the vegetation growing throughout a city that has the potential help mitigate flooding, reduce excessive heat, and improve the quality of life of urban residents. Although studies have examined the amount of UGI in relation to social vulnerability indicators (SVIs), few studies have examined the connectivity of UGI, a variable that can bolster ecosystem services provided by UGI, in relation to SVIs. This dissertation provides a novel method to quantify UGI connectivity inequity in urban centers by examining four US case studies and utilizing a series of Landscape Metrics, SVIs, Principal Component Analysis, and Mann Whitney U Tests to empirically test for inequity. For the first case study, Washington, DC, results indicate that there are disparities in tree areal coverage and connectivity between the upper 50^{th} percentile and the lower 50^{th} percentile regarding Minority %, with plots with a higher percentage of Minority residents having a significantly ($p < 0.05$) lower mean rank in Tree PLAND, Tree LPI, Tree PLADJ, and Tree Cohesion and a higher mean rank in Tree ENN_MN. The second case study, Phoenix, AZ, indicated disparities in tree and shrub connectivity, with plots in the upper 50^{th} percentile of Poverty %, No High-school Diploma %, and Age 17- % all having a lower mean rank in Tree PLADJ, Tree Cohesion, Shrub PLADJ, and Shrub Cohesion than did the plots in the lower 50^{th} percentile for those variables. In the third case study, Detroit Metropolitan Area, MI, there were no significant disparities facing vulnerable populations over the entire area. However, when comparing the city of Detroit to nearby Oakland County suburbs, results suggested that the city of Detroit, which is known to have a relatively high proportion of vulnerable residents compared to the surrounding suburbs, has a significantly lower mean rank for Tree PLAND, Tree LPI, Tree PLADJ, and Tree Cohesion and a significantly higher mean rank for Tree LSI than the suburbs of Oakland County. This suggests disparities based on city boundaries that were not exposed via this study's initial methodology. In the final case study, New York City, NY, results indicated a significantly higher mean rank for Tree ENN_MN in plots in the upper 50^{th} percentile for the SVI variables Unemployed %, Uninsured % , and Minority % than in plots in the lower 50^{th} percentile. The results of this dissertation empirically demonstrate disparities in UGI coverage in 3 of the 4 cities, and hints at disparities in the 4th, continuing the research into the identification of environmental injustices and providing a new method to quantify this facet of urban ecosystem dynamics through the lens of UGI connectivity.

Dedication

I dedicate this to my wife, Sonia Foley, who inspires me both with her brilliance and her bravery. This dissertation has been, by far, the most elaborate thing I've ever done to impress a beautiful woman.

Acknowledgments

I am deeply grateful to my advisor, Steve Macko, for his unwavering support, dedication, and patience, which have been instrumental in shaping this thesis.

My heartfelt thanks to my committee members, John Porter, Xi Yang, and Tim Beatley, for inspiring me during my academic journey and providing invaluable advice that has significantly contributed to the refinement of this work.

Special appreciation goes to Kendall Davis for her hard work on the landscape classification of Detroit, and to Laura Mogensen for her expert advice on Principal Component Analysis.

I would like to express my gratitude to my proofreading team, my parents, for slogging through pages of scientific writing to ensure accuracy and correctness, even in the minutest details.

Lastly, I extend my thanks to the University of Virginia Department of Environmental Sciences for their support, providing resources, facilities, and a collaborative environment that has been crucial in the successful completion of this research.

Contents

List of Figures

List of Tables

List of Abbreviations

CSO Combined Sewer Overflow

DC Washington, District of Columbia

DMA Detroit Metropolitan Area, Michigan (Detroit city and cities within Oakland County)

DSI Density Sprawl Index

EJ Environmental Justice

EPA United States Environmental Protection Agency

EU European Union

FHA Federal Housing Administration

HOLC Home Owners' Loan Corporation

LSM Landscape Metric

NYC New York City, New York

PC Principal Component

PCA Principal Component Analysis

PHX Pheonix, Arizona

RCP Representative Concentration Pathway

SVI Social Vulnerability Indicator

UGI	Urban Green Infrastructure
UHI	Urban Heat Island
US	United States of America

Chapter 1

Introduction

1.1 Climate Change and Urbanization

Global climate change is an enigmatic challenge that will impact many aspects of human society. The 5th Intergovernmental Panel on Climate Change Impacts, Adaptation, and Vulnerability Report[18] indicated that urban areas will see unique and acute effects of climate change. The risks associated with flooding from sea level rise, extreme precipitation events, and storm surges are increasing in coastal urban areas. This, alongside the expected stresses resulting from drought, heat waves, air pollution, and disease emergence, promises to bring unprecedented challenges to urban populations in coastal areas. Unfortunately, urban areas also struggle with a unique set of economic and societal challenges that promise to conflate the issues resulting from climate change. As of 2018, over 55% of the world's population was concentrated in urban areas, and this percentage is projected to increase beyond 68% by 2050[56]. The consolidation of these populations, as well as the complicated systemic relationships that are inherent in urban areas, may prove to pose both challenges and opportunities for urban inhabitants.

Environmentally, the migration of human populations to urban centers is not inherently hazardous for either global ecosystems or human society. In fact, there are environmental benefits to the development of high-density urban areas[36]:

- The high-density concentration of urban populations reduces the physical footprint of humans. In the context of climate change, a reduction in space occupied by human development means a reduction in both the stresses on the ecosystems we rely upon to buffer the impacts of climate change, as well as a reduction of area that requires climate adaptation.

- Generally, urban areas are more efficient in regards to resource consumption. However, the planning and design of urban areas is critical to maximizing this efficiency. A 1989 study by Newman and Kenworthy indicated that per capita gasoline consumption was inversely related to population density in large cities. This suggests that cities that grow vertically consume gasoline significantly more efficiently than those that grow horizontally through urban and suburban sprawl[40]. This is impactful both when considering the potential for climate change related resource scarcity, but also when considering the mitigation of greenhouse gases produced by the consumption of fossil fuels.

High population densities in urban centers may mean that the impact of environmental hazards will be concentrated on individuals living in these densely populated locations, many of whom are highly vulnerable[14]. In order to properly adapt to the oncoming changes associated with a warming Earth, research into the proper handling of the safety and well-being of vulnerable populations in urban centers is both morally imperative and crucial to preventing devastating loss of resources and lives.

1.1.1 Flooding

Flooding is projected to be an increasingly disruptive issue related to global climate change. In inland regions, most flooding will either be the result of riverine flooding or localized increases in the magnitude and frequency of precipitation events, coupled with the cities' geomorphologic characteristics. However, the extent to which precipitation events will increase in magnitude and frequency is difficult to predict and makes taking adaptive measures challenging to implement[18, 61]. Although different regions are likely to experience different climate extremes, at the small urban hydrology scale, projected increases in rainfall intensity range between 10% - 60% by 2100.

Many coastal regions are also likely to experience flooding resulting from extreme precipitation events, as well as increasingly recurrent flooding due to sea level rise and acute storm surges from hurricanes. It is estimated that approximately 40 million inhabitants of port cities (coastal cities with a population exceeding one million in 2005) are currently exposed to coastal flooding risks associated with climate change and, assuming current population trends and a homogeneous 0.5 meter increase in sea level, this number is expected to triple by the 2070s[23]. Additionally, a 0.5 meter rise in sea level by the 2070s is predicted to put approximately $35 trillion worth of coastal assets at risk of damage from a 1 inch 100 year storm, more than 10 times the current asset risk at $3 trillion.

1.1.2 Urban Heat Island Effect

In addition to the challenges associated with flooding, increasing global temperatures will likely exacerbate high temperatures in urban areas[18]. The urban heat island (UHI) effect, a phenomenon where areas with limited vegetation and large amounts of built structures absorb sunlight and emit heat, has already begun to impact urban centers globally. An analysis of 18 studies found that the average increase in building cooling demands resulting from the combination of UHI and global climate change between 1970 and 2010 was approximately 11%[47]. The impacts of an increase in temperature for urban areas can range from increased energy demand to increased mortality, and often these effects are more acute in socially vulnerable communities[46, 49].

1.2 Mitigation Efforts

1.2.1 Gray Infrastructure

In the United States, efforts to mitigate urban flooding can be generally defined by two categories: gray infrastructure and green infrastructure[15]. The former methodology has been historically implemented in urban areas as a means of moving water out of urban areas as quickly and efficiently as possible, often using static, inflexible infrastructure such as drains, culverts, and sewers[35]. In the early development of urban sanitation systems, this concept was applied both to sewage and stormwater, which created many “combined sewer systems”, which incorporated stormwater and sewer systems into a single infrastructure that could transport the unwanted waste elsewhere. Many of these historical combined sewer systems were designed for historical urban populations, and as these urban areas grew in size, they also outgrew the infrastructure. This, combined with the typical wear and tear associated with aging infrastructure, has resulted in thousands of combined sewer overflows (CSOs) across the United States in recent years[57]. These overflow events are often triggered by an acute influx of water into the system that overwhelms the system’s capacity, forcing the excess slurry of stormwater and wastewater to be expelled into the local watershed via intentional outfalls.

Although some applications of gray infrastructure can be used to mitigate UHI[44], the materials used to mitigate flooding are often culprits for absorbing and re-emitting heat[41]. Concrete, asphalt, and other components of the gray infrastructure used to rapidly funnel excess storm water out of urban centers frequently have low albedos and, unless combined with tactics to explicitly address UHI, will not only fail to address increases in urban temperatures, but can also add to the problem.

1.2.2 Green Infrastructure

Of the efforts to mitigate the impacts of climate change in urban regions, Urban Green Infrastructure (UGI) shows great promise as a multifaceted approach to the challenges associated with climate changes. As outlined in section 502 of the Clean Water Act, UGI is "...the range of measures that use plant or soil systems, permeable pavement or other permeable surfaces or substrates, stormwater harvest and reuse, or landscaping to store, infiltrate, or evapotranspiration stormwater and reduce flows to sewer systems or surface waters"[59]. This methodology of stormwater reduction and retention includes a wide swath of implementation, including green roofs, rain gardens, bioswales, retention ponds, and permeable pavements and surfaces.

On the US EPA website, 11 UGI elements are identified. These elements can be clumped into 2 general categories: methods that integrate new vegetation to store and slow influxes of water (Group 1), and methods that do not incorporate vegetation but alter existing infrastructure to store and slow influxes of water (Group 2).

Group 1:

- Rain Gardens
- Planter Boxes
- Bioswales
- Green Streets and Alleys
- Green Parking
- Green Roofs
- Urban Tree Canopy
- Land Conservation

Group 2:

- Permeable Pavements
- Downspout Disconnection
- Rainwater Harvesting

Evidence of the effectiveness of UGI in stormwater abatement is widely prevalent, but one of the key strengths of utilizing UGI is the potential for co-benefits. Alongside its ability to reduce stormwater flooding, studies have indicated that types of UGI can also improve ecosystem water quality and reduce the need for stormwater treatment, increase groundwater recharge, improve the energy efficiency of buildings[2, 19], improve air quality[12, 17], and abate UHI[22]. The benefits of UGI extend beyond the natural environment as well; when implemented in populated urban areas, UGI also has societal benefits. By improving urban aesthetics, offering urban recreational opportunities, reducing noise pollution, facilitating community cohesion, providing areas for urban agriculture, and supplying educational opportunities, the potential of UGI is broadly applicable.

For the purpose of this dissertation, UGI in Group 1 is of primary interest; although UGI that does not directly incorporate vegetation does help reduce and slow stormwater flooding peaks, decrease pavement temperature, and filter stormwater of contaminants, many of the co-benefits listed above are not realized without the inclusion of a vegetated component[52, 60]. Additionally, detecting and identifying UGI that does not include a vegetative element through remote sensing is challenging, as NDVI and other multi-spectral techniques cannot discriminate between gray infrastructure and UGI lacking the vegetative component (such as permeable pavement or downspout disconnection).

1.2.3 Connectivity of UGI

The amount of UGI in a city is not the only factor when considering the mitigation of climate change. How UGI covers the landscape - whether clumped in large patches, dotting the landscape in isolated parcels, or connected as a network of small clusters - factors into the effectiveness of UGI to abate climate change impacts (Figure 1.1). Many countries already consider ecosystem connectivity a priority in environmental strategy, with the European Union marking the establishment of ecological corridors as a target in the EU Biodiversity Strategy for 2030[1]. However, the emphasis on connectivity primarily focuses on the improvement and protection of biodiversity, with little mention of the benefits of ecosystem and vegetative connectivity in regards to climate change. In the United States of America (USA), even less attention is given to ecosystem connectivity, with the Environmental Protection Agency's (EPA) Green Infrastructure Strategic Agenda not mentioning corridors, networks, or connectivity as a priority in UGI planning[58].

Kim and Park found that landscapes that are less fragmented and more connected are more likely to reduce peak runoff from storm events than those that are scattered

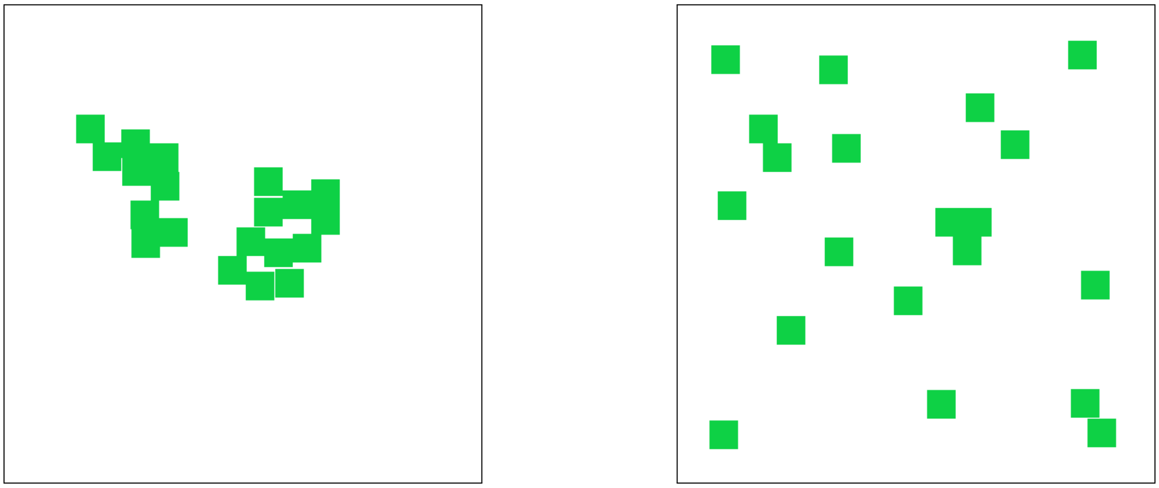

Figure 1.1: Example of two landscapes with approximately the same proportion of landscape coverage, but differing landscape connectivity. The example on the right has a lower connectivity than the landscape on the left.

and separated[29]. UHI effects are also influenced by landscape composition. Studies by Zhang et al. (2022) and Sun et al.(2018) indicate that increases in impervious surface proportion, connectivity, and shape complexity result in increases in land surface temperatures[64, 54]. Some studies even recommend the implementation of combined cooling patterns through well-structured networks of ”cold islands” to be considered when combating UHI[45]. The relationships between landscape complexity and urban land-surface temperature tends to be more complicated, but some studies show that UGI landscapes that are complex have a reduced cooling effect compared to simpler landscapes[63, 30].

Additionally, previous research has indicated that the biophysical connectivity of UGI can influence the social connectivity and resilience of communities[16, 21, 31]. Robust social connectivity has been shown to bolster the resiliency of communities to climate change related impacts and, conversely, weak social connectivity has the potential to make communities more vulnerable to these impacts[28].

1.3 Environmental Justice

Environmental Justice (EJ), as defined by the US Environmental Protection Agency (EPA), is "the fair treatment and meaningful involvement of all people regardless of race, color, national origin, or income, with respect to the development, implementation, and enforcement of environmental laws, regulations, and policies." Historically, marginalized populations in the US have endured an unequal proportion of environmental pollution[38]. Black Americans, Indigenous Americans, and other communities of color have been subject to numerous policies and actions that have actively, and passively, negatively impacted the health and function of those communities[10, 37]. In the US, the EJ movement developed in response to the many inequities in the environmental conditions endured by communities of color. Whereas this movement continues to tackle these challenges, ongoing cognizance of EJ during government decision making processes is required if missteps are to be avoided. In 1992, the EPA established the Office of Environmental Equity (later to become the Office of Environmental Justice) to address the discrepancies in environmental well-being of vulnerable populations.

Classically, EJ issues have taken the form of spatially discrete inequities caused by the direct action of corporations or government entities, often in the form of environmental pollution[4]. The proximity of point-source pollution to vulnerable communities has been a perennial issue for urban centers in the US[55, 11, 20]. However, with the challenges associated with global climate change, a different type of inequity is being exposed. These challenges are not point-source pollution problems, where a specific community experiences spatially explicit environmental degradation that can be attributed to specific actors, such as the establishment of a landfill by a municipality near low income communities of color[32]. Instead, global changes are impacting all areas regardless of socio-demographic status[18]. The crux of this problem is not the challenge of simply stopping and mitigating pollution and its impacts in vulnerable communities. It is instead ensuring that the allocation of resources to bolster the resiliency of vulnerable communities in the face of global environmental degradation is fair and equitable. When all communities are experiencing a change, those with the resources to defend against the resulting impacts will fare better than those without these resources, and this discrepancy poses an EJ problem.

Global warming and its associated impacts on urban areas, combined with an unjust distribution in UGI, exemplify this form of EJ challenge. As racial and socioeconomic segregation is found in populations globally[51, 26], identifying and understanding discrepancies in spatial characteristics of UGI connectivity and their relationships with spatial characteristics of population demographics is crucial to understanding how to avoid and address these EJ concerns in urban areas.

1.3.1 Segregation as a Source of Injustice

To fully evaluate whether spatial discrepancies in resources constitute an EJ issue, an understanding of segregation and the drivers behind this phenomenon is necessary. Urban areas are not homogeneous in socio-demographic characteristics[34]. The agent-based Schelling Model of Segregation suggests that, even when individual agents are comfortable living near those who are from different ethnicities or economic backgrounds than themselves, these agents still have mild in-group preferences that, over time, lead to segregated populations[48]. This model does not consider outside forces, such as systemic segregation, but indicates that some form of voluntary segregation is, in many ways, a predictable outcome of urban populations.

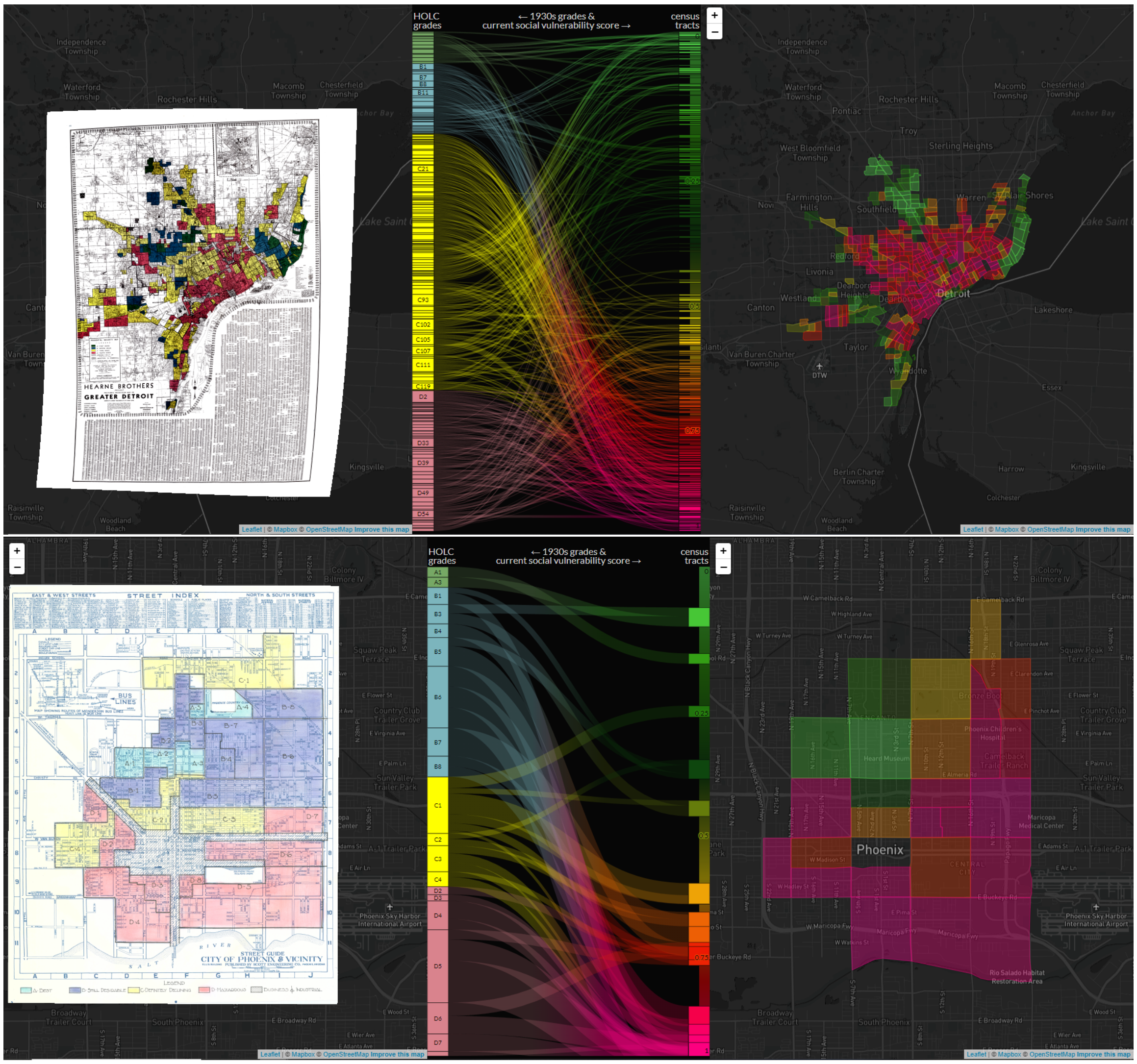

Figure 1.2: Visualization of historical HOLC ratings to 2018 SVI in Detroit, MI (top) and Phoenix, AZ (bottom). Image on the left shows an historical map of HOLC Ratings, where Green coincides with A ratings, blue with B ratings, yellow with C ratings, and red with D ratings. The image on the right shows SVI calculated from 2018 Census Data, with Green representing the least vulnerable, yellow the somewhat vulnerable, orange the vulnerable, and red the most vulnerable. The center diagram depicts the correlation between the HOLC ratings (the left bar) and SVI (the right bar) for all census districts within each city[39].

This concept offers a foundation for spatial distribution EJ issues. If we are to assume that populations will eventually segregate regardless of any outside forces or strong cultural biases, any significant discrepancies in the amount or quality of resources available to these populations based on location becomes an EJ issue[50]. Until these discrepancies are addressed, one population will unjustly lack the resources of another population.

However, populations are not only segregated via a dispersion following the Schelling Model. In the US, minority populations have been routinely forced to live in less desirable locations via systemic mechanisms and actions by neighbors with racial biases[62]. In the Post-Civil War US, ”Jim Crow Laws” were enacted to separate minorities from the white majority population. These laws were applied to both public spaces, such as laws segregating public restrooms and train cars, as well as to residential districts, i.e. laws penalizing an individual for living in areas not designated for the individual’s race[27]. These intentionally racist mechanisms have had an impact on the geographic locations of minority populations, making the EJ problem of spatial resource discrepancies even more egregious.

Legal action was not the only way that segregation was enforced in the Post-Civil War US. Violence, and threats of violence, against non-white populations were and still are used to discourage integration[7]. Urban infrastructure and transportation planning is another tool used to segregate populations[24, 3], creating conduits that both facilitate the movement of certain populations between specified locations and provide barriers to other locations. Financial mechanisms that disincentivize integration have also played a role in establishing segregated communities. One mechanism, known colloquially as redlining, has been the topic of recent EJ research for its blatantly racist intent and its lasting impact on US urban landscapes.

1.3.2 Injustice Rooted in History: Redlining and Racial Inequality

A major contributing factor in geographically-delineated inequality unique to the US stems from the historical practice of "redlining", prevalent throughout the early half of the 20th century. Redlining, a term referring to the literal red lines drawn on maps around areas designating high risk, was a process by which the Home Owners' Loan Corporation (HOLC) appraised real estate risk in urban areas during the Great Depression[25]). Areas were lumped into 4 grades, the worst of which (D grade) was given to areas that were considered "hazardous" for investors. This process proved ethically problematic, as the criteria for a D grade included the economic well-being of area households and whether the area was home to African Americans. It is believed that these historical ratings have had a profound impact on neighborhood resource distribution and the prevalence of racially driven systemic poverty and, consequentially, social vulnerability indicators (SVIs)[39]. As demonstrated by Figure 1.2, taken from *Not Even Past: Social Vulnerability and the Legacy of Redlining*, an online geographic analysis of redlining and vulnerability in urban centers by the University of Richmond's Digital Scholarship, the racially motivated D grades given by the HOLC in the 1940s frequently coincide with the census tracts deemed more vulnerable today, while the regions given A grades are typically less vulnerable today. These historical ratings, when implemented alongside other racist policies such as racially restrictive covenants, dissuaded public investment in historically vulnerable neighborhoods with primarily non-white populations. The effects of these ratings are still present today[53].

1.3.3 Identifying EJ Root Causes

A common rebuttal to EJ violation claims in urban areas questions the timeline of urban planning and its relationship with environmental hazards and resources. This argument claims that environmental problems — either lack of resources or the presence of hazards — are often found in proximity to vulnerable groups because these communities are drawn to less desirable areas, often due to a lower cost of living[5]. Studies indicate that this is not the case but rather, environmental problems are located in areas that have less political push-back, which are often areas with vulnerable residents[43]. This study is not as interested in the *Why*, although this question does merit further research. Currently, cities around the US have already started implementing UGI programs to mitigate the effects of climate change, and many of the programs have been in operation for over a decade. This study intends to serve as a window into a specific point in time and is supported by the concept that, regardless of the root cause, vulnerable groups having less environmental resources than their less vulnerable counterparts constitutes an EJ issue and deserves attention.

1.4 Significance of this Study

Although previous studies have examined the relationship between UGI and SVI, little has been done to correlate the landscape connectivity of UGI with social vulnerability. In general, the connectivity of UGI has not been adequately studied, and literature regarding this subject has focused around the effects of UGI connectivity on the impacts of climate change, rather than the past and present patterns of planning and implementation of UGI in relation to vulnerable populations. Additionally, past studies have calculated tree canopy coverage within the boundaries of political units, such as census tracts or HOLC zones, that do not have equal areas. Because area is incorporated into the calculation of connectivity[33], the size of each study area has an effect on the results of these calculations and should be standardized (Figure 1.3). By creating uniform plot sizes, some of that bias is removed.

Inventory of UGI often only includes official implementation of UGI through municipal, state, federal, or non-profit programs, ignoring grassroots efforts to green cities on the individual level[42]. These GI inventories, by not accounting for individual UGI implementation, do not include a source of UGI that is closely linked with both racial and wealth divides and thus, social vulnerability[6, 8, 13]. This study aims to close this knowledge gap by utilizing high-resolution landcover data in selected urban centers to calculate class-based landcover connectivity for sample plots within each

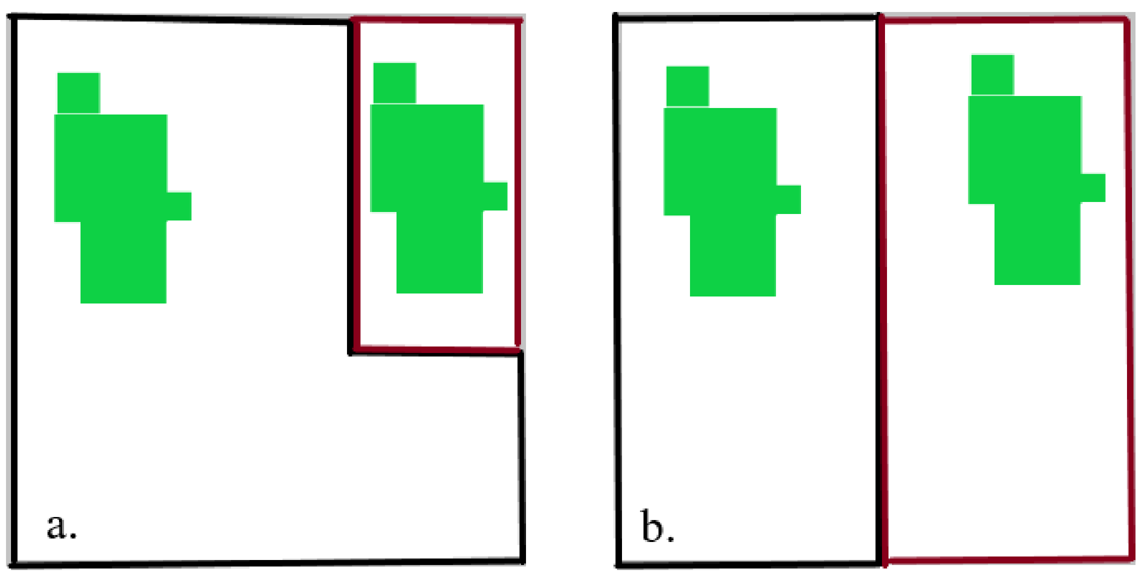

Figure 1.3: A demonstration of the importance of uniform plot area when calculating areal percentage of landcover. Both figures have two uniform patches of landcover. In Figure a., the black plot is significantly larger than the red plot, and in Figure b., the plots are equal in size. The percentage of landcover for the class in the Figure a. is much higher in the red plot than the black plot. In Figure b., they are equal. This becomes especially problematic when considering census tracts as the plot boundaries. These boundaries are generally calculated to contain areas of relatively equal populations. Thus, more densely populated tracts will be smaller in area and more easiliy influenced by subtle changes in landcover area and shape than tracts with a lower population density.

city. By utilizing high-resolution satellite imagery, any application of UGI can be detected, including those not logged by city-wide databases, and connectivity metrics of urban forests can be accurately assessed. As studies continue to reveal the impacts of climate change on urban centers, the question that must be answered is one of the equability of resource distribution: Is UGI located and configured equally when considering social vulnerability? Previous critiques of the literature surrounding EJ claim that there is a lack of quality empirical studies demonstrating that vulnerable populations are disproportionately exposed to environmental hazards[9]. This research aims to add to the body of EJ empirical studies by providing a quantitative analysis that evaluates the connectivity of UGI in selected US urban case studies and statistically compares these attributes with regional social vulnerability. Considering the history of environmental injustice in the US and the lack of emphasis on connectivity of UGI in US policy, the hypotheses of this study are as follows:

- **H1:** Discrepancies will exist in the areal coverage and connectivity of UGI between areas with a higher proportion of vulnerable residents and areas with a lower proportion of vulnerable residents.

- **H2:** Sample plots with lower percentages of residents considered vulnerable will have higher areal coverage and connectivity of UGI than plots with higher percentages of residents considered vulnerable.

This thesis aims to explore these hypotheses through four case studies selected from US cities[1]. These case studies were chosen for their unique qualities pertaining to

[1] The structure of this dissertation will include this introduction, a basic methodology, four separate case studies, and a chapter summarizing the conclusions of this study and recommending future work. Each chapter will include its own set of references. The numeric citations within each chapter will match the references of that chapter, and works that are cited by multiple chapters will be repeated in each reference section, often under a different number than in previous chapters.

politics, climate, history, and size, to determine if the methodology put forth in this study can be applicable in a variety of circumstances. The purpose of this thesis is not to definitively decide whether each city is neglecting vulnerable communities and perpetuating EJ predicaments. Instead, it serves as both a contribution to this enquiry, providing another lens through with we can view EJ in urban ecosystems, and as a starting point from which we can begin to explore the interactions between landscape connectivity, landcover type, and urban ecosystems as an EJ issue.

References

[1] Communication from the Commission to the European Parliament, the Council, the Economic and Social Committee and the Committee of the Regions. Technical Report COM(2020) 380, European Commission, Brussels, Belgium, May 2020.

[2] Hashem Akbari, Dan M. Kurn, Sarah E. Bretz, and James W. Hanford. Peak power and cooling energy savings of shade trees. *Energy and Buildings*, 25(2): 139–148, January 1997. ISSN 03787788. doi: 10.1016/S0378-7788(96)01003-1. URL https://linkinghub.elsevier.com/retrieve/pii/S0378778896010031.

[3] Kathryn Freeman Anderson and Joseph Galaskiewicz. Racial/Ethnic Residential Segregation, Socioeconomic Inequality, and Job Accessibility by Public Transportation Networks in the United States. *Spatial Demography*, 9(3):341–373, October 2021. ISSN 2364-2289, 2164-7070. doi: 10.1007/s40980-021-00093-8. URL https://link.springer.com/10.1007/s40980-021-00093-8.

[4] Spencer Banzhaf, Lala Ma, and Christopher Timmins. Environmental Justice: The Economics of Race, Place, and Pollution. *Journal of Economic Perspectives*, 33(1):185–208, February 2019. ISSN 0895-3309. doi: 10.1257/jep.33.1.185. URL https://pubs.aeaweb.org/doi/10.1257/jep.33.1.185.

[5] Vicki Been. Analyzing Evidence of Environmental Justice. *Journal of Land Use and Environmental Law*, 11, 2018. Publisher: HeinOnline.

[6] Bridget K. Behe. Comparison of Gardening Activities and Purchases of Homeowners and Renters. *Journal of Environmental Horticulture*, 24(4):217–220, De-

cember 2006. ISSN 0738-2898, 2573-5586. doi: 10.24266/0738-2898-24.4.217. URL http://meridian.allenpress.com/jeh/article/24/4/217/79663/Comparison-of-Gardening-Activities-and-Purchases.

[7] Jeannine Bell. *Hate thy neighbor: move-in violence and the persistence of racial segregation in American housing*. New York Univ. Press, New York, 2013. ISBN 978-0-8147-9144-8.

[8] Courtney Bir. Personal Gardens: Who is growing their own in the U.S.? page 7.

[9] William M. Bowen and Michael V. Wells. The Politics and Reality of Environmental Justice: A History and Considerations for Public Administrators and Policy Makers. *Public Administration Review*, 62(6):688–698, 2002. ISSN 00333352, 15406210. URL http://www.jstor.org/stable/3110327. Publisher: [American Society for Public Administration, Wiley].

[10] Robert D Bullard. The Legacy of American Apartheid and Environmental Racism. *Journal of Civil Rights and Economic Development*, 9(2):31, 1994.

[11] Jayajit Chakraborty, Timothy W. Collins, Sara E. Grineski, and Jacob J. Aun. Air pollution exposure disparities in US public housing developments. *Scientific Reports*, 12(1):9887, June 2022. ISSN 2045-2322. doi: 10.1038/s41598-022-13942-3. URL https://www.nature.com/articles/s41598-022-13942-3.

[12] Beth Anne Currie and Brad Bass. Estimates of air pollution mitigation with green plants and green roofs using the UFORE model. *Urban Ecosyst*, page 14, 2008.

[13] Jennifer H. Dennis and Bridget K. Behe. Evaluating the Role of Ethnicity on Gardening Purchases and Satisfaction. *HortScience*, 42(2):262–266, April 2007.

ISSN 0018-5345, 2327-9834. doi: 10.21273/HORTSCI.42.2.262. URL https://journals.ashs.org/view/journals/hortsci/42/2/article-p262.xml.

[14] David Dodman. URBAN DENSITY AND CLIMATE CHANGE. Technical report, United Nations Population Fund, April 2009.

[15] David Peter Dolowitz, Sarah Bell, and Melissa Keeley. Retrofitting urban drainage infrastructure: green or grey? *Urban Water Journal*, 15(1):83–91, January 2018. ISSN 1573-062X, 1744-9006. doi: 10.1080/1573062X.2017.1396352. URL https://www.tandfonline.com/doi/full/10.1080/1573062X.2017.1396352.

[16] Monika Egerer, Nakisha Fouch, Elsa C. Anderson, and Mysha Clarke. Socio-ecological connectivity differs in magnitude and direction across urban landscapes. *Scientific Reports*, 10(1):4252, December 2020. ISSN 2045-2322. doi: 10.1038/s41598-020-61230-9. URL http://www.nature.com/articles/s41598-020-61230-9.

[17] Francisco J. Escobedo and David J. Nowak. Spatial heterogeneity and air pollution removal by an urban forest. *Landscape and Urban Planning*, 90(3-4):102–110, April 2009. ISSN 01692046. doi: 10.1016/j.landurbplan.2008.10.021. URL https://linkinghub.elsevier.com/retrieve/pii/S0169204608001801.

[18] Christopher B. Field, Vicente R. Barros, and Intergovernmental Panel on Climate Change, editors. *Climate change 2014: impacts, adaptation, and vulnerability: Working Group II contribution to the fifth assessment report of the Intergovernmental Panel on Climate Change*. Cambridge University Press, New York, NY, 2014. ISBN 978-1-107-64165-5 978-1-107-05807-1 978-1-107-68386-0 978-1-107-05816-3. OCLC: ocn900613741.

[19] Josh Foster, Ashley Lowe, and Steve Winkelman. The Value of Green Infrastructure for Urban Climate Adaptation. Technical report, The Center for Clean Air Policy, February 2011.

[20] Glynis Daniels and Samantha Friedman. Spatial inequality and the distribution of industrial toxic releases: Evidence from the 1990 TR. *Social Science Quarterly (University of Texas Press)*, 80(2):224, June 1999.

[21] Mark A. Goddard, Andrew J. Dougill, and Tim G. Benton. Scaling up from gardens: biodiversity conservation in urban environments. *Trends in Ecology & Evolution*, 25(2):90–98, February 2010. ISSN 01695347. doi: 10.1016/j.tree.2009.07.016. URL https://linkinghub.elsevier.com/retrieve/pii/S0169534709002468.

[22] Heather E. Golden and Nahal Hoghooghi. Green infrastructure and its catchment-scale effects: an emerging science:. *Wiley Interdisciplinary Reviews: Water*, 5(1):e1254, January 2018. ISSN 20491948. doi: 10.1002/wat2.1254. URL http://doi.wiley.com/10.1002/wat2.1254.

[23] Susan Hanson, Robert Nicholls, N. Ranger, S. Hallegatte, J. Corfee-Morlot, C. Herweijer, and J. Chateau. A global ranking of port cities with high exposure to climate extremes. *Climatic Change*, 104(1):89–111, January 2011. ISSN 0165-0009, 1573-1480. doi: 10.1007/s10584-010-9977-4. URL http://link.springer.com/10.1007/s10584-010-9977-4.

[24] Kilian Heilmann. Transit access and neighborhood segregation. Evidence from the Dallas light rail system. *Regional Science and Urban Economics*, 73:237–250, November 2018. ISSN 01660462. doi: 10.1016/j.regsciurbeco.2018.10.007. URL https://linkinghub.elsevier.com/retrieve/pii/S0166046218301066.

[25] Amy E. Hillier. Redlining and the Home Owners' Loan Corporation. *Journal of Urban History*, 29(4):394–420, May 2003. ISSN 0096-1442, 1552-6771. doi: 10.1177/0096144203029004002. URL http://journals.sagepub.com/doi/10.1177/0096144203029004002.

[26] Paul A. Jargowsky and Christopher A. Wheeler. Economic Segregation in US Metropolitan Areas, 1970-2010. *SSRN Electronic Journal*, 2017. ISSN 1556-5068. doi: 10.2139/ssrn.3454612. URL https://www.ssrn.com/abstract=3454612.

[27] June Purcell Guild. *Black Laws of Virginia: A Summary of the Legislative Acts of Virginia concerning Negroes from Earliest Times to the Present*. Negro Universities Press, New York, NY, 1969.

[28] Amani Kafeety, Sarah B. Henderson, Amy Lubik, Jesse Kancir, Tom Kosatsky, and Michael Schwandt. Social connection as a public health adaptation to extreme heat events. *Canadian Journal of Public Health = Revue Canadienne De Sante Publique*, 111(6):876–879, December 2020. ISSN 1920-7476. doi: 10.17269/s41997-020-00309-2.

[29] Hyun Woo Kim and Yunmi Park. Urban green infrastructure and local flooding: The impact of landscape patterns on peak runoff in four Texas MSAs. *Applied Geography*, 77:72–81, December 2016. ISSN 0143-6228. doi: 10.1016/j.apgeog.2016.10.008. URL https://www.sciencedirect.com/science/article/pii/S0143622816306117.

[30] Weifeng Li, Yang Bai, Qiuwen Chen, Kate He, Xiaohua Ji, and Chunmeng Han. Discrepant impacts of land use and land cover on urban heat islands: A case study of Shanghai, China. *Ecological Indicators*, 47:171–178, December 2014.

ISSN 1470-160X. doi: 10.1016/j.ecolind.2014.08.015. URL https://www.sciencedirect.com/science/article/pii/S1470160X14003707.

[31] Zhimin Liu, Chunliang Xiu, and Chao Ye. Improving Urban Resilience through Green Infrastructure: An Integrated Approach for Connectivity Conservation in the Central City of Shenyang, China. *Complexity*, 2020:1–15, July 2020. ISSN 1076-2787, 1099-0526. doi: 10.1155/2020/1653493. URL https://www.hindawi.com/journals/complexity/2020/1653493/.

[32] Eileen Maura MacGurty. *Transforming environmentalism: Warren county, PCBS, and the origins of environmental justice*. Rutgers Univ. Press, New Brunswick, NJ, 1. paperback printing edition, 2009. ISBN 978-0-8135-4678-0 978-0-8135-3966-9.

[33] Kevin McGarigal and Barbara J. Marks. FRAGSTATS: spatial pattern analysis program for quantifying landscape structure. Technical Report PNW-GTR-351, U.S. Department of Agriculture, Forest Service, Pacific Northwest Research Station, Portland, OR, 1995. URL https://www.fs.usda.gov/treesearch/pubs/3064.

[34] Daniel P. McMillen. Employment Densities, Spatial Autocorrelation, and Subcenters in Large Metropolitan Areas. *Journal of Regional Science*, 44(2):225–244, May 2004. ISSN 0022-4146, 1467-9787. doi: 10.1111/j.0022-4146.2004.00335.x. URL https://onlinelibrary.wiley.com/doi/10.1111/j.0022-4146.2004.00335.x.

[35] Martin V. Melosi. *The sanitary city: urban infrastructure in America from colonial times to the present*. Creating the North American landscape. Johns Hopkins University Press, Baltimore, 2000. ISBN 978-0-8018-6152-9.

[36] William B Meyer. *Environmental Advantages of Cities: Countering Commonsense Antiurbanism.* MIT, Cambridge, 2014. ISBN 978-0-262-31409-1. URL http://public.eblib.com/choice/publicfullrecord.aspx?p=3339592. OCLC: 1058460376.

[37] Paul Mohai, David Pellow, and J. Timmons Roberts. Environmental Justice. *Annual Review of Environment and Resources*, 34(1):405–430, November 2009. ISSN 1543-5938, 1545-2050. doi: 10.1146/annurev-environ-082508-094348. URL https://www.annualreviews.org/doi/10.1146/annurev-environ-082508-094348.

[38] Chad Montrie. *A people's history of environmentalism in the United States.* Continuum, London ; New York, 2011. ISBN 978-1-4411-1672-7 978-1-4411-9868-6. OCLC: ocn694396591.

[39] Robert K. Nelson and Edward L. Ayers, editors. *Not Even Past: Social Vulnerability and the Legacy of Redlining.* American Panorama. The Digital Scholarship Lab and the National Community Reinvestment Coalition. URL https://dsl.richmond.edu/socialvulnerability.

[40] Peter Newman and Jeffrey R. Kenworthy. *Cities and automobile dependence: a sourcebook.* Gower Technical, Aldershot, Hants., England ; Brookfield, Vt., USA, 1989. ISBN 978-0-566-07040-2.

[41] Md. Nuruzzaman. Urban Heat Island: Causes, Effects and Mitigation Measures - A Review. *International Journal of Environmental Monitoring and Analysis*, 3 (2):67, 2015. ISSN 2328-7659. doi: 10.11648/j.ijema.20150302.15.

[42] NYC DEP. DEP Green Infrastructure, June 2021. URL https://data.cityofnewyork.us/Environment/DEP-Green-Infrastructure/spjh-pz7h.

[43] Manuel Pastor, Jim Sadd, and John Hipp. Which Came First? Toxic Facilities, Minority Move-In, and Environmental Justice. *Journal of Urban Affairs*, 23(1): 1–21, March 2001. ISSN 0735-2166, 1467-9906. doi: 10.1111/0735-2166.00072. URL https://www.tandfonline.com/doi/full/10.1111/0735-2166.00072.

[44] Jin-Da Qi, Bao-Jie He, Mo Wang, Jin Zhu, and Wei-Cong Fu. Do grey infrastructures always elevate urban temperature? No, utilizing grey infrastructures to mitigate urban heat island effects. *Sustainable Cities and Society*, 46: 101392, April 2019. ISSN 22106707. doi: 10.1016/j.scs.2018.12.020. URL https://linkinghub.elsevier.com/retrieve/pii/S221067071831686X.

[45] Wenqi Qian and Xiaoyu Li. A cold island connectivity and network perspective to mitigate the urban heat island effect. *Sustainable Cities and Society*, 94: 104525, July 2023. ISSN 22106707. doi: 10.1016/j.scs.2023.104525. URL https://linkinghub.elsevier.com/retrieve/pii/S2210670723001361.

[46] Robert J Rydman, Dino P Rumoro, Julio C Silva, Teresita M Hogan, and Linda M Kampe. The Rate and Risk of Heat-Related Illness in Hospital Emergency Departments During the 1995 Chicago Heat Disaster. page 16, 1999.

[47] M. Santamouris. Recent progress on urban overheating and heat island research. Integrated assessment of the energy, environmental, vulnerability and health impact. Synergies with the global climate change. *Energy and Buildings*, 207: 109482, January 2020. ISSN 03787788. doi: 10.1016/j.enbuild.2019.109482. URL https://linkinghub.elsevier.com/retrieve/pii/S0378778819326696.

[48] Thomas C. Schelling. Models of Segregation. *The American Economic Review*, 59(2):488–493, 1969. ISSN 00028282. URL http://www.jstor.org/stable/1823701. Publisher: American Economic Association.

[49] Leah H. Schinasi, Tarik Benmarhnia, and Anneclaire J. De Roos. Modification of the association between high ambient temperature and health by urban microclimate indicators: A systematic review and meta-analysis. *Environmental Research*, 161:168–180, February 2018. ISSN 00139351. doi: 10.1016/j.envres.2017.11.004. URL https://linkinghub.elsevier.com/retrieve/pii/S001393511731678X.

[50] David Schlosberg. *Defining environmental justice: theories, movements, and nature*. Oxford University Press, Oxford, 1. publ. in paperback edition, 2009. ISBN 978-0-19-928629-4 978-0-19-956248-0.

[51] Izhak Schnell, Ahmed Abu Baker Diab, and Itzhak Benenson. A global index for measuring socio-spatial segregation versus integration. *Applied Geography*, 58: 179–188, March 2015. ISSN 01436228. doi: 10.1016/j.apgeog.2015.01.008. URL https://linkinghub.elsevier.com/retrieve/pii/S0143622815000193.

[52] William R. Selbig. Hydraulic, water-quality, and temperature performance of three types of permeable pavement under high sediment loading conditions. Scientific Investigations Report, 2018. Series: Scientific Investigations Report.

[53] Sarah Jane Shoenfeld and Mara Cherkasky. "A Strictly White Residential Section". page 19, 2021.

[54] Ranhao Sun, Wei Xie, and Liding Chen. A landscape connectivity model to quantify contributions of heat sources and sinks in urban regions. *Landscape and Urban Planning*, 178:43–50, October 2018. ISSN 01692046. doi: 10.1016/j.landurbplan.2018.05.015. URL https://linkinghub.elsevier.com/retrieve/pii/S0169204618303591.

[55] Dorceta E. Taylor. *Toxic communities: environmental racism, industrial pollution, and residential mobility*. New York University Press, New York, 2014. ISBN 978-1-4798-0515-0. OCLC: 879551064.

[56] United Nations, Department of Economic and Social Affairs, and Population Division. *World urbanization prospects: the 2018 revision*. 2019. ISBN 978-92-1-148319-2. OCLC: 1120698127.

[57] United States EPA. Report to Congress on Impacts and Control of Combined Sewer Overflows and Sanitary Sewer Overflows. Technical Report EPA 833-R-04-001, August 2004.

[58] US Environmental Protection Agency. Green Infrastructure Strategic Agenda 2013, 2013.

[59] U.S.C. NAVIGATION AND NAVIGABLE WATERS, January 2019.

[60] Darren Waters, W Edgar Watt, and Jiri Marsalek. Adaptation of a Storm Drainage System to Accommodate Increased Rainfall Resulting from Climate Change. page 18.

[61] Patrick Willems. Impacts of Climate Change on Rainfall Extremes and Urban Drainage Systems. *Water Intelligence Online*, 11, August 2012. ISSN 14761777. doi: 10.2166/9781780401263. URL https://iwaponline.com/ebooks/book/631/.

[62] Charles E. Wynes. The Evolution of Jim Crow Laws in Twentieth Century Virginia. *Phylon (1960-)*, 28(4):416, 1967. ISSN 00318906. doi: 10.2307/274293. URL https://www.jstor.org/stable/274293?origin=crossref.

[63] Liwei Xiong, Shenxin Li, Bin Zou, Fen Peng, Xin Fang, and Yun Xue. Long Time-Series Urban Heat Island Monitoring and Driving Factors Analysis Using Remote Sensing and Geodetector. *Frontiers in Environmental Science*, 9, 2022. ISSN 2296-665X. doi: 10.3389/fenvs.2021.828230. URL https://www.frontiersin.org/articles/10.3389/fenvs.2021.828230.

[64] Yu Zhang, Yuchen Wang, Nan Ding, and Xiaoyan Yang. Spatial Pattern Impact of Impervious Surface Density on Urban Heat Island Effect: A Case Study in Xuzhou, China. *Land*, 11(12):2135, November 2022. ISSN 2073-445X. doi: 10.3390/land11122135. URL https://www.mdpi.com/2073-445X/11/12/2135.

Chapter 2

Methods Overview

2.1 Basic Methodology

Within each case study, a number, n, of study locations were selected over each study area. This number differed between case studies, and was reliant on the area of the study zone, and how many points could be used without the surrounding sample areas overlapping. For each set of random sample points (generated using the ArcGIS Pro *Generate Random Points* Tool[6], and a minimum required inter-point distance of 0.5 km), a circular buffer with a radius of 0.2 km was added around the point to create a sample plot. The radius of 0.2km was chosen as this is roughly the maximum size of a city block in many North American cities[2]. These plots were filtered to include the following criteria, with other plots being discarded:

1. Majority of plot was within areas zoned as single family residential
2. Majority of plot was not classified as water
3. Plot has a population of at least one resident according to the 2020 US Census
4. Plot has at least one dwelling according to the 2020 US Census.
5. Plot is not within a census tract that contains a prison or other forced residential situation.

Criterion 1 was deemed necessary in order to standardize the comparison between plots. Differently zoned areas will have different characteristics based on what is required by those zones. As an example, in the District of Columbia Municipal Regulations Zoning Handbook, areas zoned *Residential Apartment* required a minimum Green Area Ratio[1] of either 0.4 for low to moderate density zoned lots or 0.3 for lots zoned for medium to high density residential apartments). However, areas zoned as *Mixed Use* require a minimum Green Area Ratio of 0.2 to 0.3 (again, depending on the specific zone characteristics). Areas zoned *Single Family Residential* have no minimum Green Area Ratio, and instead include protections for trees that are not used in the former two zoning requirements[5]. Thus, by selecting only areas zoned as *Single Family Residential*, the legal baseline requirements are roughly the same for all the plots observed.

This study is focused solely on UGI, and thus, plots with a majority of water were not included in this study (Criterion 2). This is not to say that water does not also serve an important role in mitigating the effects of climate change in urban areas — in fact, water bodies have been shown to have the potential to mitigate UHI and also provide similar co-benefits to UGI[28]. However, although water bodies can lower daytime temperatures through evaporative cooling, larger water bodies have a large heat capacity and can continue to emit heat during the night, leading to diminishing returns in regards to the ability to mitigate UHI[11, 26]. Additionally, the spirit of this dissertation is to identify disparities in climate change mitigating resources as a means to invoke positive change. For most municipalities, implementing UGI through tree planting and impervious surface conversion is a much more practical and cost-effective way of improving the climate resiliency of urban communities than

[1] Ratio of the weighted value of landscape elements to lot area[5].

constructing new water bodies. As such, identifying disparities in presence of water bodies between vulnerable and non-vulnerable residents does not provide a realistic path towards change.

Criteria 3 and 4 were added simply because, without housing or people living in the plot, there were no vulnerable residents and therefore, no SVIs.

Finally, plots that contained prisons or other group quarters were disregarded because these residents neither have a choice in where they reside, nor the freedom or influence to enact change in the coverage or connectivity of UGI in their neighborhood. The issue of climate change and how it will impact residents of prisons and other group quarters is an EJ problem that merits further research, but one that this dissertation will not be addressing.

With consideration that each case study is unique and exhibits unique characteristics, site-specific criteria were sometimes included to filter the sample plots further. More details on these criteria and methods are provided in the ”Detailed Methodology” section of each chapter.

Using census tract level SVI data derived from United States Census data and prepared by the United States Center for Disease Control alongside census block level population and housing data, the percentage of the population within each plot impacted by selected SVIs detailed in Table 2.2 was calculated through polygon apportionment (Using the ArcGIS Pro *Apportion Polygon* Tool[6]). This was done using weighted points, which were centroids containing population and number of households for each DC census block. The number of residents that qualified as vulnerable were apportioned to each plot, along with the total population and the total number of households. The following variables:

- Below Poverty
- Unemployed
- No HS Diploma
- Uninsured
- Age 65+
- Age 17-
- Disability
- Limited English
- Racial Minority

were apportioned using the population field as the weight field.

The variables:

- Housing Burden
- Single-parent Household
- Household Crowding

were apportioned using the Number of Households field as the Weight field. These apportioned numbers were then used to calculate the percentage of residents within each plot that were vulnerable.

6 class-level landscape metrics (LSMs) were calculated for each plot with the R *landscapemetrics* package (Table 2.1). These LSMs were chosen due to their availability in the literature in regards to either flooding or heat mitigation. Two different types of metrics were chosen: Area/Edge metrics (PLAND and LPI, metrics pertaining to aerial coverage of landcover), and Agglomeration metrics (LSI, ENN_MN, PLADJ, and Cohesion — metrics that measure the extent to which each patch is connected to other nearby patches).

PLAND is a commonly used metric in the literature surrounding ecosystem connectivity in urban areas[15], and is simply a measure of the percentage of the study area that is a certain class[17]. LPI is similar in this regard, but instead measures the percentage of the study area that is comprised of the largest patch of a certain class, characterizing patch dominance[17, 7]. LSI in particular was chosen as a hybrid connectivity metric that also incorporates patch complexity into the consideration of agglomeration by taking the ratio of the actual edge length of class to hypothetical edge length of the simplest configuration of the landscape[17, 14]. ENN_MN is the mean Euclidean distance in meters to the nearest cell of an identical class, and measures the proximity of cells of the same class to one another as a proxy for agglomeration that has been used to quantify patch isolation[17, 22]. PLADJ is used as a measurement of the likelihood that the class of a cell is identical to its neighboring cells[17]. Cohesion represents the physical aggregation of cells of a class in a study area, incorporation perimeter, area, and number of patches[17]. As PLAND and LPI increase in a class, the areal coverage of that class increases. As PLADJ and Cohesion increase in a class, that class becomes more aggregated, and as ENN_MN increases, the class becomes more isolated. LSI functions slightly differently, starting at a value of 1 when only one squared patch exists and then increasing as the class becomes less compact. This metric shows a more complicated relationship with UHI, yet most studies indicate that complex UGI landscapes have a negative impact on the cooling properties of the UGI[30, 29, 15], and increasing LSI of impermeable surfaces has a positive effect on UHI[25].

The LSMs and SVIs were then examined using IBM SPSS Principal Component Analysis (PCA) as a form of exploratory dimension reduction[12]. PCA was chosen as a means to explore relationships between these variables because many of the SVI and

LSM variables exhibit relationships, such as LPI increasing as PLAND increases. By using PCA, the variance in the data caused by these relationships can be reduced to a component, exposing other relationships that may not be present otherwise. For each application of PCA, a Varimax rotation was used because this rotation tends to highlight a small number of important variables, simplifying the interpretation of results[4]. If the correlation matrix returned as non-positive definite on the first attempt at PCA, variables were removed from the PCA systematically, beginning with those that appeared to lack data (i.e. LSMs for landcover types not present in the study area), followed by variables that would likely have linear dependencies[1]. Following a successful PCA without a non-positive definite correlation matrix, variables that cross-loaded onto the same component were flagged to explore further. Using flagged SVI variables to separate plots into two groups by level of vulnerability, differences in the mean rank of flagged LSMs between these plot groups were then examined for significance utilizing SPSS software[12]. As the distributions of the data were rarely normal, relationships were examined using the Mann-Whitney U-Test[16].

2.2 Data

2.2.1 Landcover Classification

When available, the most recent 1m landcover classification rasters from each city's Open-Data depository are used (Appendix A.2). In the case of Detroit, MI where 1m landcover classification does not already exist, 3m multi-spectral PlanetScope satellite imagery from Planet Labs is employed alongside C-Cap High Resolution water[21], canopy[19], and impervious surface[20] cover data to classify landcover using a modified NLCD 2011 schema.

2.2.2 Social Vulnerability

For each US city, SVI data were taken from the Center for Disease Control's Social Vulnerability Index dataset[3]. These data are compiled from several social factors derived from American Community Survey data at the Census tract level deemed critical to societal vulnerability to disease and disaster[9]. Twelve of these indicators deemed relevant to this study due to their ubiquitous application to all case studies were utilized (Table 2.2).

Table 2.1: **Landscape Metrics (LSMs) used for this dissertation.** Metrics were calculated at the class level.

Metric	Formula
Percentage of Land Area (PLAND)[17]	$$PLAND = \frac{\sum_{j=1}^{n} a_{ij}}{A} * 100 \quad (2.19)$$ where a_{ij} is the area of each patch and A is the total landscape area.
Largest Patch Index (LPI)[17]	$$LPI = \frac{\max_{j=1}^{n}(a_{ij})}{A} * 100 \quad (2.20)$$ where $max_{(}a_{ij})$ is the area of the patch in square meters and A is the total landscape area in square meters.
Landscape Shape Index (LSI)[17, 13]	$$LSI = \frac{e_i}{\min e_i} \quad (2.21)$$ where e_i is the total edge length in cell surfaces and $\min_(e_i)$ the minimum total edge length in cell surfaces.
Euclidean Nearest Neighbour Mean (ENN_MN)[17, 18]	$$ENN_{MN} = mean(ENN[patch_{ij}]) \quad (2.22)$$ where $ENN[patch_{ij}]$ is the euclidean nearest-neighbor distance of each patch.
Cohesion Index (Cohesion)[17, 24]	$$Cohesion = 1 - \left(\frac{\sum_{j=1}^{n} p_{ij}}{\sum_{j=1}^{n} p_{ij}\sqrt{a_{ij}}}\right) * \left(1 - \frac{1}{\sqrt{Z}}\right)^{-1} * 100 \quad (2.23)$$ where p_{ij} is the perimeter in meters, a_{ij} is the area in square meters and Z is the number of cells.
Percentage of Like Adjacencies (PLADJ)[17]	$$PLADJ = \left(\frac{g_{ij}}{\sum_{k=1}^{m} g_{ik}}\right) * 100 \quad (2.24)$$ where g_{ij} is the number of adjacencies between cells of class i and g_{ik} is the number of adjacencies between cells of class i and k.

Table 2.2: **Social Vulnerability Indicators (SVI) used for this dissertation.** Indicators were calculated using US Census Data[9].

Indicator	Description
Below poverty %	Percentage of persons with household income below 150% of the federal poverty level
Unemployed %	Unemployment Rate Estimate
No HS diploma %	Percentage of persons age 25+ with no high school diploma
Uninsured %	Percentage of persons in the total civilian non-institutionalized population without health insurance[a]
Age 65+ %	Percentage of persons over the age of 65
Age 17- %	Percentage of persons below the age of 17
Disability %	Percentage civilian non-institutionalized population with a disability[a]
Limited English %	Percentage of persons age 5+ who speak English "less than well"
Racial minority %	Percentage of persons who are non-white and/or ethnically Hispanic or Latino
Housing burden %	Percentage of housing units with an annual income of less than $75,000 and with 30+% of income spent on housing costs[a]
Single-parent household %	Percentage of single-parent households
Household crowding %	Percentage of households with more people than rooms

[a] For Phoenix, where 2010 data was used, this variable was unavailable[8].

2.3 Case Studies

For this dissertation, 4 case studies were chosen. Each case study is predicted to experience challenges associated with climate change that could be mitigated by UGI, and each location has characteristics that makes the location unique (Figure 2.1):

- Washington, DC - A city with a unique political mechanism for UGI implementation
- Phoenix, AZ - A city in a desert environment
- Detroit, MI/Oakland County, MI - A region with a history of environmental injustices associated with economic collapse and racially-driven migration
- New York, NY - A city with a large population

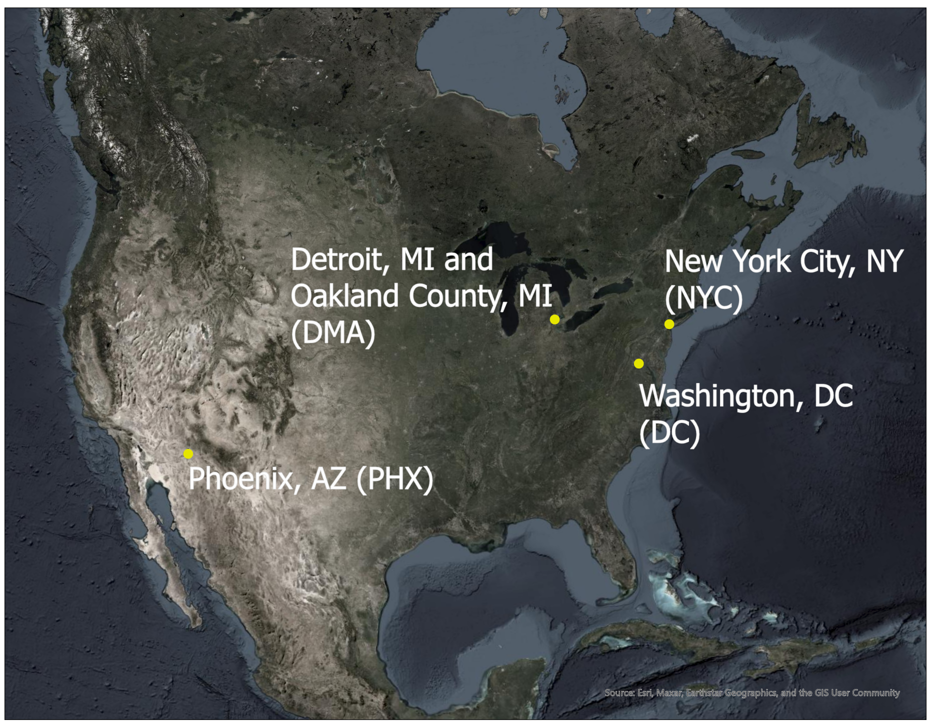

Figure 2.1: Locations of the case studies chosen for this dissertation.

Although this collection of cities does not encompass the entirety of political, geographic, or economic possibilities that may occur worldwide, it does provide a swath of differing examples to observe.

The next four chapters of this dissertation will follow a similar structure in an attempt to explore each case study fully. Each chapter will be dedicated to a single city, and begin with a brief introduction as to why the city was chosen for this study. Following this introduction, a section will be devoted to the physical aspects of the case study, including characteristics of its geographic location, such as topography and political boundaries, as well as information pertaining to its climate. As a subsection, special attention will be paid to how the climate will be impacted by future climate change.

A section of the chapter will also be devoted to a brief look into the socio-demographic landscape of the case study. The purpose of this section is to explore the social variables that will be later examined in this study through a geographic lens, identifying any trends in these variables that might appear across the landscape. It is recognized that many of these variables will exhibit spatial auto-correlation[2] considering that, as mentioned previously in Subsection 1.3.1, even without outside influences like Jim Crow laws or redlining, Schelling's Model predicts that populations with similar characteristics tend to exhibit some degree of voluntary segregation[23]. However, it is the opinion of the author that any degree of spatial auto-correlation, both in SVI variables as well as LSMs, provides evidence of any EJ infractions. This study examines built environments inhabited by populations that have the ability to alter any and all of these variables through a strictly regulated system, and thus, any spatial auto-correlation that exists is a product of this system and its laws, regulations, and policies, fulfilling the definition of EJ outlined in Section 1.3. To better understand these relationships, Moran's i will be calculated for these variables in each case study and provided in Appendix B.2.

The next section of each case study chapter will look at the political background

[2]Spatial Auto-Correlation, as defined by Getis in the Handbook of Applied Spatial Analysis, is *"the relationship between nearby spatial units, as seen on maps, where each unit is coded with a realization of a single variable"*[10]. This relates closely to Tobler's First Law of Geography, which suggests that *"everything is related to everything else, but near things are more related than distant things"*[27].

of each case study. This will include some generalized political analyses of the case study's governing bodies, as well as an historical reflection to provide context to the current state of these institutions. A subsection will be devoted to the case study's past regarding social equity, detailing systemic injustices in both race and income. A different subsection will dive into the current UGI policy of the case study, establishing the political tools and mechanisms that are working to provide UGI to the populace.

As each case study is a different set of systems with different characteristics and parameters, a more detailed methodology will be provided in the fifth section of each case study chapter which will outline the specific process by which the study was conducted. Although the differences in methods between case studies makes cross-study empirical comparisons more difficult, a qualitative comparison is still both possible and useful.

Section six of each case study chapter will provide the results from the analyses in two subsections, one for each stage of the analysis. The final seventh section will address the hypotheses outlined in Section 1.4, and go on to discuss the interpretation of these results and how it relates to the history and policies of the case study.

References

[1] *Structural Modeling by Example: Applications in Educational, Sociological, and Behavioral Research*. Cambridge University Press, Cambridge, 2010. ISBN 978-0-511-60111-8. OCLC: 900190456.

[2] City block, March 2024. URL https://en.wikipedia.org/w/index.php?title=City_block&oldid=1216099850. Page Version ID: 1216099850.

[3] Centers for Disease Control and Prevention/ Agency for Toxic Substances and Disease Registry/ Geospatial Research, Analysis, and Services Program. CDC/ATSDR Social Vulnerability Index, 2010. URL https://www.atsdr.cdc.gov/placeandhealth/svi/data_documentation_download.html.

[4] Stephens D. Hearing rehabilitation in a psychosocial framework. *Scandinavian audiology. Supplementum*, 43, 1996. ISSN 0107-8593. URL https://pubmed.ncbi.nlm.nih.gov/8738645/. Publisher: Scand Audiol Suppl.

[5] DCMR. Zoning Rgulations of 2016, 2016.

[6] ESRI. ArcGIS Pro, 2023.

[7] Rundong Feng, Fuyuan Wang, Kaiyong Wang, Hongjie Wang, and Li Li. Urban ecological land and natural-anthropogenic environment interactively drive surface urban heat island: An urban agglomeration-level study in China. *Environment International*, 157:106857, December 2021. ISSN 0160-4120. doi: 10.1016/j.envint.2021.106857. URL https://www.sciencedirect.com/science/article/pii/S0160412021004827.

[8] Geospatial Research, Analysis, and Services Program. CDC/ATSDR Social Vulnerability Index 2010 Database, Arizona, 2010.

[9] Geospatial Research, Analysis, and Services Program. CDC/ATSDR SVI 2020 Documentation, August 2022. URL https://www.atsdr.cdc.gov/placeandhealth/svi/documentation/pdf/SVI2020Documentation_08.05.22.pdf.

[10] Arthur Getis. Spatial Autocorrelation. In Manfred M. Fischer and Arthur Getis, editors, *Handbook of Applied Spatial Analysis*, pages 255–278. Springer Berlin Heidelberg, Berlin, Heidelberg, 2010. ISBN 978-3-642-03646-0 978-3-642-03647-7. doi: 10.1007/978-3-642-03647-7_14. URL https://link.springer.com/10.1007/978-3-642-03647-7_14.

[11] Patricia Gober, Anthony Brazel, Ray Quay, Soe Myint, Susanne Grossman-Clarke, Adam Miller, and Steve Rossi. Using Watered Landscapes to Manipulate Urban Heat Island Effects: How Much Water Will It Take to Cool Phoenix? *Journal of the American Planning Association*, 76(1):109–121, December 2009. ISSN 0194-4363, 1939-0130. doi: 10.1080/01944360903433113. URL http://www.tandfonline.com/doi/abs/10.1080/01944360903433113.

[12] IBM Corp. IBM SPSS Statistics for Windows, 2021.

[13] J. Bogaert, P. Van Hecke, D. Salvador-Van Eysenrode, and I. Impens. Quantifying Habitat Edge for Nature Reserve Design. *Coenoses*, 13(3):131–136, 1998.

[14] Yuqiu Jia, Lina Tang, Min Xu, and Xinyi Yang. Landscape pattern indices for evaluating urban spatial morphology – A case study of Chinese cities. *Ecological Indicators*, 99:27–37, April 2019. ISSN 1470-160X. doi: 10.1016/j.ecolind.2018.12.007. URL https://www.sciencedirect.com/science/article/pii/S1470160X18309403.

[15] Weifeng Li, Yang Bai, Qiuwen Chen, Kate He, Xiaohua Ji, and Chunmeng Han. Discrepant impacts of land use and land cover on urban heat islands: A case study of Shanghai, China. *Ecological Indicators*, 47:171–178, December 2014. ISSN 1470-160X. doi: 10.1016/j.ecolind.2014.08.015. URL https://www.sciencedirect.com/science/article/pii/S1470160X14003707.

[16] H. B. Mann and D. R. Whitney. On a Test of Whether one of Two Random Variables is Stochastically Larger than the Other. *The Annals of Mathematical Statistics*, 18(1):50–60, March 1947. ISSN 0003-4851. doi: 10.1214/aoms/1177730491. URL http://projecteuclid.org/euclid.aoms/1177730491.

[17] Kevin McGarigal and Barbara J. Marks. FRAGSTATS: spatial pattern analysis program for quantifying landscape structure. Technical Report PNW-GTR-351, U.S. Department of Agriculture, Forest Service, Pacific Northwest Research Station, Portland, OR, 1995. URL https://www.fs.usda.gov/treesearch/pubs/3064.

[18] Kevin McGarigal and William C. McComb. Relationships Between Landscape Structure and Breeding Birds in the Oregon Coast Range. *Ecological Monographs*, 65(3):235–260, August 1995. ISSN 0012-9615, 1557-7015. doi: 10.2307/2937059. URL https://onlinelibrary.wiley.com/doi/10.2307/2937059.

[19] NOAA Office for Coastal Management. 2020 NOAA C-CAP Version 2 Canopy Cover: Michigan, . URL www.coast.noaa.gov/htdata/raster1/landcover/bulkdownload/hires/.

[20] NOAA Office for Coastal Management. 2020 NOAA C-CAP Version 2 Impervious Cover: Michigan, . URL www.coast.noaa.gov/htdata/raster1/landcover/bulkdownload/hires/.

[21] NOAA Office for Coastal Management. 2020 NOAA C-CAP Version 2 Water Cover: Michigan, . URL www.coast.noaa.gov/htdata/raster1/landcover/bulkdownload/hires/.

[22] Jinyoung Rhee, Seonyoung Park, and Zhenyu Lu. Relationship between land cover patterns and surface temperature in urban areas. *GIScience & Remote Sensing*, 51(5):521–536, September 2014. ISSN 1548-1603. doi: 10.1080/15481603.2014.964455. URL https://doi.org/10.1080/15481603.2014.964455. Publisher: Taylor & Francis _eprint: https://doi.org/10.1080/15481603.2014.964455.

[23] Thomas C. Schelling. Models of Segregation. *The American Economic Review*, 59(2):488–493, 1969. ISSN 00028282. URL http://www.jstor.org/stable/1823701. Publisher: American Economic Association.

[24] Nathan H. Schumaker. Using Landscape Indices to Predict Habitat Connectivity. *Ecology*, 77(4):1210–1225, June 1996. ISSN 00129658. doi: 10.2307/2265590. URL http://doi.wiley.com/10.2307/2265590.

[25] Richard R. Shaker, Yaron Altman, Chengbin Deng, Eric Vaz, and K. Wayne Forsythe. Investigating urban heat island through spatial analysis of New York City streetscapes. *Journal of Cleaner Production*, 233:972–992, October 2019. ISSN 0959-6526. doi: 10.1016/j.jclepro.2019.05.389. URL https://www.sciencedirect.com/science/article/pii/S0959652619319328.

[26] G.J. Steeneveld, S. Koopmans, B.G. Heusinkveld, and N.E. Theeuwes. Refreshing the role of open water surfaces on mitigating the maximum urban heat island effect. *Landscape and Urban Planning*, 121:92–96, January 2014.

ISSN 01692046. doi: 10.1016/j.landurbplan.2013.09.001. URL https://linkinghub.elsevier.com/retrieve/pii/S0169204613001801.

[27] W. R. Tobler. A Computer Movie Simulating Urban Growth in the Detroit Region. *Economic Geography*, 46:234, June 1970. ISSN 00130095. doi: 10.2307/143141. URL https://www.jstor.org/stable/143141?origin=crossref.

[28] Zhijie Wu and Yixin Zhang. Water Bodies' Cooling Effects on Urban Land Daytime Surface Temperature: Ecosystem Service Reducing Heat Island Effect. *Sustainability*, 11(3):787, February 2019. ISSN 2071-1050. doi: 10.3390/su11030787. URL http://www.mdpi.com/2071-1050/11/3/787.

[29] Liwei Xiong, Shenxin Li, Bin Zou, Fen Peng, Xin Fang, and Yun Xue. Long Time-Series Urban Heat Island Monitoring and Driving Factors Analysis Using Remote Sensing and Geodetector. *Frontiers in Environmental Science*, 9, 2022. ISSN 2296-665X. doi: 10.3389/fenvs.2021.828230. URL https://www.frontiersin.org/articles/10.3389/fenvs.2021.828230.

[30] Xinping Zhang, Dexiang Wang, Hongke Hao, Fangfang Zhang, and Youning Hu. Effects of Land Use/Cover Changes and Urban Forest Configuration on Urban Heat Islands in a Loess Hilly Region: Case Study Based on Yan'an City, China. *International Journal of Environmental Research and Public Health*, 14(8):840, August 2017. ISSN 1660-4601. doi: 10.3390/ijerph14080840. URL https://www.mdpi.com/1660-4601/14/8/840. Number: 8 Publisher: Multidisciplinary Digital Publishing Institute.

Chapter 3

Washington, DC, USA

Figure 3.1: Aerial view of Washington, DC Mall, taken in 2007.[5]

3.1 Introduction

Washington (Figure 3.1), in The District of Columbia, USA was selected as a case study for its unique political infrastructure, numerous UGI implementation efforts and policies, historical instances of social and environmental injustices, and current policies that aim to address current and future injustices. As the federal Capitol of the US, this city offers a microcosm that reflects the policies and views of its residents, as well as the US at large. The city's propensity to draw residents and employees from both the US national and global professional arenas results in an urban hub with a high level of cultural diversity[12].

3.2 Geography and Climate

Washington, DC (DC) is located in the Mid-Atlantic region of the US, with its 117 km^2 footprint sharing borders with the state of Maryland to the north and the state of Virginia to the south. A smaller tributary to the Potomac, Rock Creek, flows north to south in the center-west portion of the district, emptying into the Potomac. Topographically, DC sits in part on the floodplains of the Anacostia and Potomac rivers[43]. Surrounding DC is a series of elevated ridges, with progressively rising river terraces radiating outward from the central floodplains north of the confluence of the Anacostia and Potomac. DC was established on the Atlantic Seaboard Fall Line[39], a boundary where the harder crystalline rocks of the Piedmont Plateau border the softer sediments of the Atlantic Coastal Plain. This boundary manifests itself to the west of DC as the Great Falls of the Potomac, a series of waterfalls dropping 23 meters in less than 1.6 km[31].

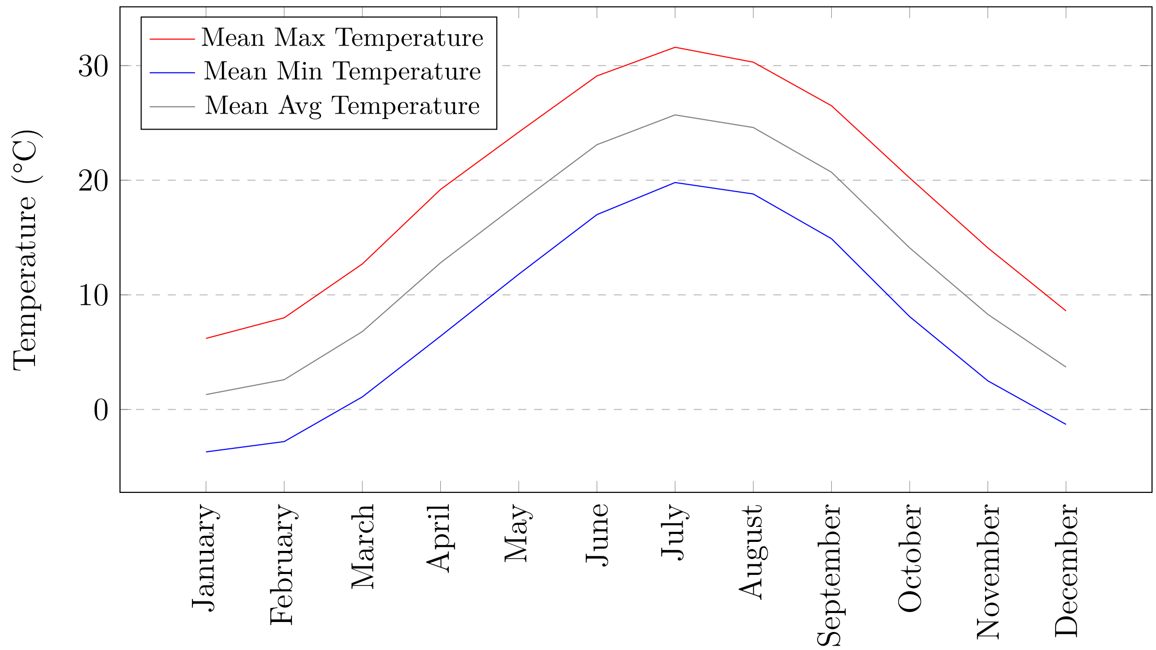

Figure 3.2: Monthly Climate Normal Temperatures for Washington, DC[46].

DC has a humid subtropical climate with a Köppen-Geiger climate classification of Cfa[38]. Summers are typically hot, with an average maximum July temperature of 32°C[1] and an average minimum July temperature of 22.4°C[1] . Winters are mild, with an average minimum January temperature of -1.1°C[1] and an average maximum monthly temperature of 7.1°C[1] (Figure 3.2).

Precipitation does not differ significantly with seasons, with an average total annual precipitation of approximately 106 cm[1] (Figure 3.3).

[1]Based on Monthly Climate Normals from 1991 to 2020[46].

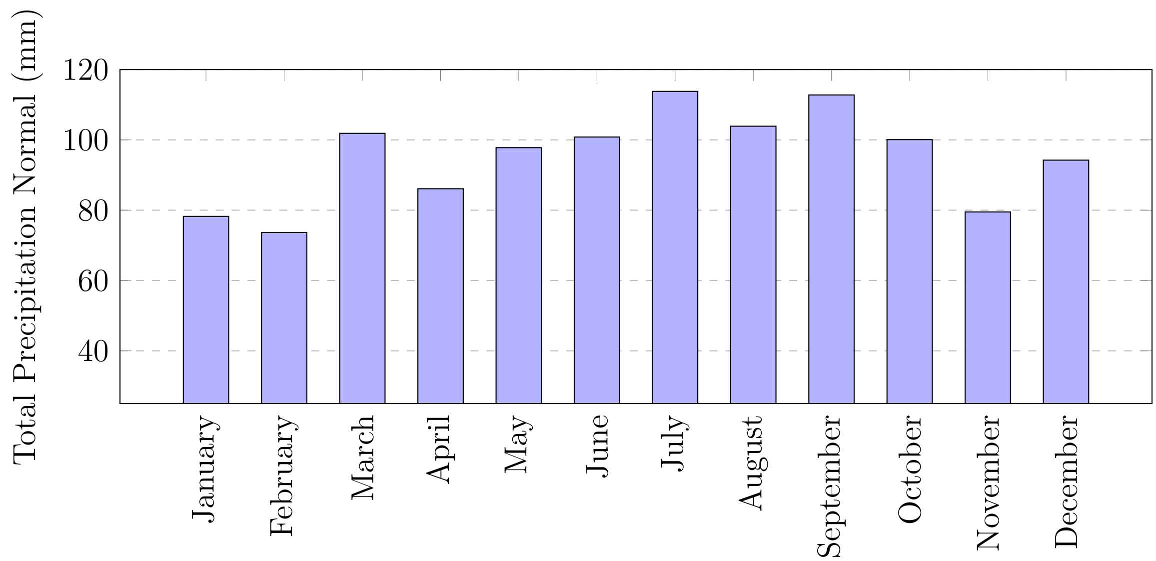

Figure 3.3: Monthly Average Total Precipitation for Washington, DC [46].

In regards to urban sprawl, DC has a lower Density Sprawl Index[2](DSI) at 38.86 for the DC metro statistical area, compared to the US average of 50.60[42]. This Index rose between 1970 and 2000, but has since lowered in 2010, indicating a recent move in population from low density sprawl to higher density inner-city residences, a deviation from the national average, which has continued upward (Figure 3.4).

[2]This *Density Sprawl Index*, introduced by Lopez and Hynes[26], is a comparison of the percentage of a population living in high density residential areas and low density areas. This index ranges from 0-100, with 0 being no sprawl and 100 being total sprawl.

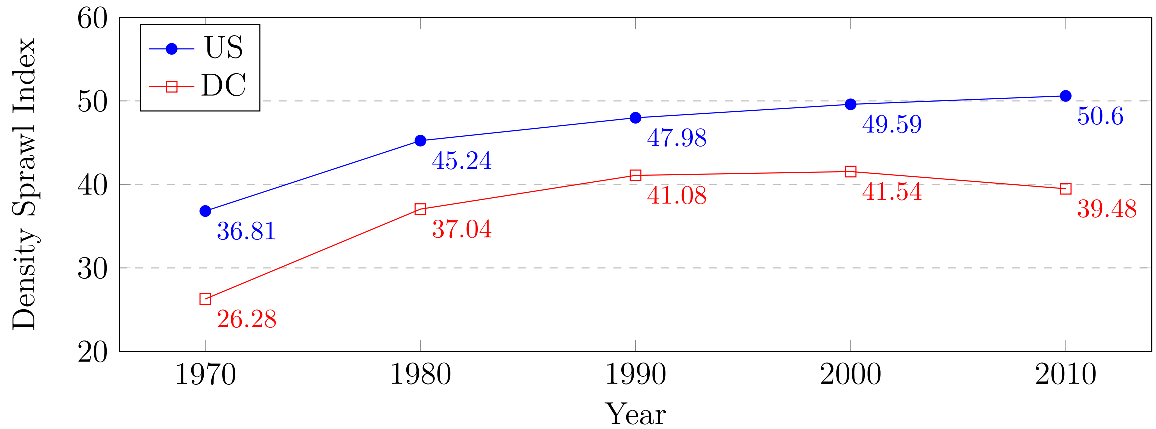

Figure 3.4: Density Sprawl Index for DC, compared with the US Average, from 1970-2010[42].

Based on 2020 landcover classification data (Figure 3.5), the highest percentage of DC's landcover is impervious surfaces, at approximately 40%. However, the next largest percentage is tree canopy, with approximately 34% of the land area (Table 3.1). Much of the impervious surface is located in downtown areas, often zoned as "mixed use" or "Apartment Residential". However, the neighborhoods surrounding the downtown area, where the areas zoned "Single Family Residential" were primarily located, had more of an abundance of tree canopy.

Table 3.1: Calculation of the percentage of landscape for each landcover class for all of Washington, DC.

	PLAND
Tree Canopy	33.71%
Grass/Shrub	15.62%
Impervious	40.31%
Water	10.20%
Barren	0.16%

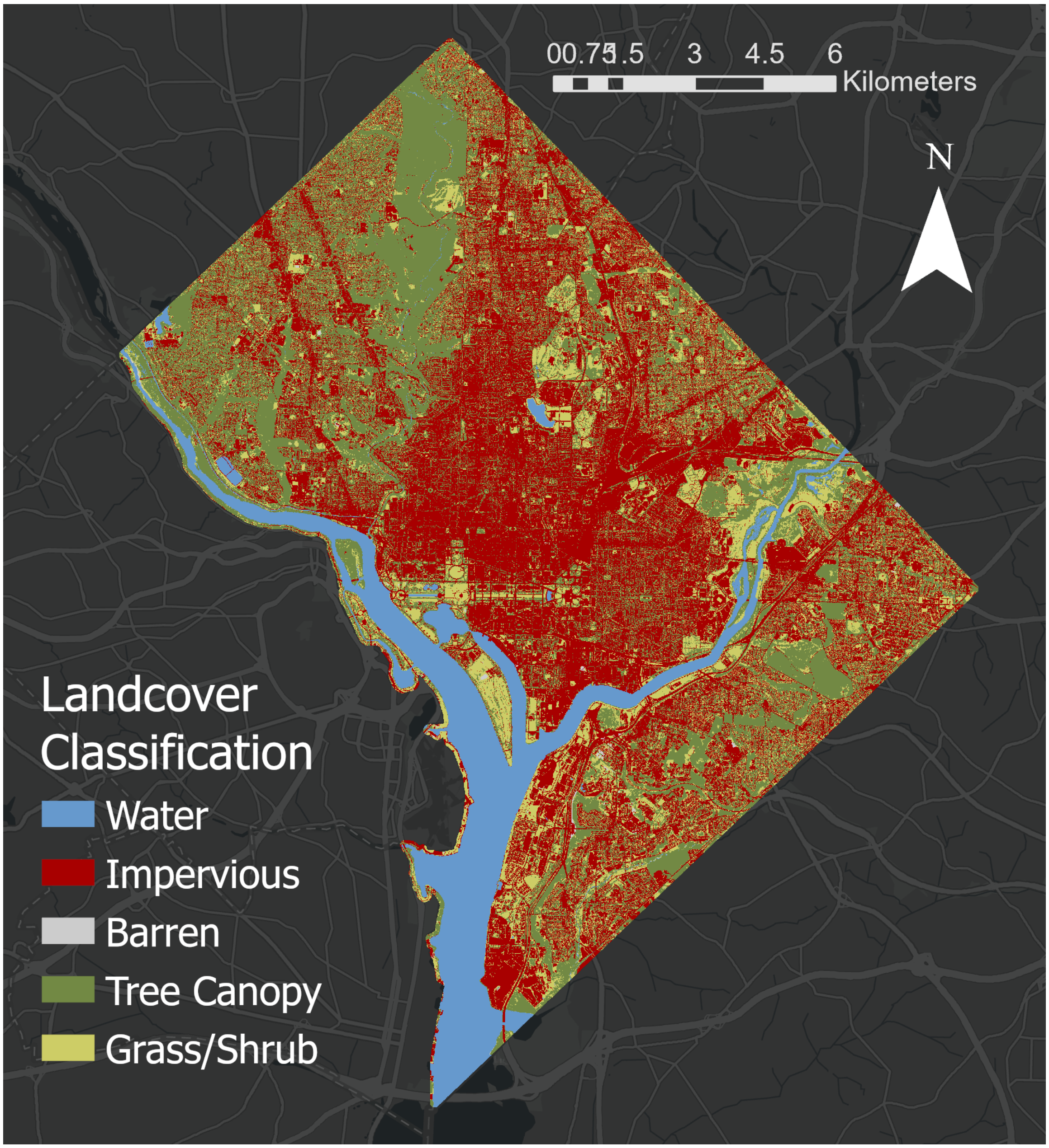

Figure 3.5: 1m landcover classification for Washington, DC.

3.2.1 Projected Climate Change

The entire northeastern region of the United States is anticipated to experience the effects of climate change, such as a rise in temperature and more frequent and intense precipitation events[47]. Located in the southernmost portion of this region, these impacts are expected to affect DC as well. Temperature increases are already expected to exacerbate the UHI effect the city currently faces — with a 1.1°C increase in annual average temperature having occurred over the past 50 years[11], and another 2.2°C projected under the Representative Concentration Pathway (RCP) 4.5. This means DC will likely experience longer heat waves with higher average temperatures, straining the city's infrastructure[29], undermining the regional economy[18], and harming its residents.

Flooding, associated with both sea level rise and overwhelming precipitation events, is already occurring and is anticipated to become more frequent[47]. While both can be devastating to DC residents, this study is focused primarily on flooding associated with high-magnitude precipitation events, as these can be mitigated with well placed UGI in any section of the city, as opposed to tidal flooding, which is best mitigated by UGI in the riparian buffer zone[20].

3.3 Socio-demographic Landscape

Table 3.2: A collection of basic information on Washington, DC.

Land Area	177 km^2
Population[a]	670,949
Per capita income[b]	$71,297
Median household income[c]	$101,722
Percent persons in poverty	13.3%

[a] Population estimates base, July 1, 2022[45]
[b] In past 12 months (in 2022 USD, 2018-2022)[45]
[c] In 2022 USD, 2018-2022[45]

The socio-demographic history of DC has been, and continues to be, dichotomic. Racial segregation is still prominent in DC[6]; as of the 2020 US Census, 39.6% of the population is considered white, with the remaining 60.4% of the population identifying as one or more minority races. This split has been present both statistically, as well as geographically. In 2000, the racial segregation index of DC was 78%. Although this has declined since then, data from 2013-2017 shows the racial segregation index at 67%. This means that 67% of the non-white population would need to physically relocate in order to reside in fully integrated white communities[6]. This separation is roughly designated on an east-west bias, with the eastern portion of DC being majority non-white and the western portion being majority white. Additionally, there appears to be a north-south geographical bias, indicating a lower percentage of residents in poverty in northern DC and a higher portion of residents in poverty in the southern portion. This pattern creates a distinct socio-economic divide, where southeastern DC is both higher in percentage of non-white residents and persons in poverty than northwestern DC (Figure 3.6).

DC's per capita income stands at $71,297, which is considerably higher than the national median of $41,261[45] (Table 3.2). The poverty rate in DC is higher than the national average, with 13.3% of the population in poverty compared to the US rate of 11.5%. Additionally, DC's median household income is significantly greater at $101,722, in contrast to the US median of $75,149.

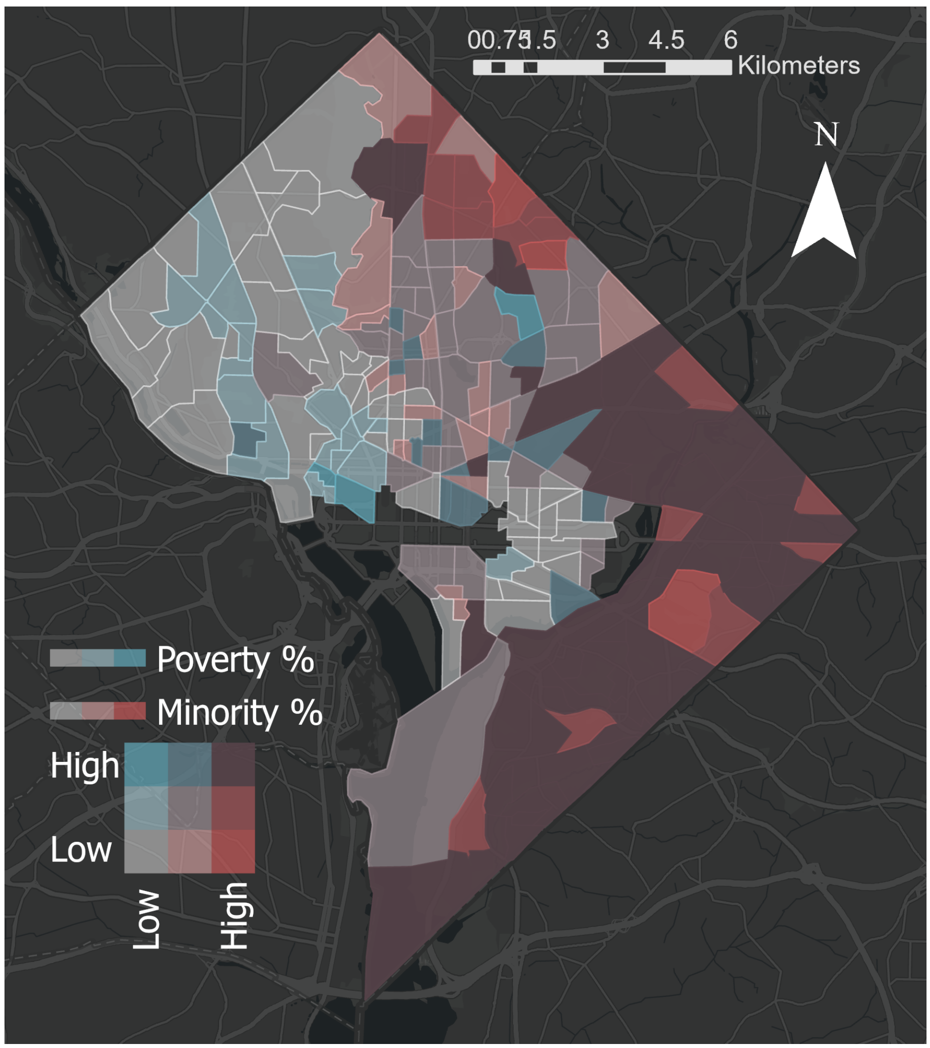

Figure 3.6: Bivariate choropleth showing the percentage of population that is a minority (shades of red) against the percentage of population that is under the poverty threshold in Washington, DC. Data collected from 2020 CDC SVI[21]

3.4 Political History

DC was officially founded in 1790 with the Residence Act, which established the location of the capital of the US on the banks of the Potomac from land donated by the states of Virginia and Maryland[9]. Prior to this event, the cities of Georgetown, Maryland, and Alexandria, Virginia were located in this selected location and, before that, the area was inhabited by the Piscataway people. The Residence Act, however, only approved the creation of the national capital, and it wasn't until the District of Columbia Organic Act of 1801 that the city was officially organized under the control of the US Federal Government.

DC is a planned city, with the capital's design being primarily credited to French architect Pierre Charles L'Enfant's 1791 L'Enfant Plan. This plan laid out a gridded street system which divided the city into four unequal quadrants around axes radiating from the US Capitol Building (Figure 3.7). Included in the L'Enfant Plan was a system of parks in varying shapes and sizes that would provide natural open spaces to the district's residents. This plan was eventually revised by Andrew and Benjamin Ellicott in 1792, but many of the original design principles were retained[32].

DC has not been granted US statehood, and instead is governed by the Council of the District of Columbia, a legislative branch comprised of a chairmen elected at large and 12 members, one from each election ward and 4 at-large members. The DC government and the powers granted to it were established by the District of Columbia Home Rule Act of 1973[34], a federal law establishing the District Charter (providing for an elected mayor and the Council), while at the same time granting the US Congress the authority to review all legislation passed by the Council. This makes DC unique in its governance: although the Council has the power to compose and vote on legislation with autonomy, all final legislation must be approved by the US Congress, and thus, the governance is a reflection of constituency of DC through a lens of the constituency of the US as a whole. Additionally, this unique configuration of governance means that organizations on both the federal and district level cooperate in regards to planning decisions. The National Capital Planning Commission oversees the development of federal property within the National Capital Region and includes 3 Presidential appointees and 2 Mayoral appointees, as well

Figure 3.7: The L'Enfant Plan, originally developed in 1791 and later revised by Andrew and Benjamin Ellicott in 1792, shaped the district into orthogonal grids radiating from the central capitol building.[2]

as 7 ex officio members including the Mayor of DC, the Chair of the DC Council, heads from the Secretary of Defense, Secretary of the Interior, an Administrator of General Services, and leaders of US Congress committees with oversight responsibility of DC[30]. District-led organizations, such as the DC Office of Planning and the DC Department of Energy and the Environment, also help to plan the National Capital Region. Owing to this environment of co-management between Federal and District level agencies, DC planning strategy is also reflective of both District politics and National US politics.

3.4.1 Social Equity in DC

The division described in Section 3.3 and illustrated by Figure 3.6 has its roots in history that can be traced back to post-Civil War Federal and District policies that encouraged racial, educational, and income segregation[3] throughout the District[6]. Among the precedents and tools used in DC to segregate and perpetuate segregation were[6]:

- **Urban Renewal**: Under the guise of improving substandard housing, populations of poor minorities were displaced and forced into worse, overcrowded conditions as housing prices increased in neighborhoods and urban blight accelerated elsewhere[48].

- **Public Housing**: Federal Housing Administration (FHA) segregationist policies barred minorities from certain public housing[28].

[3]Racial Segregation refers to residential separation of racial groups[17], education segregation refers to residential segregation by levels of education[25], and income segregation refers to residential segregation by levels of income[40]

- **Highways**: Inner-city highways were planned in ways to displace minority residents and create physical barriers between white and minority communities[27].

- **FHA Laws**: The FHA, through the post-WWII Federal Housing Administration and GI Bill, statistically financed white mortgage loans over those of minority residents and embraced racial covenants as a predictor when considering the future value of new housing developments[23].

- **Zoning**: In 1936, DC established residential zones district-wide, with stricter regulations in the northwest (i.e. no rowhouses or flats) and looser zoning regulations in the southeast[41].

- **Restrictive Covenants**: Contracts amongst private landowners refusing to rent or sell property to minorities were legal until the Supreme Court deemed them unenforceable in 1948[4].

- **Redlining**: The HOLC created maps ranking neighborhoods by credit-worthiness, based in part on the race of the residents of the neighborhoods. These were referenced by both private banks as well as the FHA when considering long-term mortgages[24].

- **Steering**: The practice of steering, where members of the real estate industry encourage and recommend segregation when assisting home-buyers and renters in finding available housing, was established policy within the Real Estate Brokers' Association of the District of Columbia until the adoption of the Fair Housing Act in 1968[19].

These policies and mechanisms ranged from subtle, such as zoning regulations prohibiting cheaper forms of housing, to blatantly-worded discrimination, i.e. racial covenants explicitly prohibiting the sale of property to non-white individuals. Collectively they provide evidence to the assumption that segregation in DC was not voluntary but, instead, was perpetuated by institutions, and that the patterns we see today were, in fact, by design. The socio-demographic distribution initiated by these historical policies have persisted to present day, as can be seen in Figure 3.6.

3.4.2 UGI Policy in DC

In 2013, DC launched the ”Sustainable DC Plan”, a strategy for increasing green infrastructure throughout the district and improving the district's waterways. This plan was directly supported by three pieces of legislation: the Sustainable DC Act of 2012, the Sustainable DC Transformation Order of 2013, and the Sustainable DC Act of 2014. The plan serves as the foundation for DC's UGI policy, yet addresses environmental concerns beyond UGI in the district.

The Sustainable DC 2.0 Plan, released in full in April 2019, is the most current iteration of this plan. Building on the former Sustainable DC Plan, Sustainable DC 2.0 was developed over the course of 20 months through an iterative process that included public input through community workshops, public polling, and technical analysis. The process was designed to be transparent and inclusive, with a focus on bringing at-risk members of the community into the conversation[1].

Sustainable DC 2.0 divides the district's environmental sustainability strategy into 13 separate topics(Table 3.3). Within these topics, the planning document is further divided into a number of Goals, Targets, and Actions. The Goals offer broad, big-picture ambitions the District intends to achieve. Each Goal is associated with a Target that provides quantifiable metrics for which success of the Goal can be measured. The Plan's Actions are mechanisms through which the District hopes to reach the associated Goal[15]. The topic of *Nature*, aiming to protect, restore, and expand ecosystems, is written to directly address increasing native green ecosystem coverage in the District, with Goals that include "Protect, restore, and expand aquatic systems", "Protect, restore, and expand land ecosystems", and "Improve human access to and stewardship of nature". These goals are supported by actions that include "planting and maintaining 10,500 new trees per year in priority areas to achieve 40% tree canopy cover by 2032" and "Creating a habitat connectivity plan to guide restoration of viable, native habitats throughout Washington, DC". The *Water* topic also intends to increase city-wide UGI, with a Goal to "Reduce the volume of stormwater runoff" with a Target of implementing UGI practices to "capture, retain, or reuse stormwater from at least 10% of the District's land area". To support this Goal and Target, DC has introduced the RiverSmart Homes program[10] to incentivize the installation of UGI on private property and encourage the retrofitting of green roofs and other stormwater abatement methods by providing guidance and implementing the Stormwater Retention Credit Trading Program.

Coupled with the Riversmart Homes Program, DC administers an impervious surface tax, the Clean Rivers Impervious Area Charge, that imposes a tax based on square footage of impervious surface and uses these funds to install improvements to reduce stormwater sewage overflow in the District. The Riversmart Program offers rebates of this tax to residents willing to reduce impermeable pavement and install UGI. Additionally, in 2016 to help meet Sustainable DC 2.0's goals, DC Water (under the Department of Energy and the Environment) issued a $25 million Environmental

Table 3.3: **13 topics targeted by *Sustainable DC 2.0.*** A summary for each topic is provided[15].

Governance

Ensuring plan implementation and accountability by the District Government

Food

Expanding urban agriculture

Increasing access to healthy food

Growing the food economy

Reducing wasted food

Equity

Improving equity in District Government planning, starting with Sustainable DC

Health

Enabling active lifestyles for residents

Increasing healthy places for residents

Improving community-level health

Built Environment

Equitably accommodating population growth

Strengthening existing neighborhoods

Making existing buildings more sustainable

Making new buildings more sustainable

Nature

Protecting and expanding aquatic wildlife and habitat

Protecting and expanding land wildlife and habitat

Improving residents' access to nature

Climate

Reducing greenhouse gas emissions (climate mitigation)

Increasing resilience to climate change (climate adaptation)

Transportation

Increasing transit use

Increasing the number of bikers and walkers

Reducing dependency on single occupant vehicles

Reducing emissions from transportation

Economy

Growing green jobs and economy

Training residents for green jobs

Waste

Reducing the amount of waste created

Increasing reuse and recovery of materials

Increasing recycling and composting

Education

Educating students about the environment

Educating community members about sustainability

Water

Making waterways fishable and swimmable

Reducing the amount of stormwater runoff

Reducing the amount of potable water used

Ensuring safe drinking water

Energy

Improving energy efficiency

Increasing renewable energy

Modernizing energy infrastructure

Impact Bond[4], the first of its kind in the US, to support the Rock Creek Project A. This was an ambitious effort to curb stormwater flooding of the Rock Creek Watershed through the implementation of UGI[14]. The majority of these projects were installed in wards 4 and 5, in the north and northeast of DC. A similar project, the Potomac River Project, was installed wards 2 and 3 in the west of the District. All together, DC committed $90 million in total to these two projects[13].

3.5 Detailed Methodology

For the sample selection process, the landcover classification was clipped to only include land using a hydrography dataset of the Anacostia and Potomac Rivers[37]. 500 random sample points were created using the methods described in Chapter 2; however, as the total area of the DC political boundaries (minus the water) did not allow for the creation of 500 points using the 0.5 km distance, only 404 sample points were created. A 0.2 km buffer radius was applied to the points to create the sample plots.

Using R code (Appendix A.1) from the landscapemetrics R package[22], the 6 LSMs detailed in Chapter 2 were computed for each plot. Of these plots, the samples that encompassed mostly water landcover, the plots that fell within any National Park boundaries[36], and the plots within the census district containing the DC correctional facilities[33] were removed. Using Zoning data[35], zonal statistics were calculated for the sample plots. Only those with a majority of "Single Family Residential" zoning

[4] An Environmental Impact Bond is a relatively new financing tool that transfers some of the performative risk of green infrastructure to bond investors. If the infrastructure shows a certain level of improvement, the District pays an outcome payment to investors. At a lower tier of function, no outcome or shared risk payment is made. At the lowest tier of function, purchasers pay the risk-share payment to the District[44].

(n = 212) were retained (Figure 3.8). For these plots, SVI variables were apportioned to each plot using the ArcGIS Pro Apportion Polygon Tool[16]. Since the percent area of barren landcover was negligible (Table 3.1) and this study is not interested in water connectivity, both LSMs for water and barren landcovers were discarded. Remaining values for SVI percentages and LSMs were analysed using PCA. Factors that were cross-loaded were examined more thoroughly with Mean Rank Analysis. Full reports for the Mean Rank Analyses can be found in Appendix B.3.

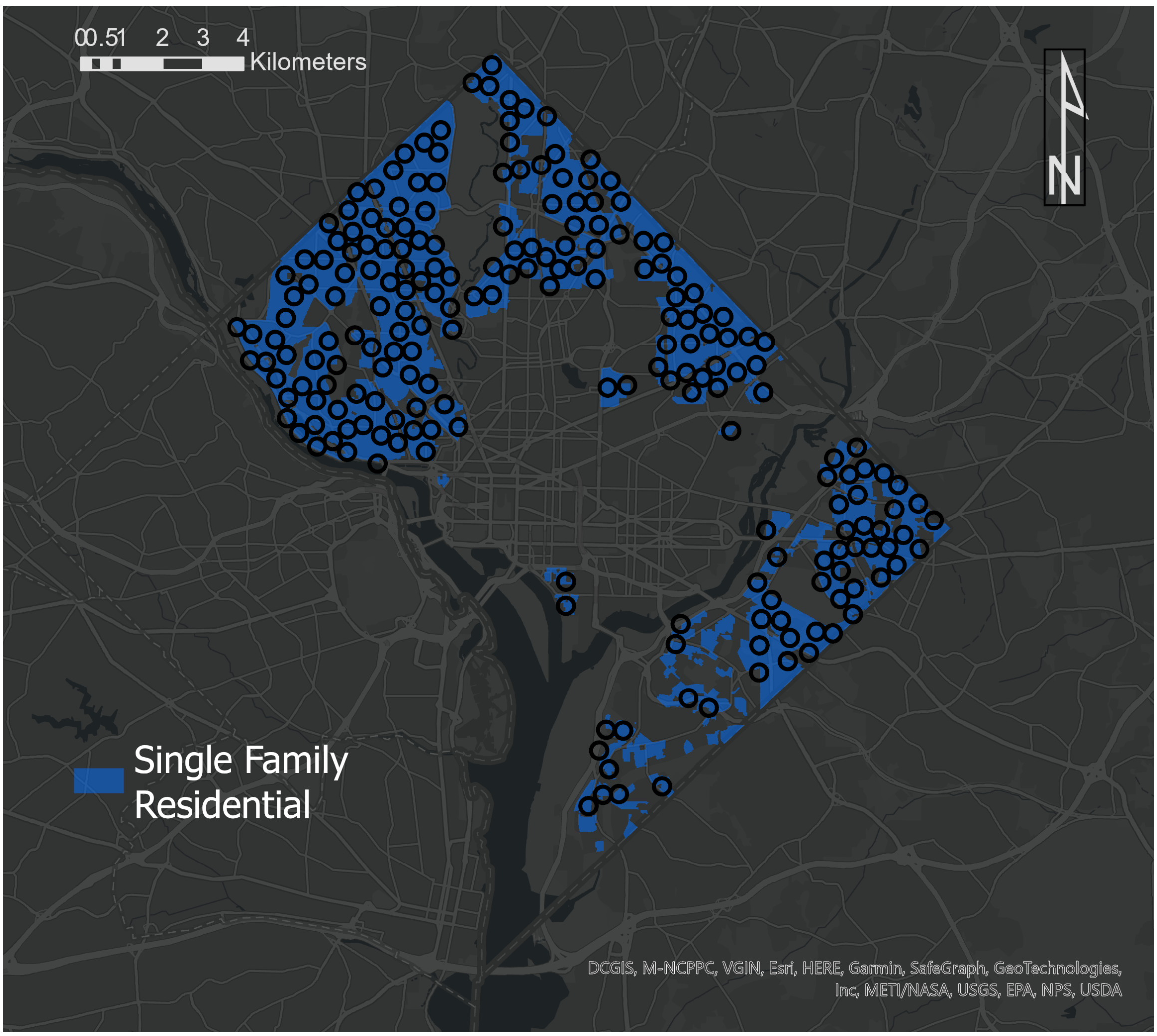

Figure 3.8: Map showing the sample plots chosen for this study (black circles). Blue zones indicate areas zoned as ”Single Family Residential”.

3.6 Results of Analysis

3.6.1 Principal Component Analysis

Using a Varimax rotation, 5 components representing 77% of the data variance were extracted with the leading 2 components explaining 52% of the variance (Table 3.4). A threshold of |0.32| was used to determine significant variable loading per component. Principal Component (PC) 1 (explaining 36% of the variance) was primarily loaded with LSMs relating to areal coverage and connectivity of both impervious surfaces and tree canopy, with tree canopy loading negatively on to PC 1 and impervious surfaces loading positively. PC 2 (explaining 17% of the variance) was loaded with the majority of the SVIvariables, with only Limited English % not significantly loading onto this component. PC 3 (explaining 12% of the variance) was primarily loaded with variables relating to landscape class complexity, PC 4 (explaining 7% of the variance) was loaded with variables relating to coverage and connectivity of the shrub/grass landcover class, and PC 5 (explaining 5% of the variance) was solely loaded with SVI variables. PC 1 was significantly cross-loaded with two SVIs: Racial Minority % and Age 65+ %. PC 2 was significantly cross loaded with one LSM: shrub/grass ENN_MN. PC 3 was cross-loaded with one SVI variable, Age 17- %, and the remaining components did not experience any cross loading between LSMs and SVIs.

The SVI variable Racial Minority % was chosen for further analysis due to it positively cross-loading onto PC 1, indicating a relationship between Racial Minority % and coverage and connectivity of tree canopy and impervious surfaces. Additionally, the landscape connectivity metric ENN_MN for the grass/shrub landcover class is cross-loaded onto PC 2, indicating a relationship between grass/shrub connectivity and vulnerability that merited further analysis.

Another relationship that appeared in the PCA connected the variable Age 65+% to PC 1, indicating there was a slight negative correlation between areas with high concentrations of 65+ age residents and connected impervious surfaces/disconnected tree canopy. This variable also showed an inverse relationship with PC 2, indicating that as the other SVI variables increased, Age 65+% decreased.

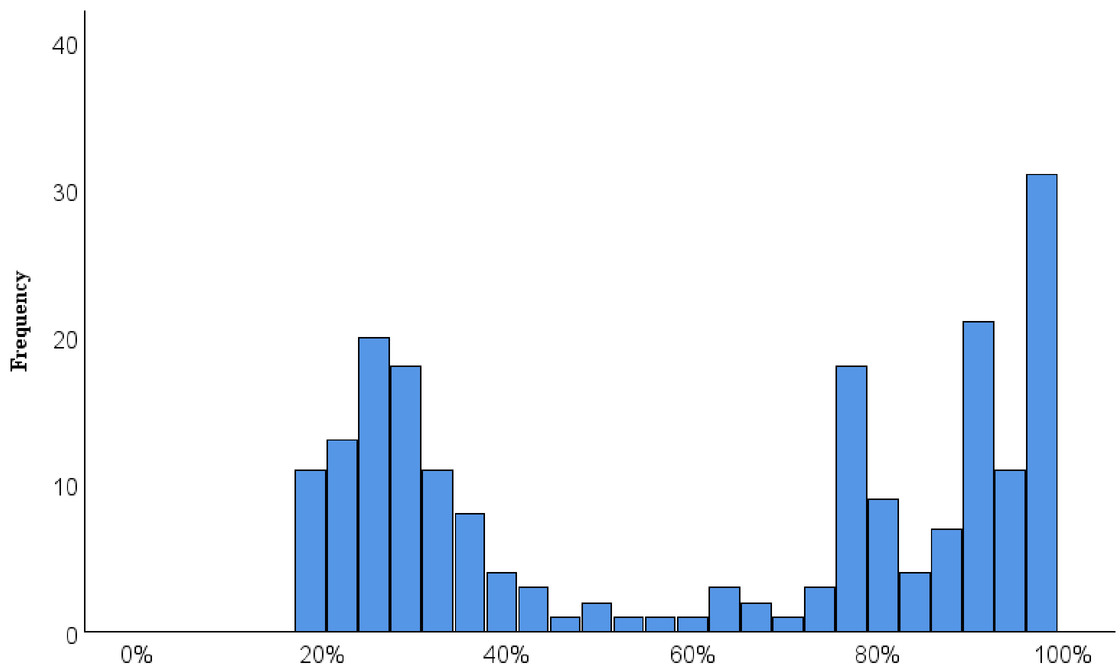

Figure 3.9: Histogram of percent minority variable of DC sample plots, displaying bimodal distribution. Plots were binned into 35 intervals.

3.6.2 Mean Rank Comparison

Owing to the bi-modal distribution of the variable Racial Minority % resulting from the racial segregation inherent in DC (Figure 3.9), the sample plots were split into 2 groups: those in the lower 50th percentile of percentage minority (M1) and those plots

Table 3.4: *PCA Rotated Component Matrix of sample plots in Washington, DC.* Rotation Method: Varimax with Kaiser Normalization. Scores below |0.32| were considered a poor correlation and not included in this component matrix[8].

Variable	Component				
	1	2	3	4	5
Below Poverty %		0.855			
Unemployed %		0.744			
No HS Diploma %		0.626			0.438
Uninsured %		0.444			0.578
Age 65+ %	-0.354	-0.379			-0.372
Age 17- %		0.393			
Disability %		0.756			
Limited English %					0.836
Racial Minority %	0.325	0.730			
Housing Burden %		0.750			
Single Parent Household %		0.754			
Household Crowding %		0.452			0.723
Impervious PLAND	0.935				
Tree PLAND	-0.904				
Shrub/grass PLAND				0.858	
Impervious LPI	0.903				
Tree LPI	-0.833				
Shrub/grass LPI				0.824	
Impervious LSI			0.934		
Tree LSI	0.588		0.732		
Shrub/grass LSI			0.790	-0.536	
Impervious enn_mn	-0.581		-0.486		
Tree enn_mn	0.624			0.413	
Shrub/grass enn_mn		-0.354	-0.748		
Impervious Cohesion	0.831				
Tree Cohesion	-0.794				
Shrub/grass Cohesion				0.865	
Impervious pladj	0.835		-0.446		
Tree pladj	-0.821		-0.487		
Shrub/grass pladj				0.896	

Kaiser-Meyer-Olkin Measure of Sampling Adequacy		.820
Bartlett's Test of Sphericity	Approx. Chi-Square	8871.208
	df	435
	Sig.	<0.001

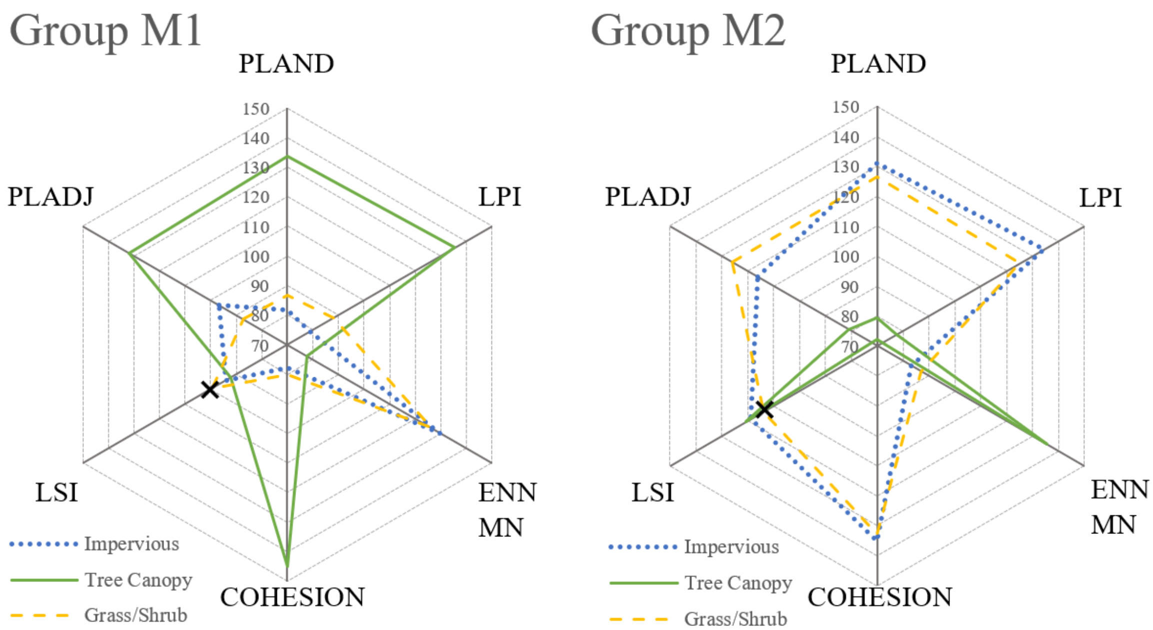

Figure 3.10: Radar plot showing mean ranks of 6 LSMs for groups M1 and M2. Mean ranks were calculated using a Mann Whitney U Test (n=212). Black "X" denotes insignificant result ($p > 0.05$).

in the upper 50th percentile of percentage minority (M2). This binary classification methodology was applied to all groups as well. The hypotheses of this dissertation are not claiming that the percentage of vulnerable residents is directly proportional to the connectivity of UGI, but instead surmise that plots with higher proportions of vulnerable residents will generally have less UGI connectivity than those with lower proportions of vulnerable residents. Thus, a binary division was deemed appropriate to evaluate this dissertation's hypotheses. A Mann-Whitney U Test determined significant differences between percentile groups in all class LSMs except Shrub/Grass LSI ($p < 0.05$) (Figure 3.10).

Regarding the areal coverage LSMs PLAND and LPI, the mean rank of M1 was higher than that of M2 for tree canopy (Figure 3.11), and lower for both shrub/grass and impervious surfaces. M1 exhibited a lower ENN_MN mean rank for tree canopy than M2, but a higher ENN_MN mean rank for both shrub/grass and impervious surfaces. For Cohesion and PLADJ, M1 exhibited a higher mean rank for tree canopy and a lower mean rank for shrub/grass and impervious surfaces than M2. For LSI, the differences in mean rank between M1 and M2 were only significant for tree canopy and impervious surfaces, and M1 had a lower mean rank in both classes.

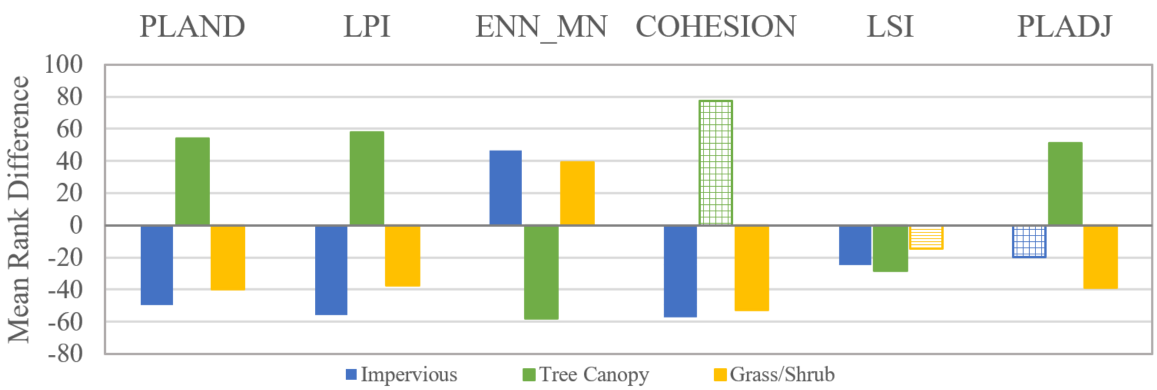

Figure 3.11: Differences in mean rank between M1 and M2 (M1-M2) for LSMs of each class. Solid colors indicate significance at $p < 0.001$. Gridded color indicates significance at $p < 0.05$. Horizontal stripes indicate insignificant differences in mean rank ($p > 0.05$).

3.7 Discussion

The results from this analysis support both hypotheses, with significant differences in mean rank favoring higher connectivity in plots with lower proportions of vulnerable residents, specifically regarding Minority % and the LSMs of each vegetation class. For nearly every vegetation class-based LSM calculated for tree canopy and grass/shrub classes, the mean rank was significantly different between groups M1 and M2. Although not directly related to either hypothesis (which solely address UGI coverage and connectivity), it should also be noted that there were significant differences in mean rank between every impervious surface-based LSM. H2 was partially supported as well — the mean rank of tree canopy LSMs in groups M1 and M2 indicated that tree canopy had higher coverage and connectivity in the plots from M1 than the plots from M2. However, coverage and connectivity of the grass/shrub landscape class appeared to be comparatively higher in the plots from M2 than in the plots from M1.

These results reveal that, while coverage and connectivity of tree canopy is, on average, less in areas with higher percentages of minorities, the coverage and connectivity of the grass/shrub landscape appears to be greater in these areas. This constitutes both an environmental justice challenge and an opportunity. Tree canopy, as an important resource for mitigating urban heat and stormwater flooding, covers less of high minority populated areas and is less connected, reducing its efficacy. However, the coverage and connectivity of vegetation that is less effective at mitigating urban heat and stormwater flooding, such as grass and shrubs, is higher in these areas. The conversion of these areas to tree canopy would be less expensive, since it does not involve the removal and disposal of impervious surfaces[3]. Additionally, this process is less disruptive to the neighborhoods in which the conversion takes place, as impervious conversion removes infrastructure in these vulnerable areas that can be vital to the communities' function, such as sidewalks and roads. More coverage and connectivity of grass, shrub, and other lower-quality vegetation means more potential for conversion to higher quality vegetation, like tree canopy.

Currently, DC policy regarding UGI aims to take into consideration connectivity of UGI. The Sustainable DC 2.0 Plan, lead by the District Department of Energy and Environment, lists habitat connectivity among its goals, with a target of 40% tree canopy cover by 2032. Equity was also listed as an important element of the Sustainable DC 2.0 Plan. Although the plan addresses the need for equity in earning and housing for non-white populations, racial disparities in tree canopy cover are not listed as a priority in the plan. Considering that persistent spatial racial segregation is often linked to historical institutional level actions including housing market discrimination[7], inadequate tree canopy coverage and connectivity in high minority areas is an EJ problem that should be considered when planning for UGI implementation. Future research of this topic should include further categorization of vegetation class. In this study, vegetation was designated as grass/shrub or tree canopy. However, vegetative quality can range dramatically within those classes. For example, an urban garden may fall in the same class as a dry, un-watered lawn, although these landcover types offer much different levels of ecosystem services. Additionally, to help better inform decision makers and stakeholders as to the best policy tools to increase coverage and connectivity of high quality urban vegetation, a better understanding of the ownership of vegetation in residential areas would be beneficial. Through the RiverSmart program, the current DC Sustainable 2.0 plan encourages and finances tree planting on both publicly owned land, such as parks and road verges, as well as on privately owned properties[15, 10]. Understanding the potential for improved connectivity in both of these sectors would allow for resources to be aptly applied where needed most in areas with vulnerable populations.

References

[1] Sustainable DC History | Sustainable DC. URL https://sustainable.dc.gov/node/1447346.

[2] Andrew Ellicott. Plan of the city of Washington in the territory of Columbia : ceded by the states of Virginia and Maryland to the United States of America, and by them established as the seat of their government after the year MDCCC, 1792. URL http://hdl.loc.gov/loc.gmd/g3850.ct004179.

[3] Antoine Kunsch and Ryan Parks. Tree Planting Cost-Benefit Analysis: A Case Study for Urban Forest Equity in Los Angeles. Technical report, Tree People, 2021.

[4] Ashley Bakelmun and Sarah Jane Shoenfeld. Open Data and Racial Segregation: Mapping the Historic Imprint of Racial Covenants and Redlining on American Cities. In Scott Hawken, Hoon Han, and Christopher Pettit, editors, *Open Cities / Open Data*, pages 57–83. Springer Nature Singapore, Singapore, 2020. ISBN 9789811366048 9789811366055. doi: 10.1007/978-981-13-6605-5_3. URL https://link.springer.com/10.1007/978-981-13-6605-5_3.

[5] Carol M. Highsmith. Aerial view of White House and downtown, Washington, D.C, April 2007. URL https://commons.wikimedia.org/wiki/File:Aerial_view_of_White_House_and_downtown,_Washington,_D.C_LCCN2010630891.tif.

[6] Jamie P Chandler and Joy Phillips. Racial, Education & Income Segregation in the District of Columbia. Technical report, District or Columbia Office of Planning, November 2020.

[7] Camille Zubrinsky Charles. The Dynamics of Racial Residential Segregation. *Annual Review of Sociology*, 29(1):167–207, August 2003. ISSN 0360-0572, 1545-2115. doi: 10.1146/annurev.soc.29.010202.100002. URL https://www.annualreviews.org/doi/10.1146/annurev.soc.29.010202.100002.

[8] Andrew L. Comrey and Howard B. Lee. *A First Course in Factor Analysis*. Psychology Press, 0 edition, November 2013. ISBN 978-1-315-82750-6. doi: 10.4324/9781315827506. URL https://www.taylorfrancis.com/books/9781317844075.

[9] HARVEY W. CREW. *CENTENNIAL HISTORY OF THE CITY OF WASHINGTON, D. C: with full outline of the natural advantages,... accounts of the indian tribes, selection of the si.* FORGOTTEN BOOKS, S.l., 2022. ISBN 978-0-331-94761-8. OCLC: 1354511023.

[10] DC Department of Energy & Environment. RiverSmart Homes. URL https://doee.dc.gov/service/riversmart-homes.

[11] DC Department of Energy & Environment. Climate Ready DC: The District of Columbia's plan to adapt to a changing climate. Technical report, Washington, D.C., 2016.

[12] DC Office of Planning. DC Cultural Plan. Technical report, Government of the District of Columbia, Washington, D.C., March 2019.

[13] DC Water. Long Term Control Plan Modification for Green Infrastructure. Executive Summary, District of Columbia Water and Sewer Authority, May 2015. URL https://www.dcwater.com/sites/default/files/green-infrastructure-exec-summary.pdf.

[14] DC Water. Rock Creek Project A Factsheet. Technical report, Department of Energy & Environment, Washington, D.C., 2018. URL https://www.dcwater.com/sites/default/files/project/documents/2020%20RCA%20Factsheet.pdf.

[15] DDOE. Sustainable DC 2.0. Comprehensive Plan, Department of Energy & Environment, Washington, D.C., April 2019.

[16] ESRI. ArcGIS Pro, 2023.

[17] John E. Farley and Gregory D. Squires. Fences and Neighbors: Segregation in 21st-Century America. *Contexts*, 4(1):33–39, February 2005. ISSN 1536-5042, 1537-6052. doi: 10.1525/ctx.2005.4.1.33. URL http://journals.sagepub.com/doi/10.1525/ctx.2005.4.1.33.

[18] Frank Ackerman and Elizabeth A. Stanton. The Cost of Climate Change: What We'll Pay if Global Warming Continues Unchecked. Technical report, Natural Resource Defence Council, May 2008.

[19] George Galster. Racial Steering by Real Estate Agents: Mechanisms and Motives. *The Review of Black Political Economy*, 19(1):39–63, June 1990. ISSN 0034-6446, 1936-4814. doi: 10.1007/BF02899931. URL http://journals.sagepub.com/doi/10.1007/BF02899931.

[20] Keryn B. Gedan, Matthew L. Kirwan, Eric Wolanski, Edward B. Barbier, and Brian R. Silliman. The present and future role of coastal wetland vegetation in protecting shorelines: answering recent challenges to the paradigm. *Climatic Change*, 106(1):7–29, May 2011. ISSN 0165-0009, 1573-1480. doi: 10.1007/s10584-010-0003-7. URL http://link.springer.com/10.1007/s10584-010-0003-7.

[21] Geospatial Research, Analysis, and Services Program. CDC/ATSDR Social Vulnerability Index 2020 - District of Columbia, October 2022.

[22] Maximilian H.K. Hesselbarth, Marco Sciaini, Kimberly A. With, Kerstin Wiegand, and Jakub Nowosad. landscapemetrics: an open-source R tool to calculate landscape metrics. *Ecography*, 42:1648–1657, 2019. doi: 10.1111/ecog.04617.

[23] Louis Lee Woods Ii. ALMOST "NO NEGRO VETERAN … COULD GET A LOAN": AFRICAN AMERICANS, THE GI BILL, AND THE NAACP CAMPAIGN AGAINST RESIDENTIAL SEGREGATION, 1917–1960. *The Journal of African American History*, 98(3):392–417, July 2013. ISSN 1548-1867, 2153-5086. doi: 10.5323/jafriamerhist.98.3.0392. URL https://www.journals.uchicago.edu/doi/10.5323/jafriamerhist.98.3.0392.

[24] Amy C. Kantor and John D. Nystuen. De Facto Redlining a Geographic View. *Economic Geography*, 58(4):309–328, 1982. ISSN 0013-0095. doi: 10.2307/143457. URL https://www.jstor.org/stable/143457. Publisher: [Clark University, Wiley].

[25] Lincoln Quillian. Does Segregation Create Winners and Losers? Residential Segregation and Inequality in Educational Attainment. *Social Problems*, 61(3):402–426, August 2014. ISSN 00377791, 15338533. doi: 10.1525/sp.2014.12193. URL https://academic.oup.com/socpro/article-lookup/doi/10.1525/sp.2014.12193.

[26] Russ Lopez and H. Patricia Hynes. Sprawl In The 1990s: Measurement, Distribution, and Trends. *Urban Affairs Review*, 38(3):325–355, January 2003. ISSN 1078-0874, 1552-8332. doi: 10.1177/1078087402238805. URL http://journals.sagepub.com/doi/10.1177/1078087402238805.

[27] Avichal Mahajan. Highways and segregation. *Journal of Urban Economics*, page 103574, June 2023. ISSN 00941190. doi: 10.1016/j.jue.2023.103574. URL https://linkinghub.elsevier.com/retrieve/pii/S0094119023000438.

[28] Mara Cherkasky. Unfinished Business in a Divided City. *Washington History*, 32(1/2):17–19, 2020. URL https://www.jstor.org/stable/26947507.

[29] Minh Nguyen, Xiaoming Wang, and Dong Chen. *An investigation of extreme heatwave events and their effects on buildings and infrastructure*. January 2011. ISBN 978-0-643-10633-8.

[30] National Capital Planning Commision. About the Commission, 2022. URL https://www.ncpc.gov/about/commission/.

[31] National Park Service. Geology - Great Falls Park (U.S. National Park Service), April 2015. URL https://www.nps.gov/grfa/learn/nature/geology.htm.

[32] National Register. The Plan of the City of Washington (L'Enfant Plan; L'Enfant-McMillan Plan) - The Plan of the City of Washington is the sole American example of a comprehensive Baroque city plan with a coordinated system of radiating avenues, parks, and vistas overlaid upon an orthogonal grid of streets., April 1997. URL https://historicsites.dcpreservation.org/items/show/478.

[33] Oak Ridge National Laboratory. Prison Boundaries, September 2020. URL https://hifld-geoplatform.opendata.arcgis.com/.

[34] Office of the General Counsel. Distict of Columbia Home Rule Act, 1973. URL https://dccouncil.us/wp-content/uploads/2018/11/Home-Rule-Act-2018-for-printing-9-13-182.pdf.

[35] Open Data DC. Zoning Regulations of 2016, April 2010. URL https://opendata.dc.gov/datasets/DCGIS::zoning-regulations-of-2016.

[36] Open Data DC. National Parks, March 2014. URL https://opendata.dc.gov/datasets/DCGIS::national-parks.

[37] Open Data DC. Waterbodies 2015, March 2016. URL https://opendata.dc.gov/datasets/DCGIS::waterbodies-2015.

[38] M. C. Peel, B. L. Finlayson, and T. A. McMahon. Updated world map of the Köppen-Geiger climate classification. *Hydrology and Earth System Sciences*, 11 (5):1633–1644, October 2007. ISSN 1607-7938. doi: 10.5194/hess-11-1633-2007. URL https://hess.copernicus.org/articles/11/1633/2007/.

[39] David C. Prowell. Cretaceous and Cenozoic tectonism on the Atlantic coastal margin. In Robert E. Sheridan and John A. Grow, editors, *The Atlantic Continental Margin*, pages 557–564. Geological Society of America, Londan, 1988. ISBN 978-0-8137-5204-4 978-0-8137-5458-1. doi: 10.1130/DNAG-GNA-I2.557. URL https://pubs.geoscienceworld.org/books/book/865/chapter/4861455/.

[40] Sean F. Reardon and Kendra Bischoff. Income Inequality and Income Segregation. *American Journal of Sociology*, 116(4):1092–1153, January 2011. ISSN 0002-9602, 1537-5390. doi: 10.1086/657114. URL https://www.journals.uchicago.edu/doi/10.1086/657114.

[41] Rufus S. Lusk. Historic Zoning Map from 1936, 1936. URL https://opendata.dc.gov/datasets/DCGIS::historic-zoning-map-from-1936/about.

[42] Russell Lopez. Urban Sprawl in the United States: 1970-2010. *Cities and the Environment*, 7(1), 2014.

[43] Noah M Schmadel and Judson W Harvey. NHD-RC: Extension of NHDPlus Version 2.1 with high-resolution river corridor attributes, 2020. URL https://www.sciencebase.gov/catalog/item/5f8e091d82ce3241879215a7.

[44] Olli Tiikkainen, Matti Pihlajamaa, and Maria Åkerman. Environmental impact bonds as a transformative policy innovation: Frames and frictions in the construction process of the Nutrient-EIB. *Environmental Innovation and Societal Transitions*, 45:170–182, December 2022. ISSN 22104224. doi: 10.1016/j.eist.2022.10.006. URL https://linkinghub.elsevier.com/retrieve/pii/S2210422422000971.

[45] United States Census Bureau. U.S. Census Bureau QuickFacts: United States. URL https://www.census.gov/quickfacts/fact/table/DC,newyorkcitynewyork,oaklandcountymichigan,detroitcitymichigan,phoenixcityarizona,US/PST045222.

[46] NOAA US Department of Commerce. Climate, 2022. URL https://www.weather.gov/wrh/Climate?wfo=lwx. Publisher: NOAA's National Weather Service.

[47] USGCRP. Fourth National Climate Assessment. Technical report, U.S. Global Change Research Program, Washington, DC, 2018. URL https://nca2018.globalchange.govhttps://nca2018.globalchange.gov/chapter/18.

[48] Alexander Von Hoffman. The lost history of urban renewal. *Journal of Urbanism: International Research on Placemaking and Urban Sustainability*, 1(3):281–301, November 2008. ISSN 1754-9175, 1754-9183. doi: 10.1080/17549170802532013. URL http://www.tandfonline.com/doi/abs/10.1080/17549170802532013.

Chapter 4

Phoenix, AZ, USA

Figure 4.1: View of Downtown Phoenix, AZ skyline[32].

4.1 Introduction

Capital and the largest city of Arizona, Phoenix (PHX) sits in the Salt River Valley in central AZ (Figure 4.1). The Salt River, for which the valley is named, has allowed the city to flourish in the otherwise inhospitable Sonoran Desert climate. PHX is a city built on irrigation — the founding of and subsequent success of this city hinged on the supply of fresh water provided by the Salt River and the network of irrigation that has been developed throughout this valley[50]. This irrigation network was constructed by Anglo settlers over previously existing irrigation canals constructed by the indigenous Hohokam people (Figure 4.2), who vacated the area prior to the arrival of these settlers[23]. By channeling water from the Salt River into the surrounding fertile, yet dry, lands, PHX was transformed into an agricultural hub and is now the 5^{th} largest city in the US. However, the Southwestern US is projected to have both a rise in average annual temperature and a decrease in snowpack and streamflow runoff due to climate change, and this runoff is crucial for PHX's survival[20]. This makes PHX incredibly interesting as a case study for UGI EJ: while UGI is a resource that will help to mitigate impending UHI effects, water is a resource that is necessary for UGI to be implemented, and the distribution of water will directly impact the potential distribution of UGI. Discrepancies in how this is distributed in regards to vulnerability could constitute an EJ problem. Because there is a limit to how much UGI can be implemented based on water availability, it is imperative that UGI is placed fairly and efficiently in PHX[54]. In the previous chapter, it could be assumed that unpaved land, without human intervention, would eventually become low-grade vegetation, likely falling under the grass/shrub category of landcover. However, in PHX, unmanaged unpaved land is more likely to be classified as barren, and any occurrence of land classified as grass/shrub would likely be intentional, as water is required to maintain this level of vegetation.

4.2 Geography and Climate

PHX is located in the northeastern Sonoran Desert, in central Arizona approximately 190 km from the US/Mexico border. PHX is surrounded by several low mountain ranges: the White Tank Mountains, the McDowell Mountains, the South Mountains,

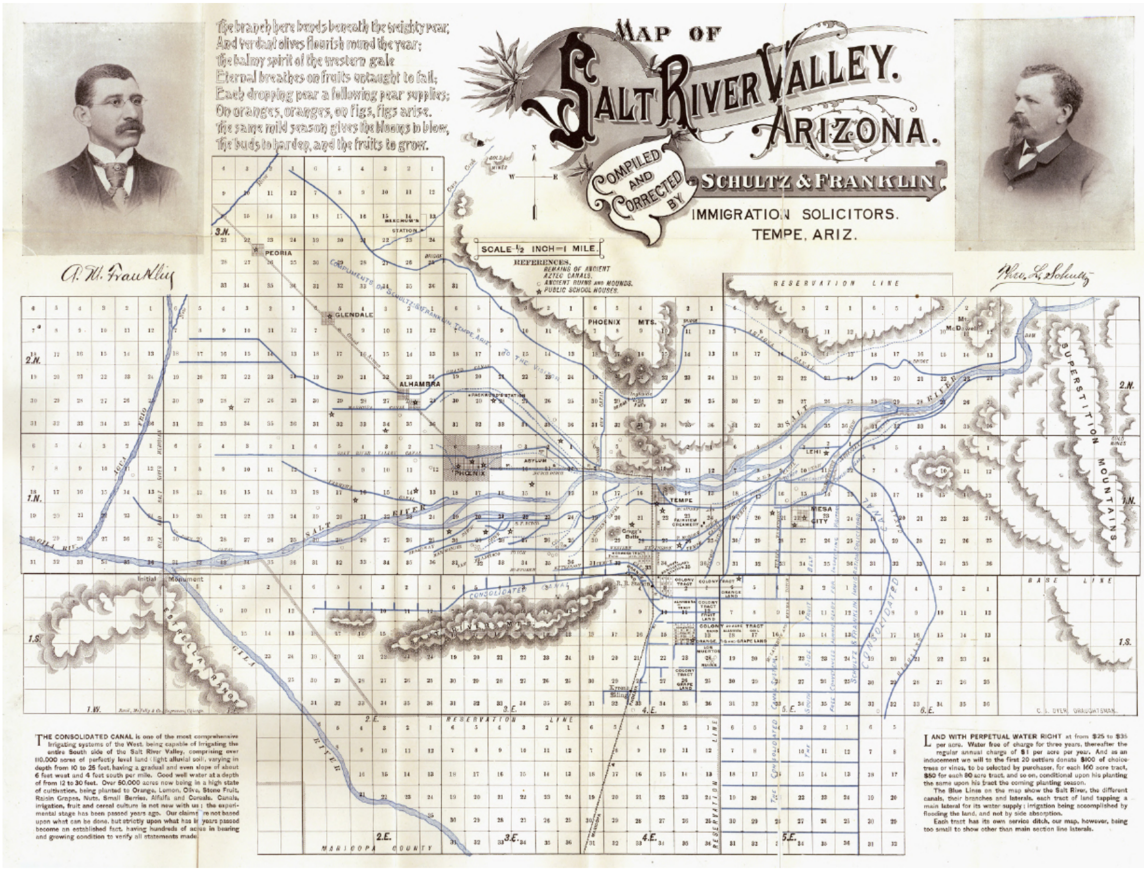

Figure 4.2: 1892 map of early Phoenix, AZ, showing the network of Hohokam canals.[19]

and the Superstitions Mountains bound the city on west, northeast, south, and east, respectively. At an elevation of 331m, PHX is generally flat; however, there are several small low-grade metamorphic mountains, including Camelback and Sunnyslope mountains, scattered within the city limits[25].

While the Salt River flows through PHX, it is not alone; the Agua Fria River, which is partially located within the city boundaries, runs in a southernly direction just west of PHX, where it meets the Salt River, which flows west through the southern half of PHX. These join to become the Gila river, which continues west until flowing into the Colorado River near Yuma, AZ[39].

The climate of PHX is a hot desert climate, Köppen climate classification BWh[26].

Summers in PHX are hot and long, winters short and mild, and the region has very little precipitation, of which most occurs during the summer monsoon season[26] (Figure 4.4). Although this climate is known for generally hot days and cold nights during the summer months, PHX, due to its UHI, often experiences less dramatically cold nighttime temperatures. Monthly mean maximum temperature normal is 41.3°C in July, while the monthly mean minimum normal temperature is 29.2°C[48] (Figure 4.3).

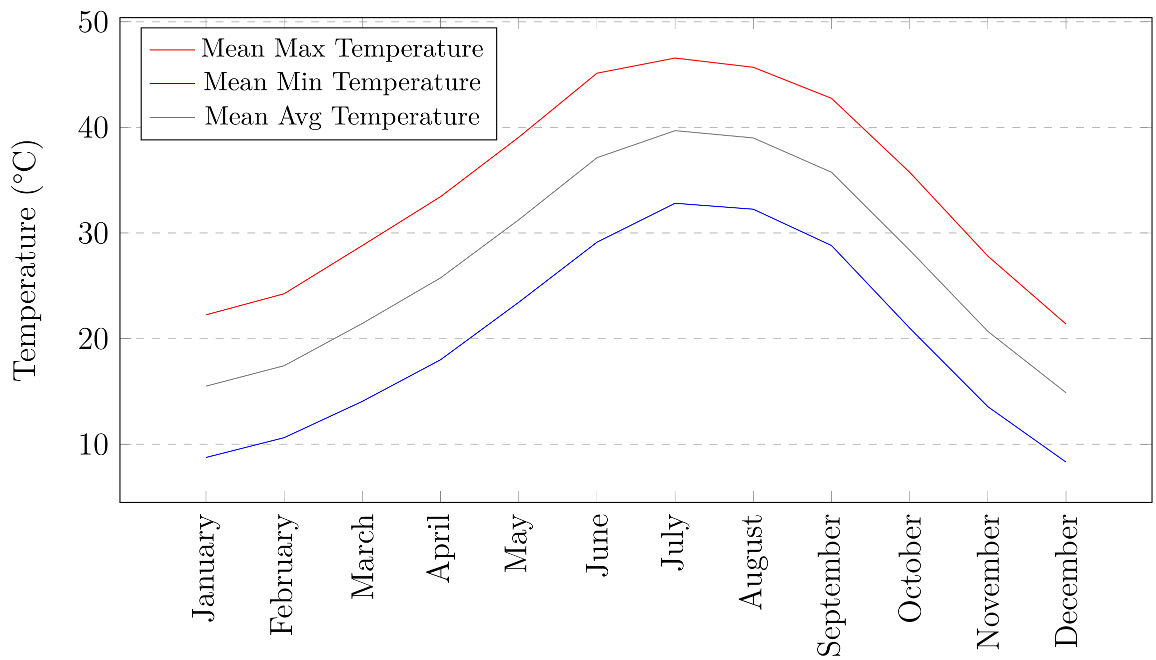

Figure 4.3: Monthly Climate Normal Temperatures for Phoenix, AZ[48].

Density Sprawl in PHX has been variable since 1970, with the PHX DSI rating slightly above the national average in 1970, after having followed the national average the previous decade, and then deviating lower in the 1990s[38] (Figure 4.5). Since 2000, there has been a slight increase, but not enough to reach the national average. However, this could be caused by PHX's rapid expansion of territory; between 1970 and 2010, PHX expanded from 642 km^2 to 1344 km^2, more than doubling in size[1]. This

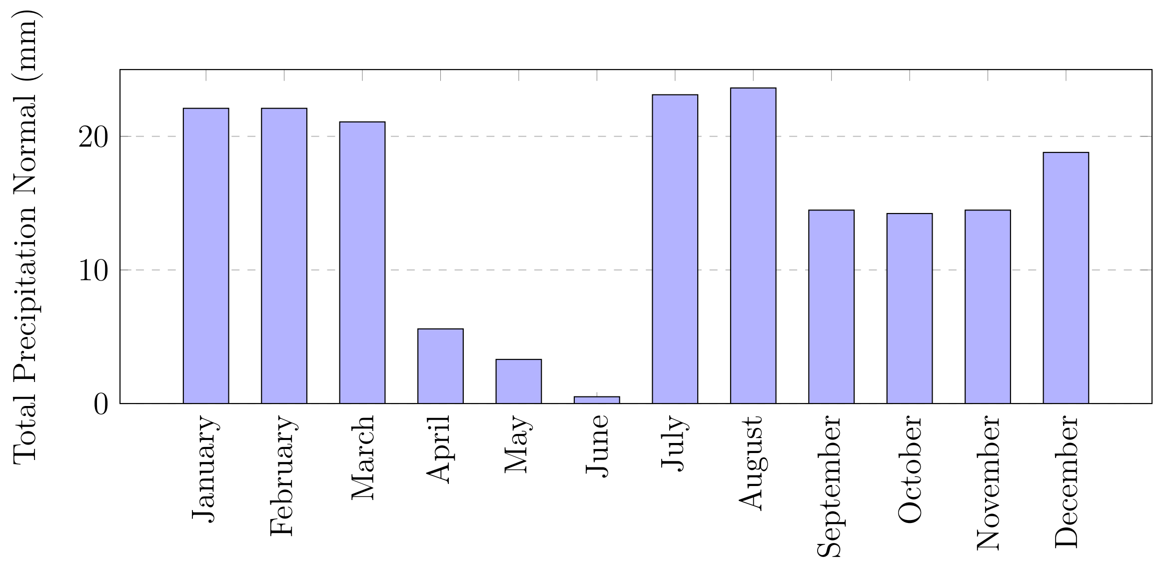

Figure 4.4: Monthly Average Total Precipitation for Phoenix, AZ [48].

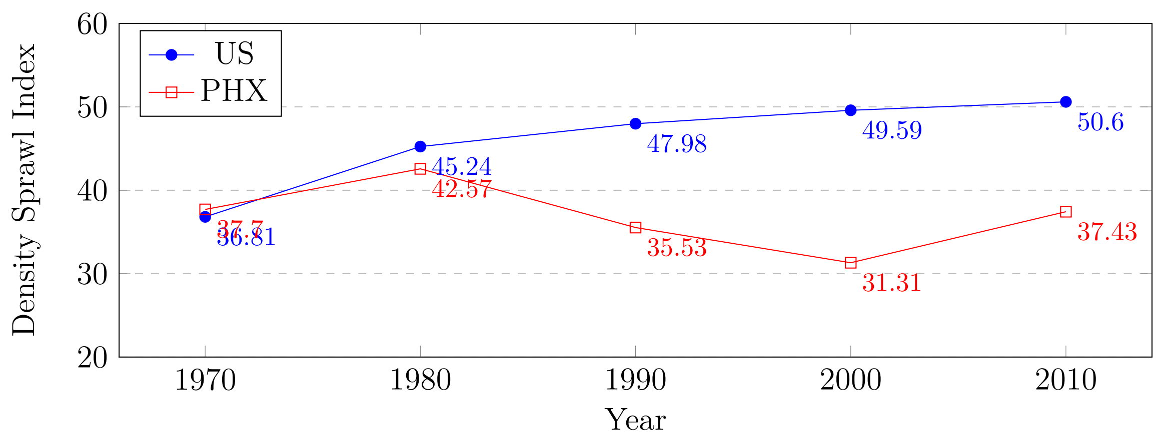

Figure 4.5: Density Sprawl Index for Phoenix Metropolitan Statistical Area (including Phoenix, Mesa, and Scottsdale AZ), compared with the US average, from 1970-2010[38].

can be attributed to ”leap frogging”, a process common throughout PHX’s history by which developers purchase large, inexpensive, and undeveloped swaths of land further outside the city center[22], which is then incorporated into the city’s boundaries. As the expansion of the city was driven by development and not population, the Development Sprawl Index formula, which incorporates the percentage of population living in low density vs. high density census tracks, could be skewed by sparsely pop-

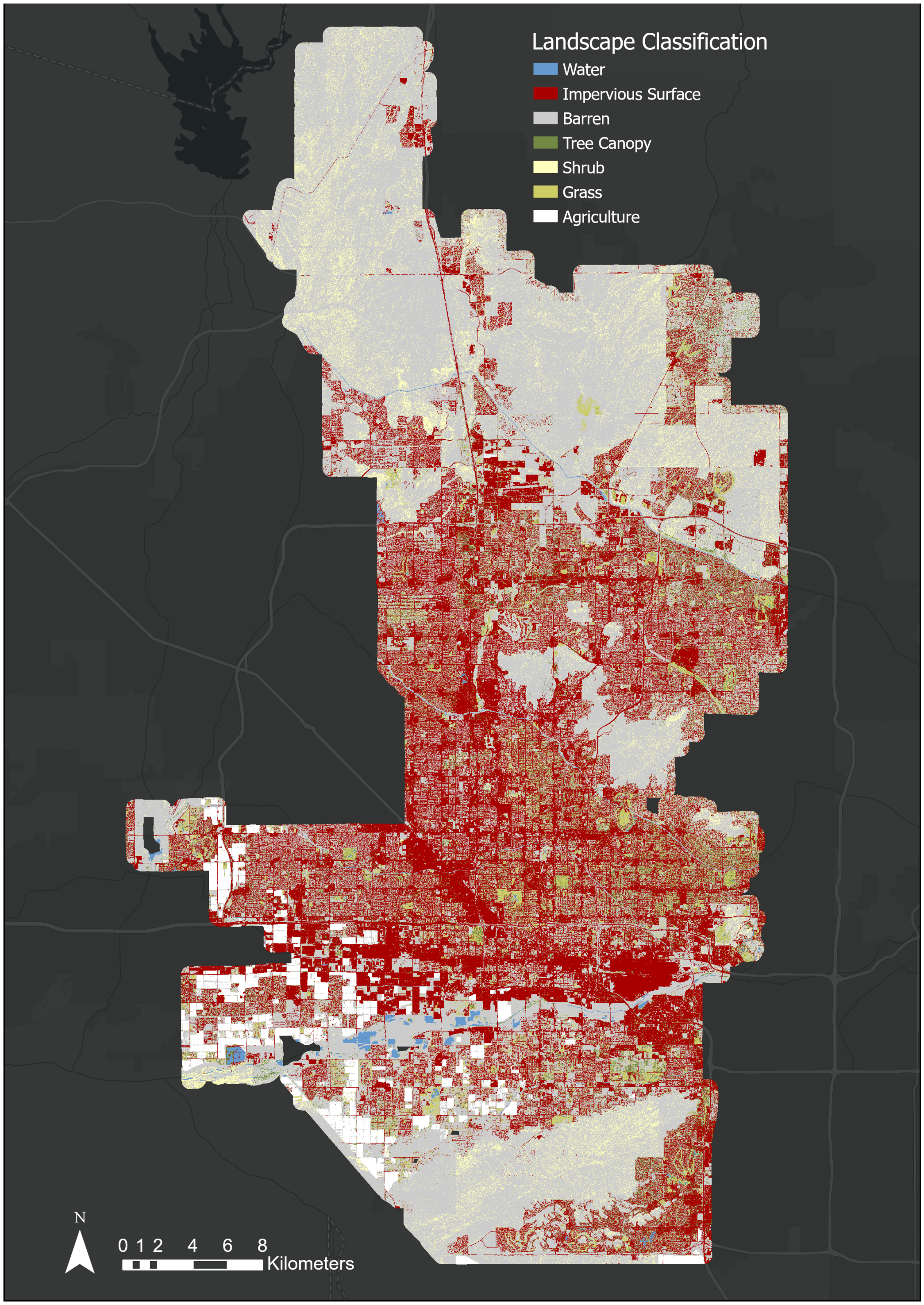

Figure 4.6: 1m landcover classification for Phoenix, AZ[49].

ulated, newly developed census tracks manifesting from rapid boundary expansion. This process, ironically, also led to an increase in urban sprawl in PHX[22].

Table 4.1: Total percentage of land area covered by each landcover class for Phoenix, AZ.

	PLAND
Tree Canopy	4.76%
Grass	5.34%
Shrub	5.92%
Impervious	28.73%
Water	0.54%
Barren	51.64%
Agriculture	3.08%

The majority of the landcover (Figure 4.6) within the PHX city boundaries can be classified as barren, at over 50% (Table 4.1). Impervious surfaces hold the next largest percentage, at over 28%. Both grass and shrubs cover more percentage of PHX than tree cover, with tree canopy only covering 4.76% and grass and shrub covering 5.34% and 5.92%, respectively.

4.2.1 Projected Climate Change

In the southwestern United States, there are several effects associated with climate change that are anticipated to be especially impactful[20, 52]. The major concerns include:

- Drought and water scarcity
- Extreme heat events
- Flooding

- Reduced air quality
- Wildfires

For this study, drought, extreme heat events, and flooding will be primarily considered.

Drought and its associated complications are expected to be particularly challenging for many urban areas in this region. The Salt River watershed, in which PHX is located, experienced some form of drought for 86% of the weeks between 2000 and 2022[47] (Figure 4.7), and these events are expected to increase in duration and intensity with climate change[52]. This is anticipated to affect both desert urban areas like PHX, with water shortages, as well as the surrounding rural areas and the agriculture within these areas that help to support the urban centers. Higher temperatures are likely to increase evapotranspiration of crops, increasing water demands and further worsening droughts. Water shortages could be exacerbated by the presence of large agribusinesses exporting crops grown in Arizona, although this process is being phased out with consideration for the ongoing, and impending, water crises[41].

In addition to the water shortages that will affect southwestern US urban centers, extreme heat events are expected to worsen with climate change. These events are expected to be both more intense, with higher maximum temperatures, and longer in duration in response to global warming[53]. Multiple models of RCPs predict the intensification of hot extremes in this region[14] and, magnified by the extensive urbanization of the PHX region, this will increase daily minimum temperatures, which is expected to impact the number of "misery days[1]" PHX experiences. This increase will add to the number of heat related deaths, and even increase violent crime in the

[1] For the study Baker et al., misery hours per day refers to hours where the Temperature-Humidity Index was above 38°C[3].

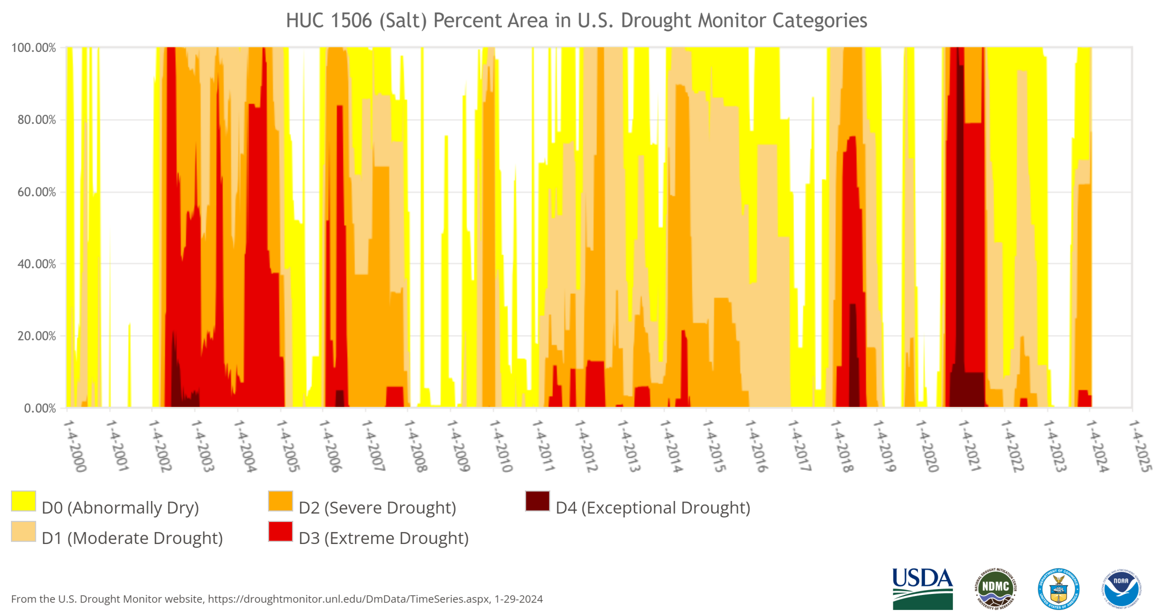

Figure 4.7: Chart showing the percentage of land experiencing varying levels of drought in the Salt River Watershed from 2000 to 2024[47].

region[3]. Vulnerable communities are expected to be disproportionately impacted by extreme heat events in PHX, with higher energy consumption for cooling and, consequentially, higher costs for already struggling communities[24].

Flooding due to increasingly intense precipitation events is also anticipated to impact PHX. Zones along the Salt River and south of the downtown districts fall within the 1% annual flood zone, many of these found in lower income, higher minority % areas[31]. With the potential for drought discussed earlier, controlling and properly utilizing stormwater to both prevent flooding and conserve water is a priority for PHX[7]. However, flooding is considered less of a risk than extreme heat events for PHX[9].

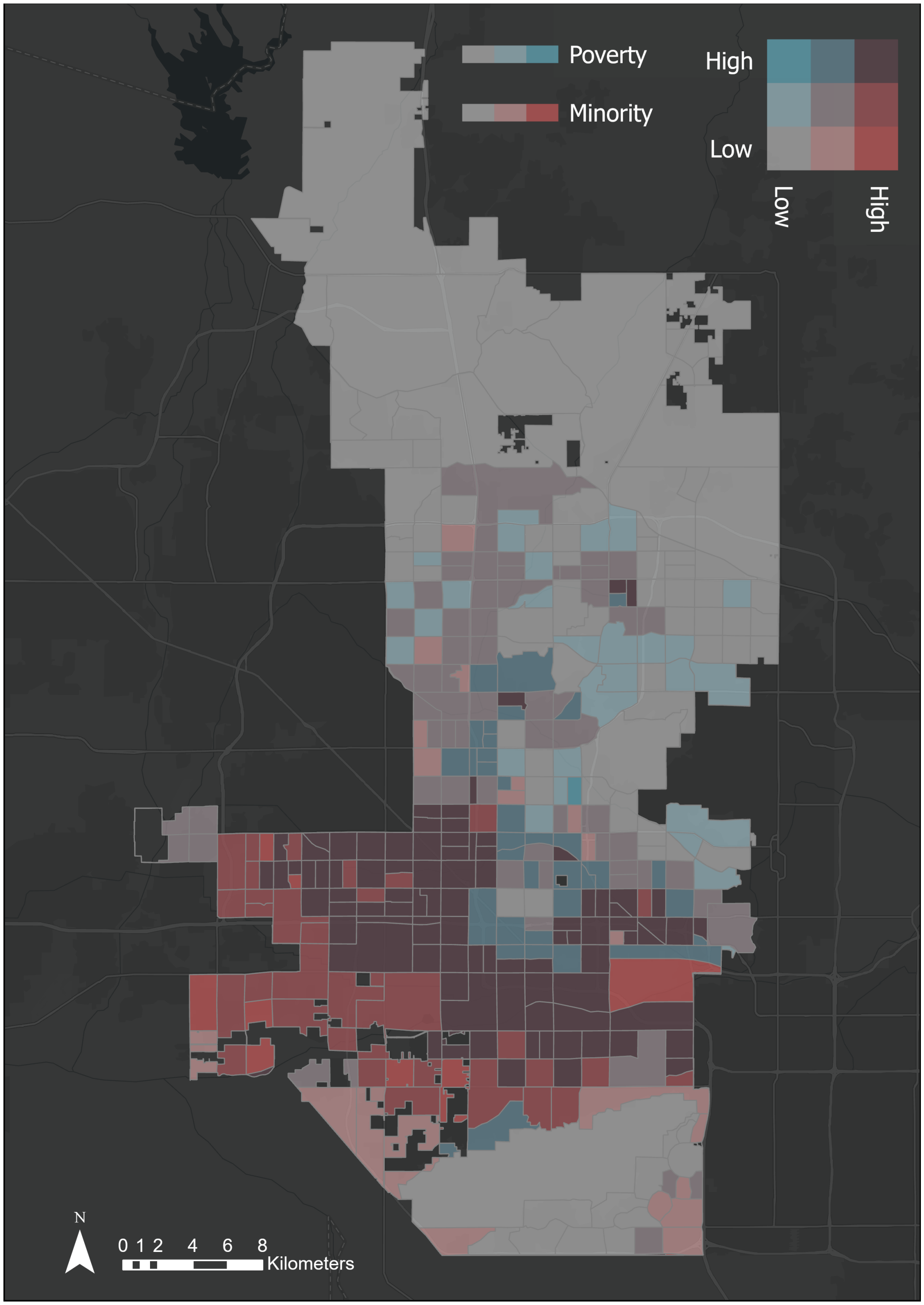

Figure 4.8: Bivariate Choropleth showing the percentage of population that is a minority (shades of red) against the percentage of population that is under the poverty threshold in Phoenix, AZ. Data collected from 2010 CDC SVI[21]

4.3 Socio-Demographic Landscape

Demographically, PHX is predominantly white (non-Hispanic), with 41.4% identifying as this group. The next largest racial/ethnic demographic is white (Hispanic), with 23%, followed by multiracial (Hispanic) with 9.52%[13]. Currently, southern PHX has a higher proportion of minority populations, and a higher proportion of residents in poverty, than northern PHX (Figure 4.8). This divide is not a straight line, but includes a cut-out of the Midtown and Downtown neighborhoods that is lower in percent minority while still relatively high in percent poverty. In the southern half of the city, the percentage of people in poverty drops the further the census tract is from the downtown area, however, the percentage of the population considered a minority remains high. Generally, other than some outlier census tracts, the further north or south from the Downtown district the census tract is, the lower the percentage of both poverty and minority population. However, this gradient is much more gradual to the south than to the north, indicating a weighted concentration of minority individuals and individuals in poverty to the south of the Downtown district.

The average per capita income of PHX is currently $33,718, lower than the US median at $41,261[43] (Table 4.2). Percentage of persons in poverty is also higher than the US average, at 14.6% compared to 11.5% for the US average, and the median household

Table 4.2: A collection of basic information on Phoenix, AZ.

Land Area	1,339 km^2
Population[1]	1,644,409
Per capita income[2]	$37,499
Median household income[3]	$72,092
Percent persons in poverty	14.6%

[a] Population estimates base, July 1, 2022[43]
[b] In past 12 months (in 2022 USD, 2018-2022)[43]
[c] In 2022 USD, 2018-2022[43]

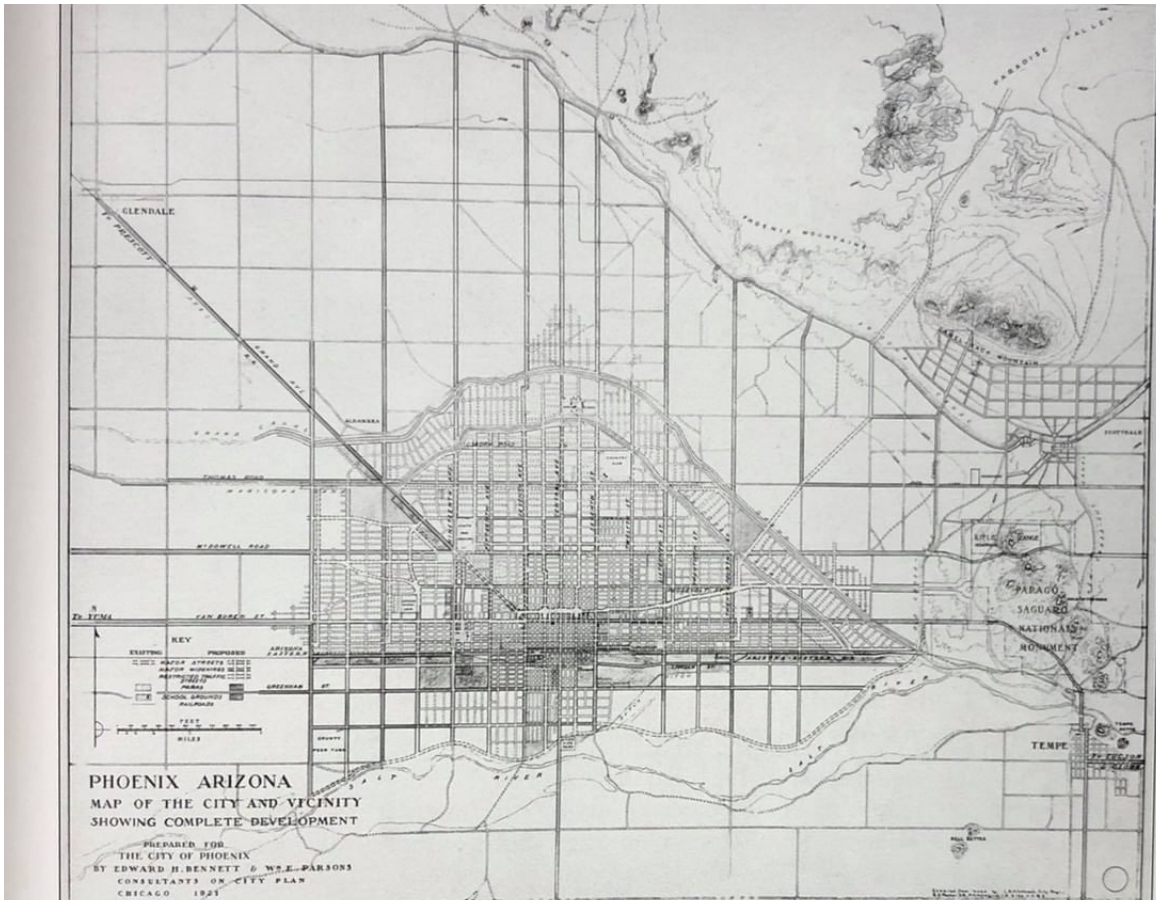

Figure 4.9: 1912 map of early Phoenix, AZ, showing the gridiron planning centered in the Salt River Valley.[16]

income of PHX, $72,092, is lower than the US median $75,149.

4.4 Political History

PHX as it exists today was settled by Anglo-Americans in the 1870s based on a gridiron plan (Figure 4.9), with the centrum near the geographical center of the Salt River Valley at the present day intersection of Washington Street and Central Avenue[29]. The settlement grew slowly but consistently, amassing a population of over 1700 by 1881, when it was officially incorporated as a city. The city continued to grow, but faced challenges, the root of which was water. Despite a network of canals previously established by the Hohokam (who had since abandoned the area), both droughts and floods threatened the growing population, and it became clear that control of the Salt River and its water was critical to continued growth and sustenance.

In 1911, the Theodore Roosevelt Dam was constructed and the Salt River Project (SRP) was initiated. By damming the Salt River, the SRP was able control flooding in PHX while also providing much needed water to irrigate the broader PHX area. Today, the SRP water service area encompasses around 100,000 hectares in PHX and Maricopa County, operating 4 dams on the Salt River and providing on average 1,172 million m^3 of water to users annually[35].

Two years after the birth of the SRP, in 1913, PHX implemented a council-manager plan as its form of government. This style of government consists of three parts: the mayor, the council, and the city manager. The mayor is elected at-large, while the 8 council members are elected within their districts. The city-manager, however, is hired by the city council and mayor, and is not an elected position. This individual oversees the day to day operations of the city while the mayor and council set policy. When the council-manager system of government was first implemented in PHX, it was one of the first major cities to utilize this system[27].

4.4.1 Social Equity in PHX

The segregation discussed in Section 4.3 stems from a combination of the location of the warehouse/industrial district in the south of PHX, as well as the tendency for the southern region, built in a floodplain, to flood. This combination brought minority populations to southern PHX in pursuit of job opportunities (as systemic racism pushed these demographics into these labor industries) and pushed those with means (primarily, wealthier white communities) away from these zones, as they fled from flooding[4]. Into the early 20th century, the railroad that supported the industrialization of PHX also represented a physical boundary, with the wealthier white communities living north of the tracks and the poorer, minority communities residing south of the tracks. Until annexation in 1959, this area south of the railroad was not officially incorporated into the City of Phoenix, and was not subject to the same land use regulations as the City of Phoenix proper[4]. This lack of regulation led to a degradation of the south PHX neighborhoods which, combined with racial prejudice, worked to push wealthier white communities north[30].

Within the minority community, Latino[2] and black residents faced different forms of discrimination. Black residents were restricted to certain geographic regions via more formal mechanisms, such as segregation laws, housing covenants, and deed restrictions[51], while Latinos were excluded from the economic opportunities that would promote integration (an obstacle the black community faced as well)[4]. The neighborhoods into which minority populations were forced were slower to acquire infrastructure that would promote health and well-being, such as potable water and sanitation, and these areas were often the site of waste disposal, housing sewage treatment facilities and landfills[4]. Although southern PHX has since acquired the utilities previously absent from the area, the precedent set by historical EJ violations has carried on into modern day, with these locations still seeing higher concentrations of pollutants than other regions of the city[5, 55].

[2] In this dissertation, "Latino" refers to individuals with a cultural connection to Latin America or Latin American descent, encompassing diverse ethnicities and nationalities.

4.4.2 UGI Policy in PHX

In August, 2013 the US EPA released a report analyzing PHX's UGI policy[45]. The report examined PHX city code and zoning ordinances using Tetra Tech's Green Infrastructure Opportunity Checklist Tool[46] and the EPA Water Quality Scorecard[44] as a framework to identify areas in existing city policy that supported UGI implementation and to find opportunities to help facilitate and improve these processes. Additionally, the report identified policies and political structures that potentially made establishing UGI in PHX more difficult. The report found that, although some of the PHX codes and ordinances were adequately working to facilitate the implementation of UGI city-wide, there were several barriers that might limit city wide implementation. Notably, although standards for new development included policies requiring the development of urban canopy and progressive storm-water management, policies encouraging and enabling the retrofitting and maintenance of existing development to promote UGI were lacking. No tree protection regulations were in place for existing private development, and street tree ordinances had strict pruning requirements compared to other municipalities which may have discouraged property owners from maintaining tree canopies. These policies had the potential to disproportionately impact vulnerable, lower income populations, as existing developments are typically more affordable than newly constructed homes[18] and exorbitant home prices prohibit low-income individuals and families from purchasing homes[11], leaving the majority of low-income residents in older, previously constructed homes. Although 91% of PHX households have access to air conditioning units for cooling[42], those that do not are most likely older construction, and most likely housing economically vulnerable residents.

At the time of the release of the 2013 EPA report, UGI policy in PHX focused in part on establishing climate-appropriate best management practices, utilizing ”Low Water Use Drought Tolerant Plants” and minimizing both lawns and high water use plants. The report claimed that the primary implementation of UGI was in bioswales or bioretention areas; many of these were retrofits, and not often used in new developments. The report suggests that more research was needed into the most appropriate species to use in these bioswale and bioretention retrofits, to maximize drought tolerance and peak stormwater mitigation[45].

PHX has implemented a climate action plan[7], detailing the policies and practices the city plans to utilize to combat the effects of climate change and minimize further greenhouse gas emissions. This plan involves seven overarching goals, three of which deal with greenhouse gas emissions, and four that build resiliency. Each goal is divided into sub-goals that address specific city improvements (Table 4.3). As a part of this plan, under the arch-goal of Heat, sub-goals H1 and H2 both intend to utilize UGI to accomplish these goals. In 2010, PHX city council implemented the Tree and Shade Master Plan[6] to further delineate these goals and provide a structure to reach them. To support this plan, a number of initiatives have been established as part of a city wide program, including the Urban Forestry Roundtable and the Urban Forest Implementation Team. The former serves as a collaboration between non-profits, private sector entities, and government representatives that works to steer policy regarding urban shade. The latter is a working group of PHX city staff that implements and monitors urban shade and tree planting projects.

Some of the programs that are currently administered by the Urban Forest Implementation Team include:

- **Citizen Forester Program:** A program that trains volunteers in planting and tree care.

- **Love Your Block**: A program that organizes tree planting events and provides grant funding for tree plantings.
- **Tree Donation Program:** Another funding tool that connects business entities with residents to provide funding for tree planting.
- **Landscape Ordinance Text Amendment:** Through the Planning and Development Department, this amendment enforces the protection and maintenance of tree plantings and ensures tree plantings are a part of new development.
- **Parks and Recreation Tree Planting Program:** A program through the Parks and Recreation Department working to reach the 25% canopy cover goal via tree plantings in parks.
- **Streets Transportation Tree Planting Program:** A tree planting program with dedicated funding to plant an average 1000 new trees annually along transportation corridors.
- **Environmental Quality and Sustainability Commission:** A group appointed by City Council to provide the council advice regarding environmental and sustainability subjects. A sub-committee, the **Urban Heat Island and Tree and Shade Sub-Committee**, is tasked with focusing primarily on UHI and tree cover.
- **Memorandum of Understanding with American Forests:** This agreement between PHX and the non-profit American Forests attempts to address UHI in PHX through "Tree Equity", focusing tree planting and preservation efforts on vulnerable areas.

Within each of these plans and programs, special attention is paid to vulnerable communities, as well as to the idea of cool corridors. Although the plans don't explicitly address UGI connectivity, the creation of cool corridors and the goal for 25% tree canopy cover by 2030 both work to increase connectivity of these resources. However, many of these policies and programs were publicized following 2010, the year from which the landcover data for this study was collected. Considering this, it

Table 4.3: Resiliency goals included in PHX's Climate Action Plan[7]. This list does not include the three greenhouse gas emission reduction goals that are also mentioned by the plan.

Air Quality	
AQ1:	Meet U.S. EPA National Ambient Air Quality Standards (NAAQS).
Local Food System	
LFS1:	All people living in Phoenix will have enough to eat and have access to affordable, healthy, local, and culturally appropriate food.
LFS2:	Businesses that produce, process, distribute, and sell local and healthy food will be recognized as integral to the economy and encouraged to grow and thrive in Phoenix.
LFS3:	Growing food in Phoenix and the region will be easy and valued, for personal or business use.
LFS4:	Food-related waste will be prevented, reused, or recycled via sustainable food production practices that maintain a healthy environment.
LFS5:	Develop food policies and actions that address local and global challenges posed by climate change, urbanization, political and economic crises, population growth and other factors.
Heat	
H1:	Create a network of 100 cool corridors in vulnerable communities by 2030 to facilitate movement of people walking, biking and using transit, particularly within and connecting to Transit Oriented Development Districts, Village Cores, and Centers.
H2:	Increase shade provided by trees or constructed shade in 'flatland parks' (not preserves) and street rights-of-ways to achieve a 25% tree and shade canopy in pedestrian areas by 2030, prioritizing communities most vulnerable to heat, particularly within and connecting to Transit Oriented Development Districts, Village Cores, and Centers.
H3:	Provide resources and services to residents to manage heat.
H4:	Increase the use of high albedo, or reflective, materials in infrastructure projects.
H5:	Develop HeatReady certification for cities in partnership with ASU by 2025.
Water	
W1:	Identify and implement infrastructure projects to ensure water security.
W2:	Improve conservation of water resources by improving stormwater management, optimizing water use, conducting water audits, and utilizing wastewater.
W3:	Increase outreach and provide programs to residents and businesses to reduce water use to 155 GPCD by 2030.

is important to recognize that this is not a critique of the policies set in place by the government of PHX, but instead serves as guidance by which to view the potential effectiveness of current policy based on previous EJ issues.

4.5 Detailed Methodology

For this chapter, 2010 PHX EnviroAtlas Meter-scale Urban Landcover Classification data was employed[49]. This data is over 10 years old at the time of this writing; however, more recent landcover data at this resolution for PHX is currently unavailable. To pair with this, 2010 CDC/ATSDR SVI data[21] was used instead of the most recent 2020 data, to better match the time frame being examined for this study. This should be noted when considering the EJ implications of the results — while this study does not encapsulate the most recent status of UGI connectivity in PHX or the most recent demographics of PHX, it establishes an EJ baseline which future decisions regarding UGI placement should consider. Additionally, the CDC/ATSDR SVI data methodology has been updated since 2010 to include the number of residents facing housing burden. Although this variable was included in the previous chapter for DC, it was not included in this study due to it being unavailable in the 2010 data.

Within the political boundaries of PHX, there is both urban/suburban land, as well as sparsely populated desert land. This study is focused on human/ecosystem dynamics and, thus, areas with no residents (for purposes of this study, ”empty space”) within the city boundaries must be disregarded when selecting sample plots. To do this, a process was employed to clip away land without a sufficient number of residents to form a study area within which the sample plots would be created.

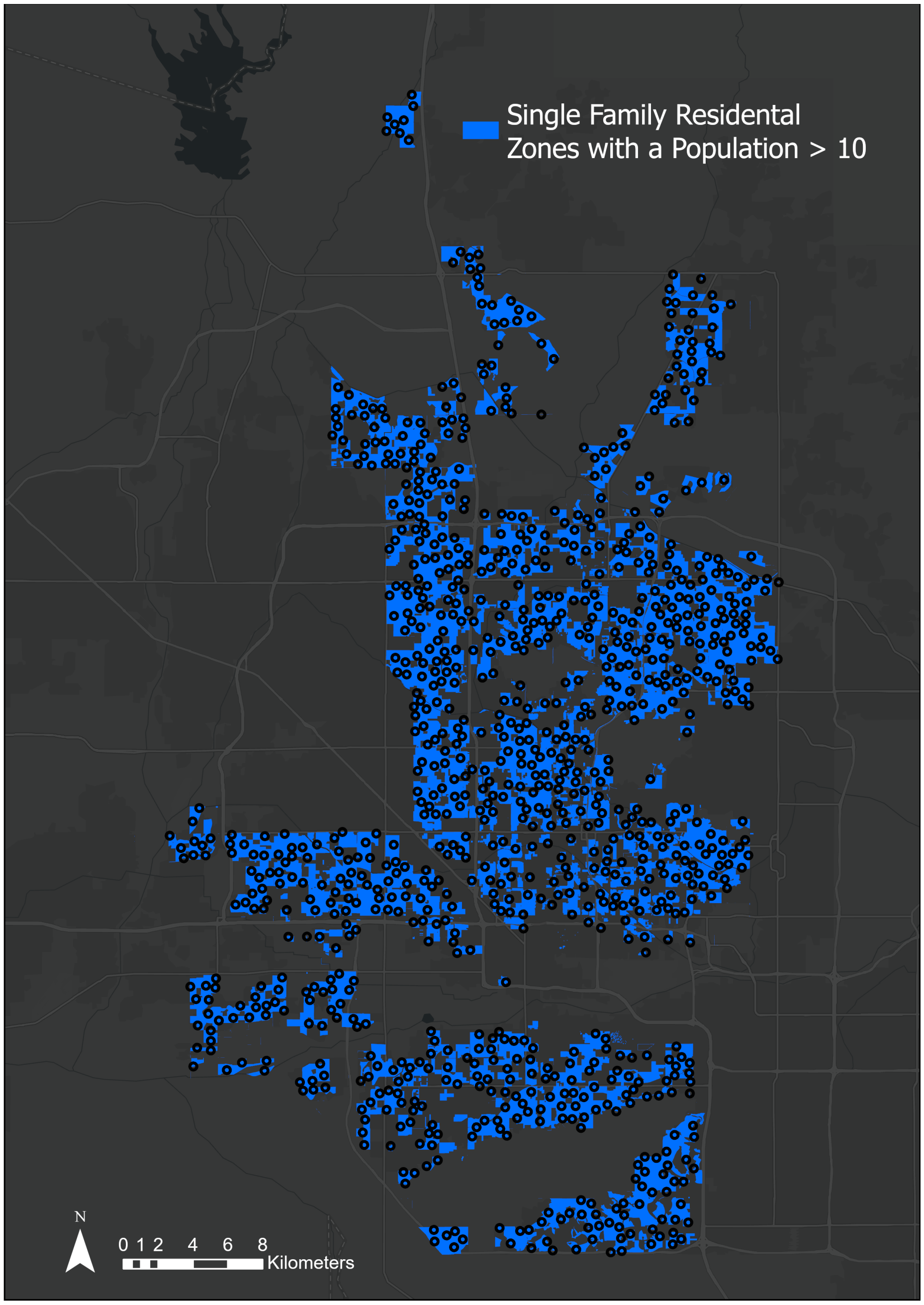

Figure 4.10: Study plots for Phoenix, AZ (n = 847). Black circles denote sample plots used in this study, blue zones represent areas deemed suitable for this study according to study criteria.

Starting with a dataset of the city boundary, all areas zoned as ”Single Family Residential” were extracted using a city zoning dataset from City of Phoenix Open Data. Next, a dataset of PHX Parks and Recreation boundaries was used to remove parkland that overlapped with these zones.

Within this study zone consisting of Single Family Residential, non-park land within the PHX city boundaries, 1000 points were generated using the ArcGIS Pro *Generate Random Sample Points* tool. However, because of the ”leapfrogging” development covered in Section 4.2, several of these plots include no residents or housing. To ensure that the study only includes urban land, rather than rural land within the city boundaries, a filter was applied to the plots to remove all plots with less a population of less than 10 (Figure 4.10). Any plots that overlapped with a census tract with a prison[34] that would contribute to the SVI variables were discarded. The remaining plots (n = 847) were processed using the methods detailed in Chapter 2. All variables were passed onto PCA except the LSMs pertaining to water and agriculture.

4.6 Results of Analysis

4.6.1 Principal Component Analysis

Using a Varimax rotation, 5 components were extracted from the data, representing 64% of the total variance (Table 4.4). PC 1 (explaining 22% of the variance) is loaded primarily with SVI variables, with the only SVI variable not loaded onto this component being unemployed %. Although the variable age 65+ % is loaded onto PC 1, it loads negatively, suggesting an inverse relationship with the other variables. Loaded onto PC 1 alongside the SVI variables is both tree canopy and shrub

PLADJ and Cohesion. Although metrics of coverage for these landcover types (such as PLAND and LPI) are not loaded onto this component, the loading of two aggregation metrics indicate a link between SVIs and the connectivity of shrub and tree cover. The remaining PCs are loaded with varying LSMs. PC 2 (explaining 18% of the variance) is loaded primarily with metrics that measure the connectivity of Barren landscape and the inverse disconnectivity of tree canopy. PC 3 (explaining 12% of the variance) is loaded with variables that indicate the connectivity of impervious surfaces and disconnectivity barren land. PC 4 (explaining 7.5% of the variance) is loaded with variables representing the connectivity of shrub landscape (as well as one variable representing a lack of areal coverage of barren land). PC 5 (explaining 5.5% of the variance) is loaded with a mix of metrics pertaining to connectivity and coverage of primarily the grass landcover, alongside weakly loaded metrics for tree connectivity and impervious disconnectivity.

Because tree PLADJ, tree Cohesion, shrub PLADJ, and shrub Cohesion loaded onto a component that is heavily loaded with SVI variables, these connectivity metrics were explored alongside poverty %, no high-school diploma %, age 65+ %, age 17- %, minority %, limited English %, single parent household %, and household crowding % using mean rank analysis to further understand the relationship.

4.6.2 Mean Rank Analysis

To prepare the data for each Mann-Whitney U Test, the sample plots were sorted into two groups for each SVI variable. Group 1 was in the lower 50^{th} percentile for each SVI variable, and Group 2 was in the upper 50^{th} percentile. Using these group designations, the Mann-Whitney U Test was conducted for each LSM to determine

Table 4.4: *PCA Rotated Component Matrix for sample plots in Phoenix, AZ.* Rotation Method: Varimax with Kaiser Normalization. Scores below |0.32| were considered a poor correlation and not included in this component matrix[10].

Variable	Component				
	1	2	3	4	5
Below Povery %	0.782				
Unemployed %					
No HS Diploma %	0.875				
Age 65+%	-0.644				
Age 17-%	0.723				
Minority %	0.904				
Limited English %	0.886				
Single Parent Household %	0.914				
Household Crowding %	0.829				
Impervious PLAND			0.837		
Barren PLAND		0.450	-0.544	0.363	
Tree PLAND		-0.832			
Shrub PLAND				0.85	
Grass PLAND					0.811
Impervious LPI			0.796		
Barren LPI		0.448	-0.554	0.395	
Tree LPI		-0.519			0.384
Shrub LPI				0.629	
Grass LPI					0.750
Impervious LSI		-0.569			-0.338
Barren LSI		-0.91			
Tree LSI		-0.843			
Shrub LSI				0.841	
Grass LSI		-0.63			
Impervious ENN_MN			-0.599		
Barren ENN_MN		0.497	0.444		
Tree ENN_MN		0.73			
Shrub ENN_MN					
Grass ENN_MN					
Impervious PLADJ			0.779		
Barren PLADJ		0.849			
Tree PLADJ	-0.465		0.356		0.390
Shrub PLADJ	-0.400			0.697	
Grass PLADJ					0.811
Impervious Cohesion			0.805		
Barren Cohesion		0.541	-0.366		
Tree Cohesion	-0.394	-0.529			0.372
Shrub Cohesion	-0.405			0.706	
Grass Cohesion					0.738
Kaiser-Meyer-Olkin Measure of Sampling Adequacy.					0.718
Bartlett's Test of Sphericity	Approx. Chi-Square				42733.359
		df			741
		Sig.			<0.001

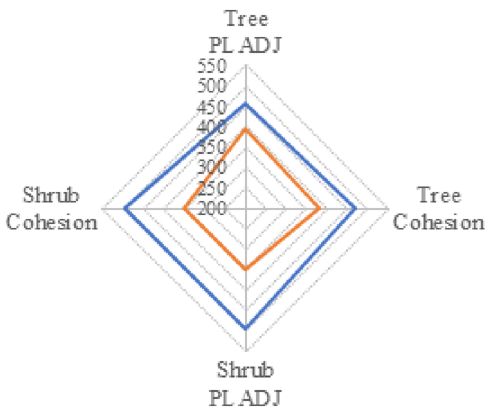

(a) Poverty

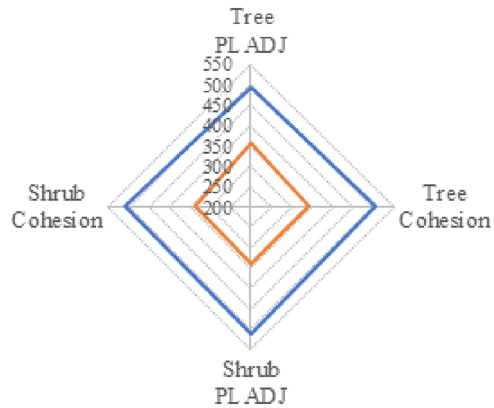

(b) No High-school Diploma

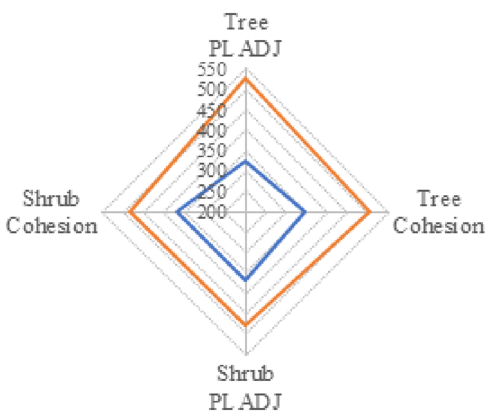

(c) Age 65+

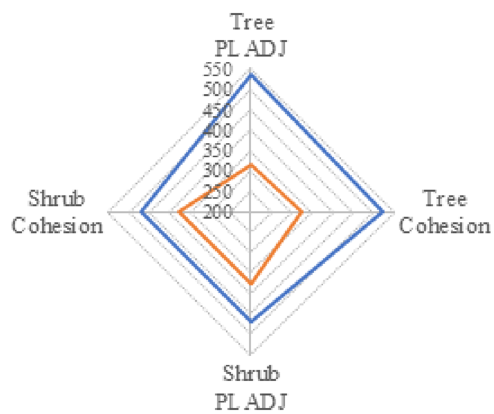

(d) Age 17-

Figure 4.11: Radar plots showing the mean rank differences of tree and shrub PLADJ and Cohesion in different vulnerability groups in PHX. Each axis is assigned a LSM examined using the Mann-Whitney U Test. Blue lines represent mean ranks of the lower 50^{th} percentile for each SVI, orange lines represent the mean ranks of the upper 50^{th} percentile group.

the mean ranks for each group and to decide whether any differences between mean rank were significant (full test results available in Appendix).

Mann-Whitney U Tests run in SPSS determined that the differences between Group 1 and Group 2 for each SVI variable was significant ($p < 0.001$) for all LSMs tested

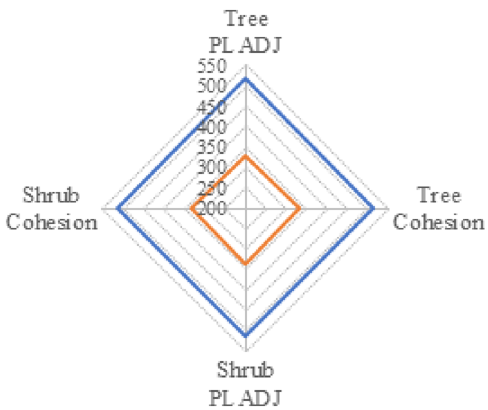

(e) Minority

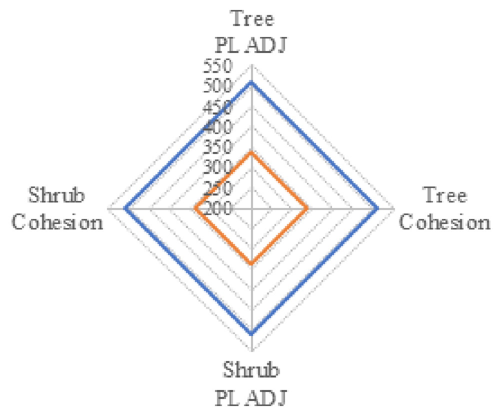

(f) Limited English

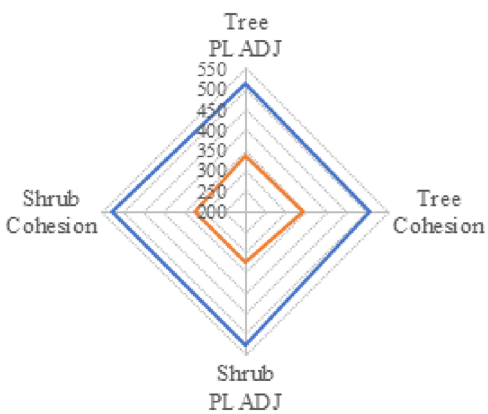

(g) Single Parent Household

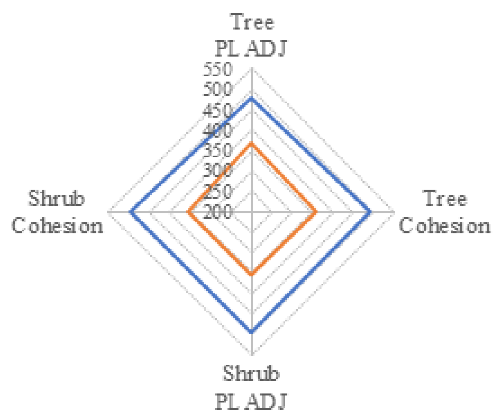

(h) Household Crowding

Radar plots showing the mean rank differences of tree and shrub PLADJ and Cohesion in different vulnerability groups in PHX. Each axis represents a LSM examined using the Mann-Whitney U Test. Blue lines represent mean ranks of the lower 50^{th} percentile for each SVI, orange lines represent the mean ranks of the upper 50^{th} percentile group (cont.).

(tree PLADJ, shrub PLADJ, tree Cohesion, and shrub Cohesion). For every variable except age 65+, Group 1 (the lower 50^{th} percentile for percentage of vulnerable plot residents) had a higher mean rank for both tree and shrub PLADJ and Cohesion than did Group 2 (the upper 50^{th} percentile for percentage of vulnerable plot residents). The inverse was true for the variable age 65+, where Group 2 had a higher mean rank. The mean rank difference was greater for both shrub LSMs than for tree LSMs in the assessments of poverty % and single parent household %, but greater for the shrub LSMs in the assessments of age 65+ %, age 17- % than the difference in mean ranks for tree based metrics. Household crowding had the smallest difference in mean rank for all LSMs, although this difference was still considered significant.

4.7 Discussion

These results support both H1 and H2, with some caveats. Mean rank analysis indicates that there are significant differences in tree and shrub PLADJ and Cohesion between the upper and lower 50^{th} percentile groups of 8 out of the 9 SVI examined ($p < 0.001$), supporting H1. Comparing the mean rank of these percentile groups, 7 out of 8 SVI have higher mean ranks of tree and shrub PLADJ and Cohesion in the lower percentile group than in the higher percentile group, supporting H2. However, the SVI Age 65+ shows an opposite, yet significant, pattern, with the higher tree and shrub PLADJ and Cohesion in the upper 50^{th} percentile group than the lower 50^{th} percentile group.

It should also be noted that, while two aggregation metrics of landscape connectivity for tree and shrub cover did exhibit relationships with SVI, none of the areal coverage metrics (PLAND or LPI) showed this same relationship. This suggests that, although there is no significant difference in how much tree and shrub coverage exists in vulnerable versus non-vulnerable areas, the way the tree and shrub cover connects is significantly different, with the trees and shrubs being better aggregated in areas with a lower percentage of their residents considered vulnerable.

An explanation for the divergence in the SVI variable Age 65+ from the other

SVI variables could be attributed to the definition of ”vulnerable” used by the CDC/ATSDR. The inclusion of this variable, in regards to the impacts of climate change, is reasonable — elderly populations are uniquely more prone to heat-related climate change impacts than other populations[37, 8]. However, the sad reality is that vulnerable populations have a shorter life span than those who are less vulnerable. The lifespans of Black Americans are both shorter and more variable than those of White Americans[17], and poverty and lack of education are both linked to disparities in life expectancy[40]. This survivor-ship bias is exhibited in the inverse relationship between population over the age of 65 and other SVI variables simply because those who have lived over the age of 65 are more likely to be less vulnerable in other regards. Regardless, this variable is important to consider when talking about climate change and, if a disparity exists, should be addressed as an EJ issue.

Comparing the differences between the mean rank of Group 1 vs. Group 2 provides several insights into the relationships between vulnerability and vegetation connectivity (Figure 4.12). Age-related SVI metrics had a larger difference between groups in tree-based LSMs than in shrub-based LSMs, although the mean rank difference between Group 1 and Group 2 was negative for the variable age 65+ |% and positive for the variable age 17- %. Variables minority %, limited English %, and No High School % all had a relatively large mean rank difference between Groups 1 and 2, and poverty % had a larger mean rank difference in shrub connectivity than tree connectivity between Group 1 and Group 2. Examining the mean rank distributions of each of these variables reveals that, although the mean rank distribution is similar in shape between groups being studied, the shape varies when comparing tree metrics with shrub metrics (Appendix B.3). Tree metrics, both PLADJ and Cohesion, exhibit a negative skew, while the shrub metrics display a complex skew, with a negative skew

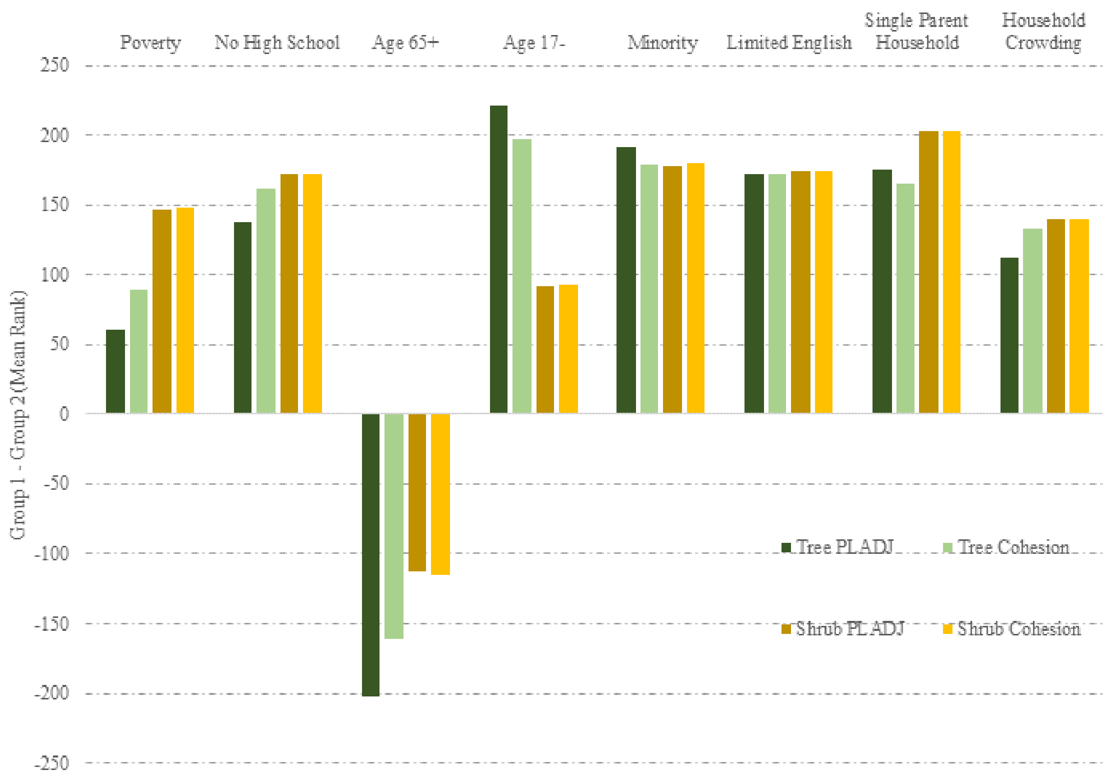

Figure 4.12: Differences in mean rank between Group 1 and Group 2 for each SVI

distorted by the number of plots that contain no shrubs and therefore exhibit zero PLADJ or Cohesion. The number of plots with this characteristic is higher in Group 2 than Group 1 for all of the SVI variables tested (except for age 65+), which likely is influencing the mean rank. This poses a challenge in interpretation: a lack of shrub coverage in vulnerable plots is an EJ issue only if there is also a lack of tree coverage, as trees provide higher levels of ecosystem services than shrubs do in regards to stormwater and heat mitigation[36]. However, as we are also seeing a disparity in tree connectivity in the plot of Group 2 for most variables, it seems that it may be a reasonable assumption that both shrubs and trees are lacking in the more vulnerable plots.

The definitions of landcover types should be considered as well when discussing these results. As Phoenix is a desert environment, land classified as barren holds a different significance than in other locations with more annual precipitation. For example, in Chapter 3, barren land was scarce and comprised very little of DC's surface area. Additionally, when it was encountered, it was anthropogenic in origin; barren land was found in construction zones, quarries, and other locations where ground was disturbed and, if that ground was left to develop without human influence, the recovery would likely transition from barren, then to grass, and eventually to tree. In Phoenix, however, the largest landcover type within the city boundaries was barren, with over 51% of the total land area (Table 4.1). It would seem that, when left without human influences, such as irrigation and cultivation, the land would default to barren, with interspersed shrub landcover, as is seen in the largely undeveloped sections within the city boundaries. This means that lack of support and funding for UGI projects will likely result in barren landcover, as opposed to grass or shrub, both of which have some cooling capacity, whereas barren landcover does not.

Current PHX UGI policy reflects the need for connectivity of UGI as well as UGI equity. The push for cool corridors in vulnerable areas is one mechanism to rectify this; however, these cool corridors will be provided along pedestrian walking routes, leaving the private property of vulnerable areas unaffected[7]. PHX's tree planting programs also target public right-of-ways, leaving private land without funding for UGI implementation. One program, the Tree Donation Program, does provide a platform, combined with the Love Your Block program, through which community members can crowd-source funding for tree plantings and other UGI projects. However, a caveat of this program is that the neighborhood improvements must be accessible to the public and, although this criterion is well-intentioned, this may prohibit the installation of UGI in much needed spaces to promote connectivity. A model similar to DC's RiverSmart Program[12], where financial incentive is provided to private property owners to replace impermeable surfaces with UGI, could work to fill the UGI connectivity gaps in vulnerable areas where PHX's current programs cannot reach.

As drought is a major concern alongside UHI in PHX, efficient use of water resources is a major concern for the metropolis. According to the 2010 landcover classification, 5.34% of PHX land area is comprised of grass, which requires significantly more water to maintain than trees do[28] and is not as effective at cooling beyond the immediate surface temperatures as trees are[2], thus being a less efficient use of water for cooling purposes. Some estimates suggest that 50% of municipal water-use in PHX is for lawns and swimming pools[15] which, while providing value to individuals for hyper-local cooling, are also primarily utilized by fewer vulnerable residents[33]. While providing more UGI to vulnerable areas may require an additional strain on water supplies, not doing so due to concerns about water supplies while still allowing residents to utilize water resources for pools and lawns would certainly constitute an EJ issue.

Considering the results of this study, 2010 PHX exhibited a disparity in UGI connectivity, where plots located in single family residential zones that were in the upper 50^{th} percentile for several SVIs, including poverty % and minority %, had significantly less connected trees and shrubs according to two aggregation metrics (PLADJ and Cohesion) than those plots in the lower 50^{th} percentile did. This could be construed as an EJ issue, where tree canopy and shrub connectivity (as a resource to mitigate UHI and flooding), are less available to more vulnerable populations. Although PHX includes both vulnerability and elements of connectivity in its plan to combat extreme heat events, the findings of this study should be included as a consideration for how best to mitigate climate change impacts equitably and efficiently.

References

[1] Phoenix 50 Years Ago: A Look Back, May 2021. URL https://kjzz.org/content/1679173/phoenix-50-years-ago-look-back.

[2] D. Armson, P. Stringer, and A.R. Ennos. The effect of tree shade and grass on surface and globe temperatures in an urban area. *Urban Forestry & Urban Greening*, 11(3):245–255, January 2012. ISSN 16188667. doi: 10.1016/j.ufug.2012.05.002. URL https://linkinghub.elsevier.com/retrieve/pii/S1618866712000611.

[3] Lawrence A. Baker, Anthony J. Brazel, Nancy Selover, Chris Martin, Nancy McIntyre, Frederick R. Steiner, Amy Nelson, and Laura Musacchio. Urbanization and warming of Phoenix (Arizona, USA): Impacts, feedbacks and mitigation. *Urban Ecosystems*, 6(3):183–203, 2002. ISSN 10838155. doi: 10.1023/A:1026101528700. URL http://link.springer.com/10.1023/A:1026101528700.

[4] Bob Bolin, Sara Grineski, and Timothy Collins. The Geography of Despair: Environmental Racism and the Making of South Phoenix, Arizona, USA. *Human Ecology Review*, 12(2):156–168, 2005. ISSN 10744827, 22040919. URL http://www.jstor.org/stable/24707530. Publisher: Society for Human Ecology.

[5] Jean Léon Boucher, Anthony M. Levenda, Caleb Carpenter, Jorge Morales-Guerrero, and Darshan M. A. Karwat. Environmental justice in Phoenix, Arizona: a neighbourhood deficit and asset score. *Local Environment*, 26(6):692–718, June 2021. ISSN 1354-9839, 1469-6711. doi: 10.1080/13549839.2021.1916899. URL https://www.tandfonline.com/doi/full/10.1080/13549839.2021.1916899.

[6] City of Phoenix. Tree and Shade Master Plan. Technical report, 2010. URL https://www.phoenix.gov/parkssite/Documents/PKS_Forestry/PKS_Forestry_Tree_and_Shade_Master_Plan.pdf.

[7] City of Phoenix. Climate Action Plan. Technical report, Phoenix, AZ, September 2021. URL https://www.phoenix.gov/oepsite/Documents/2021ClimateActionPlanEnglish.pdf.

[8] Stephanie E. Cleland, William Steinhardt, Lucas M. Neas, J. Jason West, and Ana G. Rappold. Urban heat island impacts on heat-related cardiovascular morbidity: A time series analysis of older adults in US metropolitan areas. *Environment International*, 178:108005, August 2023. ISSN 01604120. doi: 10.1016/j.envint.2023.108005. URL https://linkinghub.elsevier.com/retrieve/pii/S0160412023002787.

[9] Climate Check. Phoenix, Arizona Climate Change Risks and Hazards: Heat, Flood. URL https://climatecheck.com/arizona/phoenix.

[10] Andrew L. Comrey and Howard B. Lee. *A First Course in Factor Analysis*. Psychology Press, 0 edition, November 2013. ISBN 978-1-315-82750-6. doi: 10.4324/9781315827506. URL https://www.taylorfrancis.com/books/9781317844075.

[11] Dana Anderson. Homebuyers Must Earn $115,000 to Afford the Typical U.S. Home. That's About $40,000 More Than the Typical American Household Earns, October 2023. URL https://www.redfin.com/news/homebuyer-income-afford-home-record-high/.

[12] DDOE. Sustainable DC 2.0. Comprehensive Plan, Department of Energy & Environment, Washington, D.C., April 2019.

[13] Deloitte and Datawheel. Data USA. URL https://datausa.io/.

[14] Noah S. Diffenbaugh and Moetasim Ashfaq. Intensification of hot extremes in the United States. *Geophysical Research Letters*, 37(15), 2010. ISSN 1944-8007. doi: 10.1029/2010GL043888. URL https://onlinelibrary.wiley.com/doi/abs/10.1029/2010GL043888. _eprint: https://agupubs.onlinelibrary.wiley.com/doi/pdf/10.1029/2010GL043888.

[15] Dr. Biology. How much water are we using per year in the Phoenix area?, May 2017. URL https://askabiologist.asu.edu/questions/how-much-water-are-we-using-year-phoenix-area.

[16] Edward H Bennett and W. E. Parsons. Phoenix Arizona: Map of the City and Vicinity Showing Complete Development, 1921. URL https://www.roguecolumnist.com/.a/6a00e54fdb30b9883402788047ed90200d-800wi.

[17] Glenn Firebaugh, Francesco Acciai, Aggie J. Noah, Christopher Prather, and Claudia Nau. Why Lifespans Are More Variable Among Blacks Than Among Whites in the United States. *Demography*, 51(6):2025–2045, December 2014. ISSN 0070-3370, 1533-7790. doi: 10.1007/s13524-014-0345-2. URL https://read.dukeupress.edu/demography/article/51/6/2025/169383/Why-Lifespans-Are-More-Variable-Among-Blacks-Than.

[18] Francis Chantree. Where Is Building A Home Cheaper Than Buying? Western & South Atlantic States, With California In The Lead, February 2023. URL https://www.storagecafe.com/blog/is-it-cheaper-to-build-or-buy-a-house-in-the-us/.

[19] A. W. Franklin and Theo L. Schultz. Map of Salt River Valley, Arizona, 1892.

URL https://www.roguecolumnist.com/.a/6a00e54fdb30b988340278803f3f86200d-pi.

[20] G. Garfin, G. Franco, H. Blanco, A. Comrie, P. Gonzalez, T. Piechota, R. Smyth, R. Waskom, J.M. Melillo, Terese (T.C.) Richmond, and G. W. Yohe. Ch. 20: Southwest. Climate Change Impacts in the United States: The Third National Climate Assessment. Technical report, U.S. Global Change Research Program, 2014. URL https://nca2014.globalchange.gov/downloads.

[21] Geospatial Research, Analysis, and Services Program. CDC/ATSDR Social Vulnerability Index 2010 Database, Arizona, 2010.

[22] Carol E. Heim. Leapfrogging, Urban Sprawl, and Growth Management: Phoenix, 1950-2000. *The American Journal of Economics and Sociology*, 60(1):245–283, 2001. ISSN 0002-9246. doi: 10.1111/1536-7150.00063. URL https://www.jstor.org/stable/3487953. Publisher: [American Journal of Economics and Sociology, Inc., Wiley].

[23] J. Brett Hill, Jeffery J. Clark, William H. Doelle, and Patrick D. Lyons. Prehistoric Demography in the Southwest: Migration, Coalescence, and Hohokam Population Decline. *American Antiquity*, 69(4):689–716, October 2004. ISSN 0002-7316, 2325-5064. doi: 10.2307/4128444. URL https://www.cambridge.org/core/product/identifier/S0002731600050964/type/journal_article.

[24] Andrew Jones, Destenie Nock, Constantine Samaras, Yueming (Lucy) Qiu, and Bo Xing. Climate change impacts on future residential electricity consumption and energy burden: A case study in Phoenix, Arizona. *Energy Policy*, 183: 113811, December 2023. ISSN 0301-4215. doi: 10.1016/j.enpol.2023.113811.

URL https://www.sciencedirect.com/science/article/pii/S0301421523003968.

[25] Julia K. Johnson, Stephen J. Reynolds, and David A. Jones. Geologic Map of the Phoenix Mountains, Central Arizona. Arizona Geological Survey Digital Geologic Map 28, 2003. URL http://reynolds.asu.edu/pubs/DGM28_phx_mtns_text_8x11.pdf.

[26] Markus Kottek, Jürgen Grieser, Christoph Beck, Bruno Rudolf, and Franz Rubel. World Map of the Köppen-Geiger climate classification updated. *Meteorologische Zeitschrift*, 15(3):259–263, July 2006. ISSN 0941-2948. doi: 10.1127/0941-2948/2006/0130. URL http://www.schweizerbart.de/papers/metz/detail/15/55034/World_Map_of_the_Koppen_Geiger_climate_classificat?af=crossref.

[27] League of Arizona Cities and Towns. Council-Manager Government in Arizona. Technical report, Phoenix, AZ, June 2018. URL https://azleague.org/ArchiveCenter/ViewFile/Item/199.

[28] E. Litvak, K. F. Manago, T. S. Hogue, and D. E. Pataki. Evapotranspiration of urban landscapes in Los Angeles, California at the municipal scale. *Water Resources Research*, 53(5):4236–4252, 2017. ISSN 1944-7973. doi: 10.1002/2016WR020254. URL https://onlinelibrary.wiley.com/doi/abs/10.1002/2016WR020254. _eprint: https://agupubs.onlinelibrary.wiley.com/doi/pdf/10.1002/2016WR020254.

[29] Bradford Luckingham. Urban Development in Arizona: The Rise of Phoenix. *The Journal of Arizona History*, 22(2):197–234, 1981. URL https://www.jstor.org/stable/41859493.

[30] Bradford Luckingham. *Minorities in Phoenix: A Profile of Mexican American, Chinese American, and African American Communities, 1860-1992*. University of Arizona Press, 1994. ISBN 978-0-8165-1457-1. URL https://www.jstor.org/stable/j.ctt1bmzkbf.

[31] Maricopa County. Floodplain and Elevation Certificate Viewer. URL https://maricopa.maps.arcgis.com/apps/webappviewer/index.html?id=f1fd72bdc75f4b3982e0058f1beba159.

[32] Melikamp. English: Downtown of Phoenix AZ from an airplane. The mountain in the center is Piestewa Peak. : , . ., November 2011. URL https://commons.wikimedia.org/wiki/File:Phoenix_AZ_Downtown_from_airplane_(cropped).jpg.

[33] Jacob Napieralski, Catherine Sulich, Audrey Taylor, and Paul Draus. Mapping the link between outdoor water footprint and social vulnerability in Metro Phoenix, AZ (USA). *Landscape and Urban Planning*, 226:104498, October 2022. ISSN 01692046. doi: 10.1016/j.landurbplan.2022.104498. URL https://linkinghub.elsevier.com/retrieve/pii/S0169204622001475.

[34] Oak Ridge National Laboratory. Prison Boundaries, September 2020. URL https://hifld-geoplatform.opendata.arcgis.com/.

[35] Daniel H. Phillips, Yvonne Reinink, Timothy E. Skarupa, Charles. E. Ester, and Jon A. Skindlov. Water resources planning and management at the Salt River Project, Arizona, USA. *Irrigation and Drainage Systems*, 23(2-3):109, August 2009. ISSN 0168-6291, 1573-0654. doi: 10.1007/s10795-009-9063-0. URL http://link.springer.com/10.1007/s10795-009-9063-0.

[36] Haihong Qiu, Jiaying Zhang, Hairong Han, Xiaoqin Cheng, and Fengfeng Kang. Study on the impact of vegetation change on ecosystem services in the Loess Plateau, China. *Ecological Indicators*, 154:110812, October 2023. ISSN 1470160X. doi: 10.1016/j.ecolind.2023.110812. URL https://linkinghub.elsevier.com/retrieve/pii/S1470160X23009548.

[37] Nurfatehar Ramly, Rozita Hod, Mohd Rohaizat Hassan, Mohd Hasni Jaafar, Zaleha Isa, and Rohaida Ismail. Identifying Vulnerable Population in Urban Heat Island: A Literature Review. *International Journal of Public Health Research*, 13(2), September 2023. ISSN 2232-0245. doi: 10.17576/ijphr.1302.2023.02.07. URL https://spaj.ukm.my/ijphr/index.php/ijphr/article/view/422. Number: 2.

[38] Russell Lopez. Urban Sprawl in the United States: 1970-2010. *Cities and the Environment*, 7(1), 2014.

[39] Noah M Schmadel and Judson W Harvey. NHD-RC: Extension of NHDPlus Version 2.1 with high-resolution river corridor attributes, 2020. URL https://www.sciencebase.gov/catalog/item/5f8e091d82ce3241879215a7.

[40] Gopal K. Singh and Hyunjung Lee. Marked Disparities in Life Expectancy by Education, Poverty Level, Occupation, and Housing Tenure in the United States, 1997-2014. *International Journal of Maternal and Child Health and AIDS*, 10 (1):7–18, 2021. ISSN 2161-8674. doi: 10.21106/ijma.402. URL https://www.ncbi.nlm.nih.gov/pmc/articles/PMC7792745/.

[41] SUMAN NAISHADHAM. Arizona to cancel leases allowing Saudi-owned farm access to state's groundwater. *AP News*, October 2023. URL https://apnews

.com/article/saudi-arabia-drought-arizona-alfalfa-water-agriculture-0d13957edaf882690e15c0bd9ccfa59f.

[42] TNC. Economic Assessment of Heat in the Phoenix Metro Area. Technical report, Phoenix, AZ, 2021.

[43] United States Census Bureau. U.S. Census Bureau QuickFacts: United States. URL https://www.census.gov/quickfacts/fact/table/DC,newyorkcitynewyork,oaklandcountymichigan,detroitcitymichigan,phoenixcityarizona,US/PST045222.

[44] United States EPA. Water Quality Scorecord: Incorporating Green Infrastructure Practices at the Municipal, Neighborhood, and Site Scales. Technical Report EPA 231B09001, United States Environmental Protection Agency, Washington, D.C., October 2009. URL https://www.epa.gov/sites/default/files/2014-04/documents/water-quality-scorecard.pdf.

[45] United States EPA. Green Infrastructure Barriers and Opportunities in Phoenix, Arizona: An Evaluation of Local Codes and Ordinances. Technical Report 830-R-13-005, United States Environmental Protection Agency, Phoenix, AZ, August 2013. URL https://www.epa.gov/sites/default/files/2015-10/documents/phoenix_gi_evaluation.pdf.

[46] United States EPA. Green Infrastructure Checklists and Renderings: Tools to Assist Local Governments in Promoting and Implementing Green Infrastructure Practices. Technical Report EPA 832-R-16-006, United States Environmental Protection Agency, Denver, CO, September 2016.

[47] University of Nebraska-Lincoln, United States Department of Agriculture, and National Oceanic and Atmospheric Administration. U.S. Drought Monitor, 2024.

URL https://droughtmonitor.unl.edu/CurrentMap/StateDroughtMonitor.aspx?fips_04007.

[48] NOAA US Department of Commerce. Climate, 2022. URL https://www.weather.gov/wrh/Climate?wfo=lwx. Publisher: NOAA's National Weather Service.

[49] US Environmental Protection Agency. EnviroAtlas – Phoenix, AZ – Meter-Scale Urban Land Cover (MULC) Data (2010), September 2017.

[50] Philip R. VanderMeer. *Desert visions and the making of Phoenix, 1860-2009*. University of New Mexico Press, Albuquerque, 2010. ISBN 978-0-8263-4893-7. OCLC: 759158345.

[51] Matthew C. Whitaker. The Rise of Black Phoenix: African-American Migration, Settlement and Community Development in Maricopa County, Arizona 1868-1930. *The Journal of Negro History*, 85(3):197–209, July 2000. ISSN 0022-2992, 2325-6842. doi: 10.2307/2649077. URL http://www.journals.uchicago.edu/doi/10.2307/2649077.

[52] Dave D. White, Emile H. Elias, Kathryn A. Thomas, Cristina E. Bradatan, Mark W. Brunson, Ann Marie Chischilly, Carolyn A.F. Enquist, Leah R. Fisher, Halley E. Froehlich, Elizabeth A. Koebele, Michael Méndez, Steven M. Ostoja, Caitriana Steele, and Jennifer K. Vanos. Ch. 28. Southwest. Technical report, U.S. Global Change Research Program, Washington, DC, 2023. URL https://nca2023.globalchange.gov/chapter/28/. Publication Title: Fifth National Climate Assessment.

[53] C. Wobus, C. Zarakas, P. Malek, B. Sanderson, A. Crimmins, M. Kolian, M. Sarofim, and C. P. Weaver. Reframing Future Risks of Extreme

Heat in the United States. *Earth's Future*, 6(9):1323–1335, 2018. ISSN 2328-4277. doi: 10.1029/2018EF000943. URL https://onlinelibrary.wiley.com/doi/abs/10.1029/2018EF000943. _eprint: https://onlinelibrary.wiley.com/doi/pdf/10.1029/2018EF000943.

[54] Yuanhui Zhu, Soe W. Myint, Xin Feng, and Yubin Li. An Innovative Scheme to Confront the Trade-Off Between Water Conservation and Heat Alleviation With Environmental Justice for Urban Sustainability: The Case of Phoenix, Arizona. *AGU Advances*, 4(1):e2022AV000816, February 2023. ISSN 2576-604X, 2576-604X. doi: 10.1029/2022AV000816. URL https://agupubs.onlinelibrary.wiley.com/doi/10.1029/2022AV000816.

[55] Xiaoding Zhuo, Christopher G. Boone, and Everett L. Shock. Soil Lead Distribution and Environmental Justice in the Phoenix Metropolitan Region. *Environmental Justice*, 5(4):206–213, August 2012. ISSN 1939-4071, 1937-5174. doi: 10.1089/env.2011.0041. URL http://www.liebertpub.com/doi/10.1089/env.2011.0041.

Chapter 5

Detroit, MI, USA

Figure 5.1: Aerial view of Southwest Detroit, taken in 2015.[35]

5.1 Introduction

The city of Detroit, MI was chosen for this study because of its unique history. The city, as a major industrial hub for the automotive industry, saw an incredible boom in population during the early 20th century. This was followed by a collapse towards the end of the 20th century, with a decline in population from approximately 1,850,000 residents in 1950 to just over 670,000 residents in 2015[13]. This decline was attributed to two factors: the decentralization and volatility of the automotive industry driving workers away from the city for better opportunities and racial tensions combined with a political structure that enabled white workers with means to leave the city in exchange for the more homogeneously white suburbs[50]. The latter phenomenon, colloquially known as ”the White Flight”, occurred in many US cities during this time period.

Detroit’s decline in population and the associated migration to satellite city suburbs has had impacts that extend beyond simple population changes. ”Legacy Cities[1]” such as Detroit experience fiscal distress leading to crippled city services, property abandonment, and a myriad of other issues[77], limiting the city’s ability to cope with the impacts of climate change through urban improvement such as UGI. For this reason, Detroit makes an excellent case study for UGI connectivity and EJ.

In order to adequately consider Detroit for this study, given its history of racially driven migration from the city into surrounding suburbs, it is imperative to compare UGI placement within Detroit with that of its suburbs. For this study, cities within Oakland County, MI were also included to encompass the Detroit Metro Area (DMA). Although, semi-officially, the label ”Detroit Metropolitan Area” would also include the counties of Wayne County and Macomb County, this study will only look at Detroit City and cities within Oakland, due to availability of zoning data. From here onward, the acronym DMA will refer to these cities collectively, and the city of Detroit will be referred to as ”Detroit” and the cities within Oakland County as ”Oakland County” when distinguishing differences between the two areas.

[1] Legacy cities are characterized by a notable decline in industry and manufacturing jobs since the mid-twentieth century, leading to depopulation as residents moved en masse to suburban areas[6].

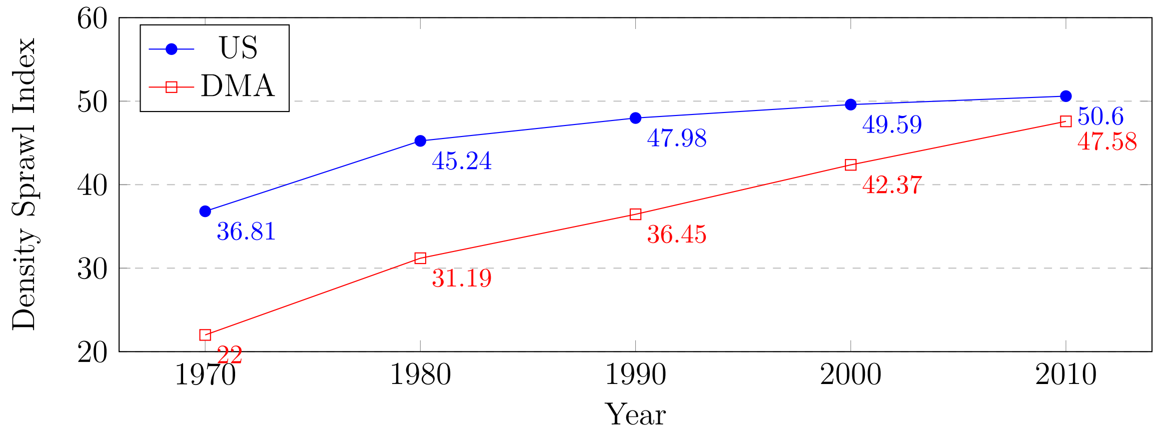

Figure 5.2: Density Sprawl Index for Detroit Metropolitan Statistical Area (including Detroit, Livonia, and Warren, MI), compared with the US Average, from 1970-2010[67].

5.2 Geography and Climate

DMA is located in the US state of Michigan near the nexus of two Great Lakes: Lake Huron to the northeast, and Lake Erie to the East. In this nexus, and just to the northeast of DMA, is a smaller lake, Lake St. Clair, and the river that connects all three, the Detroit River, is located to the southeast of DMA. On the northwestern side of the Detroit River is DMA, and the northeastern side is not just another city, but another country: Windsor, Ontario, Canada. The border between the US and Canada runs along the center of the Detroit River, with no land being shared between the two countries. The two countries are connected by three conduits: the Ambassador Bridge, the Detroit-Windsor Tunnel, and the Michigan Central Railway Tunnel.

DMA's proximity to the Detroit River provides a gradual slope from the northwest to southeast, with the majority of the smaller rivers flowing in this direction, the largest of which is the Rogue River[70]. This slope is punctuated by the Detroit Moraine, a glacial moraine that runs roughly perpendicular to the Detroit River[82]. Moving to the northwest, away from the Detroit River, the terrain becomes morainal upland

Table 5.1: Total percent landcover calculations for each landcover class in Detroit Metro Area. Table shows the total for all cities in the region, the cities only located in Oakland County, and the city of Detroit as separate columns.

	DMA Total	Cities in Oakland County	Detroit
Water	2.7%	2.5%	3.1%
Impervious	40.9%	38.9%	44.9%
Barren	3.0%	3.9%	1.3%
Tree Canopy	40.9%	44.0%	34.9%
Grass/Shrub	12.6%	10.9%	15.8%

with frequent kettle lakes as the elevation increases.

The DMA region has been experiencing increased sprawl since 1970; currently, the region is nearing the US average DSI after more than doubling this metric, from 22 in 1970 to 47.58 in 2010[48] (Figure 5.2). This is likely linked to the exodus of residents out of Detroit, chasing work in new automotive plants outside the city and fleeing from racial tensions[5]. This sprawl spread outward from Detroit city, with pockets of denser housing surrounding the satellite cities, such as Pontiac, Birmingham, and Royal Oak in Oakland County[44].

The percent landcover of impervious and tree canopy for cities in Oakland County and the City of Detroit are similar, with Detroit having slightly more impervious and slightly less tree canopy than cities in Oakland County (Table 5.1). In Oakland County, impervious surfaces are clustered within city boundaries, following major roadways. In Detroit, the highest concentration of impervious surfaces is in the Downtown district (Figure 5.3).

DMA has a hot-summer humid continental climate, Köppen climate classification Dfa[42]. Mean monthly temperatures peak in July at 28.7°C, and are coldest in January, at 0.8°C (Figure 5.4). The city of Detroit is afflicted by UHI during the

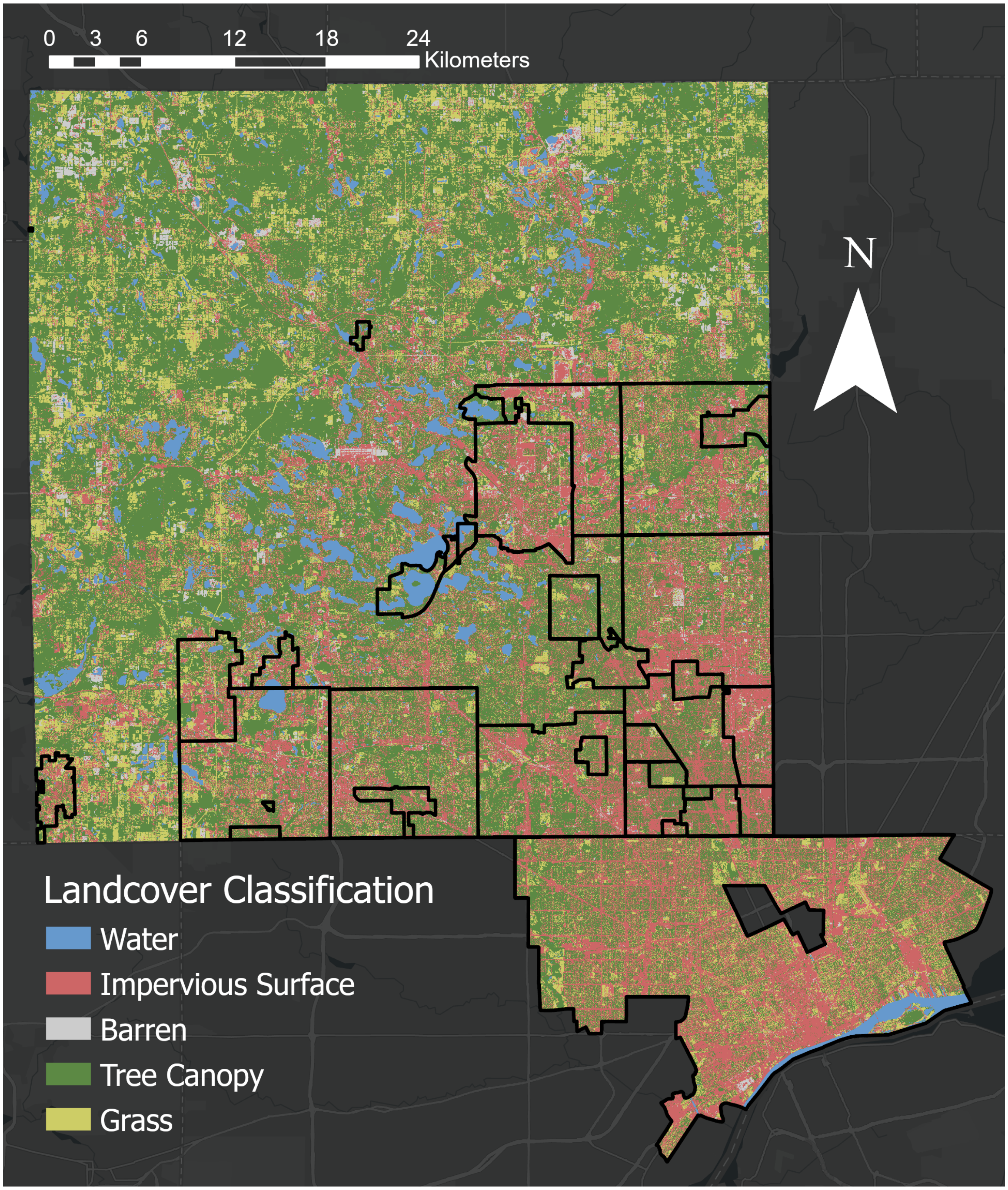

Figure 5.3: 1m landcover classification for DMA, MI. The black borders indicate city boundaries.

summer months, with estimates of 86% of its neighborhoods being over 4°C hotter due to UHI[22].

Monthly average precipitation increases in the summer months, peaking in May with a mean monthly average of 95 mm (Figure 5.5). This average is similar to that of the surrounding rural areas; however, the delivery of this precipitation differs, with DMA receiving about 20% more precipitation in the summer months than the surrounding rural areas, and less during the winter months[69].

5.2.1 Projected Climate Change

Since 1960, Detroit has experienced a warming trend of approximately 0.2°C per decade, with projected increases in average temperatures across all seasons compared to the 1980-2009 averages[38]. The number of extreme heat days is anticipated to

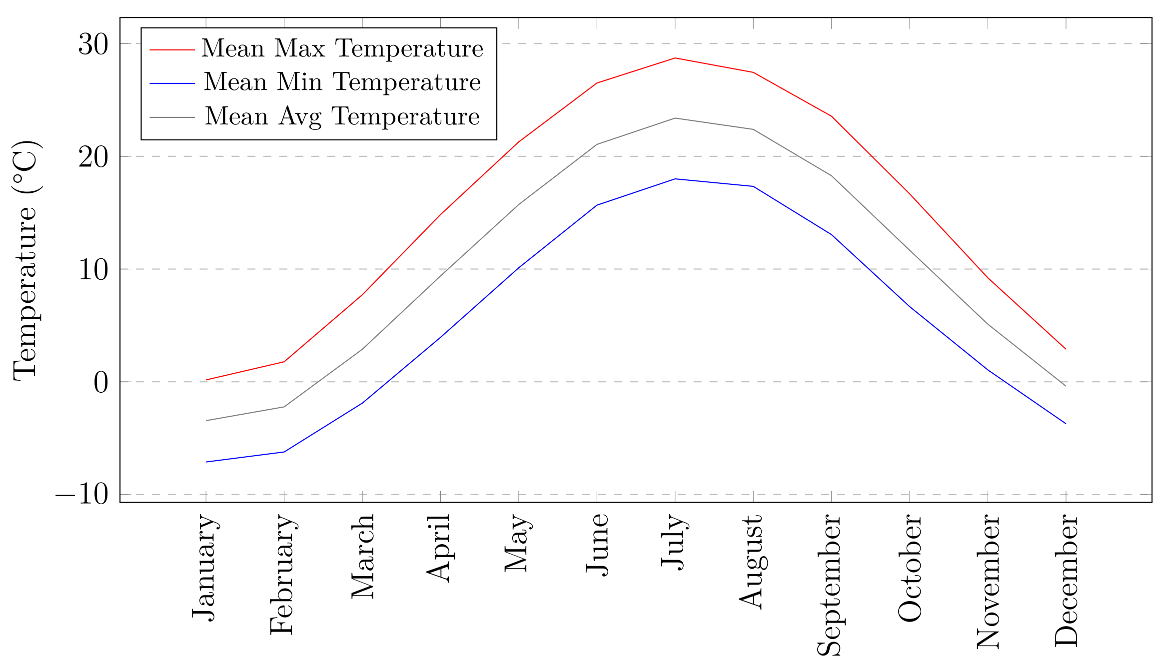

Figure 5.4: Monthly Climate Normal Temperatures for Detroit Metropolitan Area[80].

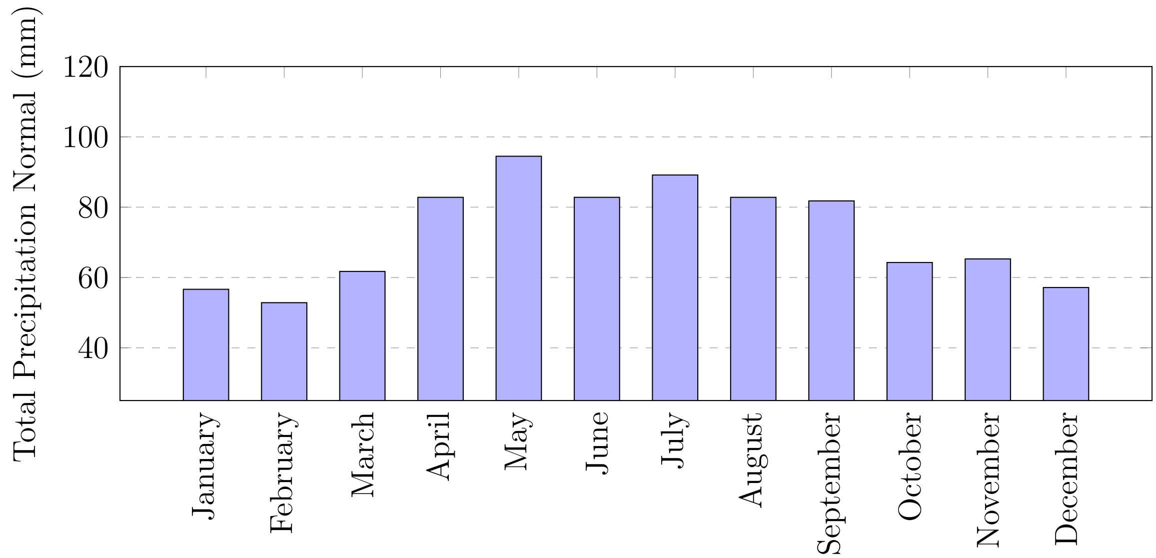

Figure 5.5: Monthly Average Total Precipitation for Detroit Metropolitan Area [80].

increase from 9 per year (the average between 1975 and 1999) to 15 per year by 2045, potentially increasing the number of summertime heat-related deaths per year by over 330%[39]. While daytime temperature averages have increased since 1975, nighttime temperatures have also rapidly increased[38]. This phenomenon is concerning, as extreme nighttime temperatures are closely linked to heat-related mortality and illness[49].

Precipitation has also been on the rise, increasing by 24 mm per decade during the same period. Spring precipitation is anticipated to continue increasing under various climate scenarios. Furthermore, heavy precipitation events are forecasted to intensify and occur more frequently. With the warming climate, precipitation events are less likely to be rain than snow, saving on snow-removal costs for the city but potentially contributing to flooding[43]. Detroit has already experienced cases of extreme flooding in modern times, most notably in 2020, when a stalled low-pressure system dropped 7-10 cm of rain on the area. This event overwhelmed the city's infrastructure, leading to flooding of over 1m in some areas[34, 54].

Table 5.2: A collection of basic information on Detroit Metropolitan Area.

	Detroit	Oakland County
Land Area	370.1 km^2	2,350 km^2
Population[1]	620,376	1,269,431
Per capita income[2]	$22,861	$53,157
Median household income[3]	$37,761	$92,620
Percent persons in poverty	31.5%	8.2%

[a] Population estimates base, July 1, 2022[78]
[b] In the past 12 months (in 2022 USD, 2018-2022)[78]
[c] In 2022 USD, 2018-2022[78]

5.3 Socio-demographic Landscape

Considering the history of DMA and the nature of this study's methods, the socio-demographic landscape of DMA should be examined in two parts: inner-city Detroit and cities within Oakland County. Overall, Oakland County has a lower percent of people in poverty, a higher per capita income, and a higher median household income than does the city of Detroit (Table 5.2). Oakland county also has a higher population than does Detroit, with over 1 million residents in total. It should be noted, however, that not all of these residents are located within the city boundaries examined by this study.

The city of Detroit can be generally divided into three parts in regards to socio-demographic make-up (Figure 5.6). The northwestern and northeastern portions, on either side of Hamtramck[2], have a relatively high percentage of both minority residents and residents below the poverty threshold. Southwestern Detroit has a high percentage of residents under the poverty threshold, as do some of the districts just

[2]Hamtramck is a city that is completely within Detroit's city boundaries but has resisted annexation. The city was historically a polish immigrant enclave, but in recent years has seen an influx of Middle Eastern immigrants. Although an interesting study in its own right, it is considered an outlier in the context of this study and therefore will not be included[84, 72]

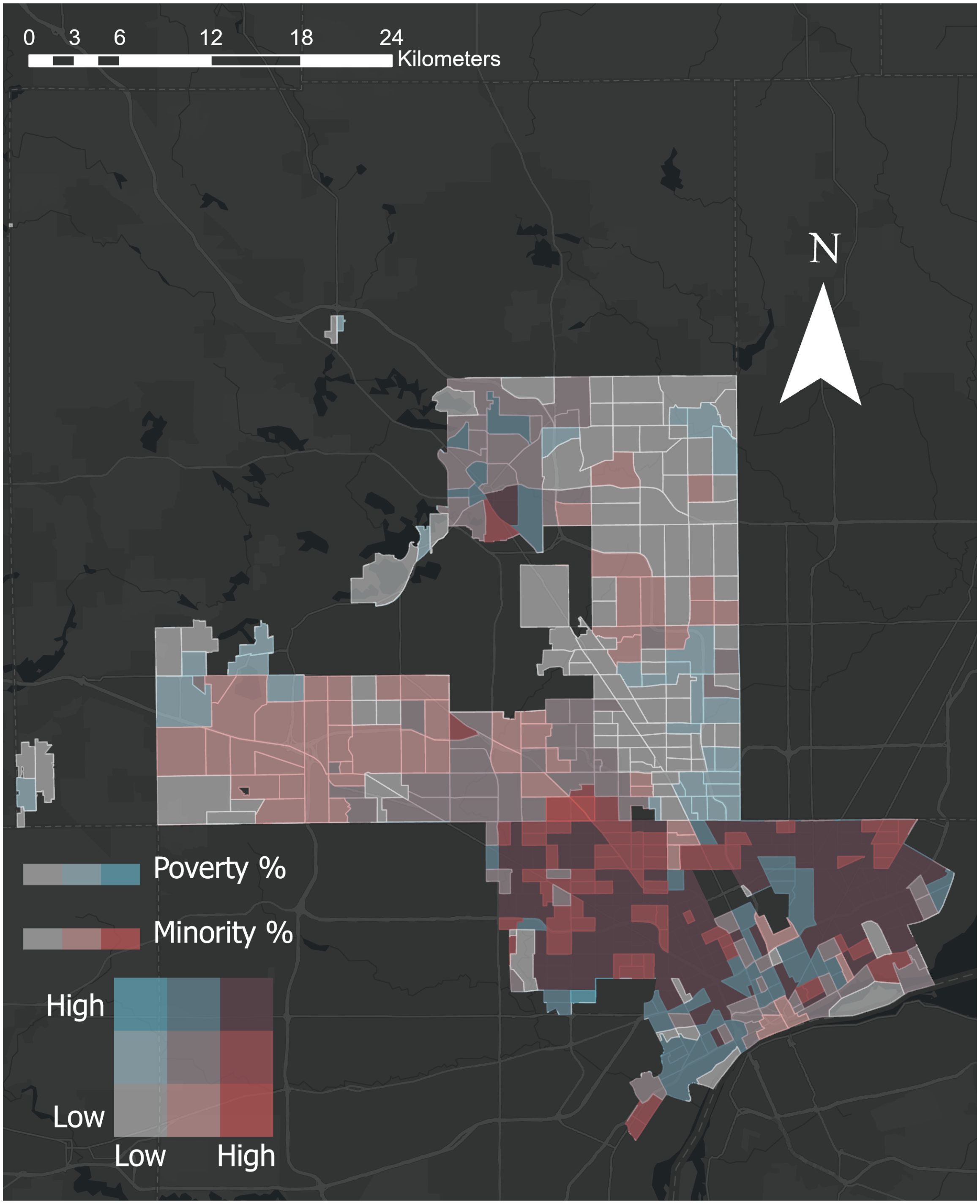

Figure 5.6: Bivariate choropleth showing the percentage of population that is a minority (shades of red) against the percentage of population that is under the poverty threshold (shades of blue) in the Detroit Metropolitan Area. Only census tracts that are within the city boundaries examined by this study are included in this image. Data collected from 2020 CDC SVI[11]

south of Hamtramck and north of the Downtown district. The Downtown district along the waterfront has the lowest percentage of both residents below the poverty threshold and minority residents.

Cities within Oakland County also exhibit a fractionalization in socio-demography. The cities in the east of Oakland County (i.e. the cities of Rochester, Rochester Hills, Bloomfield Hills, and Birmingham) have relatively low percentages of minority residents and residents below the poverty threshold. Moving west, percentages of minority residents and residents below the poverty threshold increase, but still remain low relative to Detroit (i.e the cities of Farmington, Farmington Hills, and Willowbrook). The one exception is the city of Pontiac, which contains a high concentration of both minority residents and residents in poverty.

5.4 Political History

This section will explore the history of DMA through the lens of the growth of Detroit. Although the cities in Oakland County have their own unique origin stories, their development and growth during the 1800s was closely tied to Detroit, its industry, and its location as a port city[36, 83]. Therefore, this section will focus primarily on Detroit's history, with the understanding that, although not explicitly explored through this study, the histories of Oakland County's cities are closely linked to that of Detroit.

Prior to the European settlement of Detroit, the DMA region was inhabited by a tribe of indigenous people of the Iroquois language group known as the Attawandaron[83]. Called the Neutral Nation due to the tribe's inclination to remain neutral and trade with the warring tribes of the Wyandot Nation of Georgian Bay and the Haudenosaunee

Nation of what is now western New York State, the Attawandaron were decimated during the Beaver Wars[3], when the Haudenosaunee turned on the Attawandaron after defeating the Wyandot during the mid 17th century. With the 1701 signing of the Great Peace of Montreal, the Beaver Wars were ended and French explorer Antoine de la Mothe, sieur de Cadillac pushed west from Montreal to explore the Great Lakes. Eventually, he founded Fort Pontchartrain du Détroit, a French fur trading outpost that would later become Detroit[83]. At this time, the tribes in the region were a hodgepodge of representatives of different tribes, a result of the fallout from the Beaver Wars.

The fort remained under French control until 1760, when it was ceded to the British following the French and Indian War[83]. The British held Detroit even after the Treaty of Paris ended the American Revolutionary War. In 1794 the Jay Treaty was signed, initiating the British withdrawal from the Great Lakes region as a means to avoid war and facilitate trade between the US and the British. Following this, Detroit was under US control as a part of its Michigan Territory[83]. In 1805, a fire burned almost all of Detroit, and the city's roughly 600 residents began to plan and build a village that would become the modern city of Detroit[36].

In post-1805 Detroit, Judge Augustus Brevoort Woodward created a plan where the narrow village streets of French-occupied Detroit were replaced with wider avenues that radiated outward from central nodes (Figure 5.7), inspired by the L'Enfant Plan of DC[52, 36]. This was partially adopted, with modifications more closely following a gridiron plan.

The population of Detroit did not grow rapidly until the opening of the Erie Canal

[3] The Beaver Wars were a series of conflicts fought primarily between the Haudenosaunee and the Wyandot. Allies of the Wyandot included the Algonquin tribes France[7].

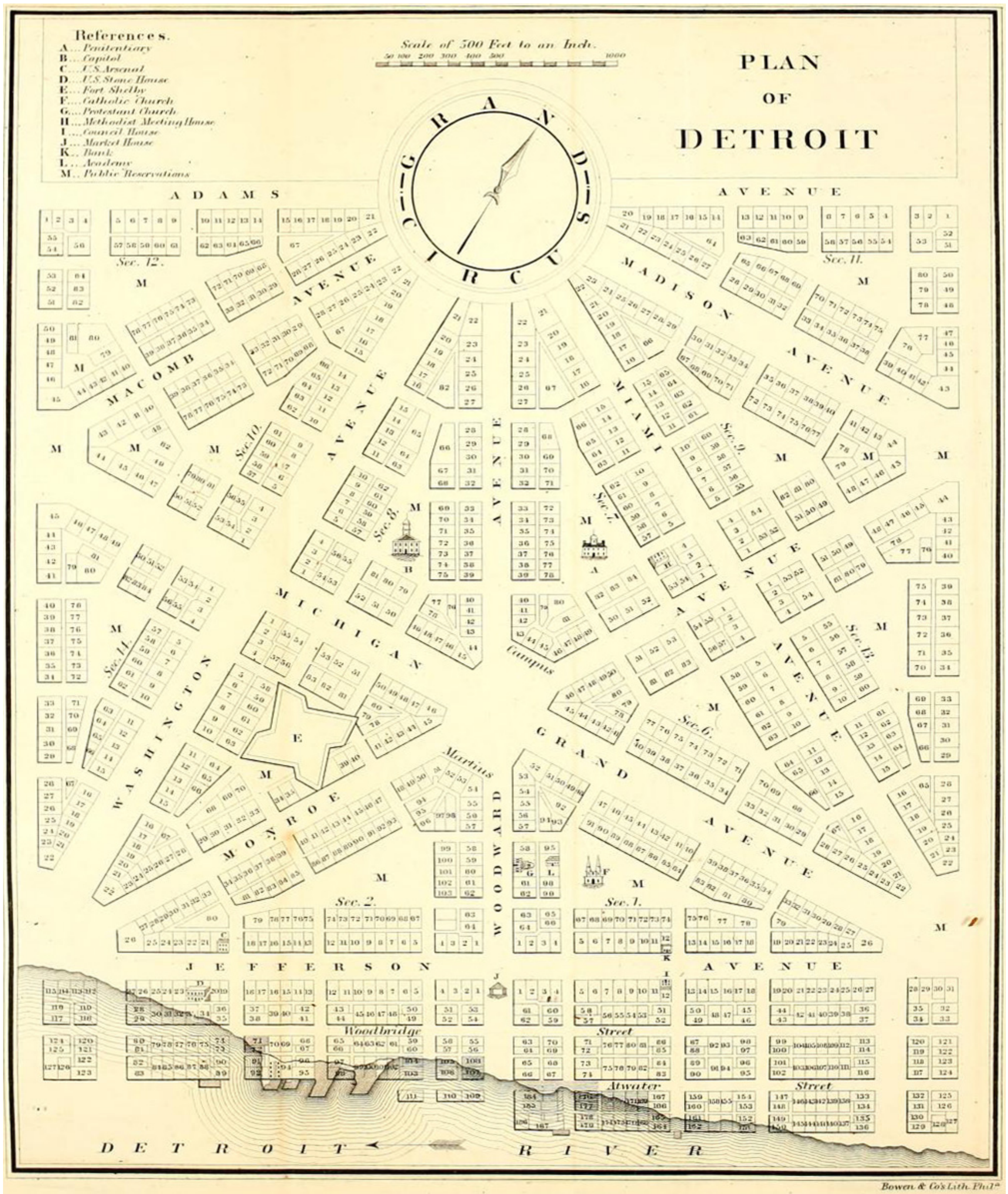

Figure 5.7: The Woodward Plan for the City of Detroit was inspired by the hub-and-spoke design of the L'Enfant Plan of Washington, DC[1]. This plan was partially adopted and combined with a gridiron plan.

in 1825, which facilitated trade and immigration from the East Coast of the US to the Great Lakes region[83]. Prior to the canal's construction, the population of Detroit grew from a population of about 600[36] in 1805 to 1,110 in 1819[83]. By 1830, five years after the Erie Canal opened, the population had grown to 2,222, and continued to boom, growing to 45,619 by 1860. Detroit became a transportation hub, and industry began to blossom in the city. The discovery of large iron deposits in the upper peninsula of Michigan in 1844 added fuel to the growth of industry in Detroit, and soon Detroit was known for the manufacturing of train parts and cast iron stoves[83].

The invention and subsequent mass production of the automobile in the late 1800s and early 1900s brought Detroit to a new level of industrial productivity. The early 20th century saw the establishment of automotive giants like the General Motors Company, the Ford Motor Company, and the Chrysler Corporation, and these automobile manufacturers brought in thousands of new residents in search of employment and opportunities[83]. The resulting second boom of Detroit increased the population from 285,704 residents in 1900 to 993,678 residents in 1920. The automotive industry flourished, with ample skilled labor, a robust network of transportation that included water and railways, and a continuous supply of iron from northern Michigan.

Following WWI, Detroit continued to see prosperity through the 1920s, until the stock market crash of 1929 that preceded the Great Depression. At this point, the automotive industry was beginning to decentralize, as this was beneficial to the production process[55]. The Great Depression greatly impacted Detroit's economy and industry, and the auto industry cut production dramatically and laid-off thousands of Detroit workers[83]. The city was in turmoil during the early 1930s, but through New Deal policies, alongside a program introduced by Detroit City Treasurer Albert

Cobo that allowed a 7 year extension for delinquent property tax payments, Detroit managed to survive the economic downturn[83].

WWII helped pull Detroit fully from its economic depression. With the US's acute need for industrial support for the military and Detroit's robust industrial infrastructure, Detroit became "the Arsenal of Democracy", producing tanks, guns, and planes for the war effort[83]. The boom in industry led to migration into the city, much of which was Black Americans from the US South during the Great Migration[4][83, 66]. This brought about social instability, as housing was limited in the city and racial tensions were high. In 1967, these tensions developed into conflict between Black Detroit residents and the Detroit Police Department, and rioting took place in the city, claiming the lives of 43 residents[47]. Although Detroit's white population had already begun an exodus from the inner city to the satellite cities surrounding Detroit, this event provided an accelerant for the racially-motivated migration. Prior to 1967, white residents were leaving Detroit at a rate of approximately 22,000 per year. In 1968, that number had skyrocketed to approximately 80,000 per year[32].

The combination of racial tensions and decentralization of the automotive industry, with the 1967 race riots as a catalyst, laid the groundwork for a transfer of population and wealth from Detroit to the surrounding cities (Figure 5.8). Thus began the downfall of Detroit. Many white residents with the means to leave did, as did the industry that once supported the city, and the tax base dwindled. In 2010, 23% of Detroit's housing was vacant, and citywide poverty peaked at 42.3% in 2012[79].

Since 2010, Detroit has been experiencing positive economic growth[4]. Unemploy-

[4]The Great Migration was a large scale exodus of Black Americans from rural regions of the southern US to northern US cities during the period between the first and second World Wars, 1915-1940. This was spurred by a pull driver, an increase in manufacturing following the war that created opportunities for Black Americans, and a push driver, the hostile societal conditions created by Post-Reconstruction southern cites[25]

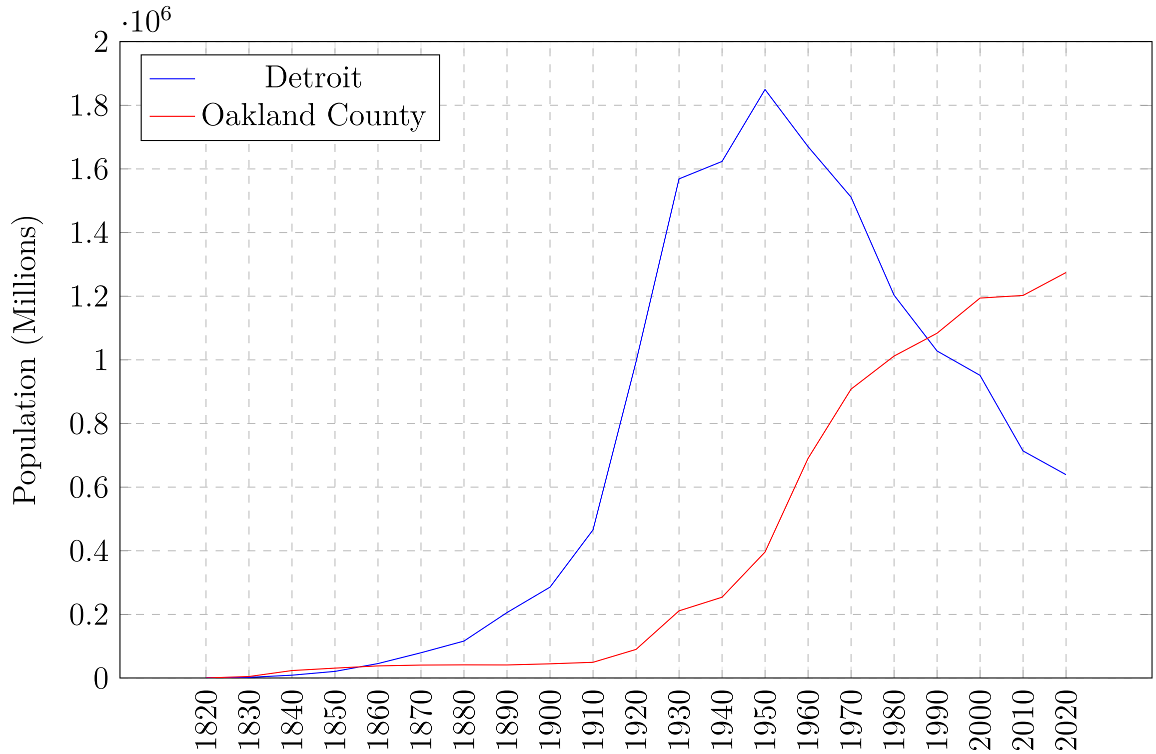

Figure 5.8: Population of Detroit, compared with Oakland County, from 1820-2020[79].

ment and poverty rates have been consistently falling, and new redevelopment projects are being planned to revitalize the city[31]. The automotive industry and the technology industry have been investing money into this revitalization process, hoping to see an economic renaissance in Detroit and to turn the city into the next ”Silicon Valley”[46].

5.4.1 Social Equity in DMA

Throughout the history of DMA, there have been many instances of social injustice. Slavery of both black and American Indian individuals was prevalent in Detroit in the 18th century. Although the Northwest Ordinance of 1787 outlawed slavery in Michigan, slavery still existed there until 1837, when Michigan became a state and prohibited slavery in its constitution[53]. Following this, instances of the marginalization of minority and immigrant communities can be found throughout DMA's history, and these can be closely linked to the current population distribution of DMA[45]. However, to succinctly summarize the lasting impacts of social inequity in DMA, this study will focus on the actions and policies from the early 1900s onwards to better understand the current state of social equity in DMA. This time period marked the greatest influx of Black Americans into the city and, consequentially, a dramatic change in the socio-demographic dynamics of DMA.

As mentioned in the previous section, DMA's status as "The Arsenal of Democracy" during WWII was a huge driver of immigration into the region. Industry in DMA was ramped up to supply the war effort with the tanks, airplanes, and guns needed to win the war, and this demanded a sizeable workforce. As social conditions in the US South were inhospitable for Black Americans due to excessive bigotry and racist policies[25], many moved to DMA in search of opportunity and prosperity. Concurrently, DMA was experiencing a dissolution of ethnic communities where, save for a couple of outliers like the Polish Hamtramck or the Hungarian Delray neighborhoods, fewer ethnically homogeneous neighborhoods existed[75]. This change in demographics morphed DMA into a dichotomous landscape and, instead of areas of the city identifying as one ethnicity or another, segregation of the city was based primarily on skin color[75].

The influx of Black Americans into DMA elicited negative reactions from many white homeowners who viewed this migration as an invasion. Black Americans who would attempt to live in areas other than the prominently poor black ghettos were met with resistance and threats of violence from their white neighbors. This, combined with a slow-down in new housing construction during the Great Depression and a lack of young, skilled construction labors (as most of the city's labor was funneled into the war efforts), led to a housing shortage during the 1940s and 1950s that disproportionately impacted Black communities[75].

The following tools were used to discriminate against Black Americans in post-WWII DMA[75]:

- Racial covenants: Clauses incorporated into property deeds with the intention of maintaining the societal homogeneity of neighborhoods. The clauses would often explicitly bar the occupation of a property by any non-white person.
- Other covenants: While racial covenants were an openly bigoted way to discriminate against Black Americans, more subtle approaches, such as occupancy lot size standards, were employed to prevent lower income individuals from purchasing property in neighborhoods
- HOLC Ratings: Racially motivated appraisals of neighborhoods made it difficult for Black Americans to obtain conventional home-financing.

Following World War II, upwards of 90 percent of Detroit's new housing developments implemented legally binding covenants prohibiting the sale to Black Americans. Because of these obstructions to the upward mobility of Black Americans, many were forced to live in crowded, low-quality ghettos in the urban inner-city. Meanwhile, the populations of the suburbs surrounding Detroit were growing at a rapid rate. Movement to these areas that were growing in both population and tax base was unobtainable to Black Americans for the aforementioned discriminatory practices. This redistribution of wealth within DMA from the inner-city to the satellite suburbs came at a time when pollution and regulatory compliance costs were climbing for inner city industries, resulting in a high concentrations of air and water pollution in largely minority communities with very little resources for mitigation[66].

Examples of EJ infractions against minority communities have been numerous since the 1960's demographic shift in DMA[66]. In regards to HOLC red-lining, studies have shown that residents living in redlined districts are at higher risk of cancers caused by air pollution[73]. However, there is little evidence for spatially-based detriments explicitly affecting vulnerable populations within Detroit boundaries. Studies examining distances to sources of air pollution have indicated that the areas directly surrounding sources of air pollution have a lower proportion of black residents than areas further away[30, 29]. A 2019 multi-city analysis found that Detroit lacked "an observable systematic UHI bias with respect to neighborhood income"[12]. This is not to say that environmental resources are being distributed completely fairly in modern times; in fact, one study[68] found that the majority of green roofs implemented in Detroit were concentrated in the wealthier, majority-white neighborhoods surrounding the Downtown district. However, the lack of empirical studies indicating egregious EJ infractions in a city with a historical record of EJ infractions, combined with the fact that Detroit is a city with over 78% of its population being non-white and over 30% being under the poverty threshold [79], indicates a need to explore EJ in context of the entirety of DMA, including its satellite suburban cities, and not just within the city boundaries.

5.4.2 UGI Policy in DMA

As DMA is a large area comprised of multiple municipalities serving over 2 million residents, there are several organizations that contribute to UGI policy and planning throughout the region, including:

- Governmental Organizations
  - Detroit Water and Sewage Department
  - Detroit Department of Recreation
  - South East Michigan Council of Governments
  - Michigan Department of Environmental Quality
  - Oakland County Water Resources Commissioner's Office
- Non-Profits
  - Detroit Future City
  - Greening of Detroit
  - Sustainable Water Works

A report published in 2014 detailing the barriers and opportunities regarding UGI implementation in DMA identified the following as potential challenges to UGI implementation in DMA[21].

- Additional Coordination: With so many players and institutions involved in UGI implementation in DMA, better coordination across organizations and departments is required to fully utilize the swath of resources at DMA's disposal.
- Antiquated Infrastructure and Approaches: Policy mechanisms are still lagging in regards to UGI implementation, and the physical infrastructure needed to implement UGI is also aging.

- Need for Increased Awareness: Simply put, there needs to be an improved understanding of how UGI works and the benefits of implementing UGI.

- Financing and Maintenance: Detroit in particular has a limited budget and, while UGI can provide future cost-savings in flood mitigation, justifying this expenditure can be challenging, especially considering the aforementioned need for an improved understanding of UGI benefits.

- Evaluating Impact: To better convince residents and practitioners of the benefits of UGI in DMA, evaluation metrics need to be improved.

Detroit's amount of vacant land is one facet of the report which identified as both a challenge and an opportunity. This poses an opportunity in that vacant land provides potential physical space for UGI, something that is often difficult to obtain in urban areas. However, this is also a challenge, as acquiring this land can be complicated when ownership of the land is ambiguous[21].

The following subsections will provide an overview of the UGI policy in Detroit (along with a brief history), and of the summary of the UGI policies found in Oakland County cities. This does not stand as a thorough policy analysis, but instead intends to provide some context regarding current and past UGI efforts in the DMA area.

The City of Detroit

From the earliest Woodward Plan, parks and green space were considered important to the planning of Detroit[24]. However, the matter of how important they were was debated in the early stages of the city's development. The Woodward Plan, as it was initially proposed, would have established a fixed ratio of public-to-private landownership, cementing the presence of publicly-owned right-of-ways through the city. Critics of this plan, primarily wealthy land owners who operated farms on the outskirts of the city, wanted to maximize profit potential for the sale of their land if they were to subdivide and, thus, opposed the provisions requiring a fixed ratio of public-to-private landownership. Some of aspects of the Woodward Plan, such as tree planting along boulevards and several of the proposed parks, were retained, but others aspects were cut out[24].

Which neighborhood should get parks was another matter that was historically debated in Detroit. In the 1880s, the governing bodies responsible for parks were involved in a battle for limited funding and, while the large riverfront park Belle Isle and other parks in wealthier neighborhoods were preserved, parks in lower-income, immigrant and Black American neighborhoods were removed. Additionally, in order to build new parks in Detroit, land must be donated (a result of the removal of the private/public fixed land ratio proposed in the Woodward Plan), and these donated projects often benefited the wealthy who had the means to donate land[24].

Today, however, Detroit places an emphasis on the need for both open space and UGI. The city of Detroit launched its Detroit Sustainability Action Agenda in 2019[15], a plan for future sustainability in Detroit which is subdivided into 4 Outcomes with 10 Goals and 43 Actions (Table 5.3). Although several of the Outcomes have Actions that would affect city-wide UGI, such as the Outcome ”Healthy, Thriving People” which includes the Actions ”Renovate existing and create new parks throughout the city” and ”Increase tree plantings in vulnerable areas”, the Outcome that explicitly addresses UGI is ”Equitable, Green City”. Under this Outcome, the Goal ”Enhance infrastructure and operations to improve resilience to climate impacts” includes the actions to ”Create neighborhood scale, distributed green infrastructure projects” and "Incorporate green stormwater infrastructure into street redesign and greenway projects". Both of these actions emphasize the need for UGI implementation specifically as a tool to abate stormwater flooding.

Between 2015 and 2017, Detroit invested $15 million in green stormwater infrastructure, and has pledged to invest $50 million by 2029. Residents are encouraged to install UGI on their private property through a stormwater rebate program[16] Additionally, non-profit organizations such as the Greening of Detroit and Detroit Future City have been providing resources and working with residents to install UGI in neighborhoods around the city[76].

Oakland County

Some, but not all, of the individual cities in Oakland County have plans dedicated to UGI implementation, but many include UGI within their Master Plan to varying degrees[14, 20, 18, 19, 17, 19]. This section will not detail each city's UGI policy by breaking down their master plans, but will instead provide a broad overview collected from the city plans and the documents cited in these plans as the basis for UGI policy.

In 2009, Oakland County released a "Green Infrastructure Vision"[60], upon which several cities have based their UGI policy on. Connectivity was included as a main focus of this vision, however, vulnerability was not listed as a priority. This plan was later built upon by the Southeast Michigan Council of Government, which created their own Green Infrastructure Vision for Southeast Michigan in 2014[74]. This vision also championed connectivity as a priority, but also failed to mention vulnerability.

This is not to say that cities in Oakland County are not taking vulnerability into account in regards to UGI placement strategy. The 2009 Pontiac, MI Parks and

Outcome	Goal	Action
Healthy, Thriving People	Increase access to healthy food, green spaces, and recreation opportunities	1. Provide nutrition and environmental education at recreation centers and parks
		2. Create local food purchasing guidelines for City-funded programs
		3. Improve access to high quality, healthy food at grocery stores
		4. Renovate existing and create new parks throughout the city
		5. Expand sports recreation opportunities for youth
	Improve air quality and reduce exposure to pollution	6. 6 Expand local air quality monitoring system
		7. Create citywide truck routing network
		8. Increase tree plantings in vulnerable areas
		9. Reduce emissions from City vehicles
	Advance equity in access to economic opportunity	10. Expand green jobs training and workforce development programs
		11. Prepare Detroit residents for City employment opportunities
		12. Launch a digital inclusion program
		13. Expand wireless internet access on City buses
		14. Launch a diversity, equity, and inclusion initiative
Affordable, Quality Homes	Reduce the total costs of housing, including utilities	15. Improve access to utility efficiency programs
		16. Expand home plumbing repair programs
		17. Implement and expand upon the Blue Ribbon Panel's water affordability recommendations
		18. Establish affordable housing preservation goals for building owners receiving City incentives
		19. Increase access to information on existing affordable housing
	Improve the health and safety of existing and new housing	20. Expand lead poisoning prevention initiatives across the city
		21. Create a residential lead abatement training pilot program
		22. Develop green building guidelines for new developments receiving City incentives
Clean, Connected Neighbor-hoods	Transform vacant lots and structures into safe, productive, sustainable spaces	23. Improve processes to purchase City owned vacant lots
		24. Support neighborhood-based efforts to care for vacant lots and structures
		25. Develop a fee structure and associated rules for irrigation only water accounts
	Reduce waste sent to landfills	26. Launch a citywide recycling campaign
		27. Expand curbside recycling to multi-family buildings
		28. Expand recycling to public spaces and all City facilities
		29. Develop a best practices framework for commercial scale compost operations
		30. Launch residential composting pilot program
	Make it easier and safer to get around Detroit without a personal vehicle	31. Improve mobility connections between neighborhoods and job centers
		32. Implement safety measures to reduce crash severity
		33. Expand Detroit's protected bike lane network
Equitable, Green City	Enhance infrastructure and operations to improve resilience to climate impacts	34. Create neighborhood scale, distributed green infrastructure projects
		35. Incorporate green stormwater infrastructure into street redesign and greenway projects
		36. Integrate climate change impacts into hazard mitigation planning
		37. Improve resident access to sustainability-related City services
		38. Expand emergency preparedness and communication tools
	Reduce municipal and citywide greenhouse gas emissions	39. Develop a greenhouse gas assessment and climate action strategy
		40. Increase the adoption of solar PV
		41. Enhance energy and water efficiency at City-owned facilities
		42. Launch Mayors' Challenge Program for Commercial Buildings
		43. Develop an electric vehicle infrastructure strategy

Table 5.3: Detroit Sustainability Action Agenda with Outcomes, Goals, and Actions[15]

Recreation Master Plan[18] recognizes the need for health equity in regards to parks and open spaces, and the city of Ferndale, MI includes a comprehensive assessment of social vulnerability in its 2020 climate change assessment[17]. However, emphasis on both connectivity and social vulnerability are not universally present in city plans regarding UGI.

Oakland County is currently piloting RainSmart Rebates, a stormwater rebate program for residents of the George W. Kuhn Drain Drainage District, an area encompassing the southeast portion of Oakland County. The program is similar to DC's RiverSmart program, offering up to $2,000 in rebates to residents who install UGI on their property[64].

5.5 Detailed Methodology

Currently, comprehensive 1m landcover classification is unavailable for the city of Detroit and Oakland County. The US National Oceanic and Atmospheric Administration's Office of Coastal Management Digital Coast program does provide 1m classifications for some areas, including the intended study area, for impervious surfaces, tree canopy, and water[56, 57, 58]. However, grass and barren surfaces are not included in these classifications. To classify this unclassified land, 3m multispectral satellite imagery from Planet Labs was used[65]. Supervised classification was accomplished using the Maximum Likelihood algorithm in ENVI 5.7[3] with 80-100 training samples for 6 classes: roads, buildings, tree canopy, grass, barren, and water. This classification was then overlain with the 1m resolution impervious surface, tree canopy, and water classification mentioned above, with these classification rasters taking precedent over the new classification. Settings for the classifier and accuracy assessments for the resulting rasters are included in Appendix A.3.

To select sample plots for DMA, datasets containing zoning and land use data for both Oakland County and Detroit were acquired[63, 27]. Using parks and recreation datasets for both regions[26, 62], park land that may be confused for Single Family Residential zoned areas was clipped out.

For Detroit city, two zoning designations, R1 and R2 (Single Family Residential and Two Family Residential) were selected as the zones of interest. R2 was included alongside R1 as the requirements for buildings were functionally similar, with the main difference being the number of families allowed to live on each lot.

Within Oakland County, only areas designated as "cities" were retained[5]. In Oakland County, there are a total of 31 cites, the boundaries of which were obtained from Access Oakland[61]. Oakland County's zoning practices differ from Detroit's, in that Oakland County's 31 cities (and numerous other populace designations) are each responsible for their own zoning practices. However, Oakland County's open data portal provides the zones decided by these cities, and includes "Single Family Residential" zones that are categorized based on lot area. Using 2021 Parcel data from City of Detroit Open Data[28], it was ascertained that the largest lot size designated as residential is 3.74 acres. For this reason, samples for Oakland County were only created in areas zoned for single family residential smaller than 5 acres. Although this may exclude some zones of the cities within Oakland County, this study assumes that the confining geography of the city of Detroit would prohibit lots from growing beyond a certain size, compared with Oakland County, where the amount of undeveloped space allows for lots greater than 5 acres to be included in city boundaries.

[5]The designation of "city" in Michigan indicates that the population center is no longer governed by the surrounding township, but has establishing its own form of self-government[2].

These larger lots, similar to the land created from ”leapfrogging” development[40] in Phoenix, AZ discussed in Chapter 4, are not so much urban land as they are land with rural characteristics within artificial urban boundaries, and were not included in this study.

Using these constraints, random sample plots were generated within both Oakland County and Detroit City using the parameters and methods outlined in Chapter 2. 1000 sample plots were created for Oakland County and, although 1000 sample plots were attempted for Detroit City, only 666 Plots were created successfully while still adhering to the 0.5km minimum distance allowed to prevent overlap. LSMs were then calculated using the R landscapemetrics package[41] (Appendix A.1), and SVI variables were apportioned using 2020 CDC/ATSDR SVI data[37] and the methods outlined in Chapter 2. Any plots that overlapped with census tracts containing prisons[59] were discarded. Sample plots with population < 10 were excluded, leaving $n = 1471$ total plots in the study (Figure 5.9). These plots were then explored for relationships using PCA.

Although these plots all reside within the same geographic region and, roughly, the same human urban ecosystem, politically they are different cities. This provides a hurdle to a quantitative analysis: although the flow of resources and residents does permeate these city boundaries[71], the management of the land within each city's boundary is up to that city's government. To overcome this, the data were explored from two perspectives. First, all sample plots were analyzed using PCA, similar to the previous two case studies. This was to establish any overarching relationships that may exist in the data as a whole. Second, plots within Detroit and plots within Oakland County were to be compared. Although each city manages land use differently, by filtering for Single Family Residential zones and implementing a maximum

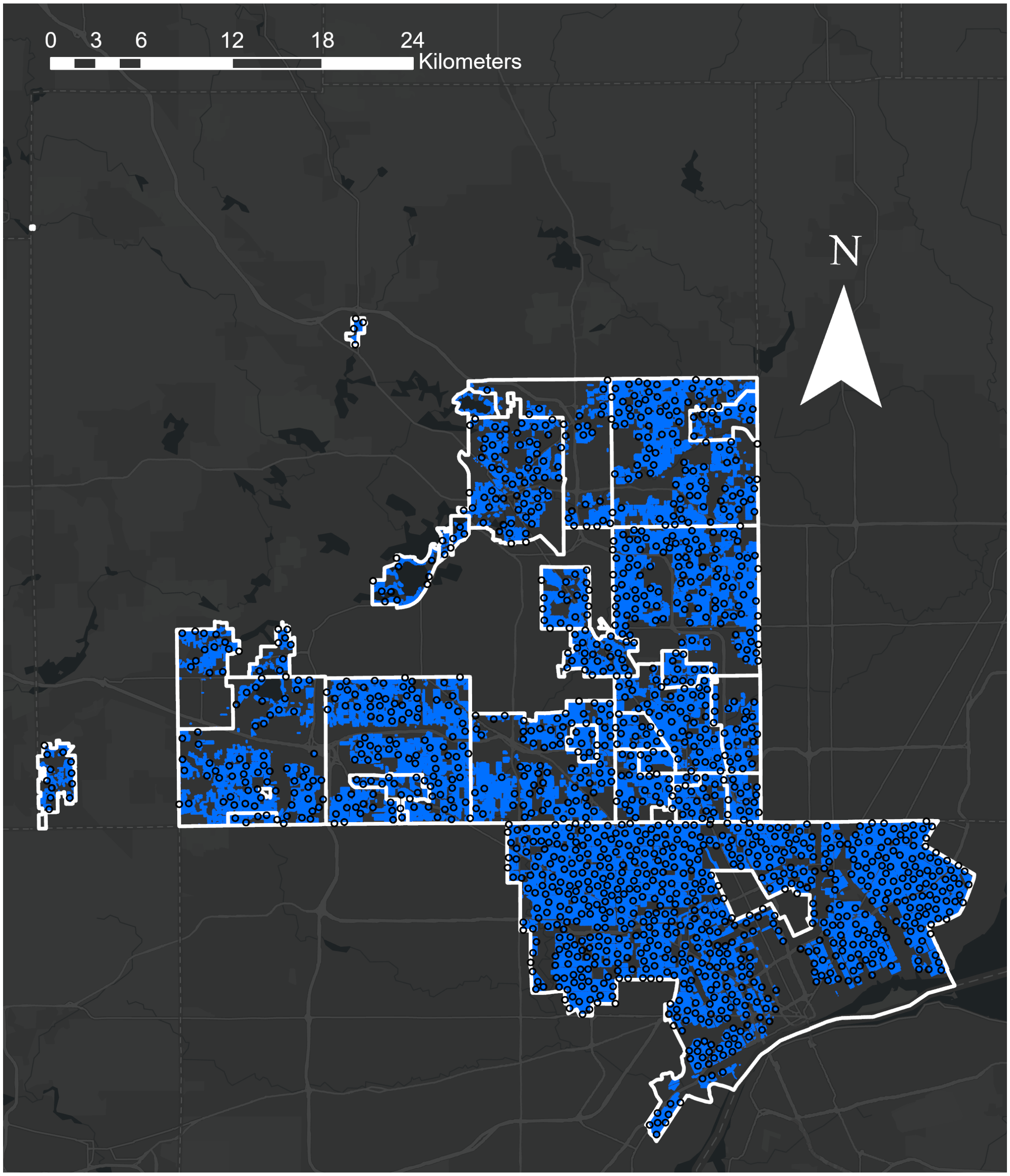

Figure 5.9: Study plots for Detroit, MI and cities in Oakland County, MI (n = 1471). Black circles denote sample plots used in this study, blue zones represent areas deemed suitable for this study according to study criteria. The white lines signify city boundaries used in this study.

lot size for analysis, it was assumed it would be reasonable to compare the plots as two separate groups that should share similar characteristics if EJ were assumed to be equitable.

Relationships that cross-loaded onto both SVI and LSM based components were explored further with a Mann Whitney U Test. Additionally, due to the historical socio-demographic shifts and the resulting segregation present in DMA, further analyses of the components derived from PCA were performed.

5.6 Results of Analysis

5.6.1 Principal Component Analysis

Using a Varimax rotation with Kaiser Normalization, 5 components were extracted explaining 59% of the variance (Table 5.4). PC 1 (representing 24% of the total variance) is loaded with variables that pertained to the areal coverage and connectivity of impervious surfaces, as well as the lack of areal coverage and connectivity of tree canopy. Of the impervious surface metrics, only Impervious LSI does not load significantly ($>|0.32|$) onto PC 1. All tree canopy metrics are loaded onto PC 1, as is Barren LSI. PC 2 (representing 17% of the total variance) is only loaded with vulnerability variables. Of these variables, only Age 65+% loaded negatively onto PC 2, behaving similarly to the data from chapters 3 and 4. Below Poverty % loads strongest onto PC 2. PC 3 (representing 10% of the total variance) has a complex set of loading variables, with Impervious LSI and grass LSI negative loading very strongly onto this component. Tree LSI also loads negatively onto this component, albeit not as strongly. The metric ENN_MN loads positively onto this component for 3 categories: impervious, tree canopy, and grass. Impervious PLADJ also loads onto PC 3. Of the SVIvariables, Minority % weakly loads negatively onto PC 3.

PC 4 (representing 7% of the total variance) is loaded with every barren LSM, with barren PLAND being the strongest. Additionally, Disability % also loads weakly negatively onto this component.

PC 5 (representing 5% of the total variance) is loaded with every grass LSM, with grass PLADJ being the strongest.

The variables of Minority % and Disability % were both binned into two groups for each variable. Plots with Minority % in the lower 50^{th} percentile and upper 50^{th} percentile were binned into groups M1 and M2, respectively, and plots with Disabled % in the lower 50^{th} percentile and upper 50^{th} percentile were binned into groups D1 and D2. Groups M1 and M2 were tested for difference in mean rank for the LSM variables Grass Pland, Impervious LSI, Grass LSI, Impervious ENN_MN, Tree ENN_MN, Grass ENN_MN, and Impervious PLADJ. Groups D1 and D2 were tested for difference in mean rank for every barren LSM.

To explore the differences between Oakland County and Detroit, plots were grouped by their locations (either Oakland County or Detroit). A Mann Whitney U Test was then conducted for these groups using the scores for PC 2 as measurements. PC 2 appears to represent the variance related to the majority of SVI variables, therefore this component could be used to determine the general vulnerability of Oakland County versus Detroit. Additionally, using these groups, a Mann Whitney U Test was performed to examine if there were differences in the LSMs for impervious surfaces and tree canopy, as these appear to have an inverse relationship according to PC 1.

Table 5.4: *PCA Rotated Component Matrix for sample plots in Detroit and Oakland County, Michigan.* Rotation Method: Varimax with Kaiser Normalization. Scores below |0.32| were considered a poor correlation and not included in this component matrix[23].

Variable	Component				
	1	2	3	4	5
Below Poverty %		0.833			
Unemployed %		0.559			
No HS Diploma %		0.774			
Uninsured %		0.703			
Age 65+ %		-0.488			
Age 17- %		0.564			
Disability %		0.501		-0.336	
Minority %		0.673	-0.342		
Limited English %		0.408			
Housing Burden %		0.576			
Single Parent Household %		0.668			
Household Crowding %		0.551			
Impervious PLAND	0.887				
Barren PLAND				0.830	
Tree PLAND	-0.898				
Grass PLAND			-0.335		0.825
Impervious LPI	0.861				
Barren LPI				0.683	
Tree LPI	-0.860				
Grass LPI					0.728
Impervious LSI			-0.928		
Barren LSI	0.443			0.538	
Tree LSI	0.504		-0.596		-0.329
Grass LSI			-0.782		
Impervious ENN_MN	-0.571		0.399		
Barren ENN_MN				-0.343	
Tree ENN_MN	0.397		0.378		
Grass ENN_MN			0.542		-0.358
Impervious PLADJ	0.617		0.685		
Barren PLADJ				0.741	
Tree PLADJ	-0.845				
Grass PLADJ					0.863
Impervious Cohesion	0.818				
Barren Cohesion				0.735	
Tree Cohesion	-0.809				
Grass Cohesion					0.810
Kaiser-Meyer-Olkin Measure of Sampling Adequacy.					0.766
Bartlett's Test of Sphericity	Approx. Chi-Square				59904.99
	df				630
	Sig.				< 0.001

5.6.2 Mean Rank Analysis

Mean Rank Analysis of the groups M1 and M2 indicated significant differences in 6 of the 7 LSMs tested (Figure 5.10a), with only Tree ENN_MN being insignificant at both levels ($p < 0.001$ and $p < 0.05$). The other LSMs showed significant differences, with Grass PLAND, Impervious LPI, and Grass LSI having a significantly lower mean rank in group M1 than in group M2. Group M1 had a significantly higher mean rank than group M2 in the metrics Impervious ENN_MN, Grass ENN_MN, and Impervious PLADJ.

Mean Rank Analysis of the groups D1 and D2 showed 4 barren LSMs, PLAND, LPI, PLADJ, and Cohesion, to have significant differences in mean rank at the level $p < 0.001$. Barren ENN_MN was significant at the level $p < 0.05$, and Barren LSI was not significant (Figure 5.10b. For Barren PLAND, LPI, ENN_MN, PLADJ, and Cohesion, group D1 had a significantly higher mean rank than group D2.

Examining the difference in mean rank between plots by location reveals that the mean rank of the PC 2 scores of plots located in Oakland County was significantly lower than those in Detroit ($p < 0.001$) (Appendix B.3). For every LSM except Tree ENN_MN, the difference in mean rank between Detroit and Oakland county plots was significant. Detroit plots had a higher mean rank for Impervious PLAND, Impervious LPI, Impervious LSI, Tree LSI, and Impervious Cohesion than did Oakland County plots. Detroit plots had a lower mean rank for Tree PLAND, Tree LPI, Impervious ENN_MN, Impervious PLADJ, Tree PLADJ, and Tree Cohesion than did Oakland County plots (Figure 5.11).

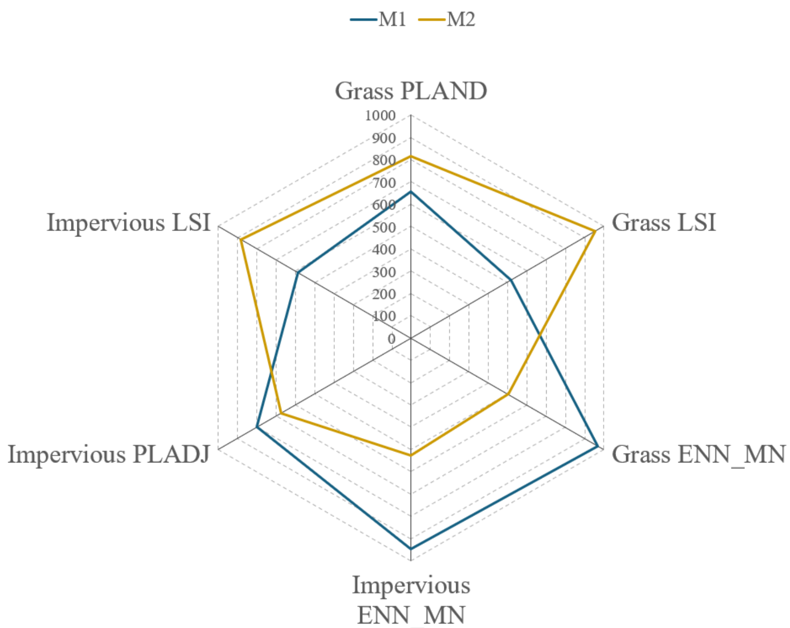

(a) Minority %

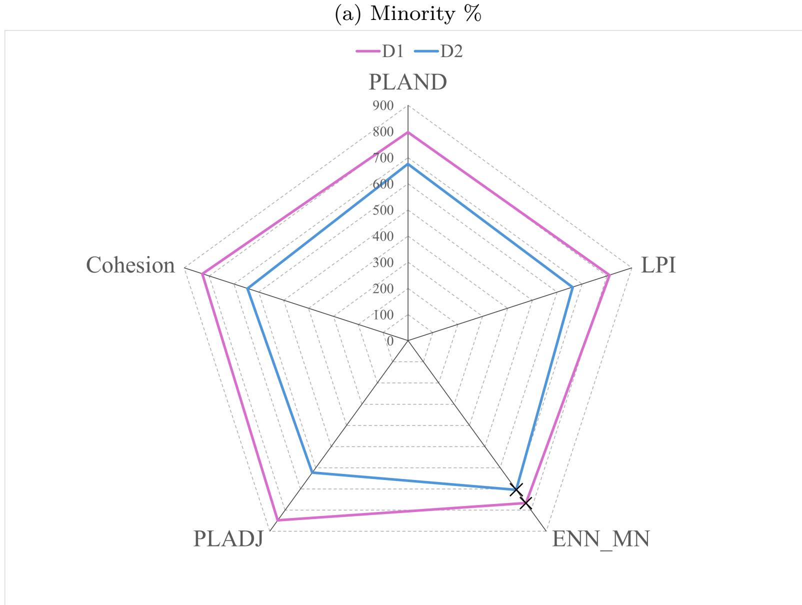

(b) Disabled %

Figure 5.10: Radar plots showing mean rank comparison for selected LSMs between tested vulnerability groups. Subfigure 5.10a shows significant mean rank comparison between Minority % groups M1 (dark blue) and M2 (gold) ($p < 0.001$). Subfigure 5.10b shows significant mean rank comparison for barren LSMs between Disability % groups D1 (pink) and D2 (blue) ($p < 0.05$, $p < 0.001$). The black X denotes a mean rank difference that is only significant at the level $p < 0.05$. Although tested, Barren LSI was not included as the differences in mean rank were found to not be significant at any level.

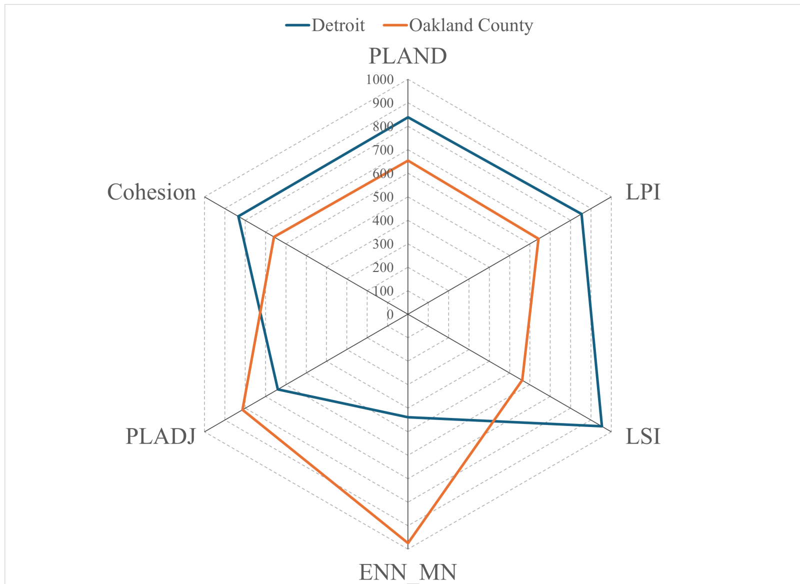

(a) Impervious Surface LSMs

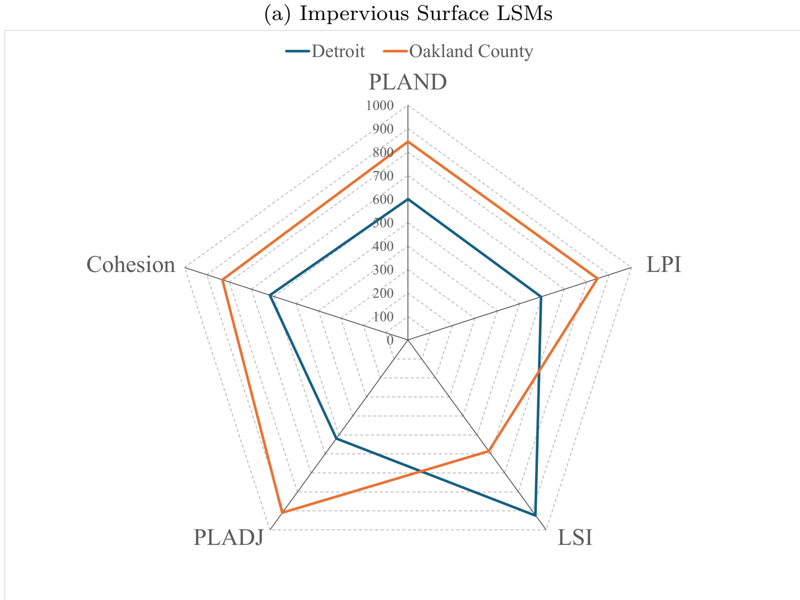

(b) Tree LSMs

Figure 5.11: Radar plot showing significant mean rank comparison for impervious surface (Subfigure 5.11a) and tree canopy (Subfigure 5.11b) LSMs for Detroit (blue) and Oakland County (orange). Tree ENN_MN was not included, as the difference in mean rank between Detroit and Oakland County plots was determined to be insignificant at all levels ($p < 0.05$, $p < 0.001$).

5.7 Discussion

When looking at the whole of DMA, some complex relationships emerge. Regarding the lower and upper 50th percentile groups for the variable Minority % (M1 and M2, respectively), grass landcover appears to have generally more percent coverage in plots from group M2 than in plots from group M1. Additionally, the shape of the grass landcover is both more complex (indicated by a higher LSI) and clustered (indicated by a lower ENN_MN) in group M2 plots than in plots from M1. At the same time, the impervious surfaces in these M2 plots are also more complex, yet not necessarily more connected or clustered (as indicated by Impervious PLADJ and Impervious ENN_MN). This suggests that areas with a higher percentage of minority population throughout DMA are more likely to have larger swaths of complex, clustered grass landcover with complex, unclustered, unconnected impervious surfaces. One possible explanation for this is the amount of vacant, derelict properties in Detroit, and the ongoing demolition of these properties. The high amount of vacant property in Detroit, although a potential opportunity for growing neighborhood UGI, has led to a high number of property demolitions in Detroit. Since 2014, approximately 20,000 homes have been demolished[8], many in vulnerable, high minority areas. With this comes other EJ issues, as the lead pollution produced by the demolition of vacant house affects nearby residents[9].

Mean rank comparison of barren LSMs for the upper and lower 50th percentile groups of the variable Disability % also displayed some interesting results. Group D1, with the lower 50th percentile of Disability %, had a higher mean rank for areal coverage of barren landcover (PLAND and LPI) and connectivity of barren landscape (PLADJ and Cohesion). The reason for this relationship is unclear, and merits a more in-depth analysis in future research.

When comparing the mean ranks between Detroit and Oakland County for impervious surface and tree canopy LSMs, a clear difference in coverage and connectivity is apparent. Detroit plots have a significantly higher mean rank for impervious areal coverage (PLAND and LPI), and impervious surface shape complexity (LPI), than do the plots in Oakland County (Figure 5.12). Additionally, Detroit plots have a lower mean rank for areal coverage (PLAND and LPI) of tree canopy than do the Oakland County plots. Regarding connectivity, the differences are more complicated. Detroit plots have a significantly higher mean rank of Impervious Cohesion, but a significantly lower mean rank of Impervious PLADJ. Cohesion measures the degree of aggregation of patches of landscape, while PLADJ measures the likelihood of an adjacent cell being the same class as any given cell of a class[51]. To be a part of a class aggregation, only one adjacent cell is required to connect patches of landcover. Therefore, it is possible, with a complex enough shape of landcover, that a patch of impervious surface is both aggregated and connected to itself, while also maintaining a low likelihood that the neighboring cells are in the same class. This is supported by the Detroit plots also having a significantly higher mean rank in both Impervious and Tree Canopy LSI than the Oakland County plots, indicating complex landcover shapes. The largest significant difference in mean rank is for Impervious ENN_MN, which suggests that patches of impervious surfaces are close together in the Detroit plots relative to the Oakland County plots.

Interpreting these results in the context of EJ requires further knowledge and some assumptions. The first hypothesis (H1), that discrepancies will exist in the areal coverage and connectivity of UGI between areas with a higher proportion of vulnerable residents and areas with a lower proportion of vulnerable residents, was affirmed by the significant differences of grass and impervious connectivity and coverage between groups M1 and M2, and groups D1 and D2. However, the second hypothesis (H2), that sample plots with lower percentages of residents considered vulnerable will have higher areal coverage and connectivity of UGI than plots with higher percentages of residents considered vulnerable, was not affirmed. Grass had higher connectivity and coverage in group M2 than in group M1, indicating that this form of UGI was in fact more connected in plots with a higher percent of minority population. Fully understanding the relationship between grass and impervious surfaces in the city of Detroit (and throughout DMA), as well as how this is affected by property demolition, may help explain this result.

However, when comparing the mean ranks of tree canopy and impervious surface coverage between Detroit and Oakland County, significant differences appear, with Detroit seemingly having a lower connectivity and coverage of tree canopy than does Oakland County. This does not support either hypothesis directly, unless we make the assumption that simply being located outside of Detroit decreases the proportion of vulnerable residents, a result of historical racially-driven migration and segregation. There is ample evidence for this claim in census data[79], and it is the belief of the author of this dissertation that this is true. However, by the constraints of this study, a direct relationship between SVI and UGI landscape connectivity was not exhibited.

These results also raise questions about urban systems and how their function can impact EJ. The political boundaries of cities are firm at any given time; residents who live on one side of the boundary pay taxes to a different governmental entity and receive a different set of services and benefits than the residents on the other side of the boundary. However, the urban ecosystem does not rigidly adhere to these boundaries. In the example of Detroit, the satellite suburbs exist as they are not

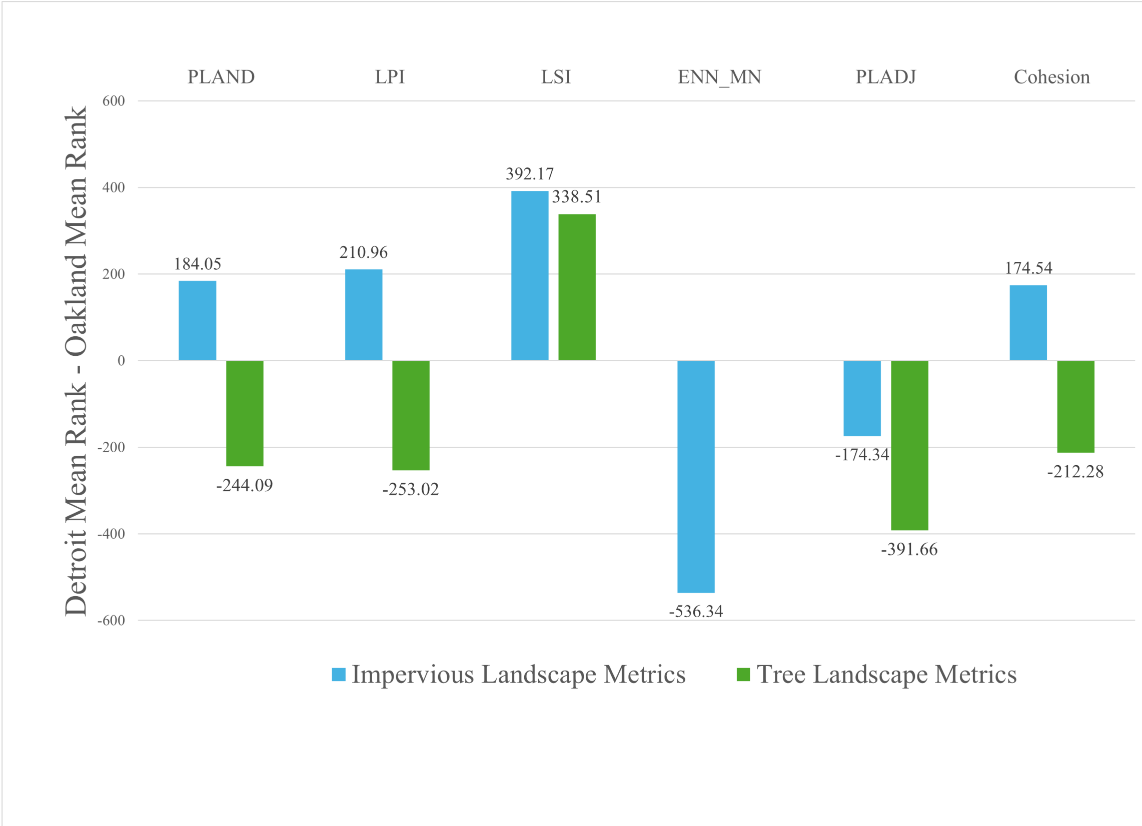

Figure 5.12: Bar graph showing the differences in mean rank between Detroit and Oakland County plots for impervious surface LSMs (blue) and tree canopy LSMs (green). A positive number indicates a higher mean rank for Detroit plots than for Oakland County plots, a negative number indicates a lower mean rank for Detroit plots than for Oakland County plots. As the difference in mean rank for Tree ENN_MN was not found to be significant ($p < 0.05$), it was not included.

in spite of Detroit, but *because* of Detroit[83, 66]. Without the port and railways of Detroit, industry would not have developed in the same way, and without the industry and the money that it brought in, the satellite suburb cities would not have formed. Yet, one of the primary barriers to UGI in Detroit is a lack of resources and funding[21], a problem that is not as prevalent in the satellite suburbs. The flow of monetary resources is artificially withheld in this urban ecosystem through political structures, regardless of the living aspects of the ecosystem, the residents and the UGI. In natural ecosystems, disturbances that limit the flow of resources reduce resiliency of the system and increase instability[81, 10], and it seems likely that this is similar in anthropogenic ecosystems as well[33]. For this reason, analyzing these EJ problems in the context of the entirety of the urban ecosystem, not just within arbitrary political boundaries, may be necessary.

References

[1] Plan of Detroit, 1832. URL https://commons.wikimedia.org/wiki/File:Old_map_1807_plan.jpg.

[2] Organization of City and Village Government in Michigan. Municipal Report, Michigan Municipal League, Ann Arbor, MI, January 2021. URL https://mml.org/pdf/mr/mr-org-of-city-and-village-govt-in-mi-jan-2021.pdf.

[3] ENVI Geospatial Software, 2022.

[4] City of Detroit Economic Outlook. Technical report, City of Detroit University Economic Analysis Partnership, Ann Arbor, MI, February 2023.

[5] Group 4. Urban Sprawl of Detroit, December 2022. URL https://storymaps.arcgis.com/stories/cd3e86480f6d4d0fa353937a1eaa4708.

[6] Alan Mallach and Lavea Brachman. Finding New Forms for America's Legacy Cities, 2012. URL https://www.lincolninst.edu/sites/default/files/pubfiles/2276_1615_Mallach_WP13AM1.pdf.

[7] Daniel P. Barr. *Unconquered: The Iroquois League at War in Colonial America*. Bloomsbury Academic, February 2006. ISBN 978-0-275-98466-3. Google-Books-ID: vi1ROx0PmI4C.

[8] Bella Contracting. A History Of The Detroit Demolition Program, March 2023. URL https://bellacontractingservices.com/a-history-of-the-detroit-demolition-program/. Section: Detroit.

[9] Carla Bezold, Samantha J. Bauer, Jessie P. Buckley, Stuart Batterman, Haifa Haroon, and Lauren Fink. Demolition Activity and Elevated Blood Lead Lev-

els among Children in Detroit, Michigan, 2014-2018. *International Journal of Environmental Research and Public Health*, 17(17):6018, August 2020. ISSN 1660-4601. doi: 10.3390/ijerph17176018.

[10] Justin D. Brookes, Kane Aldridge, Todd Wallace, Leon Linden, and George G. Ganf. Multiple Interception Pathways for Resource Utilisation and Increased Ecosystem Resilience. *Hydrobiologia*, 552(1):135–146, December 2005. ISSN 1573-5117. doi: 10.1007/s10750-005-1511-8. URL https://doi.org/10.1007/s10750-005-1511-8.

[11] Centers for Disease Control and Prevention/ Agency for Toxic Substances and Disease Registry/ Geospatial Research, Analysis, and Services Program. CDC/ATSDR Social Vulnerability Index 2020 Database, New York, 2020. URL https://www.atsdr.cdc.gov/placeandhealth/svi/data_documentation_download.html.

[12] T. Chakraborty, A. Hsu, D. Manya, and G. Sheriff. Disproportionately higher exposure to urban heat in lower-income neighborhoods: a multi-city perspective. *Environmental Research Letters*, 14(10):105003, September 2019. ISSN 1748-9326. doi: 10.1088/1748-9326/ab3b99. URL https://dx.doi.org/10.1088/1748-9326/ab3b99. Publisher: IOP Publishing.

[13] Christine Macdonald. Detroit population rank is lowest since 1850. *The Detroit News*, May 2016. URL http://www.detroitnews.com/story/news/local/detroit-city/2016/05/19/detroit-population-rank-lowest-since/84574198/.

[14] City of Bloomfield Hills. City of Bloomfield Hills Master Plan. Master Plan,

Bloomfield Hills, MI, May 2009. URL https://bloomfieldhillsmi.net/DocumentCenter/View/463/Master-Plan-PDF?bidId=.

[15] City of Detroit. Detroit Sustainability Action Agenda. Technical report, City of Detroit, Detroit, MI, 2019. URL https://detroitmi.gov/sites/detroitmi.localhost/files/2019-06/Detroit-Sustainability-Action-Agenda-Web.pdf.

[16] City of Detroit Water and Sewerage Department. Drainage Program Guide. Technical report, City of Detroit, Detroit, MI, October 2022. URL https://detroitmi.gov/sites/detroitmi.localhost/files/2022-11/Drainage%20Program%20Guide%20-%20October%202022.pdf.

[17] City of Ferndale. CLIMATE CHANGE VULNERABILITY ASSESSMENT FOR STORMWATER. Technical report, City of Ferndale, Ferndale, MI, June 2020. URL https://legistarweb-production.s3.amazonaws.com/uploads/attachment/pdf/614839/FINAL-Climate-and-Socio-Economic-Vulnerability-Assessment-for-Stormwater-FERNDALE-06.02.20.pdf.

[18] City of Pontiac, Michigan. Parks and Recreation Master Plan 2021-2025. Master Plan, Pontiac, MI, 2021. URL https://cms3.revize.com/revize/pontiacminew/Document%20Center/Departments/COMMUNITY%20DEVELOPMENT/Planning%20&%20Zoning/Parks%20&%20Recreation%20Masterplan/PontiacParkRecMasterPlan2021_2025Final.pdf.

[19] City of Royal Oak. Green Infrastructure Evaluation Report. Technical report, City of Royal Oak, Royal Oak, MI, March 2018. URL https://www.romi.gov/DocumentCenter/View/22241/Final-Report---Green-Infrastructure-Evaluation-5-6-18?bidId=.

[20] City of Troy, Michigan. Plan Troy 2040. Master Plan, Troy, MI, 2020. URL https://cms6.revize.com/revize/citytroymi/Departments/Planning/Master%20Plan/CityOfTroy_MasterPlan2040_2023-12-1.pdf.

[21] Claire Matucheski, Julia Ruedig, Kristine Schantz, and Jacob Talbot. Green Infrastructure in Detroit: Mapping Synergies and Gaps. Technical report, University of Michigan, Ann Arbor, MI, December 2014. URL https://graham.umich.edu/media/files/dow/Dow-Masters-2014-Green-Infrastructure-Detroit.pdf.

[22] Climate Central. Urban Heat Hot Spots, July 2023. URL https://www.climatecentral.org/climate-matters/urban-heat-islands-2023.

[23] Andrew L. Comrey and Howard B. Lee. *A First Course in Factor Analysis*. Psychology Press, 0 edition, November 2013. ISBN 978-1-315-82750-6. doi: 10.4324/9781315827506. URL https://www.taylorfrancis.com/books/9781317844075.

[24] Patrick Cooper-McCann. *The Promise of Parkland: Planning Detroit's Public Spaces, 1805-2018*. Thesis, 2019. URL http://deepblue.lib.umich.edu/handle/2027.42/150063. Accepted: 2019-07-08T19:48:52Z.

[25] Spencer R Crew. The Great Migration of Afro-Americans, 1915-40. *Monthly Labor Review*, pages 34–36, March 1987. URL https://www.bls.gov/opub/mlr/1987/03/art5full.pdf.

[26] Data Driven Detroit. Parks and Landmarks, Detroit, February 2014. URL https://portal.datadrivendetroit.org/datasets/D3::parks-and-landmarks-detroit.

[27] Detroit City Planning Commission. Zoning, November 2017. URL data.detroitmi.gov.

[28] Detroit Office of the Assessor. Parcels, September 2021. URL https://data.detroitmi.gov/datasets/detroitmi::parcels-2.

[29] Liam Downey. The Unintended Significance of Race: Environmental Racial Inequality in Detroit*. *Social Forces*, 83(3):971–1007, March 2005. ISSN 0037-7732. doi: 10.1353/sof.2005.0026. URL https://doi.org/10.1353/sof.2005.0026.

[30] Liam Downey. Environmental Racial Inequality in Detroit. *Social Forces*, 85(2): 771–796, December 2006. ISSN 0037-7732. doi: 10.1353/sof.2007.0003. URL https://doi.org/10.1353/sof.2007.0003.

[31] Ebony JJ Curry. Major Developments That Will Define Detroit in 2024, January 2024. URL https://www.detroitchamber.com/major-developments-that-will-define-detroit-in-2024/.

[32] Sidney Fine. *Violence in the Model City: The Cavanagh Administration, Race Relations, and the Detroit Riot of 1967*. Michigan State University Press, East Lansing, 2012. ISBN 978-1-60917-029-5. URL https://muse.jhu.edu/pub/26/monograph/book/8945.

[33] Ian Fitzsimmons. *Contemporary Effects of Natural Resource Limitation on Growing Human Populations: Socioeconomic Subsystem Evolution within Ecosystem Boundaries*. PhD thesis, University of Virginia, Charlottesville, VA, July 2022. URL https://libraetd.lib.virginia.edu/public_view/td96k349d.

[34] Frank Witsil and Kimberly P. Mitchell. Downpour floods metro Detroit as up

to 4 inches of rain soaks streets and basements. *Detroit Free Press*, August 2020. URL https://www.freep.com/story/news/local/michigan/2020/08/28/detroit-forecast-rain-flooding-roads/5654013002/.

[35] Eric Friedebach. Mexicantown - Southwest Detroit, Detroit, MI, USA, January 2015. URL https://commons.wikimedia.org/wiki/File:Mexicantown_-_Southwest_Detroit,_Detroit,_MI,_USA_-_panoramio.jpg.

[36] George N. (George Newman) Fuller. *Economic and social beginnings of Michigan;*. Lansing, Mich., Wynkoop Hallenbeck Crawford co., state printers, 1916. URL http://archive.org/details/economicsocialbe01full.

[37] Geospatial Research, Analysis, and Services Program. CDC/ATSDR Social Vulnerability Index 2020 - District of Columbia, October 2022.

[38] Great Lakes Integrated Sciences Assessment. The Potential Impacts of Climate Change on Detroit, Michigan. Technical report, June 2014. URL https://glisa.umich.edu/media/files/projects/DCAC/DCAC_Climate_Impacts.pdf.

[39] Scott Greene, Laurence S. Kalkstein, David M. Mills, and Jason Samenow. An Examination of Climate Change on Extreme Heat Events and Climate–Mortality Relationships in Large U.S. Cities. *Weather, Climate, and Society*, 3(4):281–292, October 2011. ISSN 1948-8327, 1948-8335. doi: 10.1175/WCAS-D-11-00055.1. URL https://journals.ametsoc.org/view/journals/wcas/3/4/wcas-d-11-00055_1.xml. Publisher: American Meteorological Society Section: Weather, Climate, and Society.

[40] Carol E. Heim. Leapfrogging, Urban Sprawl, and Growth Management: Phoenix, 1950-2000. *The American Journal of Economics and Sociology*, 60(1):245–283,

2001. ISSN 0002-9246. doi: 10.1111/1536-7150.00063. URL https://www.jstor.org/stable/3487953. Publisher: [American Journal of Economics and Sociology, Inc., Wiley].

[41] Maximilian H.K. Hesselbarth, Marco Sciaini, Kimberly A. With, Kerstin Wiegand, and Jakub Nowosad. landscapemetrics: an open-source R tool to calculate landscape metrics. *Ecography*, 42:1648–1657, 2019. doi: 10.1111/ecog.04617.

[42] Markus Kottek, Jürgen Grieser, Christoph Beck, Bruno Rudolf, and Franz Rubel. World Map of the Köppen-Geiger climate classification updated. *Meteorologische Zeitschrift*, 15(3):259–263, July 2006. ISSN 0941-2948. doi: 10.1127/0941-2948/2006/0130. URL http://www.schweizerbart.de/papers/metz/detail/15/55034/World_Map_of_the_Koppen_Geiger_climate_classificat?af=crossref.

[43] Kenneth E. Kunkel, Nancy E. Westcott, and David A.R. Kristovich. Assessment of potential effects of climate change on heavy lake-effect snowstorms near Lake Erie. *Journal of Great Lakes Research*, 28(4):521–536, 2002. ISSN 0380-1330. doi: 10.1016/S0380-1330(02)70603-5. URL http://www.scopus.com/inward/record.url?scp=0036961030&partnerID=8YFLogxK.

[44] Sugie Lee. Metropolitan Growth Patterns and Socio-Economic Disparity in Six US Metropolitan Areas 1970-2000: Metropolitan growth patterns and socio-economic disparity in the US. *International Journal of Urban and Regional Research*, February 2011. ISSN 03091317. doi: 10.1111/j.1468-2427.2010.01004.x. URL https://onlinelibrary.wiley.com/doi/10.1111/j.1468-2427.2010.01004.x.

[45] Daniel T. Lichter, Brian C. Thiede, and Matthew M. Brooks. Racial Diver-

sity and Segregation: Comparing Principal Cities, Inner-Ring Suburbs, Outlying Suburbs, and the Suburban Fringe. *RSF: The Russell Sage Foundation Journal of the Social Sciences*, 9(1):26–51, February 2023. ISSN 2377-8253, 2377-8261. doi: 10.7758/RSF.2023.9.1.02. URL https://www.rsfjournal.org/content/9/1/26. Publisher: RSF: The Russell Sage Foundation Journal of the Social Sciences.

[46] Jake Lingeman. U.S. automakers aim to make Detroit the next Silicon Valley, February 2023. URL https://www.newsweek.com/2023/02/17/us-automakers-aim-make-detroit-next-silicon-valley-1779611.html. Section: Autos.

[47] Hubert G. Locke. *The Detroit Riot of 1967*. Great Lakes Books. Wayne State University Press, Detroit, Michigan, 2017. ISBN 978-0-8143-4377-7. OCLC: ocn995173782.

[48] Russ Lopez and H. Patricia Hynes. Sprawl In The 1990s: Measurement, Distribution, and Trends. *Urban Affairs Review*, 38(3):325–355, January 2003. ISSN 1078-0874, 1552-8332. doi: 10.1177/1078087402238805. URL http://journals.sagepub.com/doi/10.1177/1078087402238805.

[49] George Luber and Michael McGeehin. Climate Change and Extreme Heat Events. *American Journal of Preventive Medicine*, 35(5):429–435, November 2008. ISSN 0749-3797, 1873-2607. doi: 10.1016/j.amepre.2008.08.021. URL https://www.ajpmonline.org/article/S0749-3797(08)00686-7/fulltext. Publisher: Elsevier.

[50] John F McDonald. What happened to and in Detroit? *Urban Studies*, 51(16): 3309–3329, December 2014. ISSN 0042-0980, 1360-063X. doi: 10.1177/004209

8013519505. URL http://journals.sagepub.com/doi/10.1177/0042098013519505.

[51] Kevin McGarigal and Barbara J. Marks. FRAGSTATS: spatial pattern analysis program for quantifying landscape structure. Technical Report PNW-GTR-351, U.S. Department of Agriculture, Forest Service, Pacific Northwest Research Station, Portland, OR, 1995. URL https://www.fs.usda.gov/treesearch/pubs/3064.

[52] Michigan (Ter.). *Laws of the territory of Michigan ...* Number 4 v. W.S. George & co., printers to the state, Lansing., 1871. URL //catalog.hathitrust.org/Record/002018817.

[53] Tiya Miles. *The Dawn of Detroit: A Chronicle of Slavery and Freedom in the City of the Straits*. New Press, The, La Vergne, UNITED STATES, 2017. ISBN 978-1-62097-232-8. URL http://ebookcentral.proquest.com/lib/uva/detail.action?docID=5751102.

[54] National Weather Service. Historic Flooding May 17-20, 2020, 2020. URL https://www.weather.gov/dtx/HistoricFlooding-May-17-20-2020.

[55] Neil P. Hurley. The Automotive Industry: A Study in Industrial Location on JSTOR. *Land Economics*, 35(1), 1959. doi: https://doi.org/10.2307/3144703. URL https://www-jstor-org.proxy1.library.virginia.edu/stable/3144703.

[56] NOAA Office for Coastal Management. 2020 NOAA C-CAP Version 2 Canopy Cover: Michigan, . URL www.coast.noaa.gov/htdata/raster1/landcover/bulkdownload/hires/.

[57] NOAA Office for Coastal Management. 2020 NOAA C-CAP Version 2 Impervious Cover: Michigan, . URL www.coast.noaa.gov/htdata/raster1/landcover/bulkdownload/hires/.

[58] NOAA Office for Coastal Management. 2020 NOAA C-CAP Version 2 Water Cover: Michigan, . URL www.coast.noaa.gov/htdata/raster1/landcover/bulkdownload/hires/.

[59] Oak Ridge National Laboratory. Prison Boundaries, September 2020. URL https://hifld-geoplatform.opendata.arcgis.com/.

[60] Oakland County, Michigan. Green Infrastructure Vision, 2009. URL https://www.oakgov.com/home/showpublisheddocument/48/638175152210664771.

[61] Oakland County, Michigan. OC Municipal District, October 2016. URL https://accessoakland.oakgov.com/datasets/oakgov::oc-municipal-district/about.

[62] Oakland County, Michigan. OC Recreation Land, October 2016. URL https://gisservices.oakgov.com/arcgis/rest/services/Enterprise/EnterpriseRecreationDataMapService/MapServer/0.

[63] Oakland County, Michigan. OC Current Land Use, February 2021. URL https://accessoakland.oakgov.com/maps/af7a7d054ff54bfea1e916e1a8aac7e7.

[64] Oakland County, Michigan. RainSmart Rebates, 2024. URL https://www.oakgov.com/government/water-resources-commissioner/rainsmart-rebates.

[65] Planet Labs PBC. Planet Application Program Interface: In Space for Life on Earth, 2022. URL https://api.planet.com.

[66] Josiah Rector. *Toxic debt: an environmental justice history of Detroit.* Justice, power, and politics. University of North Carolina Press, Chapel Hill, 2022. ISBN 978-1-4696-6575-7 978-1-4696-6576-4.

[67] Russell Lopez. Urban Sprawl in the United States: 1970-2010. *Cities and the Environment*, 7(1), 2014.

[68] Lino Sanchez and Tony G. Reames. Cooling Detroit: A socio-spatial analysis of equity in green roofs as an urban heat island mitigation strategy. *Urban Forestry & Urban Greening*, 44:126331, August 2019. ISSN 1618-8667. doi: 10.1016/j.ufug.2019.04.014. URL https://www.sciencedirect.com/science/article/pii/S1618866718303510.

[69] Marie Sanderson, Imaiyavalli Kumanan, Terry Tanguay, and William Schertzer. Three Aspects of the Urban Climate of Detroit-Windsor. *Journal of Applied Meteorology (1962-1982)*, 12(4):629–638, 1973. ISSN 0021-8952. doi: 10.1175/1520-0450(1973)012<0629:TAOTUC>2.0.CO;2. URL https://www.jstor.org/stable/26176773. Publisher: American Meteorological Society.

[70] Noah M Schmadel and Judson W Harvey. NHD-RC: Extension of NHDPlus Version 2.1 with high-resolution river corridor attributes, 2020. URL https://www.sciencebase.gov/catalog/item/5f8e091d82ce3241879215a7.

[71] Sean Coté. Living & Working in Detroit: LEHD Employment Statistics | Data Driven Detroit, April 2022. URL https://datadrivendetroit.org/blog/2022/04/27/living-working-lehd-employment-statistics/.

[72] Stanley S. Seidner. In Quest of a Cultural Identity: An Inquiry for the Polish Community. Technical report, 1976. ERIC Number: ED167674.

[73] Abas Shkembi, Lauren M. Smith, and Richard L. Neitzel. Linking environmental injustices in Detroit, MI to institutional racial segregation through historical federal redlining. *Journal of Exposure Science & Environmental Epidemiology*, pages 1–10, December 2022. ISSN 1559-064X. doi: 10.1038/s41370-022-00512-y. URL https://www.nature.com/articles/s41370-022-00512-y. Publisher: Nature Publishing Group.

[74] Southeast Michigan Council of Governments. Green Infrastructure Vision for Southeast Michigan. Technical report, Southeast Michigan Council of Governments, Detroit, MI, 2014. URL semcog.org/desktopmodules/SEMCOG.Publications/GetFile.ashx?filename=GreenInfrastructureVisionForSoutheastMichiganMarch2014.pdf.

[75] Thomas J. Sugrue. *The origins of the urban crisis: race and inequality in postwar Detroit*. Princeton University Press, New Jersey, first princeton classics edition edition, 2014. ISBN 978-1-4008-5121-8. OCLC: 878919151.

[76] The Greening of Detroit. greeningofdetroit.com, 2024. URL https://www.greeningofdetroit.com.

[77] J. Rosie Tighe and Stephanie Ryberg-Webster. *Legacy Cities: Continuity and Change amid Decline and Revival*. University of Pittsburgh Press, June 2019. ISBN 978-0-8229-8688-1. Google-Books-ID: 8AyfDwAAQBAJ.

[78] United States Census Bureau. U.S. Census Bureau QuickFacts: United States. URL https://www.census.gov/quickfacts/fact/table/DC,newyorkcitynewyork,oaklandcountymichigan,detroitcitymichigan,phoenixcityarizona,US/PST045222.

[79] US Census Bureau. Census.gov History, December 2020.

[80] NOAA US Department of Commerce. Climate, 2022. URL https://www.weather.gov/wrh/Climate?wfo=lwx. Publisher: NOAA's National Weather Service.

[81] Brian Walker. Conserving Biological Diversity through Ecosystem Resilience. *Conservation Biology*, 9(4):747–752, 1995. ISSN 0888-8892. doi: 10.1046/j.1523-1739.1995.09040747.x. URL https://www.jstor.org/stable/2386983. Publisher: [Wiley, Society for Conservation Biology].

[82] Wayne State University. Quaternary Geology, 2018. URL https://s.wayne.edu/urbangeology/quarternary-geology/.

[83] Frank B Woodford and Arthur M. Woodford. *All Our Yesterdays: A Brief History of Detroit*. Wayne State University Press, Detroit, UNITED STATES, 2017. ISBN 978-0-8143-4340-1. URL http://ebookcentral.proquest.com/lib/uva/detail.action?docID=5406189.

[84] Zhaoyin Feng. The US city run by Muslim Americans. *BBC News*, November 2021. URL https://www.bbc.com/news/world-us-canada-59212355.

Chapter 6

New York, New York, USA

Figure 6.1: View of New York City skyline with Brooklyn, NY in the foreground and Manhattan, NY in the background[66].

6.1 Introduction

The city of New York, New York (NYC) was chosen as a case study for this dissertation primarily due to its size. With over 8 million residents as of 2022, it is over 5 times larger in population than the next metropolis included in this dissertation, PHX. Adding to this, NYC also has a relatively small footprint for its population size, giving the city one of the highest population densities in the US, at 6870 residents per km^2[61]. Because of this, NYC has a unique challenge in implementing UGI: a balancing act of maintaining the necessary infrastructure, domiciles, and amenities required to support a large, high density population while also incorporating UGI efficiently and effectively to mitigate the impacts of climate change and improve the general well-being of the populace.

Apart from the sheer size of its population, NYC also has a complicated past concerning social justice and, more specifically, EJ. All of these factors combined with NYC's early and enthusiastic approach to implementing UGI make it an interesting and relevant case study for this dissertation.

6.2 Geography and Climate

NYC is a 783 km^2 metropolis in the Northeastern US located at the mouth of the Hudson River in the state of New York. Protected from the Atlantic Ocean by Long Island, NYC is a city among islands, with much of its geometry being established by the tidal straights between islands. These winding waterways include the East River, the Harlem River, Kill Van Kull, and New York Bay, as well as other smaller waterway divisions. NYC is both at an intersection of water as well as of land. Although, the city is within the state of New York, it shares a borders with New Jersey to the south and west and is only 16km in distance from the border of New York and Connecticut.

Five boroughs[1] make up NYC as a whole:

- Manhattan
- Brooklyn (Kings County)
- Staten Island (Richmond County)
- the Bronx
- Queens

Most of the boundaries of these boroughs are geographic, such as the Harlem River separating the Bronx and Manhattan, and Staten Island, surrounded by water, being its own borough. However, the boundary between Queens and Brooklyn is based on historical county boundaries that changed over time until 1898, when the boundary between Brooklyn and Queens was solidified[16]. To conform to the standards of this study, specific zones were chosen from the 2024 NYC Zoning Resolution[58], namely zones R1, R2, R3, and R4, which were most closely equivalent to the single family residential zones utilized in the previous case studies. Because of this, the borough of Manhattan, which has no R1, R2, R3, or R4 zones, was not included in the study.

Underlying NYC are several different geologic features that help to define its topography. Layers of glacial till overlay bedrock units that occasionally surface, creating distinct superficial features such as the exposures of the Manhattan Prong that manifest in Central Park[65, 21, 29]. NYC is extremely densely populated and, with

[1] A borough, in this case, is a self-governing city that comprises a smaller part of a larger city. The NYC government has authority over the smaller boroughs, but each borough has the ability to self-govern and provides many of the essential services required by its residents[39].

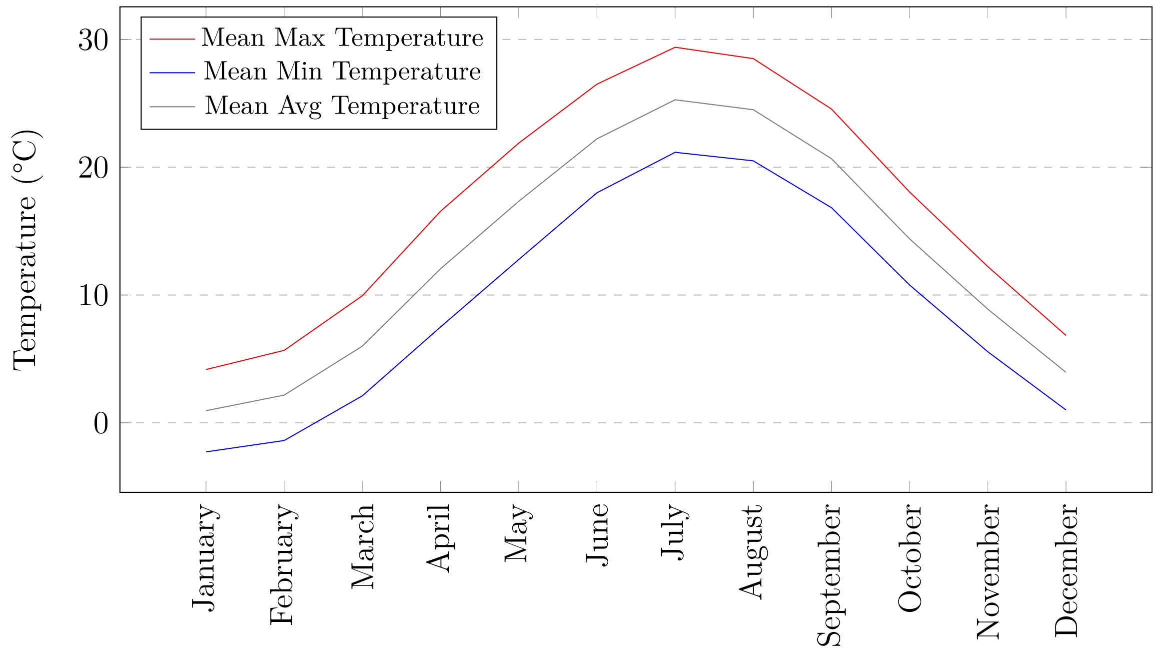

Figure 6.2: Monthly Climate Normal Temperatures for New York City (Central Park)[64].

open space for development being unavailable, some of the topological surface is anthropogenic in origin, with areas such as Battery Park in lower Manhattan and Cromwell's Creek in the South Bronx that are filled areas created to provide more living space[27, 3].

NYC has a borderline humid subtropic/humid continental climate (Köppen classification Cfa/Dfa)[23], with hot summers and cold winters, and with humidity and precipitation year round. Maximum monthly climate normals in the summer nearly reach 30°C, and minimum monthly climate normals dip below 0°C in the months of January and February (Figure 6.2). With much of NYC's urban area being a built environment, UHI is a perennial issue and significantly impacts its local temperatures during the summer months[49], with inter-city warming being up to 2°C warmer than surrounding areas during heat events[14]. In spite of the lack of seasonal precipitation (Figure 6.3), extreme precipitation-based flooding in NYC generally follows a

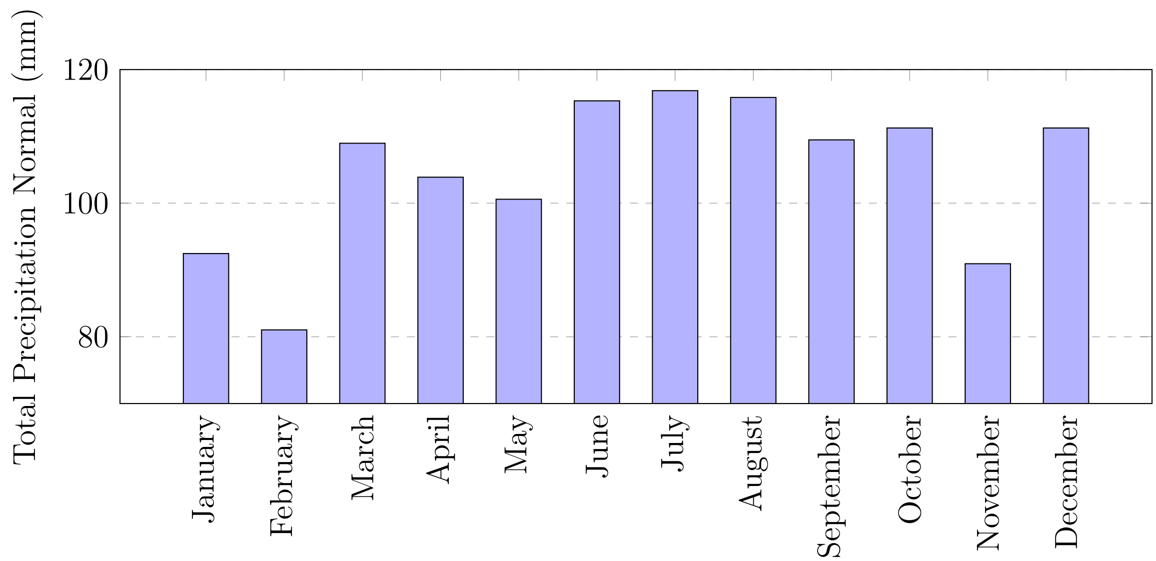

Figure 6.3: Monthly Average Total Precipitation for New York City (Central Park) [64].

seasonal pattern, with fewer occurrences in the winter months and an increase that begins in March and plateaus during the early summer[50].

Density sprawl in NYC has been much lower than the national average of the US, never cresting higher than 10 between 1970 and 2010 (Figure 6.4). The confining geography of NYC's islands contributed to this lack of sprawl and the increased pop-

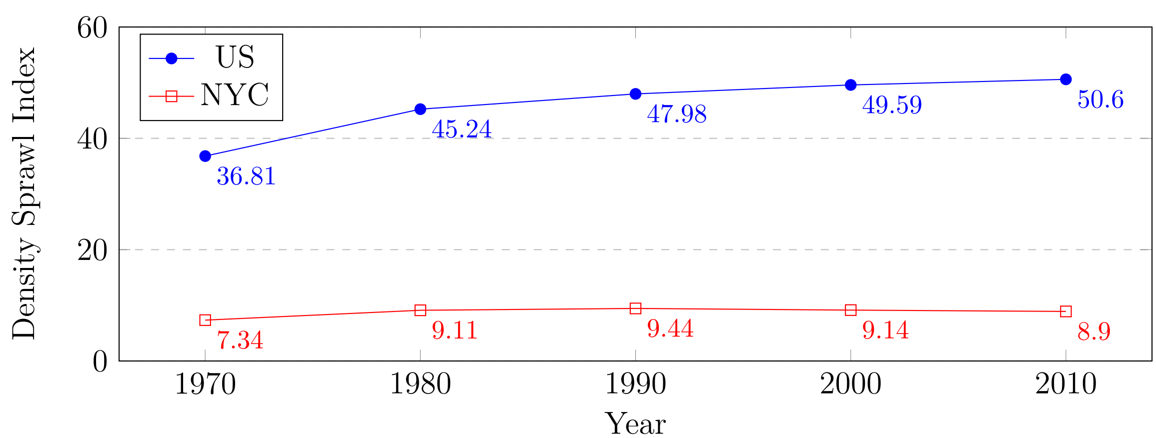

Figure 6.4: Density Sprawl Index for New York Metropolitan Division (including New York, NY, White Plains, NY, and Wayne, NJ, compared with the US Average, from 1970-2010[44].

ulation density, as outward sprawl was impossible for much of the city's history due to the bottlenecks in transportation between NYC and the mainland encouraging upward urban growth in the form of densely populated, multi-story construction[5]. This concentration has also influenced the landcover configuration of NYC; although NYC has not created the swaths of flat, low-density impermeable development associated with urban sprawl[45], NYC has a high percentage of impermeable surface landcover due to the infrastructure demanded by a high density population (Table 6.1). This leaves little physical space for vegetation such as tree canopy and grass, except for several large parks that were incorporated in planning early on in NYC's history (Figure 6.5).

Table 6.1: Total landscape PLAND calculations for New York City, NY. Calculations were made using 2017 landcover raster, and includes all areas within the NYC boundaries[] including the water bodies.

	PLAND
Tree Canopy	16.02%
Grass/Shrub	11.82%
Impervious	42.45%
Water	28.49%
Barren	1.22%

6.2.1 Projected Climate Change

Although NYC is considered among the most climate prepared cities in the world[22], global warming is still likely to have an enormous impact on its residents. There are four main climate associated challenges that NYC identifies in its 2023 AdaptNYC plan[59]:

- Coastal surge flooding

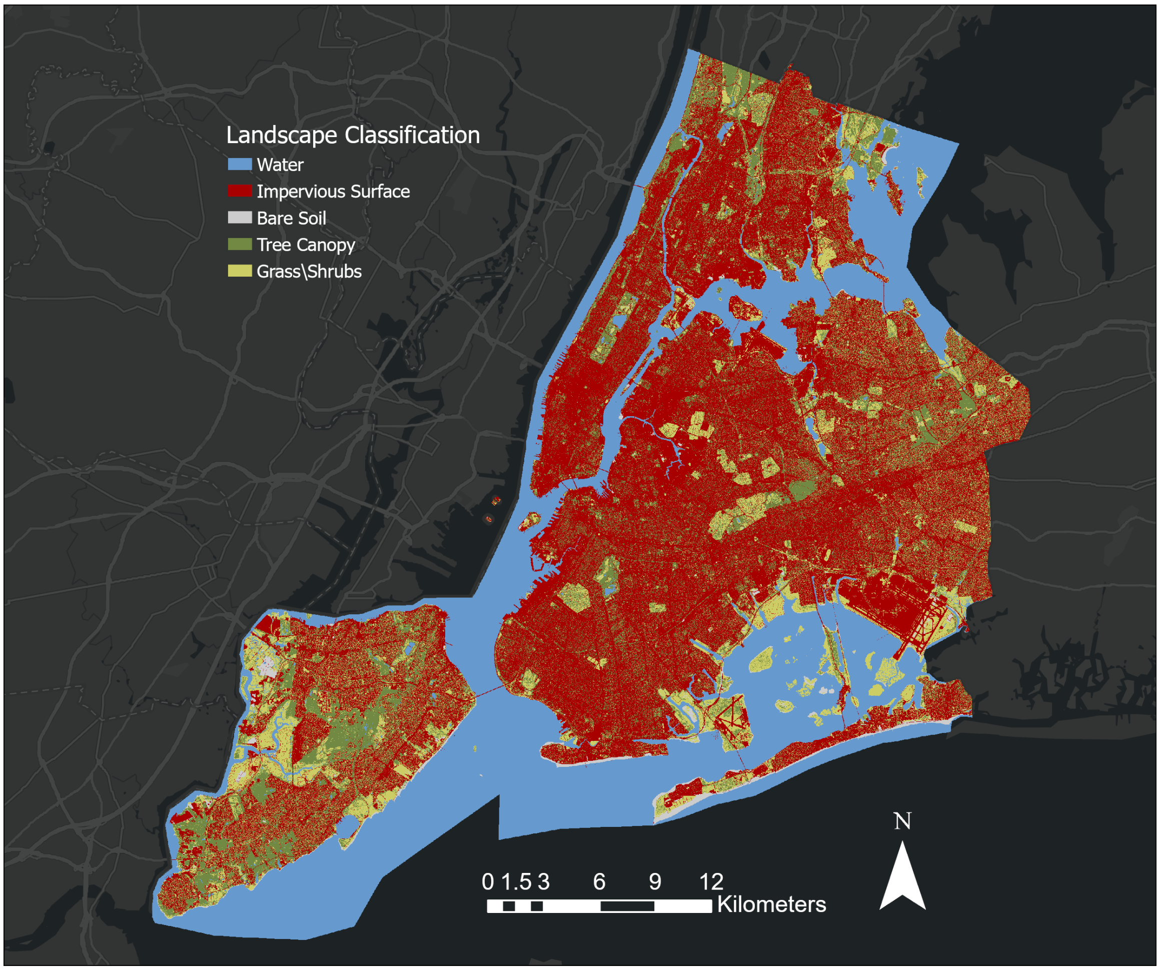

Figure 6.5: 2017 0.15 m Landcover Classification for New York City, NY[36].

- Chronic tidal flooding
- Extreme rainfall
- Extreme heat

Each of the above challenges is exacerbated by NYC's uniquely dense, built environment and its geographic location on a collection of islands at the mouth of a river.

The New York City Panel on Climate Change[37] outlined the projections for coastal flooding in a 2013 report. 100 year flood probability is expected to increase from 1.0% to between 1.4% and 5.0% in the 2050s, with the 100 year flood height increasing from a baseline of 15.0 feet to between 15.6 and 17.6 feet in the 2050s. Chronic tidal flooding is already a challenge for many coastal neighborhoods, and this is anticipated to impact over 86,000 1-2 family homes by the 2080s[59]. Although both of these are not the main focus of this study, as the UGI used to mitigate tidal and sea-level rise associated floods is restricted to coastal riparian zones, it is important to note that UGI is an important tool in addressing these challenges.

The frequency of extreme rainfall events are likely to increase as well. Since 1900, there has been a small but significant increase in the number of days per year with extreme rain events. In NYC, the four years with the highest number of rainfall events with over 2 inches of rainfall between 1900 and 2000 have occurred post 1980[37]. In the Northeastern US, of which NYC is a part of, occurrences of the extreme precipitation events have increased by 70% between 1958 and 2011[43]. The most extreme of these precipitation events, where over 3.5 inches of rain occurs, have the potential to inundate more than 116 km^2 in over 4 inches of floodwater (Figure 6.6).

Extreme heat events are anticipated to increase in both number and intensity in NYC.

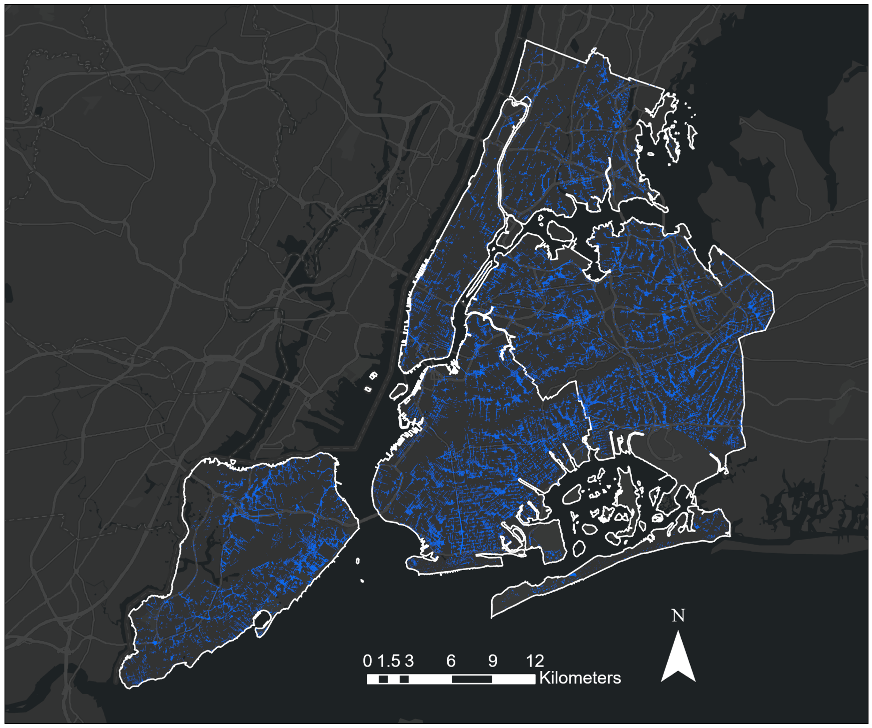

Figure 6.6: Maps of areas inundated with at least 4 inches of floodwater in the case of a 3.5 inch extreme precipitation event. Data was modeled by the City of New York for the city's 2021 Stormwater Resiliency Plan[55, 35].

The average number of days per year above 32.22°C from 1971-2000 was 18, and is expected to increase to between 24-33 by end of the 2020s, and to between 32-57 by the end of the 2050s[37]. Average air temperature was 12.22°C between 1971 and 2000, and this is expected to increase to between 13.05°C to 13.89°C by the 2020s, and 13.89°C to 15.83°C by the 2050s. The average duration of heat waves (concurrent days with a temperature above 32.22°C) is also projected to increase, from a baseline of 4 days between 1971 and 2000 to 5 days in the 2020s and 5-6 days in the 2050s[37].

6.3 Socio-Demographic Landscape

To examine the socio-demographic landscape of NYC, it may be helpful to start by dividing the city by its boroughs. Historically, the neighborhoods in each borough have changed in demographic composition over the years[5], but there are current trends in today's demographics that are rooted in history. The Bronx, specifically the South Bronx, saw a post-WWII exodus reminiscent of the "white flight" discussed in Chapter 5, transitioning from a collection of neighborhoods comprised of primarily second generation European immigrants to neighborhoods with approximately two-thirds of the residents being black or Puerto Rican, and often lower income. This has persisted through today, where there is still a considerably higher proportion of non-white individuals and of individuals below the poverty threshold in the Bronx than in the other boroughs (Figure 6.7). The borough of Staten Island, on the other hand, has both a higher proportion of white residents and lower proportion of low-income residents, much of which is attributable to this same post WWII "white flight", although Staten Island was the receiver of the racially driven migration[24].

Brooklyn and Queens are more of a patchwork regarding socio-demographic make-up. In the east of Brooklyn, neighborhoods in New Lots and Brownsville have a high proportion of both non-white populations and residents in poverty. Moving east, the percentage of non-white population remains high in the neighborhoods around Flatbush, yet the proportion of residents in poverty drops, save for a few locations. The reverse is true for the region north of Flatbush, which experiences a high proportion of residents in poverty but a lower percentage of non-white residents. The northwestern portion around Brooklyn Heights is lower in both minority population and population below poverty, but both of these metrics increase to the southwest.

Queens has a high proportion of residents who are under the poverty threshold and a low percentage of non-white residents in the south. Around the neighborhoods of Flushing and Jackson Heights, both the poverty and the non-white percentage of residents is high.

The borough of Manhattan, although not examined directly in this study, is in general low in both percent of not-white residents and in percent of persons below the poverty threshold, although both of these metrics increase in proximity to the Bronx.

The median household income of NYC is $76,607, and the per capita income is $48,066 (Table 6.2). However, these numbers are not uniform in each borough. The borough of Manhattan has a median household income of $99,880 and a per capita income of $89,702. The Bronx has the lowest median household income and per capita income with $47,036 and $25,845, respectively, and the highest rate of poverty in NYC, at 27.6%.

Table 6.2: A collection of basic information on New York City, NY.

	New York City	Brooklyn	The Bronx	Queens	Staten Island	Manhattan
Land Area	783.73 km^2	179.69 km^2	109.22 km^2	281.33 km^2	148.98 km^2	58.69 km^2
Population[1]	8,335,897	2,590,516	1,379,946	2,278,029	491,133	1,596,273
Per capita income[2]	$48,066	$43,165	$25,845	$39,201	$43,199	$89,702
Median household income[3]	$76,607	$74,692	$47,036	$82,431	$96,185	$99,880
Percent persons in poverty	17.2%	19.8%	27.6%	13.1%	11.2%	17.2%

[a] Population estimates base, July 1, 2022[62]

[b] In past 12 months (in 2022 USD, 2018-2022)[62]

[c] In 2022 USD, 2018-2022[62]

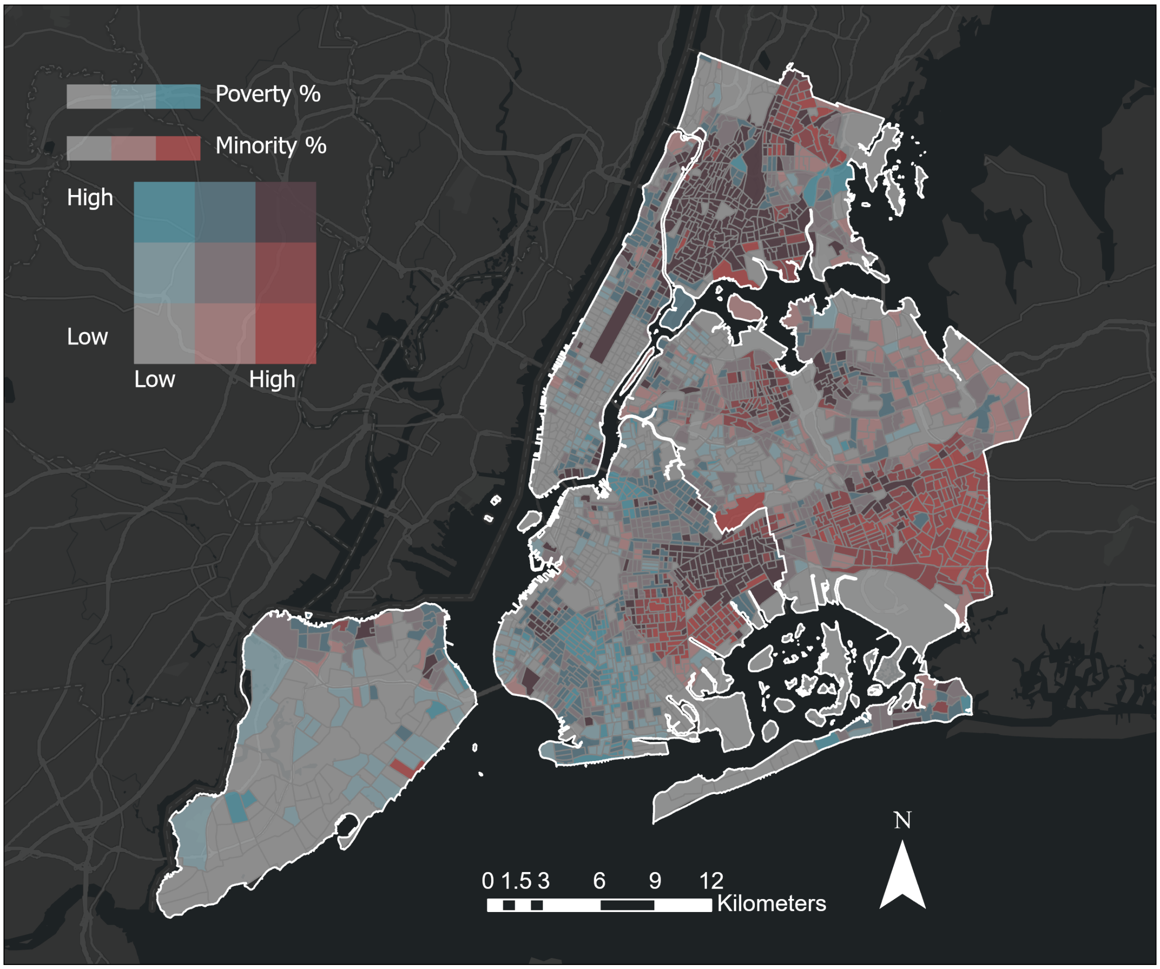

Figure 6.7: Bivariate choropleth showing the percentage of population that is a minority (shades of red) against the percentage of population that is under the poverty threshold (shades of blue) in New York City, NY. Data collected from 2020 CDC SVI[8]

6.4 Political History

Of all of the case studies included in this dissertation, NYC has perhaps the most complicated history. This section will attempt to provide a brief summary of the history of NYC, from before its founding to present day. Originally, the region was inhabited by the indigenous Algonquin people, specifically the northeastern group of Algonquin known as the Lenape[46]. Their land, known as Lenapehoking, encompassed the entire region that would later become NYC in post-European colonialism, with some population estimates at approximately 15,000 by the time of the first European appearance[5]. The groups of Lenape inhabitants were not considered well-developed tribes, and instead consisted of several autonomous groups ranging in population from a few dozen to several hundred living in a series of campsites, from which the populations would migrate seasonally. Within the area comprising the five boroughs of NYC, around 80 of these camps have been found by archaeologists, along with a network of trails connecting the sites[5].

Although the French and the Spanish were both thought to have previously visited the area [11, 70], in 1609 Henry Hudson, an Englishman in the employ of the Dutch, claimed the region for the Dutch East India Company. This visit encouraged Holland to send a group of settlers to establish a trading post on Staten Island. The trading post evolved into a bigger settlement with the formation of the Dutch West Indian Trading Company, and the Dutch land claim of New Netherland was established in 1623, stretching between the Delaware River and the Connecticut River[67, 5]. With the desire to further trade along the river now known as the Hudson, the Dutch continued to fortify their presence in the area, developing an encampment at the tip of Manhattan Island that would later become New Amsterdam and "purchasing[2]" both Manhattan Island and Staten Island from the Lenape[5].

In the 1630s, New Amsterdam continued to expand its claim outward from Manhattan Island, both to the north and across the East River, by "purchasing[2]" more land from the indigenous tribes and by establishing farms in what is now Kings, Queens, and Bronx Counties.

As a result of wars in Europe and the ambition of one Duke James Stuart of York, New Amsterdam was surrendered to the British in 1664, and New Amsterdam, with its new proprietor James Stuart, the Duke of York, became New York. This change would remain relatively permanent (save for the year of 1673, during which the Dutch captured New York and then returned New York to English following the Treaty of Westminster in 1674[42]) until the American Revolution in the 1770s. During this time, the English captured New York and used it as their headquarters in North America until the end of the war, in 1783[1]. Starting in 1785, New York served as the national capitol under the Articles of Confederation and, subsequently, the Constitution of the United States, until 1790, when the capital was moved to Philadelphia[5].

During the 1800s, NYC expanded and grew from approximately 60,000 residents to well over 3 million. This was a result of NYC's position as a sea port and its connection to the Hudson River and thus, to the Erie Canal, serving as a conduit for trade between the Atlantic US and the Midwest US. As a bustling port city with a booming economy, NYC was attractive to immigrants, and saw several surges in immigration during this time, with waves of Irish, German, Jewish, and Italian immigrants flocking to the city in search of opportunity[19, 13]. These increases in

[2] It is believed by historical scholars that the concept of purchasing land was misunderstood by the Lanape, who believed that land could not be bought or sold to an individual owner, indicating that this "purchase" may not have been made in good faith[26].

population drove the urbanization of the surrounding areas, including the counties of Queens, the Bronx, and Richmond, as well as the town of Brooklyn (Figure 6.8). This urbanization of the surrounding region was accelerated further by the building of High Bridge and Washington Bridge over the Harlem River (in 1848 and 1888, respectively), and the construction of the Brooklyn Bridge over the East River in 1883. These bridges provided conduits for the residents of the NYC region that allowed uninhibited travel throughout an urban geography segmented by waterways. The push for infrastructural connectivity of the region led to the consolidation of NYC in 1898, when each of these areas, alongside Manhattan, were joined as 5 boroughs under the overarching government of NYC[5], immediately increasing the city's footprint from 155 km^2 to 783 km^2.

From this point onward, NYC became an unprecedented experiment in urban planning, where the transition zones between the urban areas that were now consolidated as part of the NYC "urban" area included fuzzy zones of suburban and even rural regions[47]. The dynamics of these previously separate governmental entities and how they interacted with the NYC government helped shape the urban development of each region over time. NYC public servants like Andrew Haswell Green in the late 1800s and Robert Moses in the early 20^{th} century pushed for a more top-down regionalist approach to urban planning, giving these un-elected officials the power to shape the infrastructure and, concurrently, the UGI of NYC.

6.4.1 Social Equity in NYC

NYC's history is rife with events and policies that have benefited the few over the many, marginalizing vulnerable groups. Starting with the initial fraudulent "land

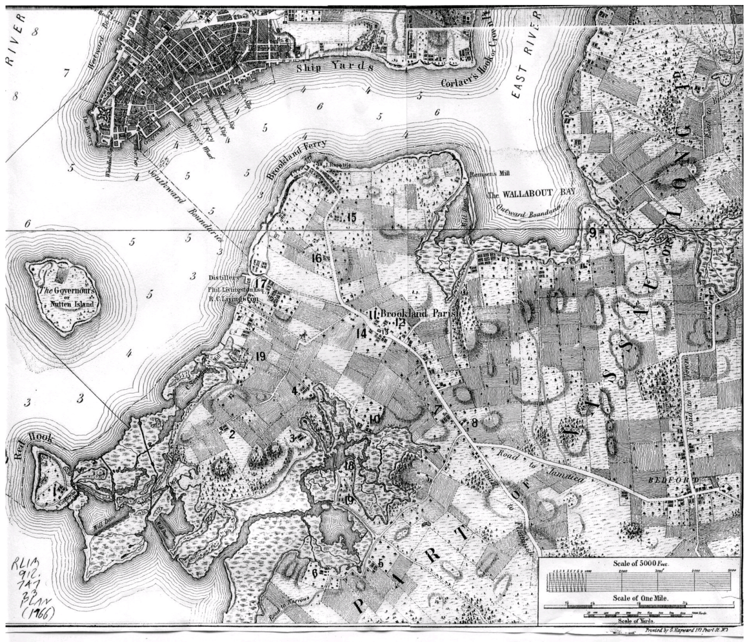

(a) Map of Brooklyn in 1766, prior to outward urbanization from Manhattan, showing little residential development and mostly agricultural use[4].

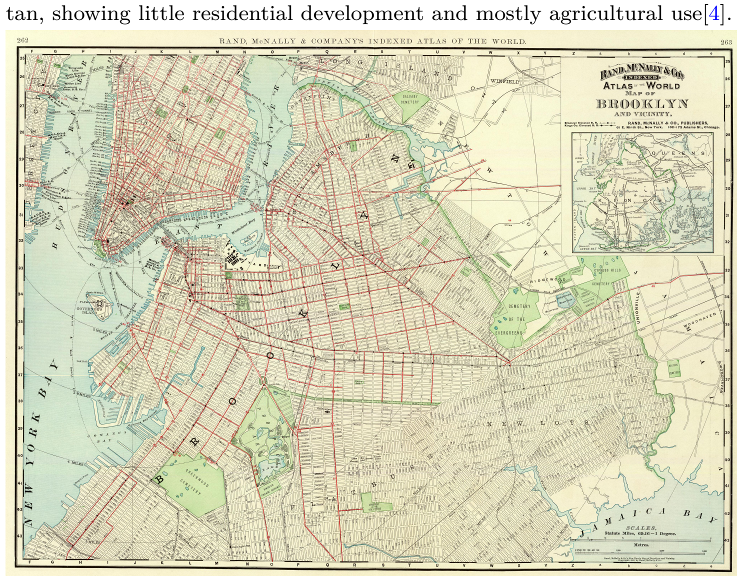

(b) Map of Brooklyn in 1897, a year before consolidation and after the construction of the Brooklyn Bridge across the East River[31].

Figure 6.8: A comparison of pre and post urbanization Brooklyn. Development of what was primarily agricultural land into residential and urban land took place in the early 1800s and was accelerated by the construction of the Brooklyn Bridge in 1833.

purchase" from the Lenape in the 1600s by Dutch capitalists, grave injustices were interspersed between the commendable feats associated with building a metropolis. Slavery existed in NYC from 1626 to 1827, when it was outlawed by the state of New York. The work of enslaved Africans can be attributed to much of the growth and success of NYC during this time[15]. Even following emancipation, black residents of NYC struggled to attain equality with their white neighbors, with low paying domestic work being the only occupations readily available to black men and women throughout the 1800s[15, 48]. This changed slightly in the 20th century, with increasing black representation in the manufacturing sector of NYC during the early 1900s following the Great Migration, yet these jobs were still low paying, leaving the black population of NYC financially burdened. A lack of economic momentum rooted in historical injustices combined with a complex system comprised of employment sectors with dominant "ethnic niches[3]" has created a racial wealth divide that exists to this day[68]. Although this dissertation does not intend to provide a comprehensive list of the well-documented mistakes made during the development of NYC, this section will examine in more detail some historical EJ problems linked closely with with NYC urban planning decisions.

In regards to NYC UGI planning, few individuals have had such a substantial impact as Robert Moses. The first Commissioner of the New York City Department of Parks and Recreation, Moses was a proponent and a driving force behind the urban renewal push of NYC in the 1940s, a movement to revitalize blighted areas in cities and replace them with public housing, highways, and parks. As an architect of NYC's park system, Moses is a polarizing figure[7]. His policies helped revitalize areas of the city,

[3] An ethnic niche, as described by Waldinger [68], refers to a sector of a city's labor market that has been historically dominated by specific ethnic groups and, consequentially, maintains this dominance as newcomers to the city are funneled into these professions via ethnic and familial ties.

providing housing and parks to residents, creating the New York State Parks system, and building 13 expressways across the city. However, he also purportedly designed policies through a racist and classist lens, killing projects that would install UGI in low income areas, attempting to discourage people of color from utilizing public recreation facilities, and showing little regard for vulnerable communities when planning large, disruptive projects, such as expressways, through their communities[7]. It is widely believed that Moses can be given credit for the push for urban renewal in NYC, as well as in the US as a whole, but it is also believed that his unchecked racist views unfairly impacted NYC's vulnerable communities.

This problematic attitude has been perpetuated into recent times, sparking backlash from residents and environmental rights groups[69]. As an example, in 1986, when the North River Sewage Treatment Plant initiated operations in West Harlem, residents of the poorer, minority-dominated community complained of noxious fumes, poor air quality, and health issues. This plant was originally planned to be located in the Upper West Side of Manhattan, but this location was changed to West Harlem as the original location was deemed "incompatible" with the development of the Upper West Side, which was a majority white neighborhood[32]. Hearings were held in 1968 regarding the siting of this plant, during which there was vehement opposition from West Harlem residents, yet the plant was still constructed after the EPA pushed the city to stop dumping sewage into the Hudson. In the rush to complete the North River Sewage Treatment Plant to avoid EPA fines, errors were made in the construction of the facility, leading to the poor air quality experienced by the neighboring residents upon its opening in 1986. In 1994, environmental activists settled a lawsuit against the city, forcing the city to fix the plant[32]. Examples like this, where top-down city planning has marginalized vulnerable communities in the push towards city-wide progress, remain a chronic problem within the city[69].

NYC has also been subject to many of the same racially prejudiced practices present in the previous case studies, including redlining by the HOLC[17]. This practice in particular continues to negatively impact the residents of these neighborhoods, many of whom are vulnerable[33]. Studies have suggested that historical redlining in NYC may be a structural determinant of preterm birth[25]. Air pollution near schools in previously redlined NYC neighborhoods continues to be higher than in other neighborhoods[18]. Exposure to Coronavirus in NYC in minority populations was linked to historical redlining[28]. These, and many other impacts, continue to plague vulnerable communities in NYC.

6.4.2 UGI Policy in NYC

In spite of (or, perhaps, because of) the injustices discussed in Subsection 6.4.1, NYC UGI policy has a keen focus on EJ and social equity. In 2007, Mayor Michael Bloomberg released PlaNYC, a comprehensive plan poised to prepare the population for expected future changes. PlaNYC included three components[51]:

- OpeNYC: A plan to address and prepare for increases in NYC's population
- MaintaiNYC: A plan to upgrade, repair, and maintain NYC's infrastructure
- GreeNYC: A plan addressing sustainability issues in NYC, including climate change and resource conservation

PlaNYC's 127 initiatives targeted ten key areas of focus:

- Housing and Neighborhoods
- Parks and Public Spaces
- Brownfields
- Waterways
- Water Supply
- Transportation
- Energy
- Air Quality
- Solid Waste
- Climate Change

Within each of these areas of interest, the Bloomberg Mayoral Office included several initiatives that contained facets related to UGI. The MillionTreesNYC initiative, a plan to plant 1 million trees in all five boroughs of NYC by 2017, was one such initiative born from this plan, and was successfully completed in 2016. The 2010 Green Infrastructure Plan[52] was another initiative, detailing the city-wide strategy to implement UGI over gray infrastructure in stormwater control scenarios. PlaNYC was rather successful quantitatively, with 97% of the proposed initiatives launched, leading to over 250,000 NYC residents having better access to parks, the creation of the Office of Environmental Remediation, and many other achievements. However, the Bloomberg Mayoral Office was criticized due to the fact that PlaNYC lacked community involvement and planning at the neighborhood level[20, 2], with complaints that certain communities were under-represented in the plan. Additionally, the catastrophe that Hurricane Sandy wrought throughout NYC exposed the need for better resiliency measures in the face of climate change adjacent disasters[34].

With the top-down regionalist governing style prevalent in NYC, the plans launched by the current NYC Mayoral Office are subject to change with shifts in management following a mayoral election. Bloomberg was ineligible for the 2013 NYC mayoral election due to NYC term-limits, and Bill de Blasio won the election and took his place. De Blasio's administration reworked PlaNYC, building on some of the environmental principles introduced in Bloomberg's plan but turned towards approaching the future of NYC with a focus on equity, renaming the plan OneNYC[54]. This plan was constructed around four principles:

- Growth
- Equity
- Sustainability
- Resiliency

By introducing equity as a main component of NYC planning, OneNYC officially made EJ a priority in NYC regional governance. However, for better or for worse, as equity became a priority, sustainability was no longer the primary focus[9]. This did not necessarily cripple environmental efforts in NYC; the de Blasio administration continued to pursue environmental sustainability with goals such as reducing waste disposal by 90% by 2030, cutting NYC greenhouse gas emissions by 80% by 2050, and expanding UGI for stormwater management. In fact, an initiative of the OneNYC plan directly addressed the need for connectivity of open space, introducing the Parks Without Borders strategy to make open spaces more accessible to residents throughout the city. Additionally, the OneNYC plan specifically addresses EJ, with plans to address flooding, brownfield redevelopment, and park improvement in vulnerable areas while acknowledging the importance of community engagement and information dissemination[54].

In 2021, another mayoral election in NYC was held and, again, the incumbent, Bill de Blasio, was ineligible to run due to term limits. This election was won by Eric Adams, who's administration again changed the comprehensive plan of NYC, changing the name to PlaNYC: Getting Sustainability Done, and restructuring the plan's goals and priorities[56]. This version of PlaNYC has a simpler structure than the Bloomberg or de Blasio plans, with 3 objectives, 10 goals, and 32 initiatives (Table 6.3).

PlaNYC: Getting Sustainability Done continues to build on previous administrations' work. The plan continues to expand on resiliency and EJ, but claims to approach climate change challenges with "concrete actions"[56]. Each initiative identified in the plan comes with a number of actions that NYC intends to take to accomplish the initiative. For example, to achieve the initiative *Achieve a 30% tree canopy cover*, the plan lists the following actions:

- Expand the Tree Risk Management Program, and in 2023, establish the Climber and Pruner Training Program pilot
- Ensure that all new buildings meet the City's street tree planting requirements through improved enforcement by 2035
- Incentivize New Yorkers to steward green spaces by 2035
- Maximize tree preservation and planting opportunities, including in areas with challenging site conditions, by 2035

Additionally, in 2022 Adams reconfigured the NYC climate change departmental teams and united them under a single entity: the Mayor's Office of Climate and Environmental Justice. This office was developed to tackle climate change and environmental issues while incorporating equity and EJ. This was an extension of the work done under the de Blasio administration in 2017, which established an Environmental Justice Advisory Board that included external EJ advocates, academics, and

Objective	Goal	Initiative
Protecting Us From Climate Threats	Extreme Heat	1. Maximize Access to indoor cooling
		2. Cool our built environment
		3. Achieve a 30% tree canopy cover
	Flooding	4. Create a new leadership structure for coastal flood resilience in 2023, headed by DEP
		5. Implement a multilayered strategy for flood resilience
		6. Launch a voluntary housing mobility and land acquisition program to provide housing counseling and facilitate future land acquisition with Federal and State funds
	Buildings	7. Support building owners in complying with Local Law 97 missions reduction goals by 2030
		8. Decarbonize affordable housing
		9. Pursue fossil fuel free City operations
		10. Reduce localized air pollution in NYC
		11. Reduce the carbon footprint of the construction industry by 2033
	Clean & Reliable Energy	12. Maximize climate infrastructure on City-owned property
		13. Connect NYC to clean electricity resources
		14. Assist building and homeowners with clean energy projects and solar installation
Improving Our Quality of Life	Green Space	15. Create an accessible and connected network of open spaces
		16. Improve the health of our forested areas
	Waterways	17. Reduce combined sewer overflows by more than 4 billion gallons per year by 2045 to improve water quality
		18. Develop a strategy to end the discharge of untreated sewage into the New York Harbor by 2060
		19. Improve the health and ecological function of wetlands
	Transportation	20. Get polluting trucks off NYC streets
		21. Prioritize public transit, walking, and biking first
		22. Ensure every New Yorker can access a bike or scooter
		23. Help New Yorkers who must drive to drive electric
	Food	24. Reduce emissions of City agency food purchases 33% by 2030
		25. Promote reduction in institutional food-related emissions 25% by 2030
		26. Reduce emissions from commercial cooking
		27. Support NYC's watershed farmers in expanding sustainability practices and food production
Building the Green Economic Engine	Green Economy	28. Launch new climate education and training programs for public schools
		29. Grow NYC's green workforce
		30. Support entrepreneurship and industry innovation
	Waste & Circular Economy	31. Collect organic materials and turn into energy and reusable assets
		32. Develop new markets and expand recycling and reuse

Table 6.3: The PlaNYC: Getting Sustainability Done plan with goals and initiatives[56]

public health experts alongside appointees from the mayors office. Under Adams, another report and data portal is currently being prepared and is planned to be released in 2024[57].

On May 19, 2023, the New York State Department of Environmental Conservation and the New York City Department of Environmental Protection publicly agreed to invest $3.5 billion in UGI for the purpose of stormwater control[38], a modification of a 2012 Consent Order put in place during the Bloomberg administration. The original consent order committed to building $1.5 billion in UGI using private and public funding, while deferring $2 billion in gray infrastructure construction projects[60].

Considering the above policies, it is crucial to note that the analyses in this chapter are executed on data that will not reflect the most recent PlaNYC policy changes, as the landcover data used is from 2017, when NYC was under the de Blasio administration. However, the direction of policy in regards to EJ and UGI placement was already progressing during this administration, and continues to be an important pillar of the city's sustainability plan.

6.5 Detailed Methodology

NYC has a relatively complex zoning system, with 10 different forms of residential zoning that are divided into subcategories[58]. For this study, residential zones R1, R2, R3, and R4, along with their subcategories were chosen. These zones were the closest comparison to the single family housing zones seen in the previous chapters. Using a zoning dataset from the NYC OpenData[40], all areas zoned as R1, R2, R3, and R4 were kept, and the remainder discarded. As the borough of Manhattan does not have any of these residential zones, it was not represented in this study. Within the boundaries of these zones, 1000 random points were created, and 2km radius buffers applied in accordance with Chapter 2 methodology. As the boundaries and the minimum distance threshold of 5 km did not allow space for 1000 plots without overlap, only 833 plots were created. Some plots fell partially outside the NYC boundaries, and these plots were discarded. Additionally, some plots were located on Governor's Island. While the zoning technically fits the study's definitions, Governor's Island does not have year-round residents[6], and these plots were discarded. Any plots with a majority of water as landcover were discarded. Any plots that overlapped with a census tract with a prison[41] that would contribute to the SVI variables were discarded.

This particular case study benefited from a very-high-resolution (6 inch) 2017 landcover raster dataset provided by the New York City Office of Technology and Innovation[36]. This landcover raster classified the NYC region with object-based detection using a combination of 2017 LiDAR and 2016 4-band orthoimagery, alongside vector GIS datasets. The landcover classification split landcover into 8 classes:

- Tree Canopy (Vegetation $>$ 8 ft. in height)
- Grass/Shrub (Vegetation $<$ 8 ft. in height)
- Bare Soil
- Water
- Buildings
- Roads
- Other Impervious Surfaces

- Railroads

For this analysis, the distinction between different types of impervious surfaces was not considered relevant, and *Buildings*, *Roads*, *Railroads*, and *Other Impervious Surfaces* were grouped under the umbrella category of impervious surfaces.

Using the created sample plots and the landcover raster, LSMs were calculated within each sample plot using R code (Appendix A.1). 2020 SVI data was utilized to apportion vulnerable populations into sample plots. Using the Apportion Polygon Tool in ArcGIS Pro[12], and 2020 census block data, the population and households fields that fit the SVI variable criteria were apportioned. Plots that contained population < 10 were discarded, leaving n = 733 plots. These plots were then analyzed using PCA. As the PLAND for bare soil is only just over 1% of the total land area coverage (Table 6.1), metrics pertaining to bare soil were removed from the PCA. Although the PLAND of water within the city boundaries is over 28%, plots were not created over the waterbodies that make up the vast majority of this landcover and, thus, sample plots did not contain a large areal coverage of water. Because of this, water LSMs were also removed from the PCA. Factors that cross-loaded were then examined more thoroughly using Mean Rank Analysis, the results of which can be found in Appendix B.3.

6.6 Results of Analysis

6.6.1 Principal Component Analysis

Using a Varimax rotation with Kaiser Normalization, 7 components were extracted explaining 78% of the variance (Table 6.4). PC 1 (explaining 28% of the variance)

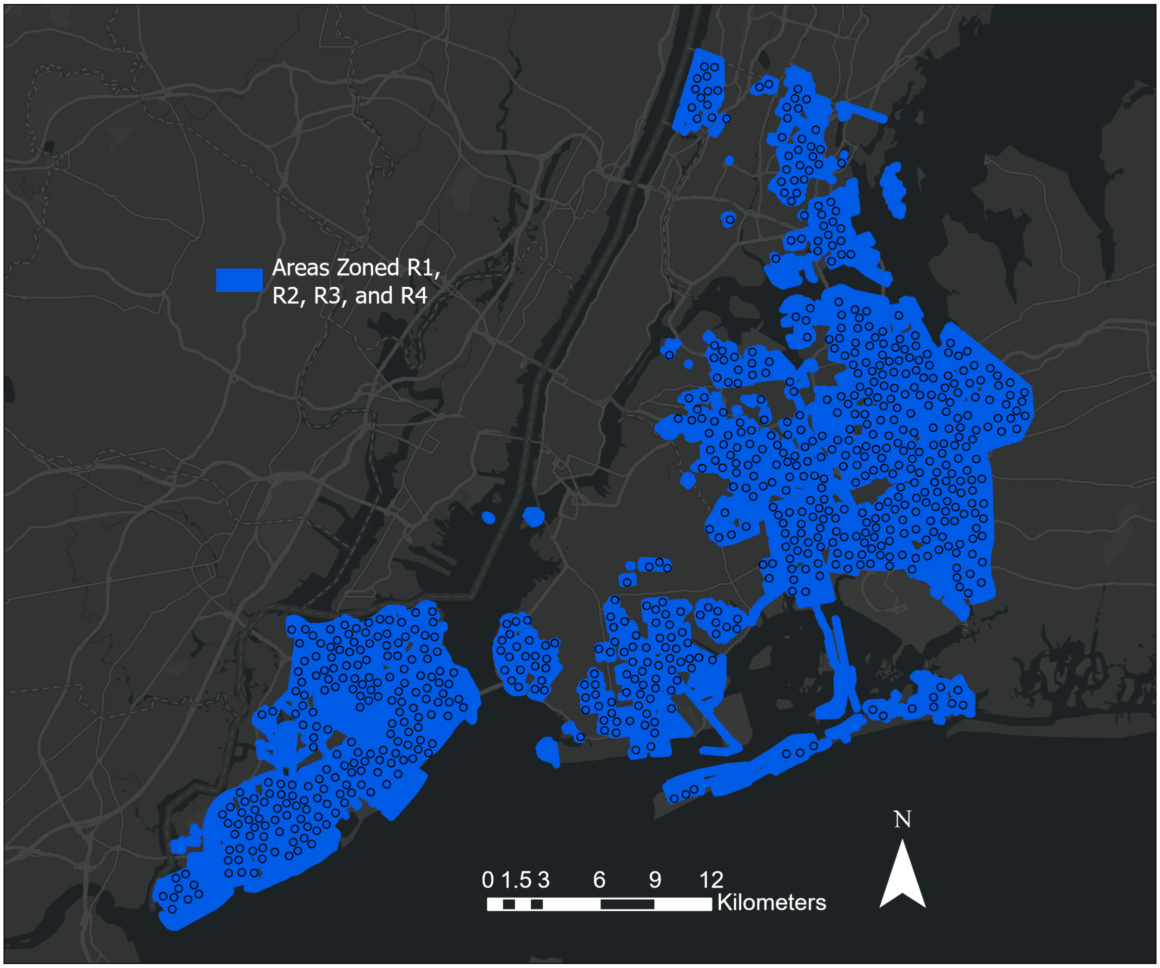

Figure 6.9: Sample plots for New York City, NY (n = 733). Black circles denote sample plots used in this study, blue zones represent areas zoned as R1, R2, R3, or R4.

is loaded with factors representing increased impervious coverage/connectivity and decreased tree canopy coverage/connectivity. Of all of the LSMs dealing with tree canopy and impervious surfaces, only Impervious LSI and Impervious ENN_MN do not significantly load onto PC 1. The factor that is loaded the strongest onto this component is Tree PLAND, at -0.943. PC 2 (explaining 15% of the variance) is loaded with more LSMs, but these factors are centered around the coverage/connectivity of grass and its inverse relationship with the coverage/connectivity of impervious surfaces. The only grass LSM that does not load onto this component is Grass ENN_MN.

The impervious LSMs that load onto PC 2 include PLAND, LPI, and ENN_MN. The factor that loads most heavily onto this component is Grass PLAND, with a loading of 0.911. PC 3 (explaining 11% of the variance) is again loaded primarily with LSMs, but these factors are associated with a combination of ENN_MN and LSI for tree canopy, grass, and impervious coverage. As the LSI for all of these landcover types is heavily negatively loaded onto PC 3, it can be assumed that this component represents the variance attributed to plots with very simple shapes for all landcover types,i.e. a single, squared patch of landcover would have an LSI of 1, and LSI would increase as the edge length of the patch (or patches) increases relative to the area. This, coupled with a positive loading of ENN_MN for all landcover types and Impervious PLADJ indicates that this component represents the ”checker-boarding” effect of urban plots, dominated by impervious surfaces with interspersed vegetation in the form of trees and grass in simple, yet small, configurations.

PC 4 (explaining 8.5% of the variance) is the first component to be loaded with SVI factors. Poverty %, No High School Diploma %, Uninsured %, Minority %, Limited English %, Household Crowding %, and Housing Burden % all loaded positively onto this component, with Limited English % loading the strongest at 0.843. PC 5 (explaining 6% of the variance) is also loaded with SVI factors, with Poverty %, Age 17- %, and Single Parent Household % loading positively and 65+ % loading negatively. This could indicate a SVIloading representing the variance attributed to single parent families. PC 6 (explaining 5% of the variance) is loaded primarily with the SVI variables Unemployed %, Uninsured %, and Minority %. However, Tree ENN_MN is also cross-loaded positively onto this component, indicating the first and only cross loading between LSMs and SVI factors. This indicates a weak positive relationship between the percentage of population within each plot that is considered

Table 6.4: *PCA Rotated Component Matrix for sample plots in New York City, NY.* Rotation Method: Varimax with Kaiser Normalization. Scores below |0.32| were considered a poor correlation and were not included in this component matrix[10].

Variable	Component						
	1	2	3	4	5	6	7
Below Poverty %				0.635	0.409		0.369
Unemployed %						0.744	
No HS Diploma %				0.776			
Uninsured %				0.699		0.360	
Age 65+ %					-0.718		0.388
Age 17- %					0.814		
Disability %							0.856
Minority %				0.451		0.649	
Limited English %				0.843			
Housing Burden %				0.619			0.352
Single Parent Household %					0.726		0.371
Household Crowding %				0.648			
Impervious PLAND	0.728	-0.581					
Tree PLAND	-0.943						
Grass PLAND		0.911					
Impervious LPI	0.751	-0.503					
Tree LPI	-0.861						
Grass LPI		0.877					
Impervious LSI			-0.928				
Tree LSI	0.428		-0.712				
Grass LSI		-0.333	-0.857				
Impervious ENN_MN		0.606	0.370				
Tree ENN_MN	0.547		0.475			0.390	
Grass ENN_MN			0.828				
Impervious PLADJ	0.434		0.748				
Tree PLADJ	-0.923						
Grass PLADJ		0.893					
Impervious Cohesion	0.667						
Tree Cohesion	-0.889						
Grass Cohesion		0.831					

Kaiser-Meyer-Olkin Measure of Sampling Adequacy.		0.753
Bartlett's Test of Sphericity	Approx. Chi-Square	27244.709
	df	435
	Sig.	< 0.001

vulnerable due to unemployment, lack of insurance, and status as a minority, and the distance between trees within that plot. Finally, PC 7 (explaining 4% of the variance) is loaded positively with more SVI factors: Poverty %, Age 65+ %, Disabled %, Single Parent Household %, and Housing Burden %. This is the only example in this entire dissertation of Age 65+ % loading positive alongside other SVI factors, and may represent the variance that can be attributed to vulnerable residents who are elderly and disabled.

6.6.2 Mean Rank Analysis

To begin, the relationship between Tree ENN_MN and the SVI variables that also loaded onto PC 5 was deemed worth exploring with Mean Rank Analysis. The plots were split into two percentile classes regarding Unemployed % (UE1 and UE2), Uninsured % (UI1 and UI2), and Minority % (M1 and M2), with one class holding all plots in the lower 50^{th} percentile (UE1, UI1, and M1) and the other class holding all plots in the upper 50^{th} percentile (UE2, UI2, M2). The Tree ENN_MN of these groups was then compared using Mann Whitney U tests to determine if there was a significant difference in the means of the upper and lower 50^{th} percentiles for each of these variables.

Results of the Mann Whitney U Test (Appendix B.5) indicate that the differences in means between the lower and upper 50^{th} percentile groups for all SVI variables tested are significant ($p < .001$). For every SVI variable tested, the mean rank was lower in the group consisting of a lower percentage of vulnerable residents (UE1, UI1, M1) than in the group consisting of a higher percentage of vulnerable residents (UE2, UI2, M2) (Figure 6.10). The largest difference in mean rank occurred between percentile

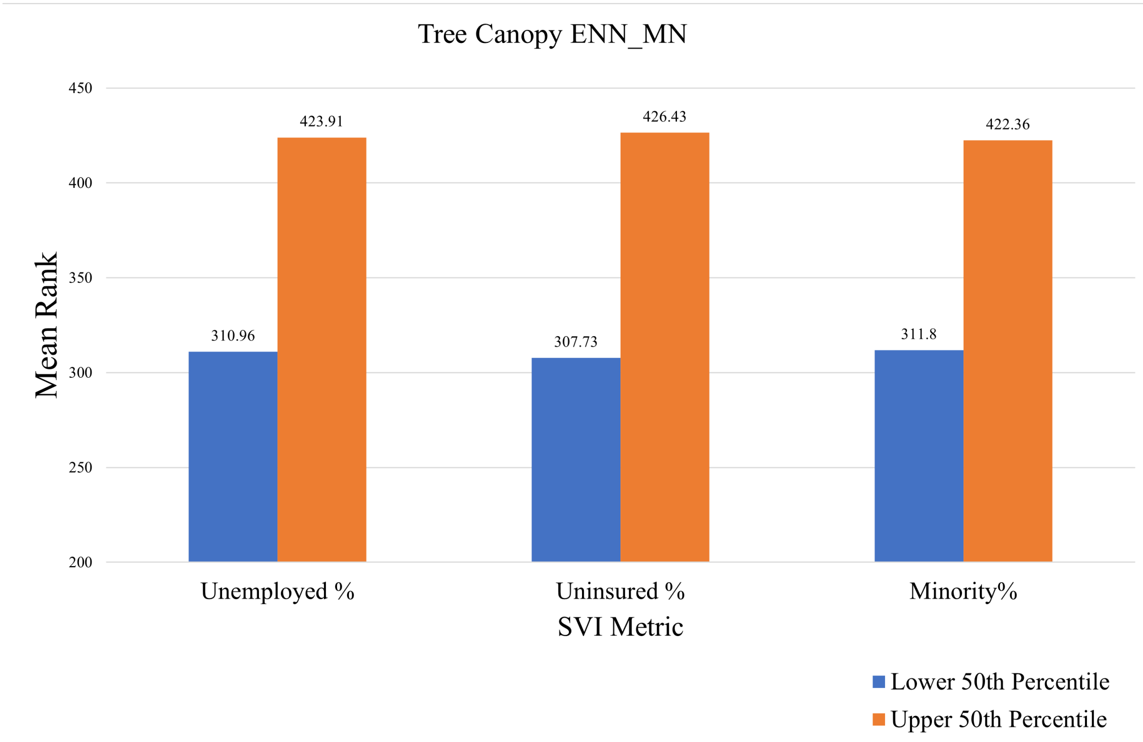

Figure 6.10: Bar graph illustrating the differences in mean rank between lower and upper percentile groups for the LSM Tree ENN_MN. Blue bars represent the groups with plots in the lower 50th percentile, orange bars represent the groups with plots in the upper 50th percentile. Numbers at the top of each bar indicate mean rank.

groups for Uninsured % (118.7), followed by Unemployed % (112.95) and Minority % (110.56).

6.7 Discussion

What is perhaps most interesting in the results of the above analyses are the relationships we did not see. Using the aforementioned methodology, no SVI variables cross-loaded onto components that were dominated by LSMs, and only one LSM (Tree ENN_MN) cross-loaded onto a component dominated by SVI variables. Mean rank analysis did yield significant differences in the means of plots in the lower and upper

50^{th} groups for Unemployed %, Uninsured %, and Minority %, with the lower percentile groups seeing a smaller ENN_MN, indicating a closer distance between trees in those plots. However, this was the only relationship exposed by PCA, supporting both hypotheses H1 and H2, but weakly.

Several factors could be attributed to these findings. NYC has had a robust and mature urban sustainability program that focuses on both a need to address EJ as well as UGI as city-wide priorities[51, 53, 54, 56]. UGI has been considered a priority since as early as 2007, with plans specifically promoting the connectivity of parks and open space. The most recent plans, since 2015, have retained these goals but also built upon them, adding EJ as a featured priority and making concerted efforts to communicate with vulnerable communities and encourage participation in the process. Successful programs, like the MillionTreesNYC program[30], have added tree canopy citywide, and ambitious tree canopy coverage goals have been included in every plan since 2007.

Another possible explanation for the lack of strong relationships seen in these analyses could stem from the design of this study. As stated in Chapter 2, this study focuses on land zoned for Single Family Residential (or a similar zoning) to help standardize the plot analysis. However, in NYC, the median value of owner-occupied housing units was $732,100 in 2018-2020[63], and the median rent for homes in NYC for 2024 is $3,200 per month. Considering that the per capita income of NYC is only $48,066 on average, and as low as $25,000 in the Bronx (Table 6.2), it seems that those prices would be unaffordable to many residents of NYC, not just those in poverty. This indicates a flaw in the methodology of this study: although the sample plots did capture a sample of vulnerable residents, it is likely that a large swath of the most vulnerable population of NYC is not being recorded when only analyzing Single

Family Residential zoned regions of the city. To better capture this population, the methodology should be adapted to include high density living situations, such as apartment buildings and high-rises.

Taking into account the need to include other zones in this particular study, it does appear that NYC's focus on UGI as a climate change mitigation strategy, as well as the city's emphasis on EJ, has encouraged some equitability in UGI connectivity in Single Family Residential zones throughout the city. The only connectivity metric that exhibited a relationship with any SVI variables was Tree ENN_MN, but these variables loaded onto PC 6, a component that only explained roughly 5% of the variance. Mean rank analysis indicated significant differences ($p < 0.001$) in this LSM for plots in the upper and lower 50^{th} percentiles of the Unemployed %, Uninsured %, and Minority % variables. This supports both hypotheses, but the lack of other LSMs exhibiting relationships may indicate NYC's effective UGI and EJ policies, as well as a weakness in the analyses for this particular case study.

References

[1] Rohit T. Aggarwala. "I want a Packet to arrive": Making New York City the headquarters of British America, 1696-1783. *New York History*, 98(1):7–39, 2017. ISSN 0146-437X. doi: 10.1353/nyh.2017.0036. URL https://www.jstor.org/stable/90018770. Publisher: Fenimore Art Museum.

[2] Tom Angotti. Is New York's Sustainability Plan Sustainable? *Hunter College Department of Urban Affairs*, January 2008. URL https://www.academia.edu/52304805/Is_New_Yorks_Sustainability_Plan_Sustainable.

[3] Austin Bradley. The Surprisingly Long History of Battery Park City – New York's Newest Neighborhood. *The Agency Journal*, July 2016. URL https://www.theagencyre.com/blog/the-surprisingly-long-history-of-battery-park-city-new-yorks-newest-neighborhood/.

[4] Bernard Ratzer. Map of Brooklyn, NY made in 1766, 1766. URL https://commons.wikimedia.org/wiki/File:BrooklynMap1766.jpg.

[5] Edwin G. Burrows and Mike Wallace. *Gotham: A History of New York City To 1898*. Oxford University Press, Incorporated, Cary, UNITED STATES, 1998. ISBN 978-0-19-972910-4. URL http://ebookcentral.proquest.com/lib/uva/detail.action?docID=5746825.

[6] Julia Carmel. A Night on Governors Island? Be Prepared to Spend for It. *The New York Times*, June 2022. ISSN 0362-4331. URL https://www.nytimes.com/2022/06/11/nyregion/governors-island.html.

[7] Robert A. Caro. *The power broker: Robert Moses and the fall of New York*. A Borzoi book. Alfred A. Knopf, New York, 1974. ISBN 978-0-394-48076-3.

[8] Centers for Disease Control and Prevention/ Agency for Toxic Substances and Disease Registry/ Geospatial Research, Analysis, and Services Program. CDC/ATSDR Social Vulnerability Index 2020 Database, New York, 2020. URL https://www.atsdr.cdc.gov/placeandhealth/svi/data_documentation_download.html.

[9] Steven Alan Cohen, Courtney Small, Madeline Silva, and Hayley Martinez. Case Study: Sustainability Planning in New York City. 2015. doi: 10.7916/D8GF0TN9. URL https://academiccommons.columbia.edu/doi/10.7916/D8GF0TN9. Publisher: Columbia University.

[10] Andrew L. Comrey and Howard B. Lee. *A First Course in Factor Analysis*. Psychology Press, 0 edition, November 2013. ISBN 978-1-315-82750-6. doi: 10.4324/9781315827506. URL https://www.taylorfrancis.com/books/9781317844075.

[11] Angie Debo. *A History of the Indians of the United States*. University of Oklahoma Press, April 2013. ISBN 978-0-8061-8965-9. Google-Books-ID: pLjYp-wiuN_wC.

[12] ESRI. ArcGIS Pro, 2023.

[13] Nancy Foner. *From Ellis Island to JFK: New York‘s Two Great Waves of Immigration*. Yale University Press, 2000. ISBN 978-0-300-08226-5. URL https://www.jstor.org/stable/j.ctt1nptw2.

[14] S. R. Gaffin, C. Rosenzweig, R. Khanbilvardi, L. Parshall, S. Mahani, H. Glickman, R. Goldberg, R. Blake, R. B. Slosberg, and D. Hillel. Variations in New York city's urban heat island strength over time and space. *Theoretical and Ap-*

plied Climatology, 94(1):1–11, September 2008. ISSN 1434-4483. doi: 10.1007/s00704-007-0368-3. URL https://doi.org/10.1007/s00704-007-0368-3.

[15] Leslie M. Harris. *In the Shadow of Slavery: African Americans in New York City, 1626-1863*. University of Chicago Press, November 2023. ISBN 978-0-226-82486-4. Google-Books-ID: KrbdEAAAQBAJ.

[16] Harry Macy Jr. Before the Five-borough City: The Old Cities, Towns, and Villages That Came Together to Form 'Greater New York', January 2021. URL https://www.newyorkfamilyhistory.org/blog/five-borough-city-old-cities-towns-and-villages-came-together-form-greater-new-york.

[17] Amy E. Hillier. Redlining and the Home Owners' Loan Corporation. *Journal of Urban History*, 29(4):394–420, May 2003. ISSN 0096-1442, 1552-6771. doi: 10.1177/0096144203029004002. URL http://journals.sagepub.com/doi/10.1177/0096144203029004002.

[18] Kyung Hwa Jung, Zachary Pitkowsky, Kira Argenio, James W. Quinn, Jean-Marie Bruzzese, Rachel L. Miller, Steven N. Chillrud, Matthew Perzanowski, Jeanette A. Stingone, and Stephanie Lovinsky-Desir. The effects of the historical practice of residential redlining in the United States on recent temporal trends of air pollution near New York City schools. *Environment International*, 169:107551, November 2022. ISSN 0160-4120. doi: 10.1016/j.envint.2022.107551. URL https://www.sciencedirect.com/science/article/pii/S0160412022004780.

[19] Natasha Iskander. America's arrival city: how immigration made New York and how immigrant exclusion almost destroyed it: commentary on "Global commerce, immigration and diversity: a New York story" by Philip Kasinitz.

Ethnic and Racial Studies, 46(11):2555–2564, August 2023. ISSN 0141-9870. doi: 10.1080/01419870.2023.2176246. URL https://doi.org/10.1080/01419870.2023.2176246. Publisher: Routledge _eprint: https://doi.org/10.1080/01419870.2023.2176246.

[20] Yosef Jabareen. An Assessment Framework for Cities Coping with Climate Change: The Case of New York City and its PlaNYC 2030. *Sustainability*, 6 (9):5898–5919, September 2014. ISSN 2071-1050. doi: 10.3390/su6095898. URL http://www.mdpi.com/2071-1050/6/9/5898.

[21] Steven J. Jaret, E. DiPadova, Lynsey Spaeth, Victoria Yuan, Riley Smith, David Randle, Keiji G. Hammond, Nicholas Tailby, and Denton S. Ebel. Field Guide for the Geology of Central Park and New York City, 2022. URL http://hdl.handle.net/2246/7307. Institution: American Museum of Natural History Research Library.

[22] Patrick L. Kinney, Thomas Matte, Kim Knowlton, Jaime Madrigano, Elisaveta Petkova, Kate Weinberger, Ashlinn Quinn, Mark Arend, and Julie Pullen. New York City Panel on Climate Change 2015 Report Chapter 5: Public Health Impacts and Resiliency. *Annals of the New York Academy of Sciences*, 1336: 67–88, January 2015. ISSN 0077-8923. doi: 10.1111/nyas.12588. URL https://www.ncbi.nlm.nih.gov/pmc/articles/PMC4749144/.

[23] Markus Kottek, Jürgen Grieser, Christoph Beck, Bruno Rudolf, and Franz Rubel. World Map of the Köppen-Geiger climate classification updated. *Meteorologische Zeitschrift*, 15(3):259–263, July 2006. ISSN 0941-2948. doi: 10.1127/0941-2948/2006/0130. URL http://www.schweizerbart.de/papers/metz/detail/15/5

5034/World_Map_of_the_Koppen_Geiger_climate_classificat?af=crossref.

[24] Daniel C. Kramer and Richard M. Flanagan. *Staten Island: conservative bastion in a liberal city*. University Press of America, Inc, Lanham, 2012. ISBN 978-0-7618-5831-7 978-0-7618-5832-4. OCLC: ocn783172502.

[25] Nancy Krieger, Gretchen Van Wye, Mary Huynh, Pamela D. Waterman, Gil Maduro, Wenhui Li, R. Charon Gwynn, Oxiris Barbot, and Mary T. Bassett. Structural Racism, Historical Redlining, and Risk of Preterm Birth in New York City, 2013–2017. *American Journal of Public Health*, 110(7):1046–1053, July 2020. ISSN 0090-0036. doi: 10.2105/AJPH.2020.305656. URL https://ajph.aphapublications.org/doi/full/10.2105/AJPH.2020.305656. Publisher: American Public Health Association.

[26] Margriet Lacey. *A Beautiful and Fruitful Place: Selected Rensselaerswijck Papers, Volume 3*. New Netherland Institute, August 2013. ISBN 978-0-9881711-9-0. Google-Books-ID: jA6AnQEACAAJ.

[27] Laura Blaszczak and The New York Public Library. The Changing Shoreline of New York City, December 2017. URL https://spacetime.nypl.org/the-changing-shoreline-of-nyc.

[28] Min Li and Faxi Yuan. Historical Redlining and Resident Exposure to COVID-19: A Study of New York City. *Race and Social Problems*, 14(2):85–100, June 2022. ISSN 1867-1756. doi: 10.1007/s12552-021-09338-z. URL https://doi.org/10.1007/s12552-021-09338-z.

[29] Louis Pope Gratacap. *Geology of the City of New York (Greater New York*. Bretano, Harvard University, 2 edition, 1901.

[30] Malcolm Pinckney. NYC Parks Celebrates One Millionth Tree With Bronx Community Members, November 2015. URL https://www.nycgovparks.org/parks/joyce-kilmer-park/dailyplant/23507.

[31] Rand McNally. Map of Brooklyn and vicinity published by Rand McNally in 1897 as part of their Atlas of the World., 1897. URL https://commons.wikimedia.org/wiki/File:1897_Brooklyn_map.jpg.

[32] Vernice D. Miller. Planning, Power and Politics: A Case Study of the Land Use and Siting History of the North River Water Pollution Control Plant. *Fordham Urban Law Journal*, 21(3):707–722, 1993. URL https://heinonline.org/HOL/P?h=hein.journals/frdurb21&i=717.

[33] Robert K. Nelson and Edward L. Ayers, editors. *Not Even Past: Social Vulnerability and the Legacy of Redlining*. American Panorama. The Digital Scholarship Lab and the National Community Reinvestment Coalition. URL https://dsl.richmond.edu/socialvulnerability.

[34] New York City Bureau of Policy and Research. Ten Years After Sandy: Barriers to Resilience. Technical report, New York City Comptroller, New York, NY, October 2022. URL https://comptroller.nyc.gov/wp-content/uploads/documents/Ten-Years-After-Sandy.pdf.

[35] New York City Department of Environmental Protection. NYC Stormwater Flood Map - Extreme Flood with 2080 Sea Level Rise, June 2021. URL https://data.cityofnewyork.us/City-Government/NYC-Stormwater-Flood-Map-Extreme-Flood-with-2080-S/w8eg-8ha6/about_data.

[36] New York City Office of Technology and Innovation. Land Cover Raster Data (2017) – 6in Resolution, September 2022. URL https://data.cityofnewyork

.us/Environment/Land-Cover-Raster-Data-2017-6in-Resolution/he6d-2qns/about_data.

[37] New York City Panel on Climate Change. Climate Risk Information 2013: Observations, Climate Change Projections, and Maps. Technical report, City of New York Special Initiative on Rebuilding and Resiliancy, New York, NY, 2013.

[38] New York Department of Environmental Protection. New York State DEC and New York City DEP Announce Agreement to Invest $3.5 Billion to Further Improve the Health of New York Harbor and Advance Climate Resilience, May 2023. URL https://www.nyc.gov/site/dep/news/23-019/new-york-state-dec-new-york-city-dep-agreement-invest-3-5-billion-further#/0.

[39] New York (N.Y.), Leonard M. Wallstein, New York (State), and N.Y.) Bureau of Municipal Research (New York. *Government of the city of New York; a survey of its organization and functions*. J.J. Little & Ives, New York, 1915. URL https://catalog.hathitrust.org/Record/001150675.

[40] NYC Department of City Planning. Zoning Districts (NYZD), January 2024. URL https://www.nyc.gov/site/planning/data-maps/open-data/dwn-gis-zoning.page.

[41] Oak Ridge National Laboratory. Prison Boundaries, September 2020. URL https://hifld-geoplatform.opendata.arcgis.com/.

[42] Peter Douglas. The Man Who Took Back New Netherland: Cornelis Evertsen the Youngest, 1642-1706, July 2022. URL https://web.archive.org/web/20220708102432/http://www.newnetherlandinstitute.org/files/2813/5680/0659/Man_Who_Took_Back_NN.pdf.

[43] U. S. Global Change Research Program. Fifth National Climate Assessment. Technical report, U.S. Global Change Research Program, Washington, DC, 2023. URL https://nca2023.globalchange.gov/chapter/24/. Publication Title: Fifth National Climate Assessment.

[44] Russell Lopez. Urban Sprawl in the United States: 1970-2010. *Cities and the Environment*, 7(1), 2014.

[45] Samuel Brody. The Characteristics, Causes, and Consequences of Sprawling Development Patterns in the United States. *Nature Education Knowledge*, 4(5), 2013. URL https://www.nature.com/scitable/knowledge/library/the-characteristics-causes-and-consequences-of-sprawling-103014747/. Cg_cat: The Characteristics, Causes, and Consequences of Sprawling Development Patterns in the United States Cg_level: ESY Cg_topic: The Characteristics, Causes, and Consequences of Sprawling Development Patterns in the United States.

[46] Eric W. Sanderson and Markley Boyle. *Mannahatta: A Natural History of New York City*. Abrams, Inc., New York, UNITED STATES, 2009. ISBN 978-1-61312-573-1. URL http://ebookcentral.proquest.com/lib/uva/detail.action?docID=4012831.

[47] Kara Murphy Schlichting. *New York Recentered: Building the Metropolis from the Shore*. University of Chicago Press, 2019. ISBN 978-0-226-61302-4 978-0-226-61316-1. doi: 10.7208/chicago/9780226613161.001.0001. URL https://www.bibliovault.org/BV.landing.epl?ISBN=9780226613161.

[48] Gunja SenGupta. *From Slavery to Poverty: The Racial Origins of Welfare*

in New York, 1840-1918. NYU Press, March 2009. ISBN 978-0-8147-4086-6. Google-Books-ID: NZs84BoIdY8C.

[49] Richard R. Shaker, Yaron Altman, Chengbin Deng, Eric Vaz, and K. Wayne Forsythe. Investigating urban heat island through spatial analysis of New York City streetscapes. *Journal of Cleaner Production*, 233:972–992, October 2019. ISSN 0959-6526. doi: 10.1016/j.jclepro.2019.05.389. URL https://www.sciencedirect.com/science/article/pii/S0959652619319328.

[50] Brianne Smith and Stephanie Rodriguez. Spatial Analysis of High-Resolution Radar Rainfall and Citizen-Reported Flash Flood Data in Ultra-Urban New York City. *Water*, 9(10):736, October 2017. ISSN 2073-4441. doi: 10.3390/w9100736. URL https://www.mdpi.com/2073-4441/9/10/736. Number: 10 Publisher: Multidisciplinary Digital Publishing Institute.

[51] The City of New York. PlaNYC: A Greener, Greater New York. Technical report, The NYC Office of the Mayor, New York, NY, 2007. URL https://www.nyc.gov/html/planyc/downloads/pdf/publications/full_report_2007.pdf.

[52] The City of New York. NYC Green Infrastructure Plan: A Sustainable Strategy for Clean Waterways. Technical report, New York City Department of Environmental Protection, New York, NY, 2010. URL https://www.nyc.gov/assets/dep/downloads/pdf/water/stormwater/green-infrastructure/nyc-green-infrastructure-plan-2010.pdf.

[53] The City of New York. PlaNYC: A Greener, Greater New York. Technical report, The NYC Office of the Mayor, April 2011. URL https://climate.cityofnewyork.us/wp-content/uploads/2023/12/planyc_2011_planyc_full_report.pdf.

[54] The City of New York. One New York: The Plan for a Strong and Just City. Technical report, The NYC Office of the Mayor, New York, NY, 2015. URL https://www.nyc.gov/html/onenyc/downloads/pdf/publications/OneNYC.pdf.

[55] The City of New York. New York City Stormwater Resiliency Plan. Technical report, NYC Mayor's Office of Resiliency, New York, NY, May 2021. URL https://www.nyc.gov/assets/orr/pdf/publications/stormwater-resiliency-plan.pdf.

[56] The City of New York. PlaNYC: Getting Sustainability Done. Technical report, The NYC Office of the Mayor, New York, NY, April 2023. URL https://climate.cityofnewyork.us/wp-content/uploads/2023/06/PlaNYC-2023-Full-Report.pdf.

[57] The City of New York. NYC Mayor's Office of Environmental Justice, 2024. URL https://climate.cityofnewyork.us/.

[58] The City of New York. Zoning Resolution, February 2024. URL https://zr.planning.nyc.gov/.

[59] The City of New York and Eric Adams. AdaptNYC. Technical report, NYC Mayor's Office of Climate and Environmental Justice, New York, NY, February 2023. URL https://climate.cityofnewyork.us/initiatives/adaptnyc/.

[60] The City of New York and The New York City Departmen of Environmental Protection. CSO Order Modification to C02-20000107-8, 2012. URL https://www1.dec.state.ny.us/docs/water_pdf/csomod2012.pdf.

[61] United States Census Bureau. Census Population Clock, . URL https://www.census.gov/popclock/embed.php?component=density.

[62] United States Census Bureau. U.S. Census Bureau QuickFacts: United States, . URL https://www.census.gov/quickfacts/fact/table/DC,newyorkcitynewyork,oaklandcountymichigan,detroitcitymichigan,phoenixcityarizona,US/PST045222.

[63] US Census Bureau. Census.gov QuickFacts, June 2021.

[64] NOAA US Department of Commerce. Climate, 2022. URL https://www.weather.gov/wrh/Climate?wfo=lwx. Publisher: NOAA's National Weather Service.

[65] U.S. Geological Survey. Geology of the New York Region. URL https://www.usgs.gov/geology-and-ecology-of-national-parks/geology-new-york-region.

[66] Kris Arnold from New York USA. Brooklyn, New York is seen in the foreground. Manhattan is the background. The Bridges are, from right to left: Williamsburg Bridge, Manhattan Bridge, Brooklyn Bridge., December 2005. URL https://commons.wikimedia.org/wiki/File:Brooklyn_from_the_Air.jpg.

[67] David Thomas Valentine and William Irving Paulding. *History of the city of New-York*. G.P. Putnam & company, New York, 1853. URL https://link.gale.com/apps/doc/CY0100939515/SABN?sid=titlelist&xid=10831588&pg=20.

[68] Roger David Waldinger. *Still the Promised City?: African-Americans and New Immigrants in Postindustrial New York*. Harvard University Press, 1999. ISBN 978-0-674-00072-8. Google-Books-ID: XIX2w_N2fCkC.

[69] Sylvia Hood Washington, Heather Goodall, and Paul C. Rosier, editors. *Echoes from the poisoned well: global memories of environmental injustice*. Lexington Books, Lanham, MD, 2006. ISBN 978-0-7391-0912-0 978-0-7391-1432-2. OCLC: ocm62858064.

[70] WPA Writer's Project. *A Maritime History of New York*. Going Coastal, Inc., 2004. ISBN 978-0-9729803-1-9.

Chapter 7

Conclusions

7.1 Discussion

In this dissertation, four cities were examined as case studies. These cities differed greatly, and were intended to represent a wide range of possible characteristics that exist in urban areas of the US. The differences between each case study were intended to be multidimensional, and included physical aspects such as area, climate, and population, as well as less tangible differences such as history, policy, and socio-demographic dynamics. The overarching question that was asked for each case study was a question of equity: do vulnerable residents enjoy the same level of areal coverage and connectivity of UGI where they live when compared to other residents? This question was specifically shaped by two hypotheses:

- **H1:** Discrepancies will exist in the areal coverage and connectivity of UGI between areas with a higher proportion of vulnerable residents and areas with a lower proportion of vulnerable residents.
- **H2:** Sample plots with lower percentages of residents considered vulnerable will have higher areal coverage and connectivity of UGI than plots with higher percentages of residents considered vulnerable.

These hypotheses were tested empirically using PCA first as an exploratory analysis to help simplify the data, followed by mean rank analysis to test relationships that were exposed with PCA.

These case studies are, by design, entirely dissimilar. Populations of the cities ranged from just over 620,000 to over 8 million, and land area ranged from 177 km^2 to 1,339 km^2 (2,720 km^2, if counting the entirety of the DMA region included in this study) (Table 7.1). Because of this, quantitative cross-comparison between the case studies is difficult. Therefore, a qualitative analysis of the differences found in each urban center was conducted.

With every urban center examined in this dissertation, demographic segregation was present. Regardless of the population or age of the city, distinct neighborhoods have developed that have higher percentages of residents that are vulnerable. In DC, we see that this occurs in the southeast. In PHX, this occurs in the central industrial districts. In DMA, the city of Detroit is much more vulnerable than the satellite cities in Oakland County. In NYC, regions in the Bronx and Brooklyn have more vulnerable residents, and Staten Island and Manhattan have less vulnerable residents. From mapping these cities, we can see that spatial patterns in SVIs exist in every city studied.

Table 7.1: Summary of the basic characteristics of each case study.

	DC	PHX	Detroit	Oakland County	NYC
Land Area	177 km^2	1,339 km^2	370 km^2	2,350km^2	784 km^2
Population[1]	670,949	1,644,409	620,376	1,269,431	8,335,897
Per capita income[2]	$71,297	$37,499	$22,861	$53,157	$48,066
Median household income[3]	$101,722	$72,092	$37,761	$92,620	$76,607
Percent persons in poverty	13.3%	14.6%	31.5%	8.2%	17.2%

[a] Population estimates base, July 1, 2022[33]
[b] In past 12 months (in 2022 USD, 2018-2022)[33]
[c] In 2022 USD, 2018-2022[33]

For the sample plots in each city, the landcover metrics had different characteristics (Figure 7.1). PHX was a major outlier in landcover type and coverage. Likely due to its climate, PHX plots had a bias towards lower values in Tree PLAND, Tree LPI, Tree PLADJ, and Tree Cohesion than did the other case studies (Figures 7.1a, 7.1b, 7.1e, 7.1f). Additionally, PHX had a bias towards higher values regarding Tree LSI, indicating that, although tree coverage was limited in spatial coverage in PHX relative to the other case studies, it was also more complex in shape (Figure 7.1c). Again, this is likely caused by PHX's climate, which requires irrigation to sustain UGI. In the other case studies, barren landscape was generally limited to construction and industrial zones. In PHX, much of the landcover is naturally barren without human influence. Adding this extra dominant class would make the landscape more complex, leading to a higher LSI for classes other than impervious surfaces (which would likely become less complex, as the simple shapes of roads, buildings, and sidewalks would not be covered by tree canopy that would increase the edge-to-area ratio of these surfaces). Additionally, the landcover raster for PHX included a separate class for shrub, which also influenced the complexity of the landscape (Table 7.2).

NYC also stood out regarding several LSMs, with higher relative values for Impervious PLAND, Impervious LPI, and Impervious LSI, as well as lower relative values for both Impervious ENN_MN and Tree ENN_MN (Figures 7.1a, 7.1b, 7.1c, 7.1d). Although this can partially be attributed to NYC's well-developed impervious infrastructure, it should be noted that some of this variance is possibly attributed to the spatial resolution of the landcover raster used for NYC. This raster had a 6 inch resolution[22] and, compared with the resolutions of the other case studies (1 meter)[29, 35, 24, 23], more details of the surface were apparent, likely adding to the complexity of the landscape, increasing LSI and revealing small patches of landcover that would

Table 7.2: Total percent landcover calculations for each landcover class in all case studies. As some classes were not calculated for every case study, the percent landcover in those case studies will be recorded as *NA* in the table.

	DC	PHX	Detroit	Oakland County	NYC
Water	33.71%	0.54%	2.5%	3.1%	28.49%
Impervious	40.31%	28.73%	38.9%	44.9%	42.45%
Barren	0.16%	51.64%	3.9%	1.3%	1.22%
Tree	33.71%	4.76%	44.0%	34.9%	16.02%
Grass	15.62%	5.34%	10.9%	15.8%	11.82%
Shrub	NA	5.92%	NA	NA	NA
Agriculture	NA	3.08%	NA	NA	NA

otherwise not be used in calculating the metrics, decreasing the ENN_MN to the next nearest patch for all landcover types.

For the metrics Impervious PLADJ and Cohesion, as well as Tree PLADJ and Cohesion, DC showed some deviation from the other case studies, with relatively low values for Impervious and Tree PLADJ and relatively high Impervious and Tree Cohesion (Figures 7.1e, 7.1f). Although it is unclear as to why this is, it indicates that both trees and impervious surfaces in DC are clumped together, so that the likelihood of having a pixel of the same class next to any given pixel is high, but the clumps are not aggregated well, leading to many clumped patches. Perhaps this is the result of the L'Enfant plan, which created regular, well-dispersed UGI in the form of pocket parks and boulevards that were not necessarily well-connected[15].

The results of each case study reflect the differences between these urban areas (Table 7.3). DC, a city with a heavy influence from the US federal government and progressive UGI policy, still exhibits inequity in tree canopy coverage and connectivity in areas with high percentages of minority residents. PHX, an urban center that faces the challenge of maintaining UGI in a desert climate with looming drought, has lower

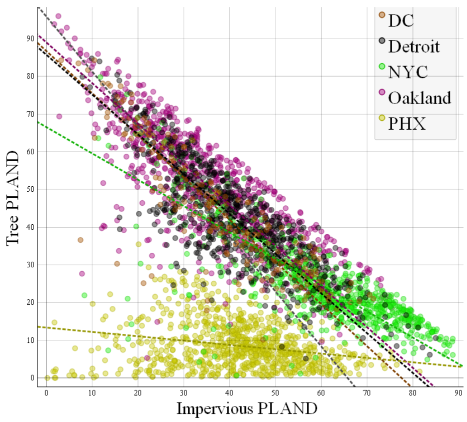

(a) Impervious PLAND vs. Tree PLAND

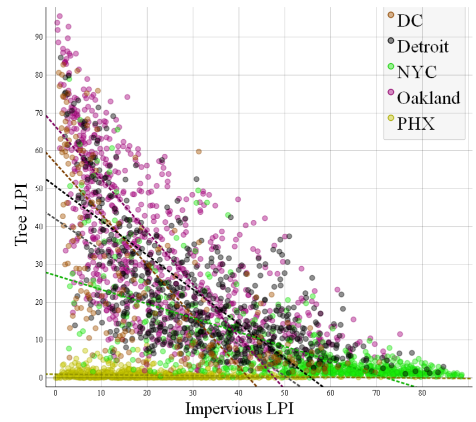

(b) Impervious LPI vs. Tree LPI

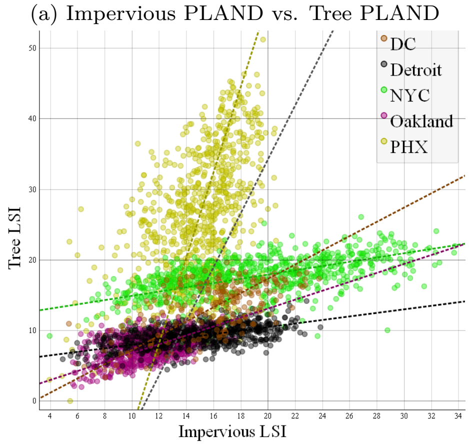

(c) Impervious LSI vs. Tree LSI

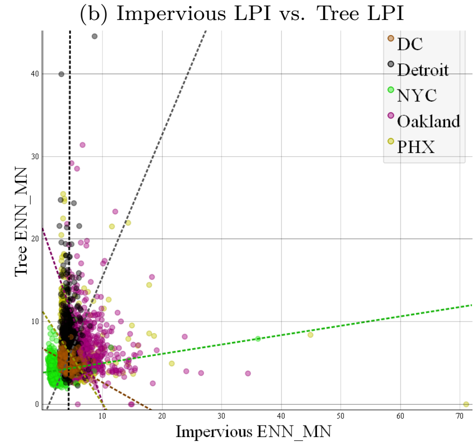

(d) Impervious ENN_MN vs. Tree ENN_MN

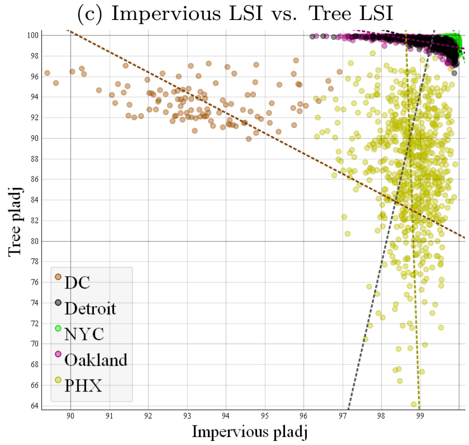

(e) Impervious PLADJ vs. Tree PLADJ

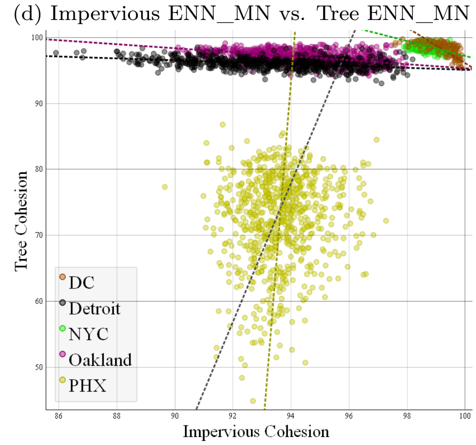

(f) Impervious Cohesion vs. Tree Cohesion

Figure 7.1: Scatter plots with trend lines comparing impervious surface and tree canopy LSMs for all cities involved in the study. DC plots are represented by brown circles, PHX plots by yellow circles, Detroit plots by blue circles, Oakland County plots by pink circles, and NYC plots by green circles.

	LSMs cross-loaded onto SVI components	SVI cross-loaded onto LSM components
DC	Grass ENN_MN	Age 65+ % **Minority %**
PHX	**Tree PLADJ** **Shrub PLADJ** **Tree Cohesion** **Shrub Cohesion**	—
DMA	—	Minority % Disabled %
NYC	**Tree ENN_MN**	—

Table 7.3: A table showing the variables that cross-loaded, meaning a LSM loading onto a primarily SVI component or a SVI variable loading onto a primarily LSM component. Variables in bold indicate support for both of this dissertation's hypotheses.

connectivity for trees and shrubs in vulnerable areas than in less-vulnerable areas. DMA did not indicate that there were strong relationships between UGI and SVIs through PCA analysis, but further exploration conducted by comparing Detroit to its surrounding cities indicated that there were indeed differences in mean rank between the city of Detroit and its satellite suburbs, showing Detroit to have a generally lower mean rank in tree coverage and conductivity than do the surrounding suburbs. NYC, with a long-running focus on UGI and equity, showed some indication that the difference between patches tree canopy was larger in areas with a higher proportion of vulnerable residents, but did not indicate strong differences in any other metrics. Hypothesis H1 was supported in every study, and H2 was supported in every study except DMA, although examination between Detroit and Oakland suggested H2 may have been supported with the assumption that Detroit is inherently more vulnerable than Oakland County.

The contribution of this dissertation to the EJ and environmental science fields is two-fold. Firstly, this study provides a generalized methodology to examine UGI connectivity in urban centers in relation to SVI. Previous studies have examined tree coverage in cities and related this to facets of EJ, including the impacts of historical injustices[17], health issues facing vulnerable populations[14, 8], and ecosystem services for under-served communities[26]. However, most of these studies have been focused solely on percentage of tree canopy cover, ignoring other impactful aspects of landscape connectivity.

Secondly, this dissertation works to continue the conversation about EJ in urban areas, linking policy and history to vulnerability and resource equity. It provides empirical evidence of inequity in UGI conductivity for three case studies using a defined methodology, and exposes potential inequity in another. Through a broad analysis of the characteristics of each urban center, this study demonstrates that, although these case studies are unique and differ widely, they share a history of injustice, they share many planning and policy ideas, and they share challenges in both protecting vulnerable populations and preparing for the impacts of climate change.

The subtext of this dissertation builds on the results of these analyses and asks a simple, yet perhaps more important question: ”why?” If the coverage and connectivity of landcover types differs between vulnerable communities and less-vulnerable communities, what historical or political factors have contributed to this and, if we are able to identify these factors, can we increase equity of UGI connectivity in urban centers and rectify these injustices? As cities are magnificently complex systems of which we are both observers and participants, this dissertation cannot and does not intend to answer that question definitively. This dissertation is intended to introduce a methodology to explore relationships between vulnerability and a UGI variable that is often overlooked in the conversation about EJ, and to provide a platform for future research to build on. Both social equity and EJ are goals that require an iterative process to appropriately address. One-off policies or singular programs lacking follow-up may address the symptoms of these problems, but to truly understand and mitigate resource inequity in urban areas, whether it be inequity in UGI, income, health care, or other necessary resources, urban centers must be monitored and treated as ever-changing, dynamic ecosystems.

As a part of the iterative process required to address EJ, studies must be built upon and amended as the conditions in urban centers change and new knowledge is exposed. This dissertation is no different, and the following section will discuss the potential blind spots in this study and ways in which to address them, as well identify directions for future research.

7.2 Future Work

7.2.1 Zoning

This dissertation focused solely on areas zoned as Single Family Residential as a means to eliminate variations in the landcover of each plot that are based on a city's zoning laws. However, in doing so, the scope of this study was narrowed considerably, creating a sizeable blind spot. Many residents in urban centers live in apartment complexes. In NYC, for example only 465,800, or 14%, of the city's housing units were Single Family Residential houses[34]. Although the methodology would need to be adapted to address the wide array of housing units that are built in areas zoned for multi-unit apartments, which includes public housing, condominiums, and garden apartments, this next step would encompass a demographic of very vulnerable residents not observed by this study's current format.

Building on this idea, it would also be useful to consider zoning as more than just a filter, and instead examine how it may impact UGI and SVI. Zoning restrictions have been blamed for the inequitable exposure of vulnerable communities to environmental hazards in many US cities including Chicago[11] and NYC[19], among others[9, 20]. Exploring this variable in further studies as a driver of EJ hazards could help better understand how to address them.

7.2.2 UGI Data

There have been several studies that have used landcover data to assess urban UGI connectivity, but often the data utilized is derived from data collected by the Landsat program, a series of satellite missions with a 30 meter resolution[18, 7, 10]. This study was able to employ 1 meter resolution data for DC[29] and PHX[35], 1 meter resolution data[24, 25, 23] supplemented with 3 meter resolution data[28] for DMA, and 6 inch resolution data for NYC[22], allowing for a much more detailed analysis for the urban areas. However, using satellite-derived data products has limitations in urban areas. Tall buildings sometime produce shadows that reduce classification accuracy[36]. Areas under canopy that contain vegetation are not visible from the top-down and, thus, are not considered when using these data products. UGI that is placed unconventionally, such as green walls, are also unable to be detected using these methods. This creates a blind spot when assessing UGI connectivity, even with high-resolution data products.

However, some researchers have pioneered innovative methodologies for identifying UGI. Several studies have developed methodologies for quantifying tree canopy utilizing Google Street View, a dataset providing ground level photography capture by cars[31, 16, 32]. Others have employed machine learning and social media to quantify UGI[27]. New technologies that will revolutionize how UGI is identified and quantified are becoming increasingly prevalent, and future studies can, and should, rely on these to improve our understanding of UGI connectivity.

7.2.3 Temporal Changes

An aspect that this study does not address that future studies should examine is temporal changes in UGI. Originally, this study had intended on including this facet. However, the time-series for high-resolution satellite imagery was deemed too short to develop any meaningful conclusions. Previous studies have used data from the Landsat program to quantify changes in UGI in urban centers[18], but, as stated previously, this data is of a lower spatial resolution and does not accurately depict small installations of UGI at a scale smaller than 30m. Understanding not just where UGI is currently located, but how UGI has been historically implemented over time in relationship to specific policies, will provide much needed context in regards to UGI policy effectiveness and equity. As more high-resolution data continues to be collected over time, future work should consider utilizing these datasets.

7.2.4 Other Case Studies

An important aspect of future work will be to apply this methodology, or an adapted version of this methodology, to other case studies. DC, PHX, DMA, and NYC are not the only cities that are experiencing the impacts of climate change, nor are they the only cities with under served vulnerable populations. HOLC maps were drawn for over 200 US cities[30], and racial covenants existed, and in some cases still exist, nationwide[5]. As was demonstrated, each urban center has its own unique barriers and opportunities to building and maintaining a robust network of UGI to help mitigate climate change impact. Expanding this study to include more cities in the US would help better understand the causes of UGI connectivity inequity.

Additionally, expanding this study to other countries could prove to be beneficial. UGI policy in the European Union operates under similar, but markedly different, principals. While the US EPA touts UGI for its benefits to humans, primarily for stormwater flooding abatement[2], the European Union includes an emphasis on habitat connectivity as a priority for UGI in its policy descriptions[1]. The difference in how UGI is viewed — as a tool to use, or as an essential ecosystem characteristic — may affect the vigor in which it is implemented in different countries, and this should be studied.

7.2.5 Unintended Consequences

Although it was not addressed in this study, this dissertation would not be complete without acknowledging the unintended consequences of rectifying EJ issues and bolstering UGI throughout cities.

One such consequence, climate gentrification, is a major concern in many urban areas. As cities are shifting resources to better accommodate populations facing climate impacts, the resulting changes in neighborhood value can have negative ramifications for vulnerable communities. In cities facing sea-level rise, property values have been positively correlated with property elevation[12], which in turn makes living in these neighborhoods too expensive for the current, sometimes vulnerable residents[4]. The same phenomenon can be observed for UGI in US cities, with research indicating a positive correlation between property value and UGI in Los Angeles, CA and a negative correlation between property value and neighborhood extreme heat[13]. This conundrum has raised calls for funding schemes to provide protections for vulnerable communities where climate resiliency is being bolstered[3]. However, this obstacle to providing vulnerable populations with robust, well-connected UGI spotlights a challenge that transcends the scope of this dissertation. The conceptual essence of climate gentrification is that, by providing the resources that would allow humans to live in a changing climate without significant loss of health or property, you are providing a resource that is cost-prohibitive for some people. It is the opinion of the author of this dissertation that this is unacceptable in a modern society, and is a symptom of the larger societal affliction that is wealth inequality. In the US, wealth inequality is high relative to other developed nations and is trending upwards[6]. Wage stagnation for middle and low-income earners, combined with inflation and rising costs of living, has made the basic essentials of living much more difficult for many Americans[21]. Considering these facts, and rejecting the premise that access to climate-mitigating resources such as UGI is a luxury and not a right, it would seem that climate gentrification is a symptom of a different problem. This being said, understanding this symptom is crucial to ensuring that actions done now do not have unintended consequences for vulnerable communities.

References

[1] Green Infrastructure (GI) — Enhancing Europe's Natural Capital, 2013. URL https://eur-lex.europa.eu/legal-content/EN/TXT/?uri=celex%3A52013DC0249.

[2] Water Infrastructure Improvement Act, January 2019.

[3] Isabelle Anguelovski, James J. T. Connolly, Hamil Pearsall, Galia Shokry, Melissa Checker, Juliana Maantay, Kenneth Gould, Tammy Lewis, Andrew Maroko, and J. Timmons Roberts. Why green "climate gentrification" threatens poor and vulnerable populations. *Proceedings of the National Academy of Sciences*, 116(52):26139–26143, December 2019. ISSN 0027-8424, 1091-6490. doi: 10.1073/pnas.1920490117. URL https://pnas.org/doi/full/10.1073/pnas.1920490117.

[4] Kyle T. Aune, Dean Gesch, and Genee S. Smith. A spatial analysis of climate gentrification in Orleans Parish, Louisiana post-Hurricane Katrina. *Environmental Research*, 185:109384, June 2020. ISSN 0013-9351. doi: 10.1016/j.envres.2020.109384. URL https://www.sciencedirect.com/science/article/pii/S0013935120302772.

[5] Richard R. W. Brooks and Carol M. Rose. *Saving the Neighborhood: Racially Restrictive Covenants, Law, and Social Norms.* Harvard University Press, Cambridge, UNITED STATES, 2013. ISBN 978-0-674-07368-5. URL http://ebookcentral.proquest.com/lib/uva/detail.action?docID=3301255.

[6] Pew Research Center. Trends in income and wealth inequality, January 2020.

URL https://www.pewresearch.org/social-trends/2020/01/09/trends-in-income-and-wealth-inequality/.

[7] Peng Chen. Inequality in heat: The role of spatial patterns of urban green infrastructure. *Urban Climate*, 53:101820, January 2024. ISSN 2212-0955. doi: 10.1016/j.uclim.2024.101820. URL https://www.sciencedirect.com/science/article/pii/S2212095524000166.

[8] Drew A. Graham, Jennifer K. Vanos, Natasha A. Kenny, and Robert D. Brown. The relationship between neighbourhood tree canopy cover and heat-related ambulance calls during extreme heat events in Toronto, Canada. *Urban Forestry & Urban Greening*, 20:180–186, December 2016. ISSN 1618-8667. doi: 10.1016/j.ufug.2016.08.005. URL https://www.sciencedirect.com/science/article/pii/S161886671630348X.

[9] Charles M. (Charles Monroe) Haar. *Land-use Planning: A Casebook on the Use, Misuse, and Reuse of Urban Land*. Law school casebook series. Little, Brown, Boston, 1959.

[10] Wei Hou and Xinpeng Li. Assessing urban green infrastructure: A simple and practical measure of its spatial distribution equity and a comprehensive evaluation. *Ecological Indicators*, 158:111408, January 2024. ISSN 1470-160X. doi: 10.1016/j.ecolind.2023.111408. URL https://www.sciencedirect.com/science/article/pii/S1470160X23015509.

[11] Charles Isaacs. Environmental Justice in Little Village: A Case for Reforming Chicago's Zoning Law Notes and Comments. *Northwestern Journal of Law and Social Policy*, 15(3):357–402, 2019. URL https://heinonline.org/HOL/P?h=hein.journals/nwjlsopo15&i=357.

[12] Jesse M. Keenan, Thomas Hill, and Anurag Gumber. Climate gentrification: from theory to empiricism in Miami-Dade County, Florida. *Environmental Research Letters*, 13(5):054001, April 2018. ISSN 1748-9326. doi: 10.1088/1748-9326/aabb32. URL https://dx.doi.org/10.1088/1748-9326/aabb32. Publisher: IOP Publishing.

[13] Junsik Kim, Reid Ewing, and Alessandro Rigolon. Does Green Infrastructure Affect Housing Prices Via Extreme Heat and Air Pollution Mitigation? A Focus on Green and Climate Gentrification in Los Angeles County, 2000-2021, October 2023. URL https://papers.ssrn.com/abstract=4591592.

[14] Sungmin Lee, Juha Baek, Se Woong Kim, and Galen Newman. Tree canopy, pediatric asthma, and social vulnerability: An ecological study in Connecticut. *Landscape and Urban Planning*, 225:104451, September 2022. ISSN 0169-2046. doi: 10.1016/j.landurbplan.2022.104451. URL https://www.sciencedirect.com/science/article/pii/S0169204622001001.

[15] Pierre Charles L'Enfant. Plan of the city intended for the permanent seat of the government of t[he] United States : projected agreeable to the direction of the President of the United States, in pursuance of an act of Congress, passed on the sixteenth day of July, MDCCXC, "establishing the permanent seat on the bank of the Potowmac", 1991. URL http://hdl.loc.gov/loc.gmd/g3850.ct000091.

[16] Xiaojiang Li, Chuanrong Zhang, Weidong Li, Robert Ricard, Qingyan Meng, and Weixing Zhang. Assessing street-level urban greenery using Google Street View and a modified green view index. *Urban Forestry & Urban Greening*, 14 (3):675–685, January 2015. ISSN 1618-8667. doi: 10.1016/j.ufug.2015.06.006.

URL https://www.sciencedirect.com/science/article/pii/S1618866715000874.

[17] Dexter H. Locke, Billy Hall, J. Morgan Grove, Steward T. A. Pickett, Laura A. Ogden, Carissa Aoki, Christopher G. Boone, and Jarlath P. M. O'Neil-Dunne. Residential housing segregation and urban tree canopy in 37 US Cities. *npj Urban Sustainability*, 1(1):1–9, March 2021. ISSN 2661-8001. doi: 10.1038/s42949-021-00022-0. URL https://www.nature.com/articles/s42949-021-00022-0. Publisher: Nature Publishing Group.

[18] Yin Ma, Xinqi Zheng, Menglan Liu, Dongya Liu, Gang Ai, and Xueye Chen. Spatio-temporal evolution characteristics analysis and optimization prediction of urban green infrastructure: a case study of Beijing, China. *Scientific Reports*, 12(1):10702, June 2022. ISSN 2045-2322. doi: 10.1038/s41598-022-14613-z. URL https://www.nature.com/articles/s41598-022-14613-z. Publisher: Nature Publishing Group.

[19] Juliana Maantay. Industrial Zoning Changes in New York City: A Case Study of "Expulsive" Zoning. *Projections: the Planning Journal of Massachusetts Institute of Technology (MIT)*, pages 63–108, January 2002.

[20] Juliana Maantay. Zoning Law, Health, and Environmental Justice: What's the Connection? *Journal of Law, Medicine & Ethics*, 30(4):572–593, December 2002. ISSN 1073-1105, 1748-720X. doi: 10.1111/j.1748-720X.2002.tb00427.x. URL https://www.cambridge.org/core/journals/journal-of-law-medicine-and-ethics/article/zoning-law-health-and-environmental-justice-whats-the-connection/5010FBAB6A61A58BBF759630123306CE.

[21] Lawrence Mishel, Elise Gould, and Josh Bivens. WAGE STAGNATION IN NINE CHARTS. *Economic Policy Institute*, January 2015.

[22] New York City Office of Technology and Innovation. Land Cover Raster Data (2017) – 6in Resolution, September 2022. URL https://data.cityofnewyork.us/Environment/Land-Cover-Raster-Data-2017-6in-Resolution/he6d-2qns/about_data.

[23] NOAA Office for Coastal Management. 2020 NOAA C-CAP Version 2 Canopy Cover: Michigan, . URL www.coast.noaa.gov/htdata/raster1/landcover/bulkdownload/hires/.

[24] NOAA Office for Coastal Management. 2020 NOAA C-CAP Version 2 Impervious Cover: Michigan, . URL www.coast.noaa.gov/htdata/raster1/landcover/bulkdownload/hires/.

[25] NOAA Office for Coastal Management. 2020 NOAA C-CAP Version 2 Water Cover: Michigan, . URL www.coast.noaa.gov/htdata/raster1/landcover/bulkdownload/hires/.

[26] Charity Nyelele and Charles N. Kroll. The equity of urban forest ecosystem services and benefits in the Bronx, NY. *Urban Forestry & Urban Greening*, 53:126723, August 2020. ISSN 1618-8667. doi: 10.1016/j.ufug.2020.126723. URL https://www.sciencedirect.com/science/article/pii/S161886671930500X.

[27] Charity Nyelele, Catherine Keske, Min Gon Chung, Han Guo, and Benis N. Egoh. Using social media data and machine learning to map recreational ecosystem services. *Ecological Indicators*, 154:110606, October 2023. ISSN 1470-160X. doi:

10.1016/j.ecolind.2023.110606. URL https://www.sciencedirect.com/science/article/pii/S1470160X23007483.

[28] Planet Labs PBC. Planet Application Program Interface: In Space for Life on Earth, 2022. URL https://api.planet.com.

[29] PlanIT Geo, LLC. Generalized Land Cover 2020, April 2022. URL http://opendata.dc.gov.

[30] Price V. Fishback, Jessica LaVoice, Allison Shertzer, and Randall Walsh. The HOLC Maps: How Race and Poverty Influenced Real Estate Professionals' Evaluation of Lending Risk in the 1930s. Working Paper 28146, National Bureau of Economic Research, Cambridge, MA, 2021.

[31] Daniel R. Richards and Peter J. Edwards. Quantifying street tree regulating ecosystem services using Google Street View. *Ecological Indicators*, 77:31–40, June 2017. ISSN 1470-160X. doi: 10.1016/j.ecolind.2017.01.028. URL https://www.sciencedirect.com/science/article/pii/S1470160X17300341.

[32] Andrew G. Rundle, Michael D. M. Bader, Catherine A. Richards, Kathryn M. Neckerman, and Julien O. Teitler. Using Google Street View to Audit Neighborhood Environments. *American Journal of Preventive Medicine*, 40(1):94–100, January 2011. ISSN 0749-3797. doi: 10.1016/j.amepre.2010.09.034. URL https://www.sciencedirect.com/science/article/pii/S0749379710005623.

[33] United States Census Bureau. U.S. Census Bureau QuickFacts: United States. URL https://www.census.gov/quickfacts/fact/table/DC,newyorkcitynewyork,oaklandcountymichigan,detroitcitymichigan,phoenixcityarizona,US/PST045222.

[34] US Census Bureau. 2021 New York City Housing and Vacancy Survey Microdata, 2021. URL https://www.census.gov/data/datasets/2021/demo/nychvs/microdata.html. Section: Government.

[35] US Environmental Protection Agency. EnviroAtlas – Phoenix, AZ – Meter-Scale Urban Land Cover (MULC) Data (2010), September 2017.

[36] Weiqi Zhou, Ganlin Huang, Austin Troy, and M. L. Cadenasso. Object-based land cover classification of shaded areas in high spatial resolution imagery of urban areas: A comparison study. *Remote Sensing of Environment*, 113(8):1769–1777, August 2009. ISSN 0034-4257. doi: 10.1016/j.rse.2009.04.007. URL https://www.sciencedirect.com/science/article/pii/S0034425709001199.

Appendices

Appendix A

Additional Methodology

A.1 Landscape Metrics R Code

The LSM analyses in this study were coded using R programming language[22] in R-Studio[21]. Packages utilized for this code include:

- shiny[6]
- shinyjs[2]
- shinyFiles[18]
- labelled[11]
- landscapemetrics[8]
- sf[16]
- rgdal[5]
- raster[9]
- spatstat[3]
- ENMTools[24]

- sp[17]
- dplyr[25]
- maptools[4]
- terra[10]
- leaflet[7]

```r
#
# This application is designed to take a landcover classification Raster
    (.tif)
# and, using a zipped polygon shapefile (.zip), calculate zonal class
   based
# landscape metrics using the landscapemetrics r package developed by
   Maximilian
# H. K. Hesselbarth (https://orcid.org/0000-0003-1115-9918)
# (https://r-spatialecology.github.io/landscapemetrics/)
#

#

library(shiny)
library(shinyjs)
library(shinyFiles)
library(labelled)
library(landscapemetrics)
library(sf)
library(rgdal)
library(raster)
library(spatstat)
library(ENMTools)
library(sp)
library(dplyr)
library(maptools)
library(terra)
library(leaflet)

# UI for Application - Includes file uploads for zipped shapefile and
```

```
  raster,
# as well as checkboxes for which landscape metrics should be calculated
ui <- fluidPage(
  shinyjs::useShinyjs(),
  # Application title
  titlePanel("Zonal Class Based Landscape Metrics"),

  # Sidebar with a file input for shp and an input for landscape class

  sidebarPanel(
    fileInput("shp", "Choose Zipped Zonal Shapefile (.zip)", accept = ".zip"),
    fileInput("landclass", "Choose Landscape Classification Raster (.tif)", accept = ".tif"),
    helpText("Check all class metrics you would like calculated"),
    checkboxInput("PLAND", "Percentage of landscape of class (Area and Edge metric)", value = FALSE),
    checkboxInput("LPI", "Largest patch index (Area and Edge metric)", value = FALSE),
    checkboxInput("GYRATE", "Mean radius of gyration (Area and edge metric)", value = FALSE),
    checkboxInput("LSI", "Landscape shape index (Aggregation metric)", value = FALSE),
    checkboxInput("CLUMPY", "Clumpiness index (Aggregation metric)", value = FALSE),
    checkboxInput("ENN", "Mean of euclidean nearest-neighbor distance (Aggregation metric)", value = FALSE),
    checkboxInput("DIVISION", "Landscape division index (Aggregation metric)", value = FALSE),
    checkboxInput("PD", "Patch density (Aggregation metric)", value = FALSE),
```

```
    checkboxInput("AI", "Aggregation index (Aggregation metric)", value
    = FALSE),
    checkboxInput("PLADJ", "Percentage of Like Adjacencies (Aggregation
    metric)", value = FALSE),
    checkboxInput("COHESION", "Patch Cohesion Index (Aggregation metric)
    ", value = FALSE),
    checkboxInput("SHAPE", "Shape index (Shape metric)", value = FALSE),
    actionButton("goButton","Go!", class="btn-success"),

  ),

  mainPanel(
    shiny::textInput("wat","Class value for water"),
    shiny::textInput("imp","Class value for developed"),
    shiny::textInput("bar","Class value for barren"),
    shiny::textInput("fst","Class value for forest"),
    shiny::textInput("shrb","Class value for shrubland"),
    shiny::textInput("grs","Class value for herbaceous/grass"),
    shiny::textInput("plt","Class value for planted/cultivated"),
    shiny::textInput("wl","Class value for wetlands"),
    checkboxInput("NLCD", "Use NLCD standard?", value=TRUE),
    shinyjs::disabled(downloadButton("downloadData", "Download .CSV"))

  )
)

# Define server logic required to run LSM
server <- function(input, output, session) {

  options(shiny.maxRequestSize=30000*1014^10)

```

```r
fileready<-reactiveValues(ok =FALSE)

observeEvent(input$goButton, {
  shinyjs::disable("goButton")
  log <- reactiveValues(outputText ='')
  tmpdir <- tempdir()

  log$outputText <- paste(log$outputText,"Preparing Shapefile...",'<br
  >')
  shinyjs::html(id='log',log$outputText)

  shpzip <- input$shp
  unzip(shpzip$datapath, exdir = tmpdir)

  #  Validate correct formats
  zonefile <- input$shp
  ext <- tools::file_ext(zonefile$datapath)
  req(zonefile)
  validate(need(ext == "zip", "Please upload a zip file"))
  landfile <- input$landclass
  ext <- tools::file_ext(landfile$datapath)
  req(landfile)
  validate(need(ext == "tif", "Please upload a tif file"))

  # Import Shapefiles
  shpzip <- list.files(tmpdir, pattern = "\\.shp$")

  setwd(tmpdir)

  shpzip <- paste0("/", shpzip)

```

```
    shp <- read_sf(paste0(tmpdir,shpzip))

    # Convert shp to RDS for speed
    saveRDS(shp, "shp.RDS")
    shp <- readRDS('shp.RDS')

    # Add "plot_id" field to create index

    print("Preparing Raster...")

    # Import as raster
    landclass <- raster(landfile$datapath)

    # Establish classes as a vector
    print("Establishing Classes")

    classes<- data.frame()
    if(input$NLCD==FALSE){
      classes[1,1] <- renderText({input$wat})
      classes[2,1] <- renderText({input$imp})
      classes[3,1] <- renderText({input$bar})
      classes[4,1] <- renderText({input$fst})
      classes[5,1] <- renderText({input$shrb})
      classes[6,1] <- renderText({input$grs})
      classes[7,1] <- renderText({input$plt})
      classes[8,1] <- renderText({input$wt})
    } else{
      classes <- c(10,20,30,40,52,70,80,90)
    }

    # Convert raster to RDS for speed
```

```
    saveRDS(landclass, "landclass.rds")
    landclassRDS <- readRDS(file="landclass.rds")

    # Standardize Projections
    #landclassRDS <- projectRaster(landclassRDS, crs = crs(shp))

    # Drop NA Classes if applicable
    classes <- classes[!is.na(classes)]

    # Establish Master Table
    metrics <- data.frame()

    metrics <- shp[,3]

    metrics <- st_drop_geometry(metrics)
    colnames(metrics)<-c("plot_id")
    plotids<-metrics

    # Establish Temporary table
    metric_merge = data.frame()

    # Run PLAND
    if(input$PLAND == TRUE) {
      print("Calculating PLAND. This may take several minutes.")
      # Run PLAND
      smplemet <- sample_lsm(landclassRDS, y = shp, what = "lsm_c_pland"
)

      # Sort and append Classes
      for(x in classes){

```

```
      i <- merge(plotids, subset(smplemet, class == x ), by.x = "plot_id", by.y = "plot_id", all.x=TRUE)
      i[is.na(i)] = 0
      i <- i[c(1,7)]

      names(i)[names(i) == "value"] <- paste0(as.character(x), "_PLAND")

      metric_merge <- st_drop_geometry(i)
      metrics <- merge(metrics, metric_merge , by.x = "plot_id", by.y = "plot_id")
    }
  }

  # Run LPI
  if(input$LPI == TRUE) {
    print("Calculating LPI. This may take several minutes.")

    # Run LPI
    smplemet <- sample_lsm(landclassRDS, y = shp, what = "lsm_c_lpi")

    # Sort and append Classes
    for(x in classes){

      i <- merge(plotids, subset(smplemet, class == x ), by.x = "plot_id", by.y = "plot_id", all.x=TRUE)
      i[is.na(i)] = 0
      i <- i[c(1,7)]

      names(i)[names(i) == "value"] <- paste0(as.character(x), "_LPI")

```

```
      metric_merge <- st_drop_geometry(i)
      metrics <- merge(metrics, metric_merge , by.x = "plot_id", by.y = "plot_id")
    }
  }

  # Run GYRATE
  if(input$GYRATE == TRUE) {
    print("Calculating mean radius of gyration. This may take several minutes.")

    # Run gyrate_mn
    smplemet <- sample_lsm(landclassRDS, y = shp, what = "lsm_c_gyrate_mn")

    # Sort and append Classes
    for(x in classes){

      i <- merge(plotids, subset(smplemet, class == x ), by.x = "plot_id", by.y = "plot_id", all.x=TRUE)
      i[is.na(i)] = 0
      i <- i[c(1,7)]

      names(i)[names(i) == "value"] <- paste0(as.character(x), "_gyrate_mn")

      metric_merge <- st_drop_geometry(i)

      metrics <- merge(metrics, metric_merge , by.x = "plot_id", by.y = "plot_id")
    }
```

```
  }

  # Run LSI
  if(input$LSI == TRUE) {
    print("Calculating LSI. This may take several minutes.")
    # Run LSI
    smplemet <- sample_lsm(landclassRDS, y = shp, what = "lsm_c_lsi")

    # Sort and append Classes
    for(x in classes){

      i <- merge(plotids, subset(smplemet, class == x ), by.x = "plot_id", by.y = "plot_id", all.x=TRUE)
      i[is.na(i)] = 0
      i <- i[c(1,7)]

      names(i)[names(i) == "value"] <- paste0(as.character(x), "_LSI")

      metric_merge <- st_drop_geometry(i)

      metrics <- merge(metrics, metric_merge , by.x = "plot_id", by.y = "plot_id")
    }
  }

  # Run CLUMPY
  if(input$CLUMPY == TRUE) {
    print("Calculating Clumpiness index. This may take several minutes.")

    # Run CLUMPY
```

```
    smplemet <- sample_lsm(landclassRDS, y = shp, what = "lsm_c_clumpy")

    # Sort and append Classes
    for(x in classes){

      i <- merge(plotids, subset(smplemet, class == x ), by.x = "plot_id", by.y = "plot_id", all.x=TRUE)
      i[is.na(i)] = 0
      i <- i[c(1,7)]

      names(i)[names(i) == "value"] <- paste0(as.character(x), "_CLUMPY")

      metric_merge <- st_drop_geometry(i)

      metrics <- merge(metrics, metric_merge , by.x = "plot_id", by.y = "plot_id")
    }
  }

  # Run ENN_MN
  if(input$ENN == TRUE) {
    print("Calculating mean of euclidean nearest-neighbor distance. This may take several minutes.")

    # Run enn_mn
    smplemet <- sample_lsm(landclassRDS, y = shp, what = "lsm_c_enn_mn")

    # Sort and append Classes
```

```
    for(x in classes){

      i <- merge(plotids, subset(smplemet, class == x ), by.x = "plot_id", by.y = "plot_id", all.x=TRUE)
      i[is.na(i)] = 0
      i <- i[c(1,7)]

      names(i)[names(i) == "value"] <- paste0(as.character(x), "_enn_mn")

      metric_merge <- st_drop_geometry(i)

      metrics <- merge(metrics, metric_merge , by.x = "plot_id", by.y = "plot_id")
    }
  }

  # Run DIVISION
  if(input$DIVISION == TRUE) {
    print("Calculating Landscape Division index. This may take several minutes.")

    # Run division
    smplemet <- sample_lsm(landclassRDS, y = shp, what = "lsm_c_division")

    # Sort and append Classes
    for(x in classes){

      i <- merge(plotids, subset(smplemet, class == x ), by.x = "plot_id", by.y = "plot_id", all.x=TRUE)
```

```
      i[is.na(i)] = 0
      i <- i[c(1,7)]

      names(i)[names(i) == "value"] <- paste0(as.character(x), "_division")

      metric_merge <- st_drop_geometry(i)

      metrics <- merge(metrics, metric_merge , by.x = "plot_id", by.y = "plot_id")
    }
  }

  # Run PD
  if(input$PD == TRUE) {
    print("Calculating patch density. This may take several minutes.")

    # Run pd
    smplemet <- sample_lsm(landclassRDS, y = shp, what = "lsm_c_pd")

    # Sort and append Classes
    for(x in classes){

      i <- merge(plotids, subset(smplemet, class == x ), by.x = "plot_id", by.y = "plot_id", all.x=TRUE)
      i[is.na(i)] = 0
      i <- i[c(1,7)]

      names(i)[names(i) == "value"] <- paste0(as.character(x), "_pd")

      metric_merge <- st_drop_geometry(i)
```

```
      metrics <- merge(metrics, metric_merge , by.x = "plot_id", by.y = "plot_id")
    }
  }

  # Run AI
  if(input$AI == TRUE) {
    print("Calculating Aggregation Index. This may take several minutes.")
    # Run ai
    smplemet <- sample_lsm(landclassRDS, y = shp, what = "lsm_c_ai")

    # Sort and append Classes
    for(x in classes){

      i <- merge(plotids, subset(smplemet, class == x ), by.x = "plot_id", by.y = "plot_id", all.x=TRUE)
      i[is.na(i)] = 0
      i <- i[c(1,7)]

      names(i)[names(i) == "value"] <- paste0(as.character(x), "_ai")

      metric_merge <- st_drop_geometry(i)
      metrics <- merge(metrics, metric_merge , by.x = "plot_id", by.y = "plot_id")
    }
  }

  # Run PLADJ
  if(input$PLADJ == TRUE) {
```

```
    print("Calculating percentage of like adjacencies. This may take several minutes.")

    # Run PLADJ
    smplemet <- sample_lsm(landclassRDS, y = shp, what = "lsm_c_pladj")

    # Sort and append Classes
    for(x in classes){

      i <- merge(plotids, subset(smplemet, class == x ), by.x = "plot_id", by.y = "plot_id", all.x=TRUE)
      i[is.na(i)] = 0
      i <- i[c(1,7)]

      names(i)[names(i) == "value"] <- paste0(as.character(x), "_pladj")

      metric_merge <- st_drop_geometry(i)

      metrics <- merge(metrics, metric_merge , by.x = "plot_id", by.y = "plot_id")
    }
  }

  # Run COHESION
  if(input$COHESION == TRUE) {
    print("Calculating Cohesion Index. This may take several minutes.")
    # Run COHESION
    smplemet <- sample_lsm(landclassRDS, y = shp, what = "lsm_c_
```

```
cohesion")

    # Sort and append Classes
    for(x in classes){

      i <- merge(plotids, subset(smplemet, class == x ), by.x = "plot_id", by.y = "plot_id", all.x=TRUE)
      i[is.na(i)] = 0
      i <- i[c(1,7)]

      names(i)[names(i) == "value"] <- paste0(as.character(x), "_cohesion")

      metric_merge <- st_drop_geometry(i)

      metrics <- merge(metrics, metric_merge , by.x = "plot_id", by.y = "plot_id")
    }
  }

  # Run SHAPE
  if(input$SHAPE == TRUE) {
    print("Calculating mean shape index. This may take several minutes.")
    # Run shape_mn
    smplemet <- sample_lsm(landclassRDS, y = shp, what = "lsm_c_shape_mn")
    # Sort and append Classes
    for(x in classes){

      i <- merge(plotids, subset(smplemet, class == x ), by.x = "plot_
```

```
id", by.y = "plot_id", all.x=TRUE)
        i[is.na(i)] = 0
        i <- i[c(1,7)]

        names(i)[names(i) == "value"] <- paste0(as.character(x), "_shape
_mn")

        metric_merge <- st_drop_geometry(i)

        metrics <- merge(metrics, metric_merge , by.x = "plot_id", by.y
= "plot_id")

      }
    }

    # Prepare dataframe as csv
    output$downloadData <- downloadHandler(
      filename = function() {
        # Use the selected dataset as the suggested file name
        paste0(as.character(input$shp), "_LSM.csv")
      },
      content = function(file) {
        # Write the dataset to the `file` that will be downloaded
        write.csv(st_drop_geometry(metrics), file)
      }
    )
    shinyjs::enable("downloadData")

    print("FINISHED")

  })
```

```
}

# Run the application
shinyApp(ui=ui, server=server, options = list(display.mode = 'showcase')
    )
```

A.2 High-Resolution Landcover Rasters

The table below provides details regarding the high-resolution landcover rasters utilized in this dissertation. For DMA, a landcover classification was created to supplement the C-CAP impervious surface, tree canopy, and water datasets (Appendix A.3).

Case Study	Resolution	Year	Derived from	Number of classes	Overall Accuracy	Source
DC	1m	2020	Pleiades satellite and DC LiDAR data	5	97%	Planit Geo, LLC[20]
PHX	1m	2010	USDA NAIP (National Agricultural Imagery Program) 4-band aerial imagery	7	75%	EnviroAtlas Meter-Scale Urban Land Cover[23]
DMA	1m	2020	Various commercial satellites and LiDAR	1 for each product	80-90%	NOAA Coastal Change Analysis Program High-Resolution Land Cover[13, 14, 15]
NYC	6in	2017	LiDAR point clouds, orthoimagery, vector GIS datasets	8	98%	New York City Office of Technology and Innovation[12]

Table A.1: Landcover classifications used in this dissertation.

A.3 DMA Classification

The DMA landcover classification was accomplished with the help of an Undergraduate researcher, Kendall Davis. For this classification, Planetscope 3m resolution data from July, 2020 was employed[19]. Using the Classification Workflow tool in ENVI version 4.8[1], 80-100 training samples were created for each of 6 classes:

- Water
- Buildings
- Roads
- Barren
- Tree Canopy
- Grass.

These samples were modified using the Region of Interest tool in ENVI. The Maximum Likelihood Classification algorithm was run on these samples using the following settings:

- No probability threshold
- Multiple values for maximum distance error
- Distance error of 10000000
- Rule images were not computed.

Accuracy assessments were run on Detroit (Table A.2a) and Oakland County (Table A.2b) separately.

	Class						
	Roads	Barren	Water	Buildings	Grass	Tree	Prod. Accuracy
Unclassified	0%	0%	0%	0%	0%	0%	—
Roads	90.95%	4.66%	0.04%	12.92%	0%	0.04%	90.95%
Barren	6.09%	93.32%	0%	0.42%	1.5%	0%	93.32%
Water	0%	0%	98.1%	0%	0%	0%	98.10%
Buildings	2.62%	1.55%	1.79%	86.2%	1.04%	0%	86.20%
Grassland	0.34%	0.47%	0.06%	0.46%	91.48%	3.73%	91.48%
Forestland	0%	0%	0%	0%	7.48%	96.24%	96.24%
User Accuracy	90.23%	67.32%	100.00%	87.57%	91.89%	95.62%	—

κ Coefficient: 0.9249

Overall Accuracy: 94.6392%

(a) Accuracy Assessment for City of Detroit

	Class						
	Roads	Barren	Water	Buildings	Grass	Tree	Prod. Accuracy
Unclassified	0%	0%	0%	0%	0%	0%	—
Roads	91.39%	2.72%	0%	43.01%	0%	0.01%	91.39%
Barren	1.05%	95.77%	0%	3.46%	1.5%	0%	95.77%
Water	0%	0%	97.6%	0%	0%	0%	97.60%
Buildings	7.24%	1.03%	2.38%	52.96%	0.12%	0%	52.96%
Grassland	0.32%	0.49%	0.01%	0.58%	97.49%	2.94%	97.49%
Forestland	0%	0%	0%	0%	0.89%	97.05%	97.05%
User Accuracy	80.16%	95.14%	100.00%	52.31%	88.26%	99.78%	—

κ Coefficient: 0.9371

Overall Accuracy: 95.5619%

(b) Accuracy Assessment for Oakland County

Table A.2: Accuracy assessments for DMA landcover classification.

References

[1] ENVI Geospatial Software, 2022.

[2] Dean Attali. shinyjs: Easily improve the user experience of your shiny apps in seconds. manual, 2021. URL https://CRAN.R-project.org/package=shinyjs.

[3] Adrian Baddeley and Rolf Turner. spatstat: An R package for analyzing spatial point patterns. *Journal of Statistical Software*, 12(6):1–42, 2005. doi: 10.18637/jss.v012.i06.

[4] Roger Bivand and Nicholas Lewin-Koh. maptools: Tools for handling spatial objects. manual, 2023. URL https://CRAN.R-project.org/package=maptools.

[5] Roger Bivand, Tim Keitt, and Barry Rowlingson. rgdal: Bindings for the 'geospatial' data abstraction library. manual, 2023. URL https://CRAN.R-project.org/package=rgdal.

[6] Winston Chang, Joe Cheng, JJ Allaire, Carson Sievert, Barret Schloerke, Yihui Xie, Jeff Allen, Jonathan McPherson, Alan Dipert, and Barbara Borges. shiny: Web application framework for R. manual, 2024. URL https://shiny.posit.co/.

[7] Joe Cheng, Barret Schloerke, Bhaskar Karambelkar, and Yihui Xie. leaflet: Create interactive web maps with the JavaScript 'leaflet' library. manual, 2023. URL https://CRAN.R-project.org/package=leaflet.

[8] Maximilian H.K. Hesselbarth, Marco Sciaini, Kimberly A. With, Kerstin Wie-

gand, and Jakub Nowosad. landscapemetrics: an open-source R tool to calculate landscape metrics. *Ecography*, 42:1648–1657, 2019. doi: 10.1111/ecog.04617.

[9] Robert J. Hijmans. raster: Geographic data analysis and modeling. manual, 2023. URL https://CRAN.R-project.org/package=raster.

[10] Robert J. Hijmans. terra: Spatial data analysis. manual, 2023. URL https://CRAN.R-project.org/package=terra.

[11] Joseph Larmarange. labelled: Manipulating labelled data. manual, 2023. URL https://CRAN.R-project.org/package=labelled.

[12] New York City Office of Technology and Innovation. Land Cover Raster Data (2017) – 6in Resolution, September 2022. URL https://data.cityofnewyork.us/Environment/Land-Cover-Raster-Data-2017-6in-Resolution/he6d-2qns/about_data.

[13] NOAA Office for Coastal Management. 2020 NOAA C-CAP Version 2 Canopy Cover: Michigan, . URL www.coast.noaa.gov/htdata/raster1/landcover/bulkdownload/hires/.

[14] NOAA Office for Coastal Management. 2020 NOAA C-CAP Version 2 Impervious Cover: Michigan, . URL www.coast.noaa.gov/htdata/raster1/landcover/bulkdownload/hires/.

[15] NOAA Office for Coastal Management. 2020 NOAA C-CAP Version 2 Water Cover: Michigan, . URL www.coast.noaa.gov/htdata/raster1/landcover/bulkdownload/hires/.

[16] Edzer Pebesma. Simple features for R: Standardized support for spatial vector

data. *The R Journal*, 10(1):439–446, 2018. doi: 10.32614/RJ-2018-009. URL https://doi.org/10.32614/RJ-2018-009.

[17] Edzer J. Pebesma and Roger Bivand. Classes and methods for spatial data in R. *R News*, 5(2):9–13, November 2005. URL https://CRAN.R-project.org/doc/Rnews/.

[18] Thomas Lin Pedersen, Vincent Nijs, Thomas Schaffner, and Eric Nantz. shinyFiles: A server-side file system viewer for shiny. manual, 2022. URL https://CRAN.R-project.org/package=shinyFiles.

[19] Planet Labs PBC. Planet Application Program Interface: In Space for Life on Earth, 2022. URL https://api.planet.com.

[20] PlanIT Geo, LLC. Generalized Land Cover 2020, April 2022. URL http://opendata.dc.gov.

[21] Posit team. RStudio: Integrated development environment for R. manual, Posit Software, PBC, Boston, MA, 2023. URL http://www.posit.co/.

[22] R Core Team. R: A language and environment for statistical computing. manual, R Foundation for Statistical Computing, Vienna, Austria, 2023. URL https://www.R-project.org/.

[23] US Environmental Protection Agency. EnviroAtlas – Phoenix, AZ – Meter-Scale Urban Land Cover (MULC) Data (2010), September 2017.

[24] Dan Warren and Russell Dinnage. ENMTools: Analysis of niche evolution using niche and distribution models. manual, 2023.

[25] Hadley Wickham, Romain François, Lionel Henry, Kirill Müller, and Davis Vaughan. dplyr: A grammar of data manipulation. manual, 2023. URL https://CRAN.R-project.org/package=dplyr.

Appendix B

Additional Results

B.1 PCA Scree Plots

Figure B.1: Below are a set of scree plots from the PCA of each case study, showing the eigenvalues for each component extracted. Components were extracted visually, using a qualitatively determined point where eigenvalue was no longer reducing rapidly. For each city, the red dashed line indicates this point.

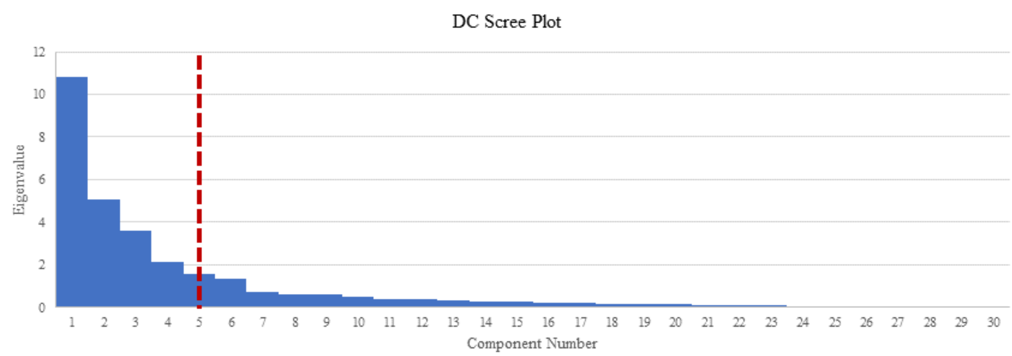

(a) Scree Plot for DC PCA. 5 components extracted explaining 77% of the variance.

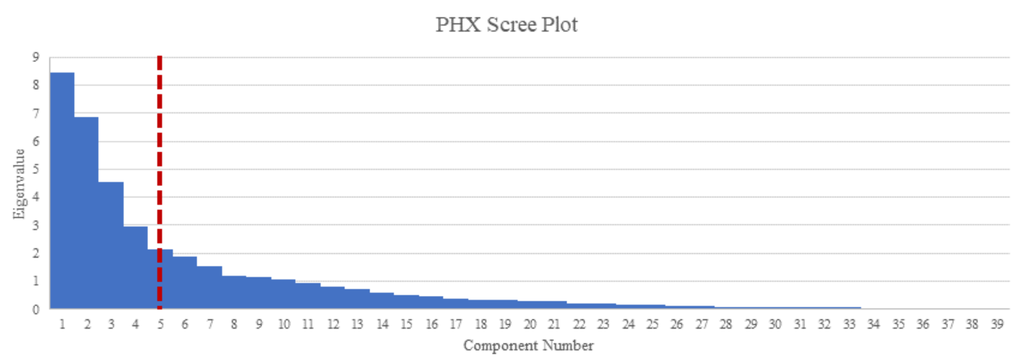

(b) Scree Plot for PHX PCA. 5 components extracted explaining 64% of the variance.

Below are a set of scree plots from the PCA of each case study, showing the eigenvalues for each component extracted. Components were extracted visually, using a qualitatively determined point where eigenvalue was no longer reducing rapidly. For each city, the red dashed line indicates this point (cont.).

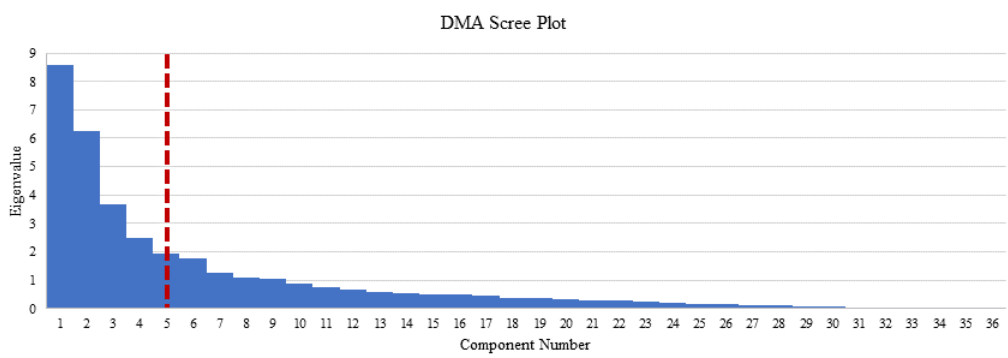

(c) Scree Plot for DMA PCA. 5 components extracted explaining 64% of the variance.

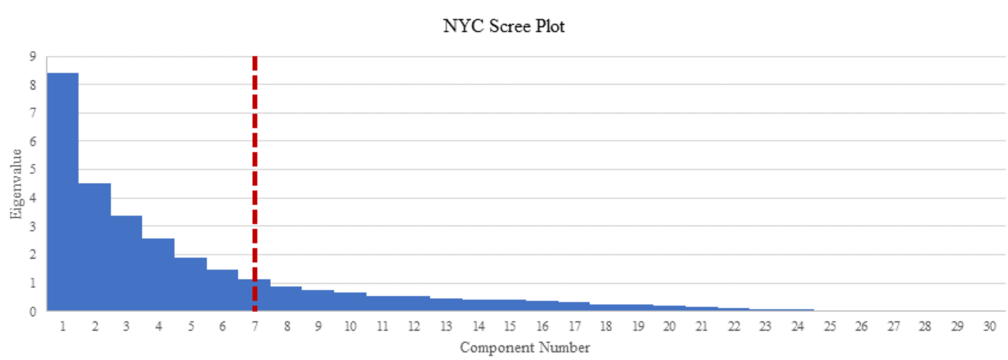

(d) Scree Plot for NYC PCA. 7 components extracted explaining 78% of the variance.

B.2 Measures of Spatial Auto-correlation

Spatial auto-correlation of each variable was measured with Global Moran's i, using a fixed distance band conceptualization of spatial relationships set to a Euclidean distance of 800m.

	Moran's Index	Expected Index	Variance	z-score	p-value
Below Poverty %	0.750662	-0.004739	0.00287	14.0931	0
Unemployed %	0.699745	-0.004739	0.00277	13.3791	0
No HS Diploma %	0.631809	-0.004739	0.00287	11.8733	0
Uninsured %	0.518724	-0.004739	0.00287	9.77752	0
Age 65+ %	0.542238	-0.004739	0.00289	10.1811	0
Age 17- %	0.612669	-0.004739	0.00288	11.5131	0
Disabled %	0.792673	-0.004739	0.00287	14.8878	0
Limited English %	0.454182	-0.004739	0.00274	8.76692	0
Minority %	0.974108	-0.004739	0.00291	18.1485	0
Housing Burden %	0.724897	-0.004739	0.0029	13.5612	0
Single Parent Household %	0.588781	-0.004739	0.00278	11.2585	0
Household Crowding %	0.401386	-0.004739	0.00276	7.72836	0
Impervious PLAND	0.469629	-0.004739	0.0029	8.81323	0
Tree PLAND	0.608615	-0.004739	0.0029	11.3996	0
Shrub & Grass PLAND	0.174741	-0.004739	0.00281	3.38734	0.000706
Impervious LPI	0.445089	-0.004739	0.0029	8.35644	0
Tree LPI	0.621797	-0.004739	0.00289	11.6507	0
Shrub & Grass LPI	0.033081	-0.004739	0.00265	0.73466	0.462548
Impervious LSI	0.200053	-0.004739	0.00288	3.81391	0.000137
Tree LSI	0.33656	-0.004739	0.00289	6.35195	0
Shrub & Grass LSI	0.178557	-0.004739	0.00288	3.41579	0.000636
Impervious ENN__MN	0.342115	-0.004739	0.00285	6.49313	0
Tree ENN__MN	0.439938	-0.004739	0.00288	8.28343	0
Shrub & Grass ENN__MN	0.419698	-0.004739	0.00283	7.97464	0
Impervious Cohesion	0.519105	-0.004739	0.00287	9.77346	0
Tree Cohesion	0.65356	-0.004739	0.00289	12.2441	0
Shrub & Grass Cohesion	0.239107	-0.004739	0.00289	4.53932	0.000006
Impervious PLADJ	0.359796	-0.004739	0.00289	6.77763	0
Tree PLADJ	0.518128	-0.004739	0.0029	9.7153	0
Shrub & Grass PLADJ	0.114715	-0.004739	0.00288	2.22515	0.026071

Table B.1: Moran's i calculations for DC

	Moran's Index	Expected Index	Variance	z-score	p-value
Below Poverty %	0.747451	-0.00118	0.001615	18.62874	0
Unemployed %	0.578035	-0.00118	0.001612	14.42496	0
No HS Diploma %	0.936646	-0.00118	0.001619	23.30778	0
Age 65+ %	0.83507	-0.00118	0.001606	20.86411	0
Age 17- %	0.859257	-0.00118	0.001619	21.38376	0
Minority %	0.942322	-0.00118	0.001621	23.43494	0
Limited English %	0.908876	-0.00118	0.001617	22.63404	0
Single Parent Household %	0.884511	-0.00118	0.00162	22.00522	0
Household Crowding %	0.893809	-0.00118	0.001614	22.27875	0
Impervious PLAND	0.349205	-0.00118	0.001618	8.710253	0
Barren PLAND	0.457423	-0.00118	0.001616	11.40662	0
Tree PLAND	0.767089	-0.00118	0.001617	19.1031	0
Shrub PLAND	0.279493	-0.00118	0.001559	7.108553	0
Grass PLAND	0.416153	-0.00118	0.001599	10.43785	0
Impervious LPI	0.270762	-0.00118	0.001615	6.766103	0
Barren LPI	0.303385	-0.00118	0.001607	7.597608	0
Tree LPI	0.495403	-0.00118	0.001588	12.45972	0
Shrub LPI	0.06369	-0.00118	0.000747	2.373703	0.017611
Grass LPI	0.27397	-0.00118	0.001492	7.122304	0
Impervious LSI	0.180449	-0.00118	0.001617	4.517132	0.000006
Barren LSI	0.609321	-0.00118	0.001618	15.17669	0
Tree LSI	0.769551	-0.00118	0.00162	19.1492	0
Shrub LSI	0.454568	-0.00118	0.00161	11.35657	0
Grass LSI	0.62552	-0.00118	0.001618	15.57774	0
Impervious ENN_MN	0.059463	-0.00118	0.001196	1.75393	0.079443
Barren ENN_MN	0.392512	-0.00118	0.001605	9.826747	0
Tree ENN_MN	0.686231	-0.00118	0.001607	17.14952	0
Shrub ENN_MN	0.255941	-0.00118	0.001557	6.516151	0
Grass ENN_MN	0.567131	-0.00118	0.00134	15.52592	0
Impervious PLADJ	0.210081	-0.00118	0.001426	5.595189	0
Barren PLADJ	0.637929	-0.00118	0.001619	15.88565	0
Tree PLADJ	0.636474	-0.00118	0.001602	15.92906	0
Shrub PLADJ	0.63238	-0.00118	0.001621	15.73513	0
Grass PLADJ	0.236145	-0.00118	0.001585	5.961399	0
Impervious Cohesion	0.195684	-0.00118	0.00148	5.116668	0
Barren Cohesion	0.567876	-0.00118	0.001609	14.18765	0
Tree Cohesion	0.596543	-0.00118	0.001562	15.12335	0
Shrub Cohesion	0.632013	-0.00118	0.001622	15.72429	0
Grass Cohesion	0.16488	-0.00118	0.001529	4.246982	0.000022

Table B.2: Moran's i calculations for PHX

	Moran's Index	Expected Index	Variance	z-score	p-value
Below Poverty %	0.911633	-0.00068	0.000621	36.60282	0
Unemployed %	0.714418	-0.00068	0.00062	28.72876	0
No HS Diploma %	0.875708	-0.00068	0.00062	35.18354	0
Uninsured %	0.761969	-0.00068	0.00062	30.63569	0
Age 65+ %	0.683236	-0.00068	0.00062	27.45725	0
Age 17- %	0.719047	-0.00068	0.000621	28.89055	0
Disabled %	0.815646	-0.00068	0.000621	32.76715	0
Limited English %	0.820454	-0.00068	0.000613	33.16763	0
Minority %	0.95527	-0.00068	0.000621	38.34785	0
Housing Burden %	0.774346	-0.00068	0.000621	31.1022	0
Single Parent Household %	0.749676	-0.00068	0.00062	30.13594	0
Household Crowding %	0.693189	-0.00068	0.000617	27.92775	0
Impervious PLAND	0.430994	-0.00068	0.000621	17.32482	0
Barren PLAND	0.336566	-0.00068	0.000611	13.64292	0
Tree PLAND	0.431024	-0.00068	0.000621	17.32589	0
Grass PLAND	0.558131	-0.00068	0.00062	22.43499	0
Impervious LPI	0.381177	-0.00068	0.000621	15.32412	0
Barren LPI	0.103796	-0.00068	0.000548	4.462606	0.000008
Tree LPI	0.424189	-0.00068	0.000621	17.05366	0
Grass LPI	0.125595	-0.00068	0.000617	5.08242	0
Impervious LSI	0.412675	-0.00068	0.000621	16.58985	0
Barren LSI	0.567054	-0.00068	0.000621	22.78487	0
Tree LSI	0.46641	-0.00068	0.000621	18.74836	0
Grass LSI	0.67469	-0.00068	0.000621	27.10543	0
Impervious ENN_MN	0.479213	-0.00068	0.000611	19.40679	0
Barren ENN_MN	0.179548	-0.00068	0.000545	7.719974	0
Tree ENN_MN	0.111622	-0.00068	0.000612	4.540984	0.000006
Grass ENN_MN	0.572097	-0.00068	0.000591	23.55334	0
Impervious PLADJ	0.295991	-0.00068	0.000621	11.90783	0
Barren PLADJ	0.356931	-0.00068	0.000616	14.40351	0
Tree PLADJ	0.545146	-0.00068	0.000621	21.90813	0
Grass PLADJ	0.315991	-0.00068	0.000585	13.09836	0
Impervious Cohesion	0.309748	-0.00068	0.000617	12.49602	0
Barren Cohesion	0.341701	-0.00068	0.000614	13.81985	0
Tree Cohesion	0.408789	-0.00068	0.00062	16.45082	0
Grass Cohesion	0.237021	-0.00068	0.00049	10.74206	0

Table B.3: Moran's i Calculations for DMA

	Moran's Index	Expected Index	Variance	z-score	p-value
Below Poverty %	0.483426	-0.00137	0.001112	14.53655	0
Unemployed %	0.381445	-0.00137	0.001114	11.47143	0
No HS Diploma%	0.579458	-0.00137	0.001116	17.38358	0
Uninsured %	0.569498	-0.00137	0.001115	17.0961	0
Age 65+ %	0.438849	-0.00137	0.001088	13.34431	0
Age 17- %	0.404149	-0.00137	0.001116	12.14027	0
Disabled %	0.395396	-0.00137	0.001109	11.91639	0
Minority %	0.873058	-0.00137	0.001119	26.13646	0
Limited English %	0.792002	-0.00137	0.001112	23.78764	0
Single Parent Household %	0.503496	-0.00137	0.001102	15.20507	0
Household Crowding %	0.442866	-0.00137	0.001112	13.32274	0
Housing Burden %	0.365422	-0.00137	0.001111	11.00445	0
Impervious PLAND	0.468805	-0.00137	0.001117	14.06737	0
Tree PLAND	0.402502	-0.00137	0.001113	12.10463	0
Grass Pland	0.318068	-0.00137	0.001104	9.612324	0
Impervious LPI	0.474044	-0.00137	0.001118	14.21889	0
Tree LPI	0.323376	-0.00137	0.001098	9.798383	0
Grass LPI	0.144821	-0.00137	0.001054	4.503021	0.000007
Impervious LSI	0.490012	-0.00137	0.001118	14.69319	0
Tree LSI	0.198093	-0.00137	0.001116	5.971221	0
Grass LSI	0.438576	-0.00137	0.001118	13.15898	0
Impervious ENNMN	0.001973	-0.00137	0.000597	0.136663	0.891297
Tree ENNMN	0.392748	-0.00137	0.001099	11.89098	0
Grass ENNMN	0.646714	-0.00137	0.001113	19.4222	0
Impervious PLADJ	0.509238	-0.00137	0.001116	15.2855	0
Tree PLADJ	0.369628	-0.00137	0.001107	11.15057	0
Grass PLADJ	0.311635	-0.00137	0.001117	9.366697	0
Impervious Cohesion	0.221673	-0.00137	0.001071	6.816758	0
Tree Cohesion	0.368927	-0.00137	0.001109	11.12183	0
Grass Cohesion	0.446389	-0.00137	0.001117	13.39666	0

Table B.4: Moran's i calculations for NYC

B.3 Results of Mann-Whitney U Test

The following charts show the results from Mann Whitney U Tests conducted as a form of Mean Rank Analysis. Variables to test were chosen based on relationships that were revealed through PCA. Figure B.2 shows the results of the tests for DC, Figure B.3 shows the results for PHX, Figure B.4 shows the results for DMA, and Figure B.5 shows the results for NYC. Significance was determined at two levels: $p < 0.05$ and $p < 0.001$.

Figure B.2: Results of the Mann Whitney U Tests conducted on DC data.

Independent-Samples Mann-Whitney U Test: Minority %

M1 M2

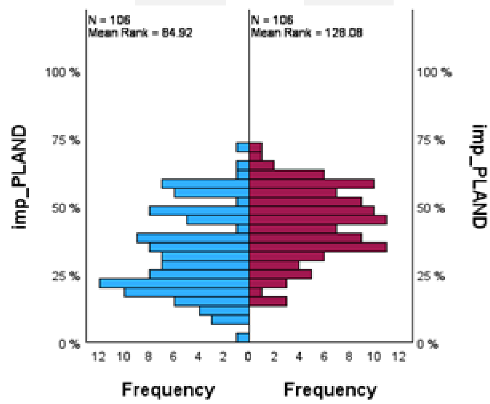

Independent-Samples Mann-Whitney U Test Summary

Total N	212
Mann-Whitney U	7905.000
Wilcoxon W	13576.000
Test Statistic	7905.000
Standard Error	446.586
Standardized Test Statistic	5.121
Asymptotic Sig.(2-sided test)	<.001

Independent-Samples Mann-Whitney U Test: Age Minority %

M1 M2

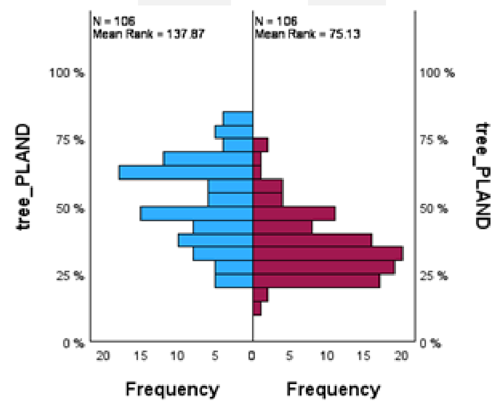

Independent-Samples Mann-Whitney U Test Summary

Total N	212
Mann-Whitney U	2293.000
Wilcoxon W	7964.000
Test Statistic	2293.000
Standard Error	446.586
Standardized Test Statistic	-7.445
Asymptotic Sig.(2-sided test)	<.001

Independent-Samples Mann-Whitney U Test: Minority %

M1 M2

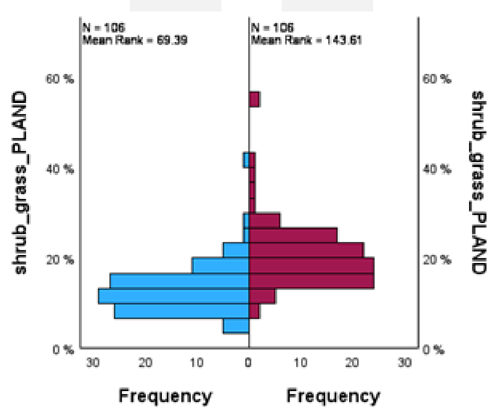

Independent-Samples Mann-Whitney U Test Summary

Total N	212
Mann-Whitney U	9552.000
Wilcoxon W	15223.000
Test Statistic	9552.000
Standard Error	446.586
Standardized Test Statistic	8.809
Asymptotic Sig.(2-sided test)	<.001

Independent-Samples Mann-Whitney U Test: Minority %

M1 M2

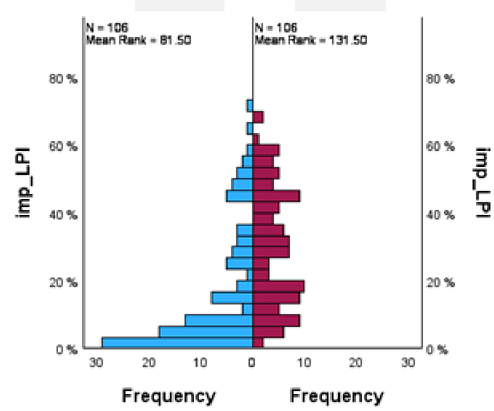

Independent-Samples Mann-Whitney U Test Summary

Total N	212
Mann-Whitney U	8268.000
Wilcoxon W	13939.000
Test Statistic	8268.000
Standard Error	446.586
Standardized Test Statistic	5.934
Asymptotic Sig.(2-sided test)	<.001

Results of the Mann Whitney U Tests conducted on DC data (cont.).

Independent-Samples Mann-Whitney U Test: Minority %

M1 M2

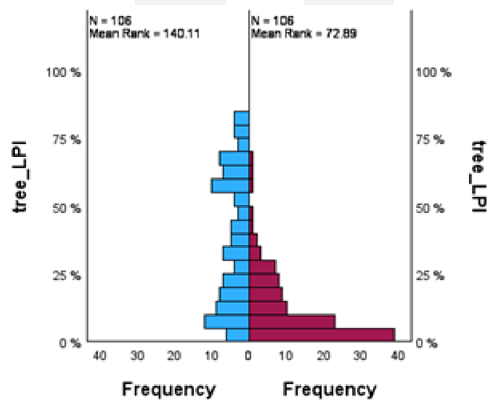

Independent-Samples Mann-Whitney U Test Summary

Total N	212
Mann-Whitney U	2055.000
Wilcoxon W	7726.000
Test Statistic	2055.000
Standard Error	446.586
Standardized Test Statistic	-7.978
Asymptotic Sig.(2-sided test)	<.001

Independent-Samples Mann-Whitney U Test: Age Minority %

M1 M2

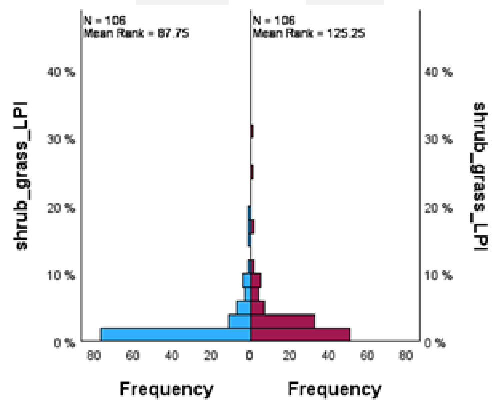

Independent-Samples Mann-Whitney U Test Summary

Total N	212
Mann-Whitney U	7605.000
Wilcoxon W	13276.000
Test Statistic	7605.000
Standard Error	446.586
Standardized Test Statistic	4.449
Asymptotic Sig.(2-sided test)	<.001

Independent-Samples Mann-Whitney U Test: Minority %

M1 M2

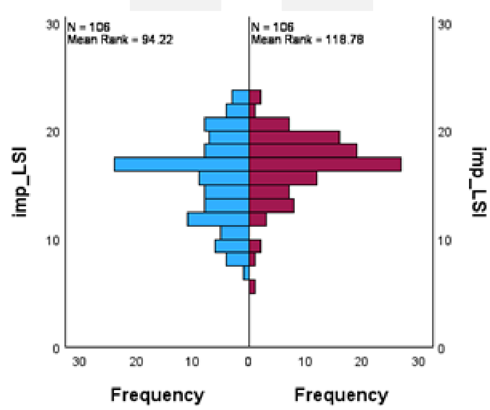

Independent-Samples Mann-Whitney U Test Summary

Total N	212
Mann-Whitney U	6920.000
Wilcoxon W	12591.000
Test Statistic	6920.000
Standard Error	446.586
Standardized Test Statistic	2.915
Asymptotic Sig.(2-sided test)	.004

Independent-Samples Mann-Whitney U Test: Minority %

M1 M2

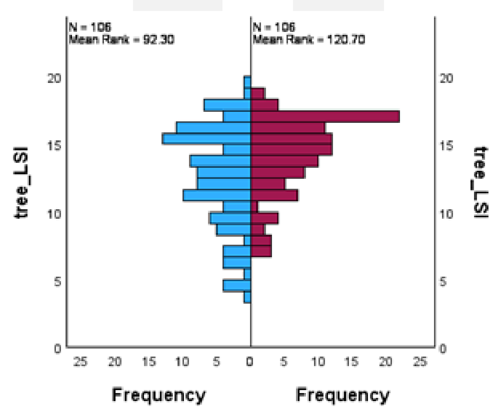

Independent-Samples Mann-Whitney U Test Summary

Total N	212
Mann-Whitney U	7123.000
Wilcoxon W	12794.000
Test Statistic	7123.000
Standard Error	446.586
Standardized Test Statistic	3.370
Asymptotic Sig.(2-sided test)	<.001

Results of the Mann Whitney U Tests conducted on DC data (cont.).

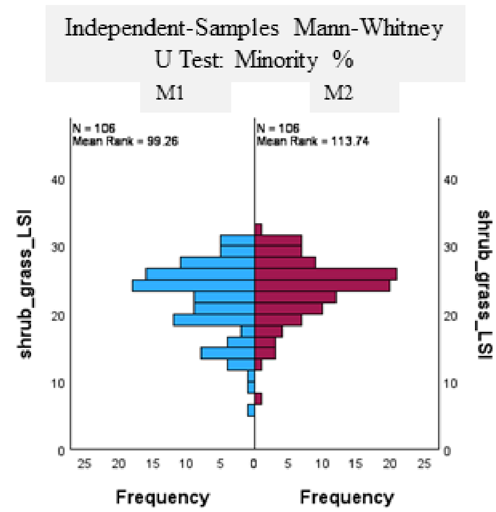

Independent-Samples Mann-Whitney U Test Summary

Total N	212
Mann-Whitney U	6385.000
Wilcoxon W	12056.000
Test Statistic	6385.000
Standard Error	446.586
Standardized Test Statistic	1.717
Asymptotic Sig.(2-sided test)	.086

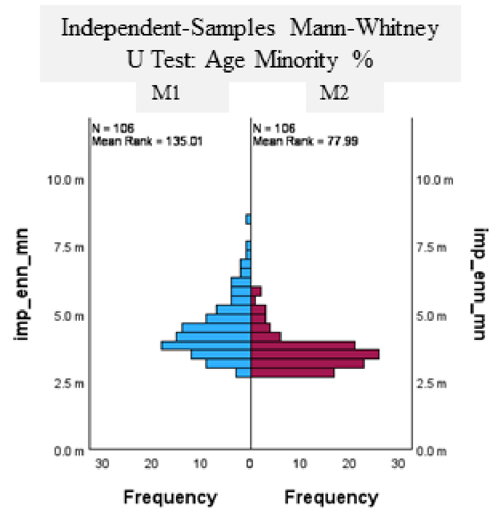

Independent-Samples Mann-Whitney U Test Summary

Total N	212
Mann-Whitney U	2596.000
Wilcoxon W	8267.000
Test Statistic	2596.000
Standard Error	446.586
Standardized Test Statistic	-6.767
Asymptotic Sig.(2-sided test)	<.001

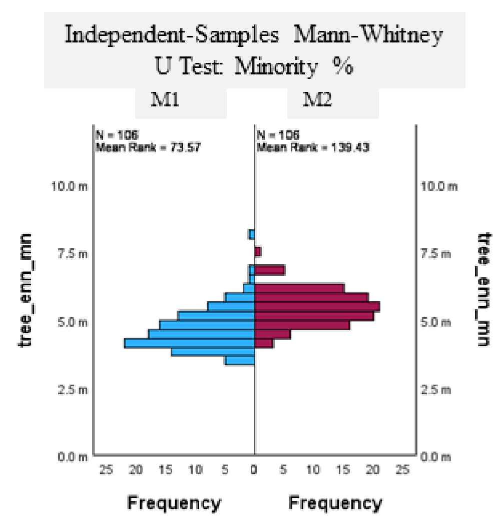

Independent-Samples Mann-Whitney U Test Summary

Total N	212
Mann-Whitney U	9109.000
Wilcoxon W	14780.000
Test Statistic	9109.000
Standard Error	446.586
Standardized Test Statistic	7.817
Asymptotic Sig.(2-sided test)	<.001

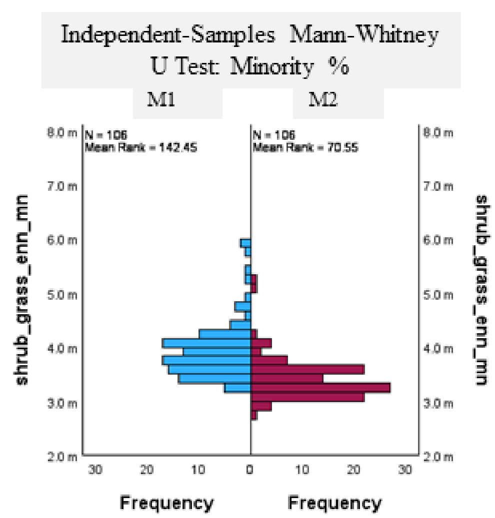

Independent-Samples Mann-Whitney U Test Summary

Total N	212
Mann-Whitney U	1807.000
Wilcoxon W	7478.000
Test Statistic	1807.000
Standard Error	446.586
Standardized Test Statistic	-8.534
Asymptotic Sig.(2-sided test)	<.001

Results of the Mann Whitney U Tests conducted on DC data (cont.).

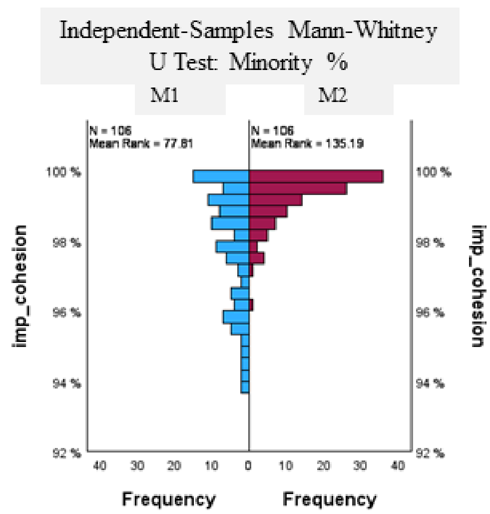

Independent-Samples Mann-Whitney U Test Summary

Total N	212
Mann-Whitney U	8659.000
Wilcoxon W	14330.000
Test Statistic	8659.000
Standard Error	446.586
Standardized Test Statistic	6.809
Asymptotic Sig.(2-sided test)	<.001

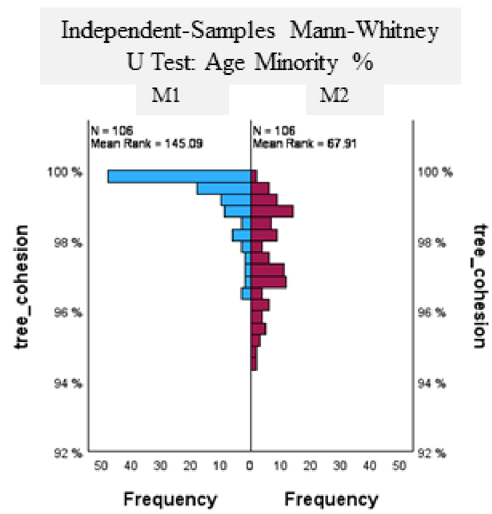

Independent-Samples Mann-Whitney U Test Summary

Total N	212
Mann-Whitney U	1527.000
Wilcoxon W	7198.000
Test Statistic	1527.000
Standard Error	446.586
Standardized Test Statistic	-9.161
Asymptotic Sig.(2-sided test)	<.001

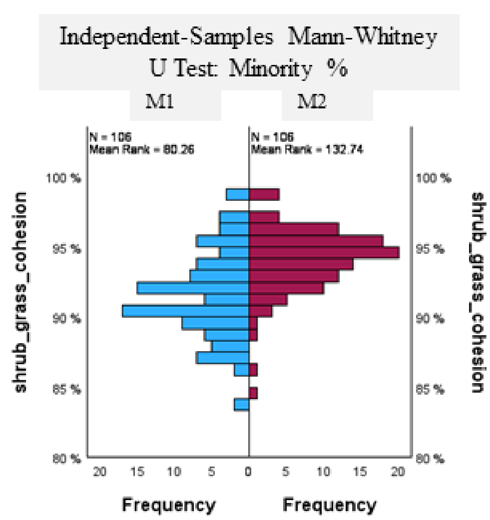

Independent-Samples Mann-Whitney U Test Summary

Total N	212
Mann-Whitney U	8399.000
Wilcoxon W	14070.000
Test Statistic	8399.000
Standard Error	446.586
Standardized Test Statistic	6.227
Asymptotic Sig.(2-sided test)	<.001

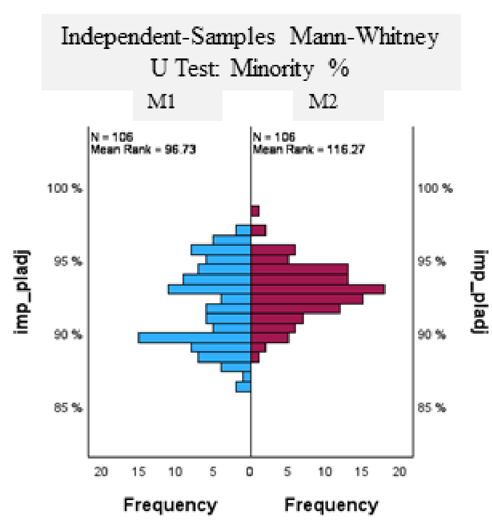

Independent-Samples Mann-Whitney U Test Summary

Total N	212
Mann-Whitney U	6654.000
Wilcoxon W	12325.000
Test Statistic	6654.000
Standard Error	446.586
Standardized Test Statistic	2.320
Asymptotic Sig.(2-sided test)	.020

Results of the Mann Whitney U Tests conducted on DC data (cont.).

Independent-Samples Mann-Whitney U Test: Minority %

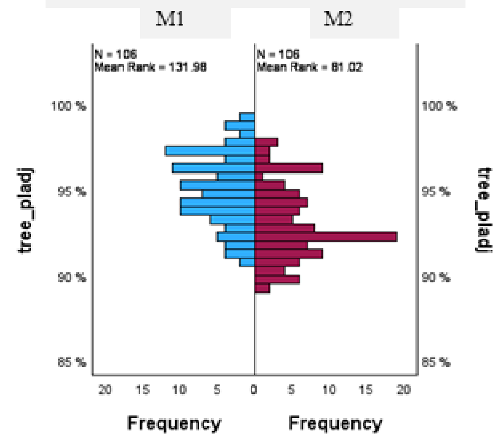

Independent-Samples Mann-Whitney U Test Summary

Total N	212
Mann-Whitney U	2917.000
Wilcoxon W	8588.000
Test Statistic	2917.000
Standard Error	446.586
Standardized Test Statistic	-6.048
Asymptotic Sig.(2-sided test)	<.001

Independent-Samples Mann-Whitney U Test: Age Minority %

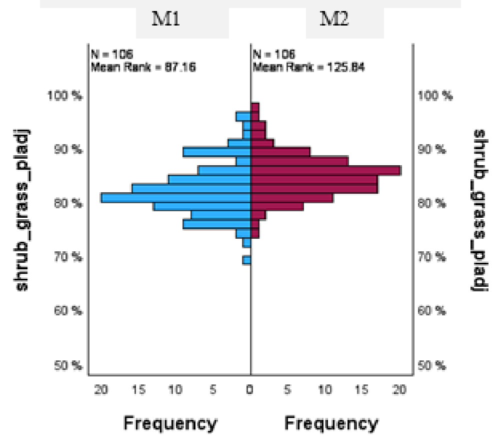

Independent-Samples Mann-Whitney U Test Summary

Total N	212
Mann-Whitney U	7668.000
Wilcoxon W	13339.000
Test Statistic	7668.000
Standard Error	446.586
Standardized Test Statistic	4.590
Asymptotic Sig.(2-sided test)	<.001

Independent-Samples Mann-Whitney U Test: Age 65+ %

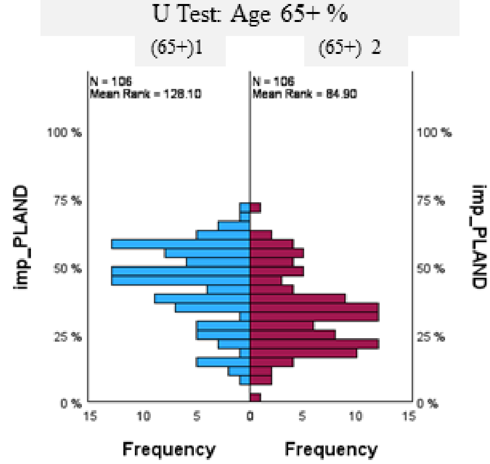

Independent-Samples Mann-Whitney U Test Summary

Total N	212
Mann-Whitney U	3328.000
Wilcoxon W	8999.000
Test Statistic	3328.000
Standard Error	446.586
Standardized Test Statistic	-5.128
Asymptotic Sig.(2-sided test)	<.001

Independent-Samples Mann-Whitney U Test: Age 65+ %

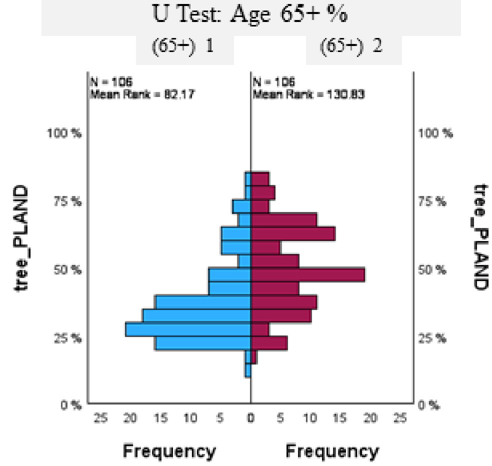

Independent-Samples Mann-Whitney U Test Summary

Total N	212
Mann-Whitney U	8197.000
Wilcoxon W	13868.000
Test Statistic	8197.000
Standard Error	446.586
Standardized Test Statistic	5.775
Asymptotic Sig.(2-sided test)	<.001

Results of the Mann Whitney U Tests conducted on DC data (cont.).

Independent-Samples Mann-Whitney U Test: Age 65+ %

(65+)1 (65+) 2

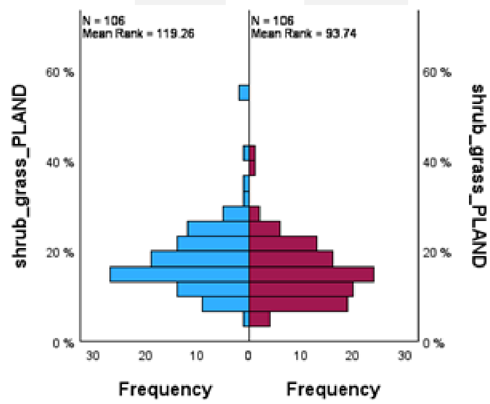

Independent-Samples Mann-Whitney U Test Summary

Total N	212
Mann-Whitney U	4265.000
Wilcoxon W	9936.000
Test Statistic	4265.000
Standard Error	446.586
Standardized Test Statistic	-3.030
Asymptotic Sig.(2-sided test)	.002

Independent-Samples Mann-Whitney U Test: Age 65+ %

(65+) 1 (65+) 2

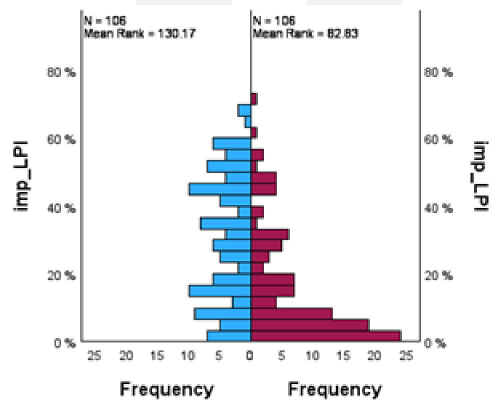

Independent-Samples Mann-Whitney U Test Summary

Total N	212
Mann-Whitney U	3109.000
Wilcoxon W	8780.000
Test Statistic	3109.000
Standard Error	446.586
Standardized Test Statistic	-5.618
Asymptotic Sig.(2-sided test)	<.001

Independent-Samples Mann-Whitney U Test: Age 65+ %

(65+) 1 (65+) 2

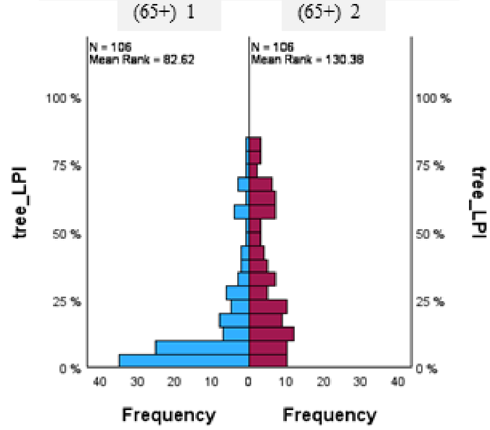

Independent-Samples Mann-Whitney U Test Summary

Total N	212
Mann-Whitney U	8149.000
Wilcoxon W	13820.000
Test Statistic	8149.000
Standard Error	446.586
Standardized Test Statistic	5.667
Asymptotic Sig.(2-sided test)	<.001

Independent-Samples Mann-Whitney U Test: Age 65+ %

(65+) 1 (65+) 2

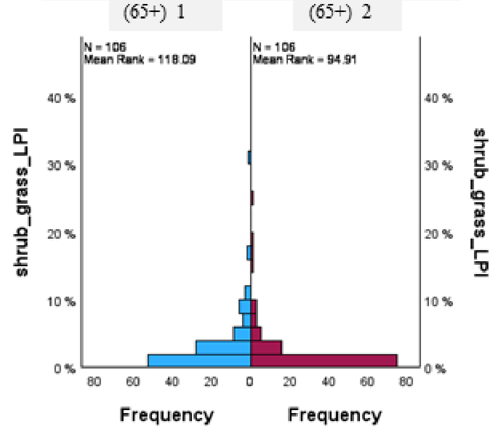

Independent-Samples Mann-Whitney U Test Summary

Total N	212
Mann-Whitney U	4389.000
Wilcoxon W	10060.000
Test Statistic	4389.000
Standard Error	446.586
Standardized Test Statistic	-2.752
Asymptotic Sig.(2-sided test)	.006

Results of the Mann Whitney U Tests conducted on DC data (cont.).

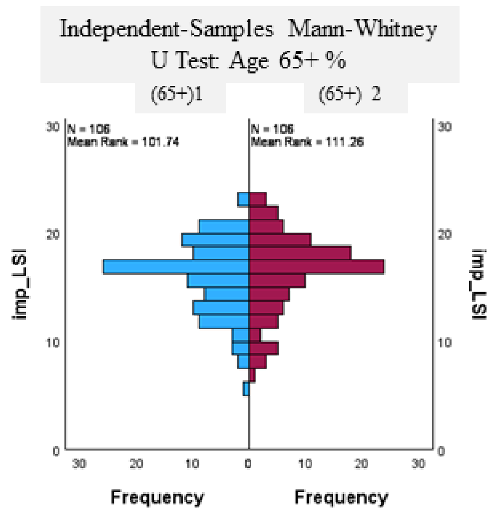

Independent-Samples Mann-Whitney U Test Summary

Total N	212
Mann-Whitney U	6123.000
Wilcoxon W	11794.000
Test Statistic	6123.000
Standard Error	446.586
Standardized Test Statistic	1.131
Asymptotic Sig.(2-sided test)	.258

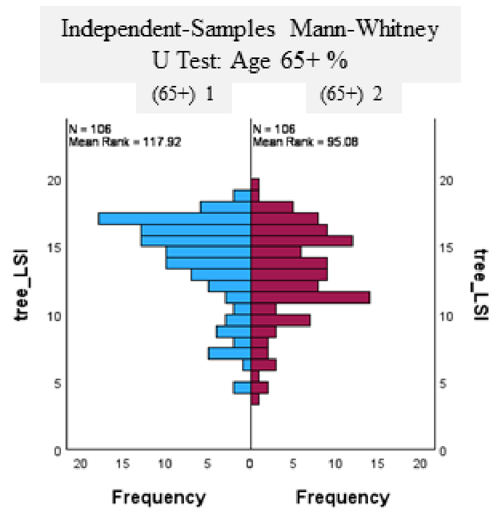

Independent-Samples Mann-Whitney U Test Summary

Total N	212
Mann-Whitney U	4407.000
Wilcoxon W	10078.000
Test Statistic	4407.000
Standard Error	446.586
Standardized Test Statistic	-2.712
Asymptotic Sig.(2-sided test)	.007

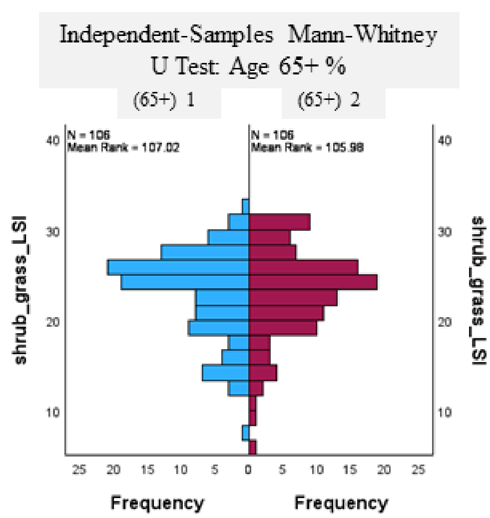

Independent-Samples Mann-Whitney U Test Summary

Total N	212
Mann-Whitney U	5563.000
Wilcoxon W	11234.000
Test Statistic	5563.000
Standard Error	446.586
Standardized Test Statistic	-.123
Asymptotic Sig.(2-sided test)	.902

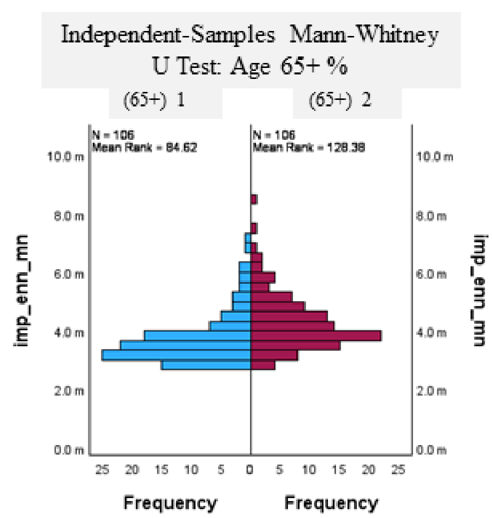

Independent-Samples Mann-Whitney U Test Summary

Total N	212
Mann-Whitney U	7937.000
Wilcoxon W	13608.000
Test Statistic	7937.000
Standard Error	446.586
Standardized Test Statistic	5.193
Asymptotic Sig.(2-sided test)	<.001

Results of the Mann Whitney U Tests conducted on DC data (cont.).

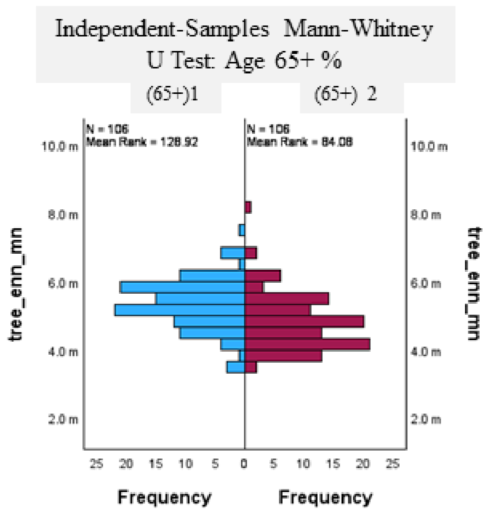

Independent-Samples Mann-Whitney U Test Summary

Total N	212
Mann-Whitney U	3242.000
Wilcoxon W	8913.000
Test Statistic	3242.000
Standard Error	446.586
Standardized Test Statistic	-5.320
Asymptotic Sig.(2-sided test)	<.001

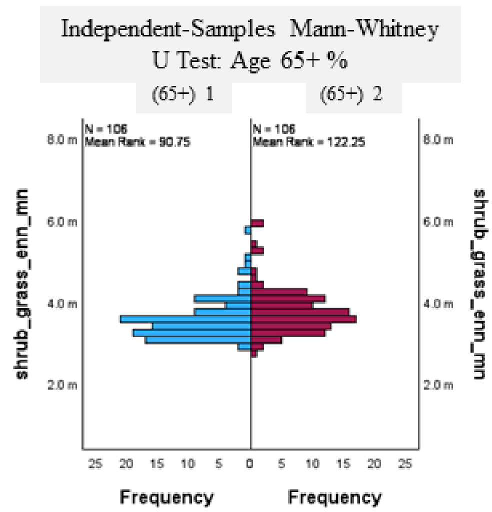

Independent-Samples Mann-Whitney U Test Summary

Total N	212
Mann-Whitney U	7287.000
Wilcoxon W	12958.000
Test Statistic	7287.000
Standard Error	446.586
Standardized Test Statistic	3.737
Asymptotic Sig.(2-sided test)	<.001

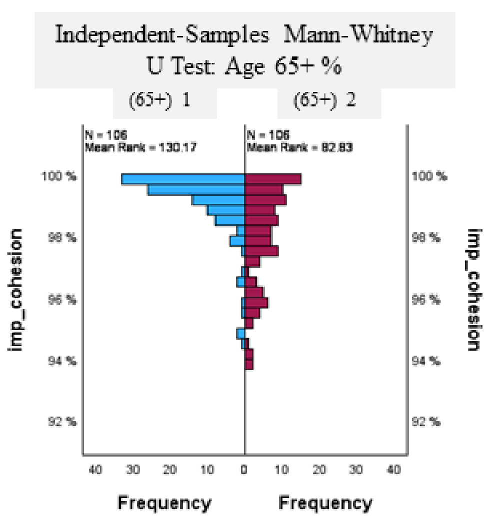

Independent-Samples Mann-Whitney U Test Summary

Total N	212
Mann-Whitney U	3109.000
Wilcoxon W	8780.000
Test Statistic	3109.000
Standard Error	446.586
Standardized Test Statistic	-5.618
Asymptotic Sig.(2-sided test)	<.001

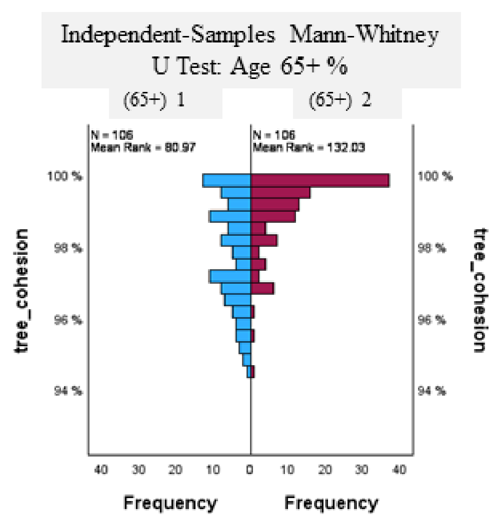

Independent-Samples Mann-Whitney U Test Summary

Total N	212
Mann-Whitney U	8324.000
Wilcoxon W	13995.000
Test Statistic	8324.000
Standard Error	446.586
Standardized Test Statistic	6.059
Asymptotic Sig.(2-sided test)	<.001

Results of the Mann Whitney U Tests conducted on DC data (cont.).

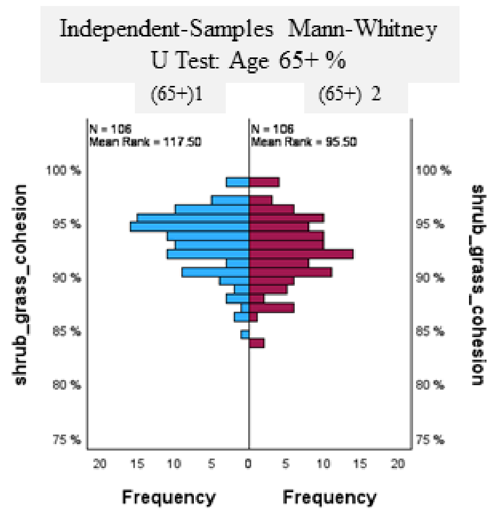

Independent-Samples Mann-Whitney U Test Summary

Total N	212
Mann-Whitney U	4452.000
Wilcoxon W	10123.000
Test Statistic	4452.000
Standard Error	446.586
Standardized Test Statistic	-2.611
Asymptotic Sig.(2-sided test)	.009

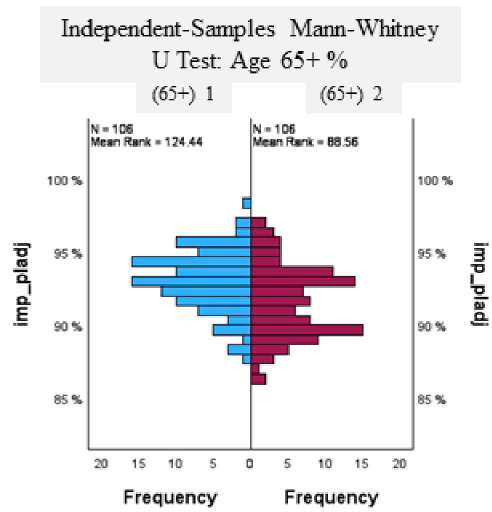

Independent-Samples Mann-Whitney U Test Summary

Total N	212
Mann-Whitney U	3716.000
Wilcoxon W	9387.000
Test Statistic	3716.000
Standard Error	446.586
Standardized Test Statistic	-4.259
Asymptotic Sig.(2-sided test)	<.001

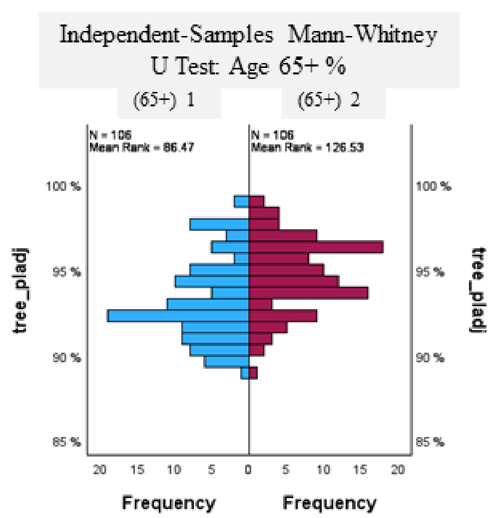

Independent-Samples Mann-Whitney U Test Summary

Total N	212
Mann-Whitney U	7741.000
Wilcoxon W	13412.000
Test Statistic	7741.000
Standard Error	446.586
Standardized Test Statistic	4.754
Asymptotic Sig.(2-sided test)	<.001

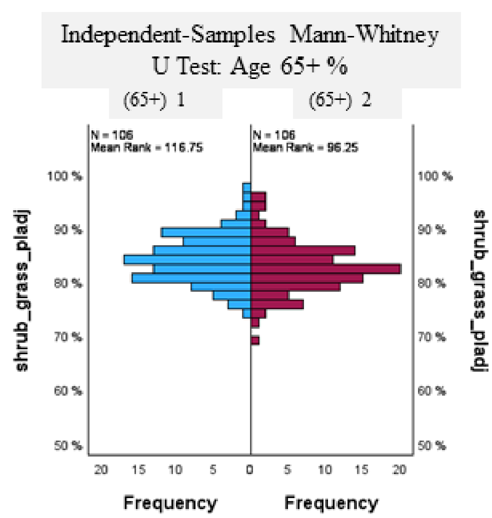

Independent-Samples Mann-Whitney U Test Summary

Total N	212
Mann-Whitney U	4531.000
Wilcoxon W	10202.000
Test Statistic	4531.000
Standard Error	446.586
Standardized Test Statistic	-2.434
Asymptotic Sig.(2-sided test)	.015

Figure B.3: Results of the Mann Whitney U Tests conducted on PHX data.

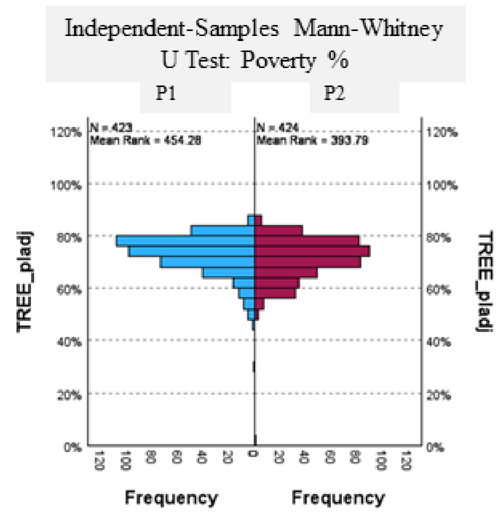

Independent-Samples Mann-Whitney U Test Summary

Total N	847
Mann-Whitney U	76866.000
Wilcoxon W	166966.000
Test Statistic	76866.000
Standard Error	3560.085
Standardized Test Statistic	-3.598
Asymptotic Sig.(2-sided test)	<.001

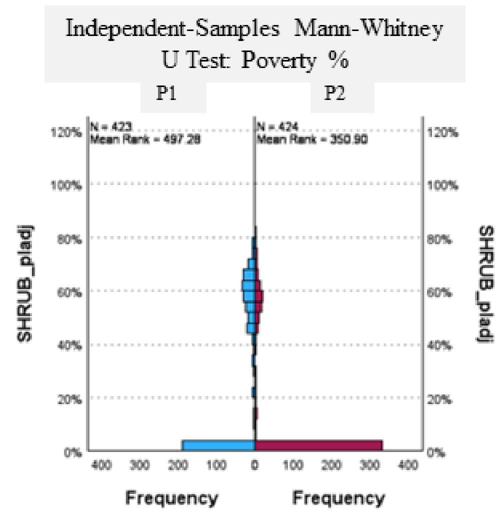

Independent-Samples Mann-Whitney U Test Summary

Total N	847
Mann-Whitney U	58680.500
Wilcoxon W	148780.500
Test Statistic	58680.500
Standard Error	3129.200
Standardized Test Statistic	-9.905
Asymptotic Sig.(2-sided test)	<.001

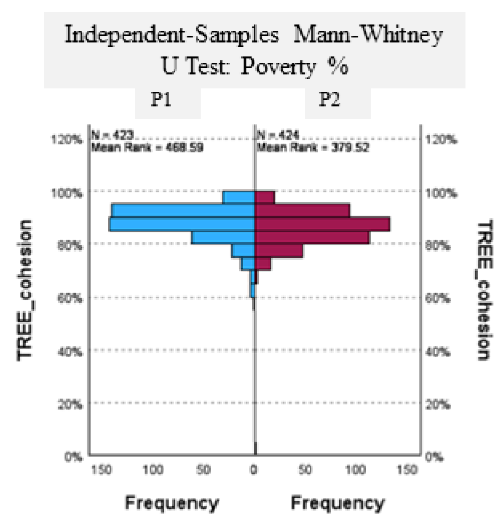

Independent-Samples Mann-Whitney U Test Summary

Total N	847
Mann-Whitney U	70816.000
Wilcoxon W	160916.000
Test Statistic	70816.000
Standard Error	3560.085
Standardized Test Statistic	-5.298
Asymptotic Sig.(2-sided test)	<.001

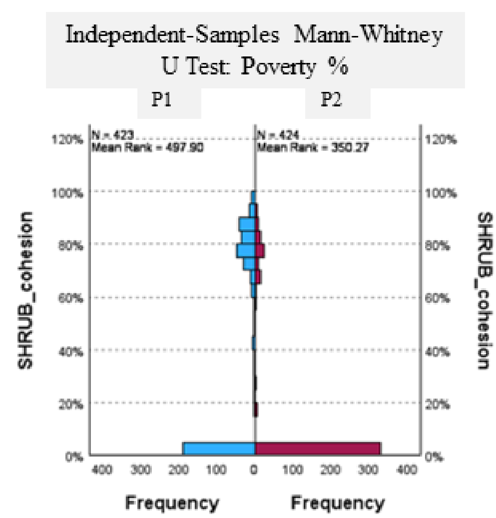

Independent-Samples Mann-Whitney U Test Summary

Total N	847
Mann-Whitney U	58414.500
Wilcoxon W	148514.500
Test Statistic	58414.500
Standard Error	3129.200
Standardized Test Statistic	-9.990
Asymptotic Sig.(2-sided test)	<.001

Results of the Mann Whitney U Tests conducted on PHX data (cont.).

Independent-Samples Mann-Whitney U Test: No High School Diploma %

HS1 HS2

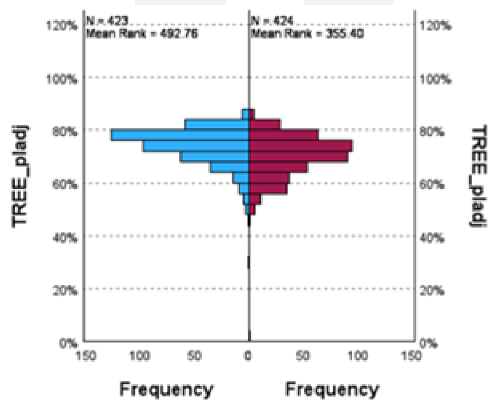

Independent-Samples Mann-Whitney U Test Summary

Total N	847
Mann-Whitney U	60589.000
Wilcoxon W	150689.000
Test Statistic	60589.000
Standard Error	3560.085
Standardized Test Statistic	-8.170
Asymptotic Sig.(2-sided test)	<.001

Independent-Samples Mann-Whitney U Test: No High School Diploma %

HS1 HS2

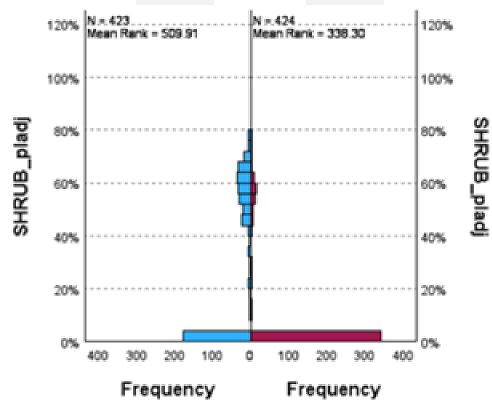

Independent-Samples Mann-Whitney U Test Summary

Total N	847
Mann-Whitney U	53338.000
Wilcoxon W	143438.000
Test Statistic	53338.000
Standard Error	3129.200
Standardized Test Statistic	-11.613
Asymptotic Sig.(2-sided test)	<.001

Independent-Samples Mann-Whitney U Test: No High School Diploma %

HS1 HS2

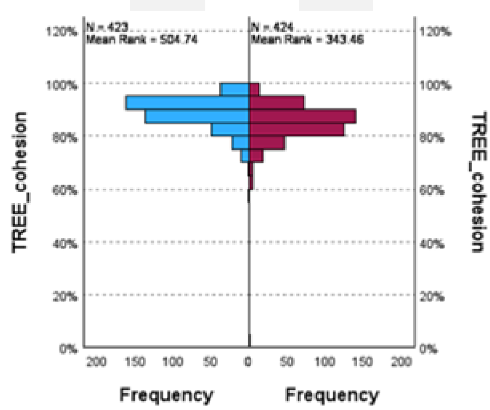

Independent-Samples Mann-Whitney U Test Summary

Total N	847
Mann-Whitney U	55525.000
Wilcoxon W	145625.000
Test Statistic	55525.000
Standard Error	3560.085
Standardized Test Statistic	-9.593
Asymptotic Sig.(2-sided test)	<.001

Independent-Samples Mann-Whitney U Test: No High School Diploma %

HS1 HS2

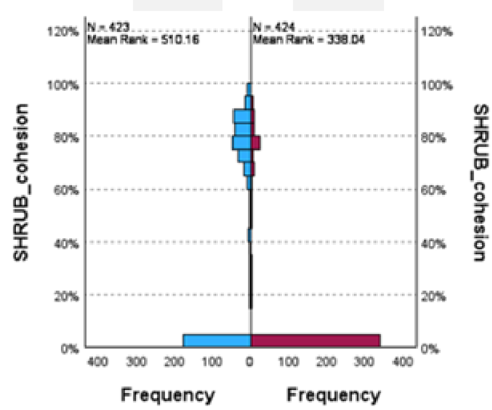

Independent-Samples Mann-Whitney U Test Summary

Total N	847
Mann-Whitney U	53229.500
Wilcoxon W	143329.500
Test Statistic	53229.500
Standard Error	3129.200
Standardized Test Statistic	-11.647
Asymptotic Sig.(2-sided test)	<.001

Results of the Mann Whitney U Tests conducted on PHX data (cont.).

Independent-Samples Mann-Whitney U Test Summary

Total N	847
Mann-Whitney U	132493.000
Wilcoxon W	222169.000
Test Statistic	132493.000
Standard Error	3560.085
Standardized Test Statistic	12.027
Asymptotic Sig.(2-sided test)	<.001

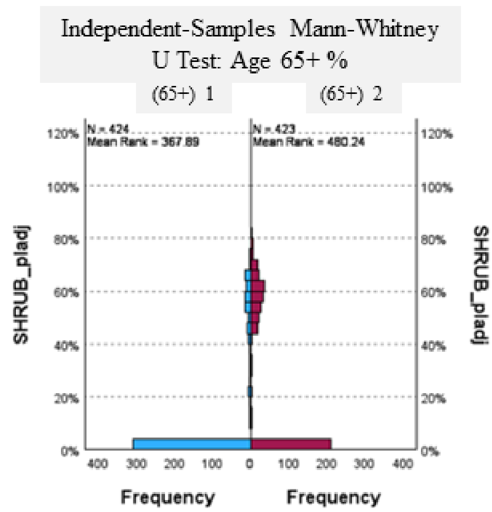

Independent-Samples Mann-Whitney U Test Summary

Total N	847
Mann-Whitney U	113467.000
Wilcoxon W	203143.000
Test Statistic	113467.000
Standard Error	3129.200
Standardized Test Statistic	7.603
Asymptotic Sig.(2-sided test)	<.001

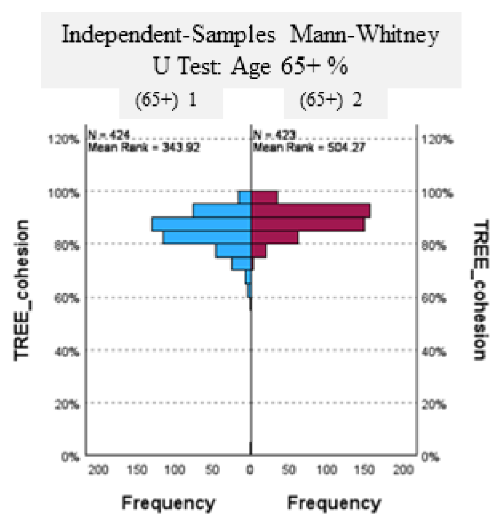

Independent-Samples Mann-Whitney U Test Summary

Total N	847
Mann-Whitney U	123630.000
Wilcoxon W	213306.000
Test Statistic	123630.000
Standard Error	3560.085
Standardized Test Statistic	9.537
Asymptotic Sig.(2-sided test)	<.001

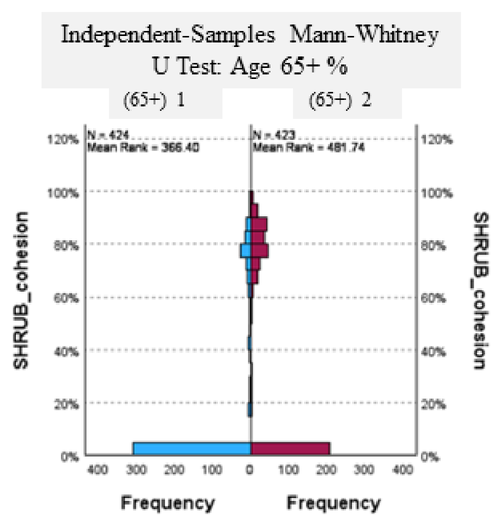

Independent-Samples Mann-Whitney U Test Summary

Total N	847
Mann-Whitney U	114100.500
Wilcoxon W	203776.500
Test Statistic	114100.500
Standard Error	3129.200
Standardized Test Statistic	7.805
Asymptotic Sig.(2-sided test)	<.001

Results of the Mann Whitney U Tests conducted on PHX data (cont.).

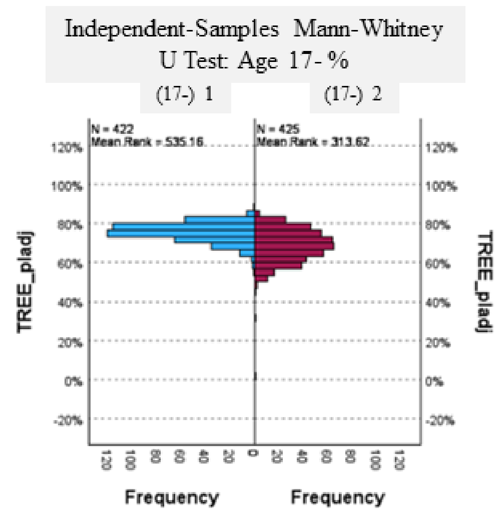

Independent-Samples Mann-Whitney U Test Summary

Total N	847
Mann-Whitney U	42765.000
Wilcoxon W	133290.000
Test Statistic	42765.000
Standard Error	3560.066
Standardized Test Statistic	-13.177
Asymptotic Sig.(2-sided test)	<.001

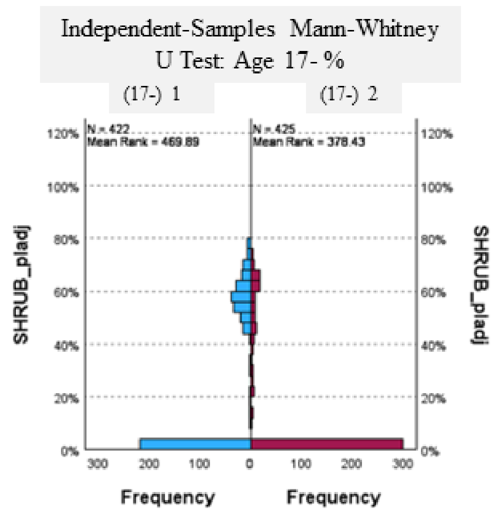

Independent-Samples Mann-Whitney U Test Summary

Total N	847
Mann-Whitney U	70308.000
Wilcoxon W	160833.000
Test Statistic	70308.000
Standard Error	3129.183
Standardized Test Statistic	-6.189
Asymptotic Sig.(2-sided test)	<.001

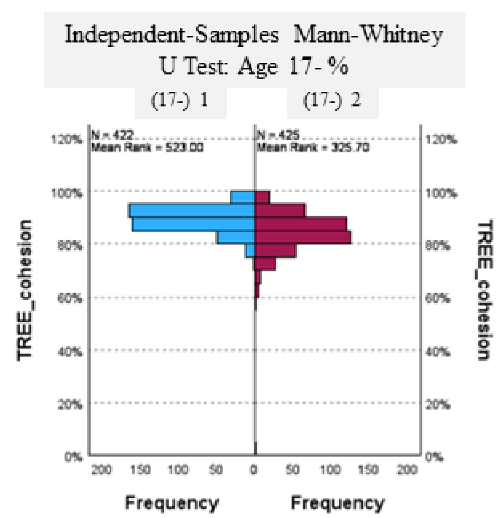

Independent-Samples Mann-Whitney U Test Summary

Total N	847
Mann-Whitney U	47896.000
Wilcoxon W	138421.000
Test Statistic	47896.000
Standard Error	3560.066
Standardized Test Statistic	-11.735
Asymptotic Sig.(2-sided test)	<.001

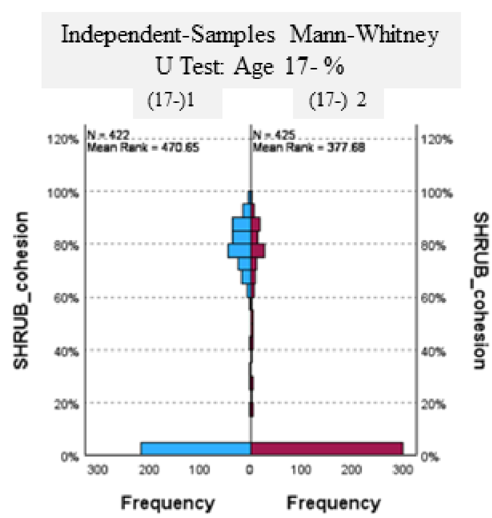

Independent-Samples Mann-Whitney U Test Summary

Total N	847
Mann-Whitney U	69989.500
Wilcoxon W	160514.500
Test Statistic	69989.500
Standard Error	3129.183
Standardized Test Statistic	-6.291
Asymptotic Sig.(2-sided test)	<.001

Results of the Mann Whitney U Tests conducted on PHX data (cont.).

Independent-Samples Mann-Whitney U Test: Minority %

M1 M2

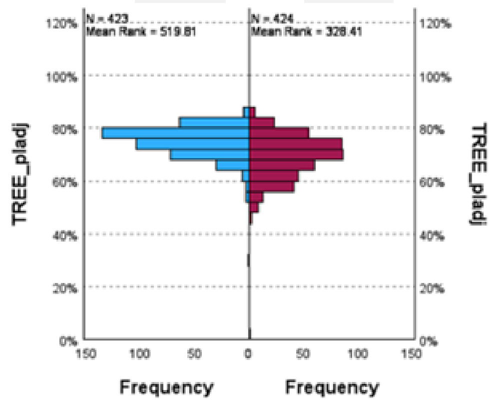

Independent-Samples Mann-Whitney U Test Summary

Total N	847
Mann-Whitney U	49147.000
Wilcoxon W	139247.000
Test Statistic	49147.000
Standard Error	3560.085
Standardized Test Statistic	-11.384
Asymptotic Sig.(2-sided test)	<.001

Independent-Samples Mann-Whitney U Test: Age Minority %

M1 M2

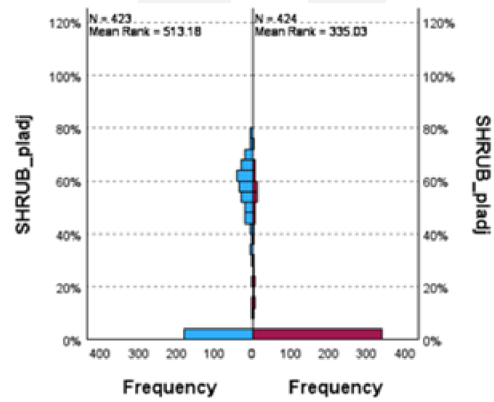

Independent-Samples Mann-Whitney U Test Summary

Total N	847
Mann-Whitney U	51954.000
Wilcoxon W	142054.000
Test Statistic	51954.000
Standard Error	3129.200
Standardized Test Statistic	-12.055
Asymptotic Sig.(2-sided test)	<.001

Independent-Samples Mann-Whitney U Test: Minority %

M1 M2

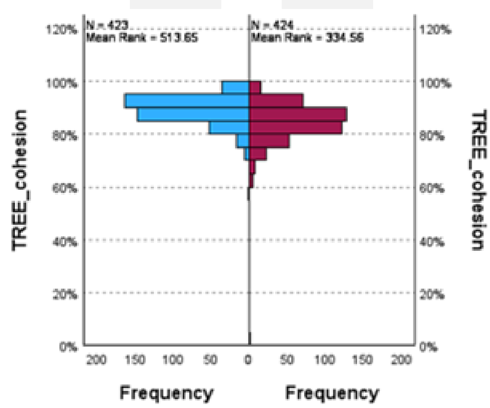

Independent-Samples Mann-Whitney U Test Summary

Total N	847
Mann-Whitney U	51755.000
Wilcoxon W	141855.000
Test Statistic	51755.000
Standard Error	3560.085
Standardized Test Statistic	-10.652
Asymptotic Sig.(2-sided test)	<.001

Independent-Samples Mann-Whitney U Test: Minority %

M1 M2

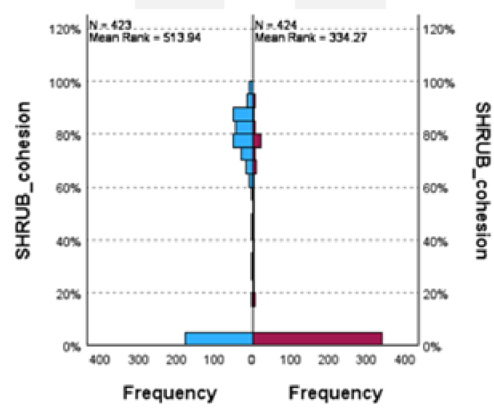

Independent-Samples Mann-Whitney U Test Summary

Total N	847
Mann-Whitney U	51631.500
Wilcoxon W	141731.500
Test Statistic	51631.500
Standard Error	3129.200
Standardized Test Statistic	-12.158
Asymptotic Sig.(2-sided test)	<.001

Results of the Mann Whitney U Tests conducted on PHX data (cont.).

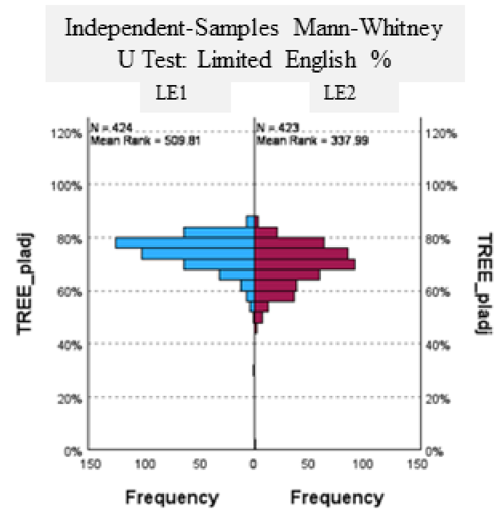

Independent-Samples Mann-Whitney U Test Summary

Total N	847
Mann-Whitney U	53294.000
Wilcoxon W	142970.000
Test Statistic	53294.000
Standard Error	3560.085
Standardized Test Statistic	-10.219
Asymptotic Sig.(2-sided test)	<.001

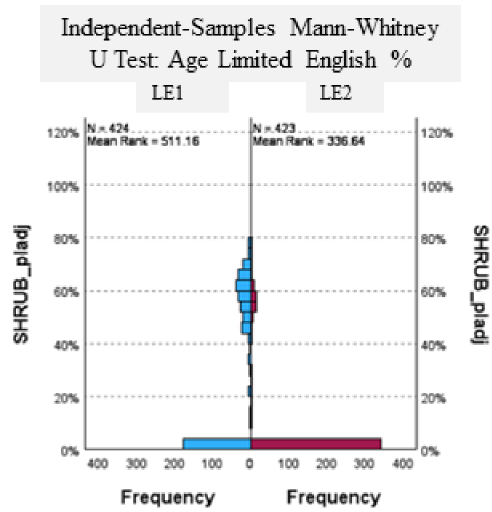

Independent-Samples Mann-Whitney U Test Summary

Total N	847
Mann-Whitney U	52722.000
Wilcoxon W	142398.000
Test Statistic	52722.000
Standard Error	3129.200
Standardized Test Statistic	-11.809
Asymptotic Sig.(2-sided test)	<.001

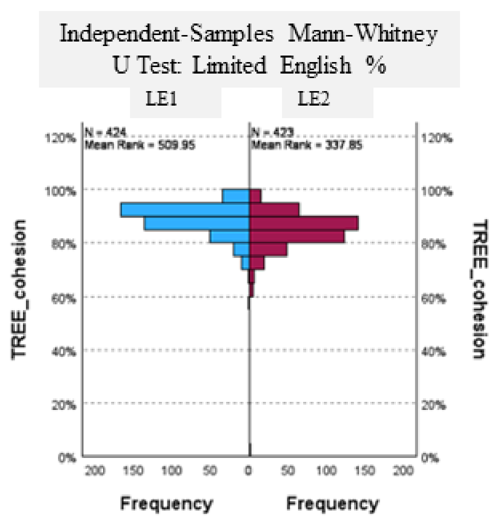

Independent-Samples Mann-Whitney U Test Summary

Total N	847
Mann-Whitney U	53233.000
Wilcoxon W	142909.000
Test Statistic	53233.000
Standard Error	3560.085
Standardized Test Statistic	-10.237
Asymptotic Sig.(2-sided test)	<.001

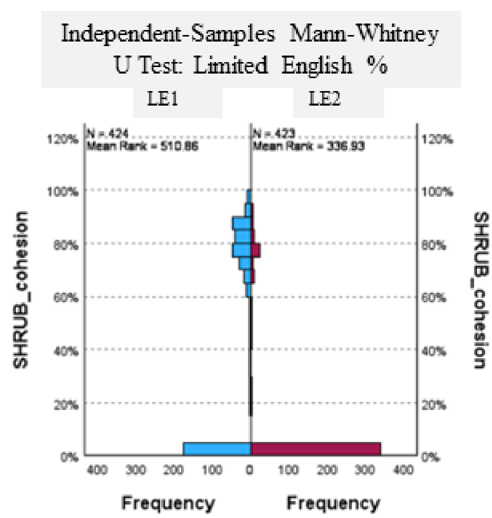

Independent-Samples Mann-Whitney U Test Summary

Total N	847
Mann-Whitney U	52847.500
Wilcoxon W	142523.500
Test Statistic	52847.500
Standard Error	3129.200
Standardized Test Statistic	-11.769
Asymptotic Sig.(2-sided test)	<.001

Results of the Mann Whitney U Tests conducted on PHX data (cont.).

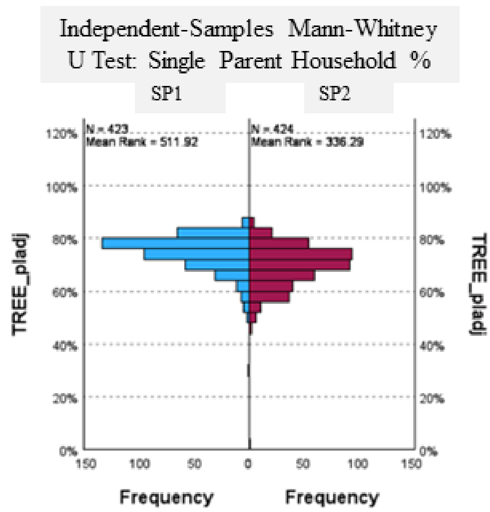

Independent-Samples Mann-Whitney U Test Summary

Total N	847
Mann-Whitney U	52485.000
Wilcoxon W	142585.000
Test Statistic	52485.000
Standard Error	3560.085
Standardized Test Statistic	-10.447
Asymptotic Sig.(2-sided test)	<.001

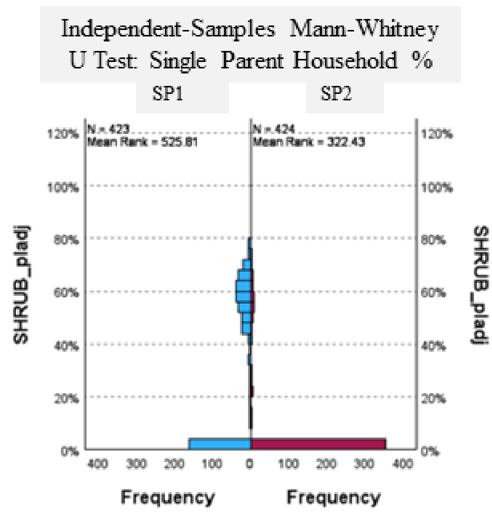

Independent-Samples Mann-Whitney U Test Summary

Total N	847
Mann-Whitney U	46611.000
Wilcoxon W	136711.000
Test Statistic	46611.000
Standard Error	3129.200
Standardized Test Statistic	-13.762
Asymptotic Sig.(2-sided test)	<.001

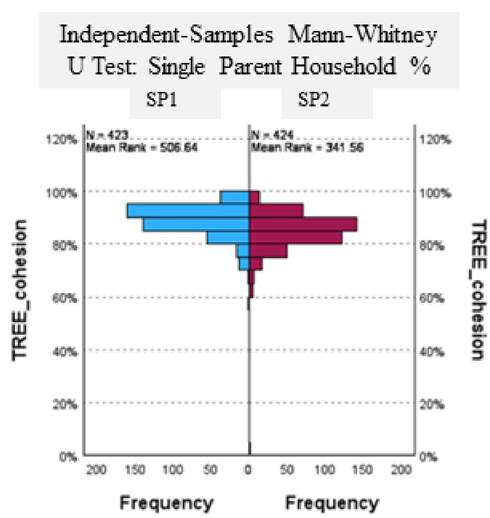

Independent-Samples Mann-Whitney U Test Summary

Total N	847
Mann-Whitney U	54720.000
Wilcoxon W	144820.000
Test Statistic	54720.000
Standard Error	3560.085
Standardized Test Statistic	-9.819
Asymptotic Sig.(2-sided test)	<.001

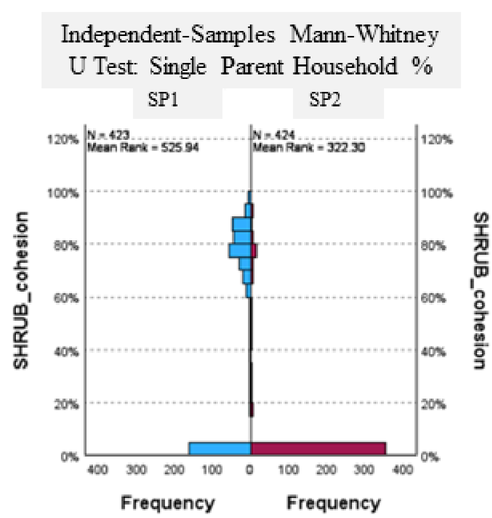

Independent-Samples Mann-Whitney U Test Summary

Total N	847
Mann-Whitney U	46555.500
Wilcoxon W	136655.500
Test Statistic	46555.500
Standard Error	3129.200
Standardized Test Statistic	-13.780
Asymptotic Sig.(2-sided test)	<.001

Results of the Mann Whitney U Tests conducted on PHX data (cont.).

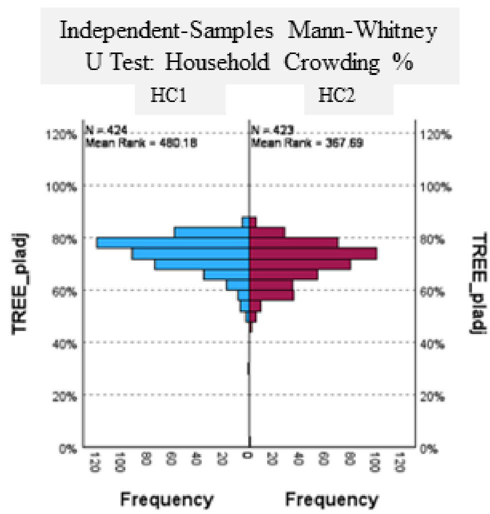

Independent-Samples Mann-Whitney U Test Summary

Total N	847
Mann-Whitney U	65856.000
Wilcoxon W	155532.000
Test Statistic	65856.000
Standard Error	3560.085
Standardized Test Statistic	-6.691
Asymptotic Sig.(2-sided test)	<.001

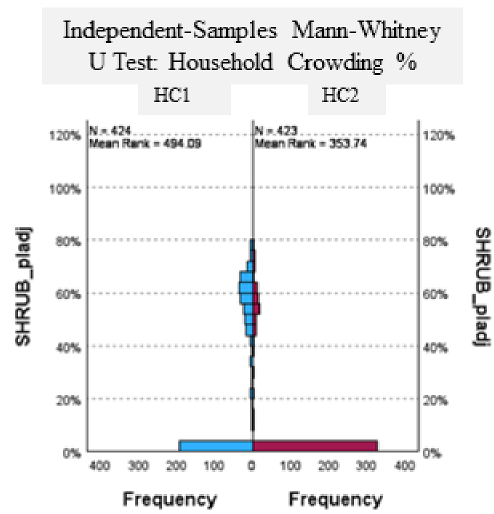

Independent-Samples Mann-Whitney U Test Summary

Total N	847
Mann-Whitney U	59958.000
Wilcoxon W	149634.000
Test Statistic	59958.000
Standard Error	3129.200
Standardized Test Statistic	-9.497
Asymptotic Sig.(2-sided test)	<.001

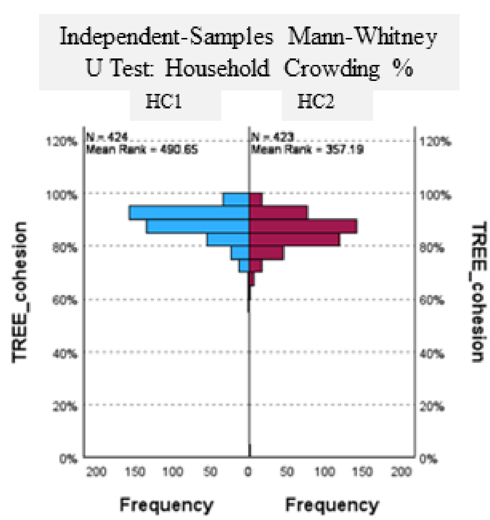

Independent-Samples Mann-Whitney U Test Summary

Total N	847
Mann-Whitney U	61417.000
Wilcoxon W	151093.000
Test Statistic	61417.000
Standard Error	3560.085
Standardized Test Statistic	-7.938
Asymptotic Sig.(2-sided test)	<.001

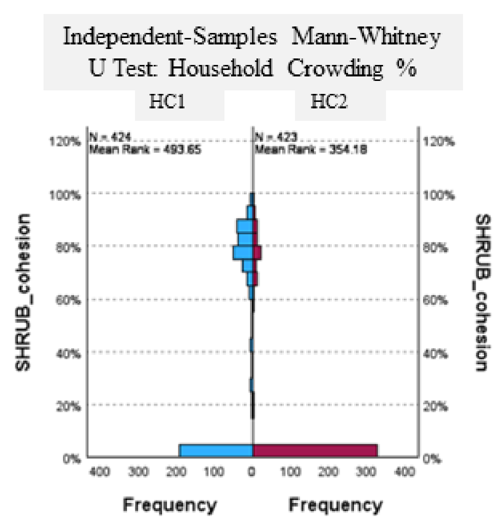

Independent-Samples Mann-Whitney U Test Summary

Total N	847
Mann-Whitney U	60143.000
Wilcoxon W	149819.000
Test Statistic	60143.000
Standard Error	3129.200
Standardized Test Statistic	-9.438
Asymptotic Sig.(2-sided test)	<.001

Figure B.4: Results of the Mann Whitney U Tests conducted on DMA data.

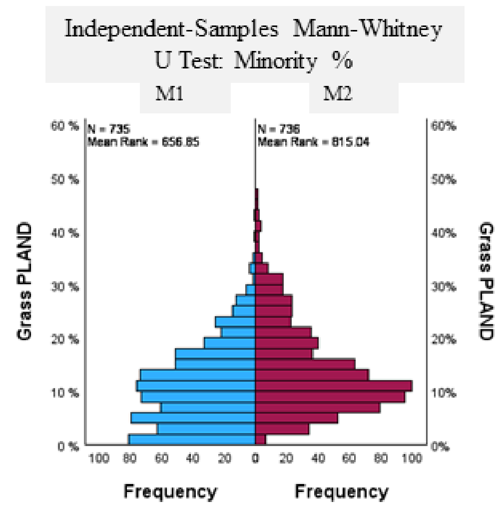

Independent-Samples Mann-Whitney U Test Summary

Total N	1471
Mann-Whitney U	328656.000
Wilcoxon W	599872.000
Test Statistic	328656.000
Standard Error	8146.027
Standardized Test Statistic	7.142
Asymptotic Sig.(2-sided test)	<.001

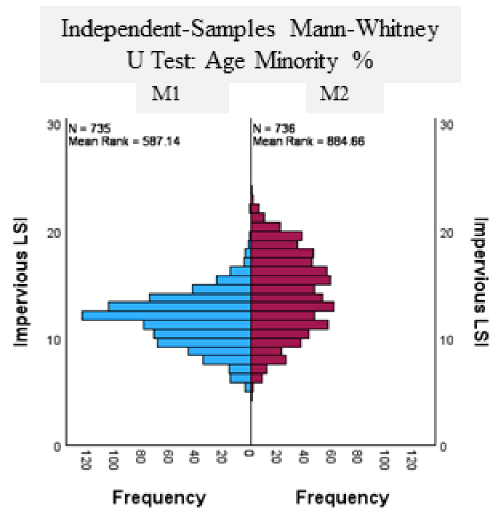

Independent-Samples Mann-Whitney U Test Summary

Total N	1471
Mann-Whitney U	379891.500
Wilcoxon W	651107.500
Test Statistic	379891.500
Standard Error	8146.027
Standardized Test Statistic	13.431
Asymptotic Sig.(2-sided test)	<.001

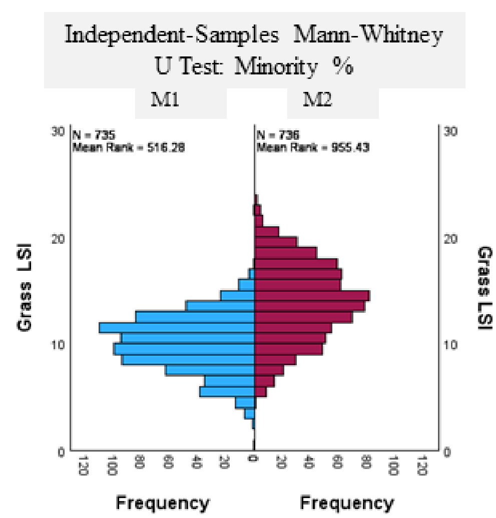

Independent-Samples Mann-Whitney U Test Summary

Total N	1471
Mann-Whitney U	431977.500
Wilcoxon W	703193.500
Test Statistic	431977.500
Standard Error	8146.027
Standardized Test Statistic	19.825
Asymptotic Sig.(2-sided test)	<.001

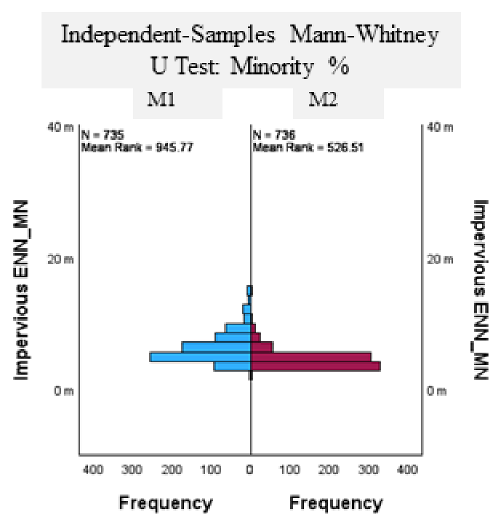

Independent-Samples Mann-Whitney U Test Summary

Total N	1471
Mann-Whitney U	116299.000
Wilcoxon W	387515.000
Test Statistic	116299.000
Standard Error	8146.027
Standardized Test Statistic	-18.927
Asymptotic Sig.(2-sided test)	<.001

Results of the Mann Whitney U Tests conducted on DMA data (cont.).

Independent-Samples Mann-Whitney U Test: Minority %

M1 M2

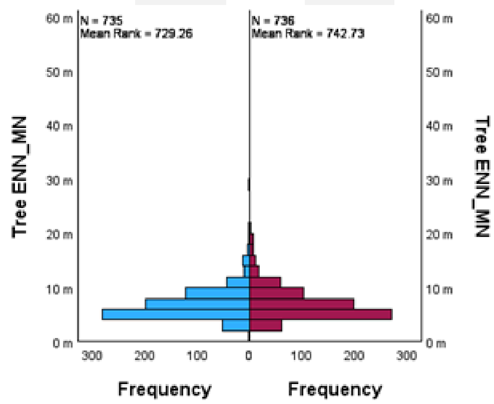

Independent-Samples Mann-Whitney U Test Summary

Total N	1471
Mann-Whitney U	275436.000
Wilcoxon W	546652.000
Test Statistic	275436.000
Standard Error	8146.027
Standardized Test Statistic	.608
Asymptotic Sig.(2-sided test)	.543

Independent-Samples Mann-Whitney U Test: Age Minority %

M1 M2

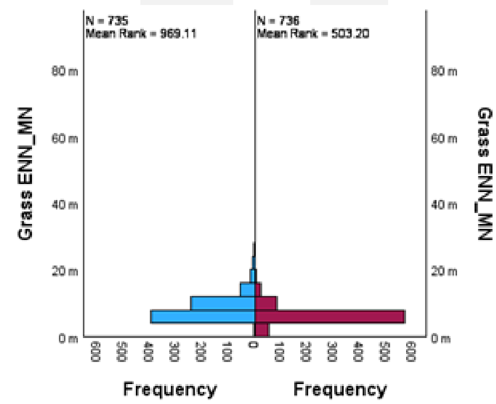

Independent-Samples Mann-Whitney U Test Summary

Total N	1471
Mann-Whitney U	99141.000
Wilcoxon W	370357.000
Test Statistic	99141.000
Standard Error	8146.027
Standardized Test Statistic	-21.033
Asymptotic Sig.(2-sided test)	<.001

Independent-Samples Mann-Whitney U Test: Minority %

M1 M2

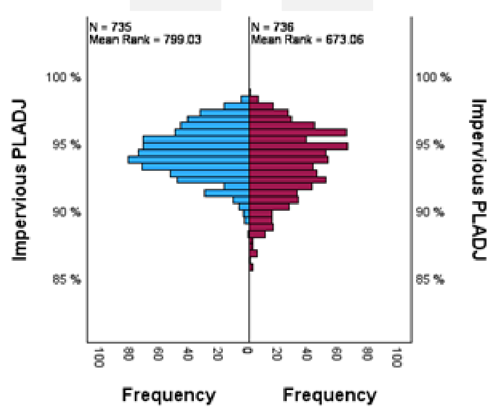

Independent-Samples Mann-Whitney U Test Summary

Total N	1471
Mann-Whitney U	224153.000
Wilcoxon W	495369.000
Test Statistic	224153.000
Standard Error	8146.027
Standardized Test Statistic	-5.687
Asymptotic Sig.(2-sided test)	<.001

Independent-Samples Mann-Whitney U Test: Disabled %

D1 D2

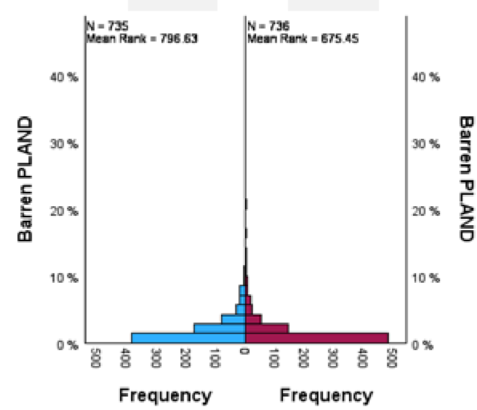

Independent-Samples Mann-Whitney U Test Summary

Total N	1471
Mann-Whitney U	225917.500
Wilcoxon W	497133.500
Test Statistic	225917.500
Standard Error	8146.027
Standardized Test Statistic	-5.470
Asymptotic Sig.(2-sided test)	<.001

Results of the Mann Whitney U Tests conducted on DMA data (cont.).

Independent-Samples Mann-Whitney U Test: Disabled %

D1 D2

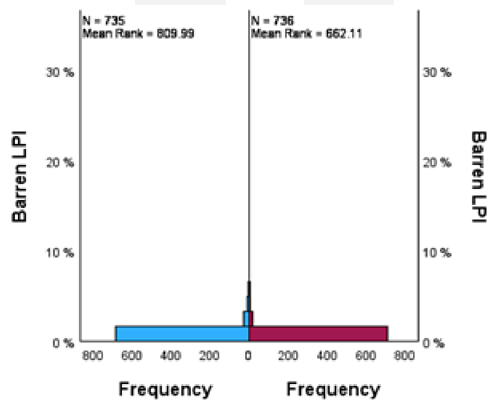

Independent-Samples Mann-Whitney U Test Summary

Total N	1471
Mann-Whitney U	216095.000
Wilcoxon W	487311.000
Test Statistic	216095.000
Standard Error	8146.026
Standardized Test Statistic	-6.676
Asymptotic Sig.(2-sided test)	<.001

Independent-Samples Mann-Whitney U Test: Age Disabled %

D1 D2

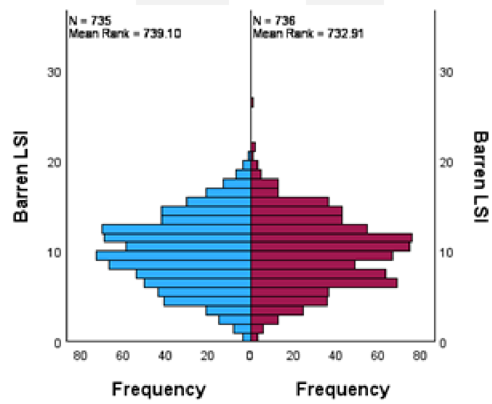

Independent-Samples Mann-Whitney U Test Summary

Total N	1471
Mann-Whitney U	268203.000
Wilcoxon W	539419.000
Test Statistic	268203.000
Standard Error	8146.024
Standardized Test Statistic	-.280
Asymptotic Sig.(2-sided test)	.780

Independent-Samples Mann-Whitney U Test: Disabled %

D1 D2

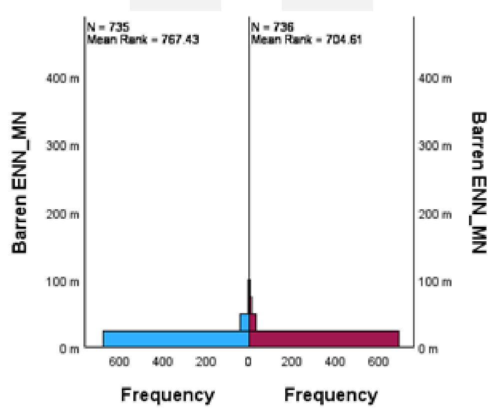

Independent-Samples Mann-Whitney U Test Summary

Total N	1471
Mann-Whitney U	247376.500
Wilcoxon W	518592.500
Test Statistic	247376.500
Standard Error	8146.026
Standardized Test Statistic	-2.836
Asymptotic Sig.(2-sided test)	.005

Independent-Samples Mann-Whitney U Test: Disabled %

D1 D2

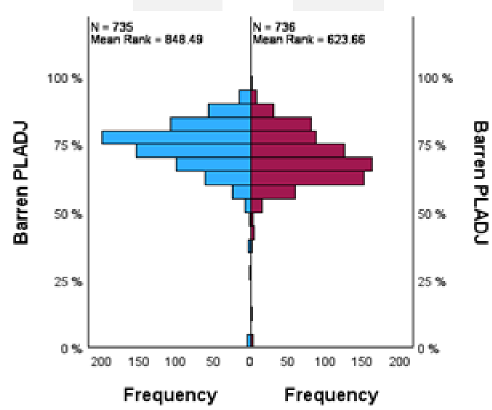

Independent-Samples Mann-Whitney U Test Summary

Total N	1471
Mann-Whitney U	187800.500
Wilcoxon W	459016.500
Test Statistic	187800.500
Standard Error	8146.027
Standardized Test Statistic	-10.150
Asymptotic Sig.(2-sided test)	<.001

Results of the Mann Whitney U Tests conducted on DMA data (cont.).

Independent-Samples Mann-Whitney U Test: Disabled %

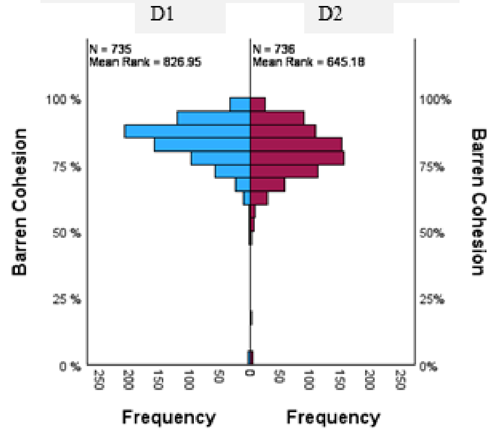

Independent-Samples Mann-Whitney U Test Summary

Total N	1471
Mann-Whitney U	203633.000
Wilcoxon W	474849.000
Test Statistic	203633.000
Standard Error	8146.027
Standardized Test Statistic	-8.206
Asymptotic Sig.(2-sided test)	<.001

Independent-Samples Mann-Whitney U Test: Factor Score PC 2

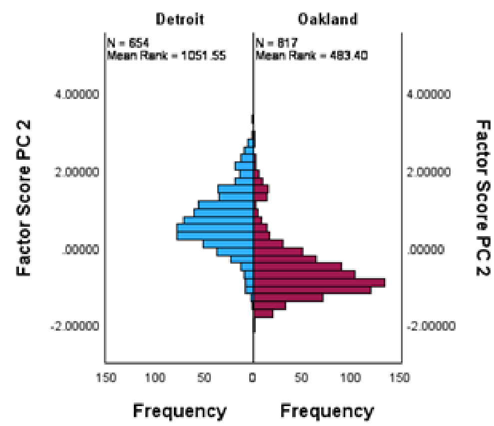

Independent-Samples Mann-Whitney U Test Summary

Total N	1471
Mann-Whitney U	60788.000
Wilcoxon W	394941.000
Test Statistic	60788.000
Standard Error	8095.864
Standardized Test Statistic	-25.491
Asymptotic Sig.(2-sided test)	<.001

Independent-Samples Mann-Whitney U Test

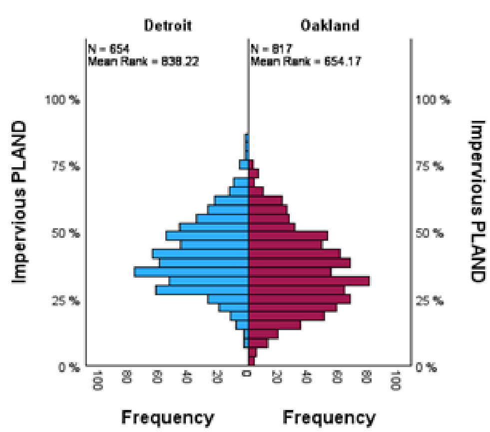

Independent-Samples Mann-Whitney U Test Summary

Total N	1471
Mann-Whitney U	200305.000
Wilcoxon W	534458.000
Test Statistic	200305.000
Standard Error	8095.864
Standardized Test Statistic	-8.258
Asymptotic Sig.(2-sided test)	<.001

Independent-Samples Mann-Whitney U Test

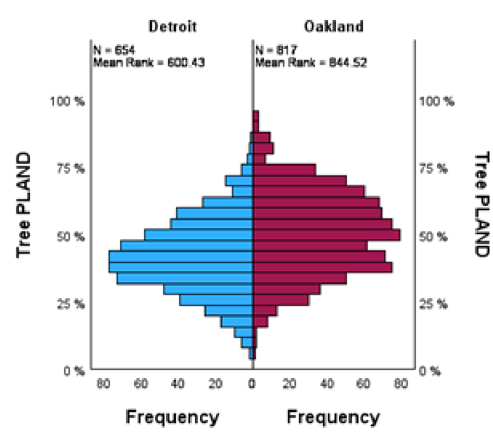

Total N	1471
Mann-Whitney U	355822.000
Wilcoxon W	689975.000
Test Statistic	355822.000
Standard Error	8095.864
Standardized Test Statistic	10.952
Asymptotic Sig.(2-sided test)	<.001

Figure B.5: Results of the Mann Whitney U Tests conducted on NYC data.

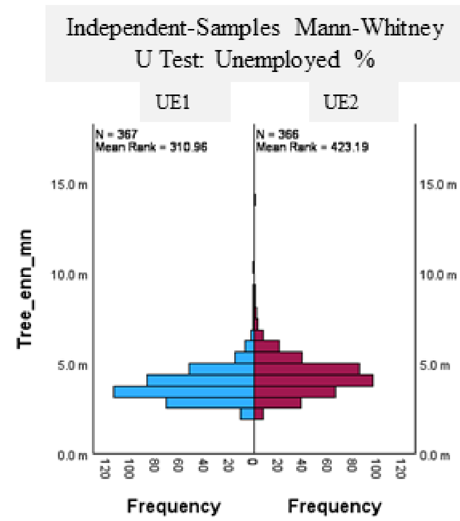

Independent-Samples Mann-Whitney U Test Summary

Total N	733
Mann-Whitney U	87728.000
Wilcoxon W	154889.000
Test Statistic	87728.000
Standard Error	2866.362
Standardized Test Statistic	7.175
Asymptotic Sig.(2-sided test)	<.001

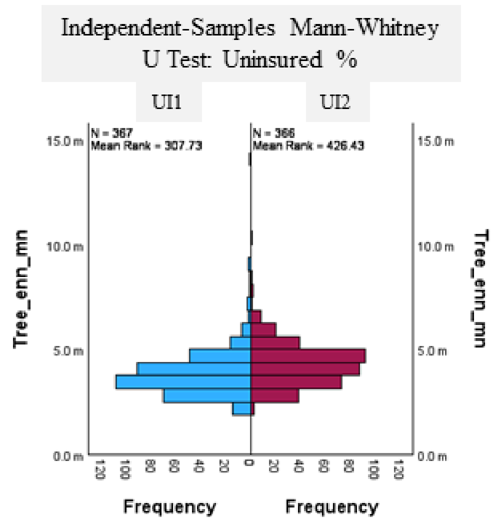

Independent-Samples Mann-Whitney U Test Summary

Total N	733
Mann-Whitney U	88914.000
Wilcoxon W	156075.000
Test Statistic	88914.000
Standard Error	2866.362
Standardized Test Statistic	7.589
Asymptotic Sig.(2-sided test)	<.001

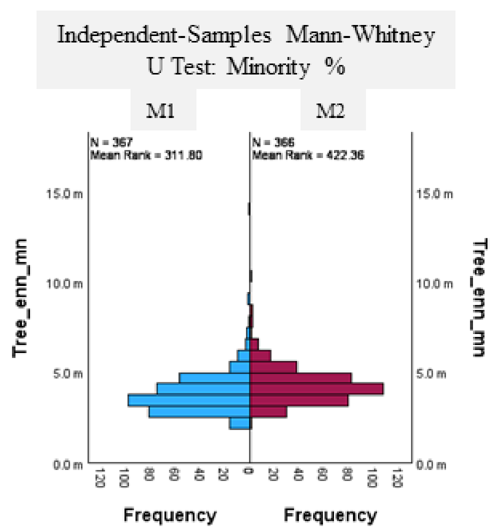

Independent-Samples Mann-Whitney U Test Summary

Total N	733
Mann-Whitney U	87421.000
Wilcoxon W	154582.000
Test Statistic	87421.000
Standard Error	2866.362
Standardized Test Statistic	7.068
Asymptotic Sig.(2-sided test)	<.001